Gene therapy for axon regeneration

Adeno-associated viral vector-mediated delivery of SaCas9 and phosphoinositide 3-kinases in cortical neurons

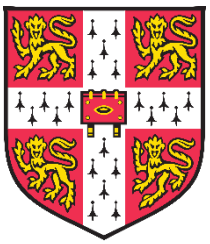

Bart Nieuwenhuis

University of Cambridge

King's college

Supervised by:

Professor James W. Fawcett

John van Geest Centre for Brain Repair

Department of Clinical Neuroscience

University of Cambridge

Professor Joost Verhaagen

Netherlands Institute for Neurosciences

Royal Netherlands Academy of Arts and Sciences (KNAW)

This dissertation is submitted for the degree of Doctor of Philosophy

March 2019

DECLARATION

This dissertation is the result of my own work and includes nothing that is the outcome of work done in collaboration except as declared at the beginning of each dissertation chapter.

The material in this dissertation has not been submitted for any other degree, diploma or qualifications at the University of Cambridge or other universities.

This dissertation does not exceed the word limit specified by the Clinical Medicine and Clinical Veterinary Medicine Degree Committee.

This work was funded by a Nathalie Rose Barr award (NRB110) from the International Spinal Research Trust, a grant from the Medical Research Council (G1000864), an ERA-NET NEURON grant AxonRepair (013-16-002), and support from the laboratory for regeneration of sensorimotor systems at the Netherlands Institute for Neuroscience. The funders had no role in study design, data collection and analysis, decision to publish, or preparation of the dissertation.

The following publications were part of my PhD training and were published before submitting this dissertation:

- **Nieuwenhuis B**, Haenzi B, Andrews MR, Verhaagen J, Fawcett JW (2018) Integrins promote axonal regeneration after injury of the nervous system. Biological Reviews 8:35.
- **Nieuwenhuis B**, Eva R (2018a) Linking axon transport to regeneration using in vitro laser axotomy. Neural Regen Res 13:410–412.
- **Nieuwenhuis B**, Eva R (2018b) ARF6 and Rab11 as intrinsic regulators of axon regeneration. Small GTPases 1–10.

For my mother

Anneke Erkamp

And in memory of my father

Gradus Barend Nieuwenhuis

TABLE OF CONTENTS

ACKNOWLEDGMENTS

I would like to take the opportunity to thank the people that contributed to the work of this dissertation and also those who made my stay at Cambridge a memorable period of my life.

First of all, I would like to thank my supervisors James W. Fawcett and Joost Verhaagen. James, thanks for giving me the opportunity to work as a PhD student in your laboratory and for introducing me to your international network of scientists. I am grateful for your support and also acknowledge the freedom that you gave me to pursue my own ideas. Joost, thanks for your trust since the beginning of my master's degree at the VU University Amsterdam to the end of my PhD degree at the University of Cambridge. I learned a lot from you. You are both excellent mentors in my journey to become a scientist.

I thank Andras Lakatos and Simone Di Giovanni for being the examiners of my doctoral dissertation.

I give a special thanks to Barbara Haenzi. Your experience in scientific writing and animal work was a great help for my PhD training. This dissertation would have been thinner without your support. Thanks for your patience when I was struggling with the mice and rats. You were also a listening ear and could provide great advice when needed.

Also a special thanks to Richard Eva. You taught me a lot about microscopy and this contributed to the nice images in my thesis. You also gave me the freedom to work on PI3Ks in cultured cortical neurons. It was probably the best decision of my PhD to move into this project. These experiments were the fun part of my PhD.

Veselina Petrova, I am happy that we could support each other during the tough way to graduation. I also enjoyed the many conferences that we attended together. Can you name them all? I am happy to have found a great friend throughout this dissertation.

Sam 'Soldier' Hilton, You were always there for me at work and as friend. A great thank you for your technical support in the combined facility and tissue processing (Chapter IV). I mainly thank you for our squash and 'breakfast club' sessions at King's college and for introducing me to the sport rugby. We should visit the pub again soon and import Danish Christmas beer. I will provide the stroopwaffels.

Alejandro ‘Guapo’ Carnicer-Lombarte, You were a great buddy throughout the PhD. Thanks for spending hours with me to make the ImageJ Macro for image analysis to count eGFP positive neurons (Chapter IV). It was also nice to spend some game-hours together and the trip to South-Spain and Gibraltar is also very memorable. That monkey… Finally, I acknowledge the support of your almost-always empty desk in the PhD room. Yes, I hijacked it all the time.

Craig Pearson, it was great to have you around during the first year of my PhD. Your positivity and passion for your research had an impact on me. Furthermore, the writing sessions in the libraries of many colleges contributed to passing the first year report. Our holiday in Italy was also great fun. Now tell me… Where is ‘Dino’?

Marco Vermeer, working with you in the fashion store offered me the necessary distraction from the scientific community. I also developed translational skills such as alertness, listening, a positive attitude, and most importantly being personable. The past ten years as salesman were fun.

Andrea ‘Cornetto’ Loreto, who are you? What a driving adventures we had! The Chelsea – Atlético Madrid football game was an absolute highlight. Thanks for all the banter inside and outside the Brain Repair Centre.

I thank Daniella Massias for the fun moments in the first year of my PhD. It was great to explore all the social events that Cambridge had to offer during our studies. Your wedding in Gibraltar is also an unforgettable memory.

Barbara Hobo, Fred de Winter and Matthew Mason, thank you for teaching me the fine tricks of making adeno-associated virus and lentivirus (Chapter IV). It was a great pleasure to work with you.

I acknowledge Cara Brodie for giving me access to the fluorescent scanning service of the Cancer Research UK Cambridge institute. Thank you for the beautiful overview images of the virus transduced brains (Chapter IV).

Hiro Koseki, the king of cell culture, thanks for teaching me how to grow cortical neurons in a dish.

Joachim Fuchs and Britta Eickholt, thanks for sharing the staining protocol for PIP_3. It was great to collaborate and the method became a crucial part of Chapter IV.

Menghon Cheah and Melissa Andrews, thank you both for setting the fundamentals for the work on integrins. Melissa, also thank you for your contribution to the review article (Chapter I).

William Hendriks, thanks for sharing your experience regarding the CRISPR-Cas9 system (Chapter II). I wouldn't be able to set up this technique in Amsterdam and Cambridge without your guidance.

Simona Foscarin, I want to thank you for optimizing the Ankyrin-G genotyping protocol during my intermission of study.

Sara Soleman and Jessica Kwok, both of you played a significant role by guiding me during my internship and at the beginning of my PhD training. Thank you for the good start.

Elise Laperrousaz, thanks for your cell culture support near the end of my PhD. I hope that the CRISPR-Cas9 constructs for EFA6 will be useful for your post-doc role in Cambridge.

Matthew Rasband contributed to my research by sharing their transgenic Ankyrin-G conditional knockout mouse. Thank you.

Thanks to Andy Osborn and Keith Martin for your enthusiasm about my viral vector and promoter study. I am excited for our follow-up project in eye.

I thank Rachel Evans and Amanda Barber for their work on PI3K in animal models. I look forward to the final manuscript in which both our work is combined for publication.

Thanks to Damiano Barone, Heleen van 't Spijker, Ruwani Wijeyekoon, Katie Hall, James Henderson, Raquel Conceicao, Tasneem Khatib, Peter Arthur-Farraj, Shaline Fazal, and

Stuart Few for the fun moments in Cambridge.

Thanks to the staff in phenomics and the combined facility for looking after the animals, in particularly thanks to Ali Robinson and Damian Quigley.

I would like to thank King's College for becoming my second home during the PhD. The College also provide financial support to attend two great science meetings, EMBO (Crete, Greece) and SfN (San Diego, USA), and was also caring during my intermission of study. I especially thank Bert Vaux, Tim Flack and College nurse Vicky Few. The college porters also can't be forgotten for their daily assistance.

I would like to thank the friends that I have made at King's college, in particular to Martin Smoragiewicz, Alex Young-il Seo, Oscar Wilsby, Katrin Heider, Ahmed Mudassar, Lera Shumaylova, and Elisabeth Vargas-Holguin. I also thank the members of the 2015 and 2016 King's college boat club.

Thanks to all other colleagues of the Brain Repair Centre and the Netherlands Institute for Neuroscience for creating a pleasurable work environment.

Lieve Nina, I am so happy that we met during our PhD degrees in Cambridge. You have been an infinite support through the hard and good times. I am thankful for the beautiful moments together. Ευχαριστώ Πολύ.

A huge thanks to my brother Joost. You may have given the biggest contribution to this dissertation by looking after mum and dad in the Netherlands. I am thankful for all your support at home, while I was abroad. I am also proud that you are doing great at your studies.

This dissertation wouldn't have been possible without the endless support of my parents. Lieve mam, bedankt voor alles wat jij doet. Ik kan niet in woorden uitdrukken hoe belangrijk mijn zorgeloze jeugd was om uiteindelijk hier met een PhD diploma van Cambridge te staan. Ik draag daarom dit proefschrift op aan jou en pap.

Finally, I would like to acknowledge my own determination and commitment to complete this PhD degree. I had a long road with lots of ups and downs. Nevertheless, I always persisted to make this PhD work.

GENERAL INTRODUCTION

Injury to the brain and spinal cord has devastating consequences because adult neurons in the central nervous system (CNS) do not regenerate. Traumatic CNS injuries are a significant clinical problem and have life-changing consequences for patients. There are 130.000 new cases of spinal cord injury (SCI) per year worldwide and currently affects more than 2.5 million people (International Spinal Research Trust). Spinal cord injury often results in loss of essential bodily functions including sexual function, bladder control, and motor and sensory function. SCI mainly occurs among young adults and generates a psychological burden for both the patients and their caregivers. Furthermore, SCI is a substantial economic problem, as the UK national cost was estimated at one billion pounds per year. With these facts in mind, there is currently enormous interest in developing treatments for patients who are living with SCI.

There are many factors that contribute to the failure of axon regeneration in the CNS. Generally speaking, the problem of axon regeneration can be subdivided in at least two aspects: 1) the growth-repulsive environment surrounding the injured axon and 2) the low intrinsic regeneration potential of adult CNS neurons.

SCI initiates drastic molecular and cellular changes at the site of insult. The primary injury is the direct mechanical trauma to the neurons, glia and blood vessels in the spinal cord. The ruptured vascular system contributes to ischemia-induced cell death and entry of inflammatory and other cells to the site of injury (reviewed in Oudega, 2012). Scar tissue is formed within a few days after an injury and consists of edema, and includes many cells types and an orchestra of molecules. Astrocytes react to the injury by forming a dense net within the scar and secrete a variety of molecules including chondroitin sulfate proteoglycans (CSPGs) including aggrecan (reviewed in Silver & Miller, 2004; Gervasi, Kwok, & Fawcett, 2008). Fibroblasts, derived from connective tissue, also enter the site of injury and produce axon repulsive molecules such as class III semaphorins (reviewed in Mecollari, Nieuwenhuis, & Verhaagen, 2014). On top of that, Wallerian degeneration occurs and myelin debris accumulates in the scar and along the denervated nerve tracts. Several of the myelin-derived molecules, including Nogo-A, MAG and OMgp, are known to be repulsive for axon regeneration (reviewed in Schweigreiter & Bandtlow, 2006; Alizadeh, Dyck, & Karimi-Abdolrezaee, 2015; Boghdadi, Teo, & Bourne, 2017). Thus, the scar tissue holds multiple molecular components that hinder axonal regeneration. Yet, there are also studies suggesting that certain components of the scar are regeneration-supportive, such as laminins, thrombospondin-1 and certain CSPGs (Tyzack *et al.*, 2014; Anderson *et al.*, 2016).

Mechanisms within neurons also restrict axonal regeneration in the adult CNS. First of all, the primary injury causes apoptosis of many CNS neurons at the injury site. Only the surviving neurons have the possibility to promote axonal regeneration. However, many CNS neurons survive the injury, in particular the neurons of the large descending and ascending tracts of the spinal cord. Successful axon regeneration requires the formation of a growth cone and synthesis of cytoskeleton and regeneration-associated proteins to extend and lengthen the injured axon (reviewed in Liu *et al.*, 2011; Bradke, Fawcett, & Spira, 2012). However, adult CNS neurons are unsuccessful to activate regeneration-associated genes (reviewed in van Kesteren *et al.*, 2011; Fagoe, van Heest, & Verhaagen, 2014). The mechanism how the axon regeneration response declines during maturation is unknown. Our laboratory has the hypothesis that (epi-) genetic changes and selective polarized transport that occurs during neuronal polarization contribute to the decline in the axonal regeneration response of CNS neurons (reviewed in Nieuwenhuis & Eva, 2018). Developing neurons have a high dendritic and axonal growth capacity, while matured CNS neurons develop an axon initial segment, propagate action potentials, form spines and synapses and importantly have a low capacity for axonal growth. Some of the evidence that highlight the decline in the intrinsic axonal regeneration response in adult CNS neurons is briefly reviewed below.

Neurons of adult motor tracts that fail to regenerate lack regeneration-associated receptors in their axon. Integrins are cell-surface receptors that are important for axonal growth in embryonic CNS tissue, but are excluded from the axonal compartment of corticospinal tract and cerebellum in adulthood, and are also not upregulated after injury (Pinkstaff *et al.*, 1999; Andrews *et al.*, 2009). The cell-surface receptor TrkB is also not found in the axons of the adult corticospinal tract, nor upregulated after injury (Yan *et al.*, 1997; Liebl *et al.*, 2001; Lu, Blesch, & Tuszynski, 2001). Insulin-like growth factor receptors are also important during development of the corticospinal tract (Arlotta *et al.*, 2005; Ozdinler & Macklis, 2006), but are not found in the axon when matured (Hollis *et al.*, 2009a). The absence of growth-promoting receptors that interact with the environment of the CNS is one mechanism that contributes to axon regeneration failure.

Studies that aimed to re-introduce regeneration-associated receptors in the corticospinal tract were unsuccessful to get the receptors transported in the axonal compartment. Adeno-associated viral vector mediated delivery of integrins (Andrews *et al.*, 2016), TrkB (Hollis *et al.*, 2009b), and IGFR-1 (Hollis *et al.*, 2009a) in the corticospinal tract resulted in localisation of the receptors in the somatodendritic compartment of the neuron in the cortex, but not in the axon in the spinal cord. This suggests that the adult corticospinal tract has mechanisms in place that prevent growth-promoting receptors to enter

the axon. The axon initial segment is an important component of selective polarised transport in multipolar neurons (reviewed in Rasband, 2010). The mechanisms how the AIS regulates axonal transport is not completely understood, but it is a known barrier for the axonal transport of many proteins including integrins (Bi *et al.*, 2001; Hedstrom, Ogawa, & Rasband, 2008; Sobotzik *et al.*, 2009; Franssen *et al.*, 2015). In addition, changes in the axonal transport machinery contribute to exclusion of regeneration-associated receptors. Rab11 is a small-GTPases that marks endosomes containing integrins, TrkB, and IGFR-1 (reviewed in Nieuwenhuis & Eva, 2018). Rab11-positive recycling endosomes are largely excluded from axons in adult cortical neurons (Sheehan *et al.*, 1996; Koseki *et al.*, 2017). This is most likely the consequence of a steep-upregulation of GTP exchange factors (GEFs), such as EFA6 and ARNO (Sakagami *et al.*, 2006; Bi *et al.*, 2001; Franssen *et al.*, 2015; Eva *et al.*, 2017), which direct these endosomes away from the axon. Modifications in actin and microtubules also contribute to selective polarised transport in cortical neurons (Franssen *et al.*, 2015).

An age-dependent decline in axonal regeneration is observed in cultured cortical neurons (Koseki *et al.*, 2017) and in the corticospinal tract *in vivo* (Geoffroy *et al.*, 2016). Multiple intrinsic mechanisms, in which some are depended on upstream axonal receptor signalling, which are beneficial for axonal regeneration are down-regulated during maturation. For instance, there is a decline of phosphoinositide 3-kinases in cortical neurons *in vitro* and *in vivo* (Eickholt *et al.*, 2007; Koseki *et al.*, 2017). There is also a decline in the number of activated ribosomal proteins in CNS neurons in line with maturation *in vivo* (Park *et al.*, 2008; Liu *et al.*, 2010). An age-associated decline in cyclic adenosine monophosphate (cAMP) which correlates with loss of axonal growth has also been reported (Cai *et al.*, 2001). A down-regulation of histone acetyltransferases has also been observed which results in more compact chromatin during maturation and may contribute to the decline in the ability of regeneration-associated transcription factors to promote axonal regeneration in CNS neurons (Gaub *et al.*, 2011; and reviewed in Danzi *et al.*, 2018).

The low intrinsic axon regeneration capacity of adult CNS neurons is an important component restricting functional recovery after spinal cord injury. This dissertation focuses on genetic approaches to enhance the axonal regeneration capacity of cortical neurons. Changes in integrin receptor biology are a good example of molecular changes leading to restricted axonal regeneration in the adult CNS. Several studies have shown that targeting integrins and related regeneration-associated molecules can promote axonal regeneration after injury of the nervous system. The tools used for the discovery of integrins and approaches to manipulate them could also act as a model for other mechanisms that limit axonal

regeneration. Strategies that aim to promote axonal transport of regeneration-associated receptors and downstream axonal growth signalling are therefore topics of this thesis. Work in this thesis aimed to explore whether dismantling the axon initial segment could enhance the transport of regeneration-associated receptors in the axon. Another approach investigated whether improving axonal growth signalling, downstream of receptor signal transduction, promotes axon regeneration in CNS neurons. Adeno-associated viral (AAV) vectors are the preferred carriers to transduce CNS neurons, and were also used in this thesis to deliver transgenes into cortical neurons and the corticospinal tract. Part of this dissertation focussed on optimising AAV-mediated transduction of the corticospinal tract because regeneration of this neuronal pathway is a key event to restore motor function after spinal cord injury. Gene therapy is a promising strategy to promote axonal regeneration. The overall objectives of this dissertation were the following: (i) to enhance axon regeneration in cortical neurons *in vitro;* and (ii) to optimize AAV-mediated transduction of the corticospinal tract *in vivo*.

OUTLINE OF THIS DOCTORAL DISSERTATION

Chapter I is a literature review about the cell surface receptors integrins and their role in axonal regeneration. Integrins contribute to the spontaneous axon regeneration in the peripheral nervous system by interacting with ligands in the extracellular matrix. Integrin biology is different in the CNS. These receptors are transported into the axon of developing neurons, but selective axonal transport limits the regenerative response in adult CNS neurons. Manipulation of integrins and related molecules that control their transport and activation state is a promising tool to promote robust regeneration in the CNS. The platforms and experimental therapies used in integrin research are also relevant for other mechanisms limited axon regeneration.

Chapter II is based on the hypothesis that the axon initial segment is a barrier for the axonal transport of integrins and other growth-promoting receptors. The aim was to dismantle the axon initial segment by knockout of the cytoskeletal scaffolding protein Ankyrin-G. Two genetic tools were made and tested to knockout Ankyrin G: (1) a short hairpin RNA, and (2) a dual promoter AAV viral vector that drives the expression of a CRISPR-associated endonuclease 9 from *Staphylococcus aures* and one guide RNA targeting Ankyrin-G.

Chapter III is based on the hypothesis that low axonal PtdIns-3,4,5-P3 (PIP_3) signalling, due to the absence of growth-promoting receptors in the axon, contributes to regenerative failure in the CNS. This chapter investigates whether overexpression of phosphoinositide 3-kinases (PI3Ks), which generates PIP_3, can promote axon regeneration in cultured cortical neurons.

Chapter IV aimed to identify the best method to deliver transgenes into the corticospinal tract by using AAVs. The choice of serotype and promoter has a crucial impact on gene therapy as it can ultimately depict whether it will be successful or unsuccessful. This study consisted of a direct comparison between the AAV1 and AAV5 viral vector serotypes and four promoters (CMV, PGK, sCAG, synapsin) in their efficiency to express eGFP following injection at the sensory-motor cortex in mice and rats.

Chapter V is a summary and general discussion of the obtained results in dissertation. It highlights future perspectives of the current work and how the research contributes to advance the field of gene therapy and axon regeneration.

CHAPTER I - Integrins promote axonal regeneration after injury of the nervous system

Declaration:

 The citation is: Nieuwenhuis, B., Haenzi, B., Andrews, M. R., Verhaagen, J. and Fawcett, J. W. (2018), Integrins promote axonal regeneration after injury of the nervous system. Biol Rev, 93: 1339-1362. doi:10.1111/brv.12398.

This literature review was written in collaboration with the above authors. The contribution of each author is the following:

Barbara Haenzi wrote sub-section VII.*2* 'Developmental changes in the integrin transport machinery', made figure 1 and figure 4, and edited early versions of the manuscript.

Melissa Andrews wrote Section II 'The localisation of integrins in the nervous system and implications for axonal regeneration' and sub-section VII.1 'Exclusion of integrins from the axon of certain adult central nervous system neurons'.

Joost Verhaagen contributed by critical reading and editing of the manuscript.

James Fawcett edited the final version of the manuscript before submission to the journal.

I, Bart Nieuwenhuis, initiated the literature review, made the text, figures and tables that are not mentioned above, and I am the corresponding author of the published article.

I. INTRODUCTION

The integrin receptor family plays a role in a variety of processes including the development of various tissues (reviewed in Danen & Sonnenberg, 2003; Avraamides, Garmy-Susini, & Varner, 2008), the formation of the nervous system (reviewed in Colognato & Tzvetanova, 2011; Gardiner, 2011; Kazanis & ffrench-Constant, 2011; Myers, Santiago Medina, & Gomez, 2011), the immune response (reviewed in Means & Luster, 2010), cancer (reviewed in Guo & Giancotti, 2004; Desgrosellier & Cheresh, 2010; Schittenhelm, Tabatabai, & Sipos, 2016; Paolillo, Serra, & Schinelli, 2016), synaptic plasticity (reviewed in Park & Goda, 2016) and axonal regeneration in the peripheral nervous system (PNS) (reviewed in Gardiner, 2011; Eva & Fawcett, 2014). This review describes and discusses the role of integrins in axonal regeneration and their use as therapeutic targets to stimulate repair after spinal cord injury.

(1) Structure

The structure of integrins is well characterised and has been described in many reviews (Takada, Ye, & Simon, 2007; Wegener *et al.*, 2007; Arnaout, Goodman, & Xiong, 2007; Campbell & Humphries, 2011; Hu & Luo, 2013). Integrins are heterodimeric receptors that consist of one alpha (α) and one beta (β) subunit. In mammals, 18 α and 8 β subunits have been identified giving rise to 24 unique integrin receptors (reviewed in Hynes, 2002). Integrins are type I (C-terminus located intracellularly) glycoproteins. The ectodomain is the largest part of both the α and β subunits containing the metal-ion and extracellular-matrix (ECM) ligand-binding sites. The interaction between the transmembrane domains of the subunits determines the conformation and therefore the activation state of the receptor. Inactivated integrins exist in a bent orientation as the two transmembrane domains interact closely. By contrast, activated integrins have less interaction between the transmembrane parts, resulting in a straight conformation and allowing them to bind to ligands in the ECM. The cytoplasmic tails of integrins are relatively short. They lack enzymatic activity and integrins are therefore reliant on multi-protein complexes for signal transduction. The particularly short tail of the α subunit indicates a limited role for this subunit in intracellular processes. The cytoplasmic tail of the β subunit is also short, but contains two NPXY motifs that can interact with phosphotyrosine binding domains of intracellular proteins, such as talins (Tadokoro *et al.*, 2003), kindlins (Moser *et al.*, 2008; Harburger, Bouaouina, & Calderwood, 2009) and various other signalling and scaffolding molecules.

(2) Signalling

Each integrin bears a unique binding affinity for components in the heterogeneous ECM (reviewed in van der Flier & Sonnenberg, 2001; Hynes, 2002; Humphries, 2006), such as laminin, fibronectin, collagen and tenascin-C. Importantly, integrins mediate bi-directional signalling between the extracellular matrix and the cytoskeleton across the plasma membrane. Activated integrins bind to specific ECM ligands and induce signalling to the intracellular compartment of the cell, a process known as 'outside-in' signalling. The activated integrin signalling regulates the actin cytoskeleton *via* many proteins. Firstly, talin, which interacts with the cytoplasmic tail of integrins, links them directly, or *via* vinculin, to the actin cytoskeleton. Secondly, focal adhesion kinase (FAK) is recruited to activated integrins and is a key signalling scaffold protein that activates downstream proteins such as paxillin and Src. Thirdly, integrin-linked kinase (ILK) is another important signalling scaffold protein that phosphorylates downstream proteins. Conversely, 'inside-out' signalling refers to the mechanism in which intracellular proteins bind integrins thereby inducing a conformational change that enhances the binding activity of integrins towards their ligands in the ECM, enabling intracellular signalling. Talin and kindlin, the main mediators of inside-out signalling, are subject to various regulatory pathways that thereby affect integrin function (reviewed in Calderwood, Campbell, & Critchley, 2013; Ye, Lagarrigue, & Ginsberg, 2014; Rognoni, Ruppert, & Fässler, 2016). Importantly, the integrin receptor family can form hundreds of protein complexes to link the ECM with the cytoskeleton. These protein complexes are also referred to as the integrin adhesome (Zaidel-Bar *et al.*, 2007; Robertson *et al.*, 2015; Horton *et al.*, 2015; reviewed in Winograd-Katz *et al.*, 2014; Humphries *et al.*, 2015).

(3) Integrin subunit knockouts

Whole-system and tissue-specific knockout studies of integrins have been fruitful in demonstrating their functional importance. It has been demonstrated in integrin-knockout mice that integrins are important for tissue development. Depending on which integrin subunit is knocked out, the mouse phenotypes range from mild developmental defects to embryonic or perinatal lethality (reviewed in Hynes, 2002; Bouvard *et al.*, 2013). The architecture and function of the nervous system is also reliant on the coordinated expression of integrin receptors and components of the ECM. Several studies examining deletion of different integrin subunits have shown varying degrees of impairment and/or changes in gross morphology, thereby confirming their fundamental role in the development and maintenance of the nervous system. For example, mutant mice carrying brain-specific (neurons and glia) deletion of α6 integrin had abnormalities in the foliation of the cerebellum along with a reduction in process outgrowth of the Bergmann glia, yet the cerebral cortex developed normally (Marchetti *et al.*, 2013). Selective deletion of αV integrin in the brain resulted in severe neurological abnormalities including seizures and ataxia as well as cerebral haemorrhage (beginning *in utero*), leading to death by four weeks of age in the majority of cases (McCarty *et al.*, 2005). Deletion of the β1 subunit influences the majority of integrin heterodimers and not surprisingly a whole-body knockout is embryonically lethal (Fässler & Meyer, 1995). Deletion of β1 integrins in the brain leads to death shortly after birth (Graus-Porta *et al.*, 2001) highlighting that expression of β1 integrin heterodimers in neurons and glia is essential. Several integrins have specific roles in axon regeneration that are discussed below (see Sections III and IV.*i*). The fact that integrins are located at the growth cone (Robles & Gomez, 2006) and respond to diverse extracellular molecular signals present in the environment of the injured PNS and central nervous system (CNS) makes them an interesting target to study axonal regeneration (**Fig. 1**).

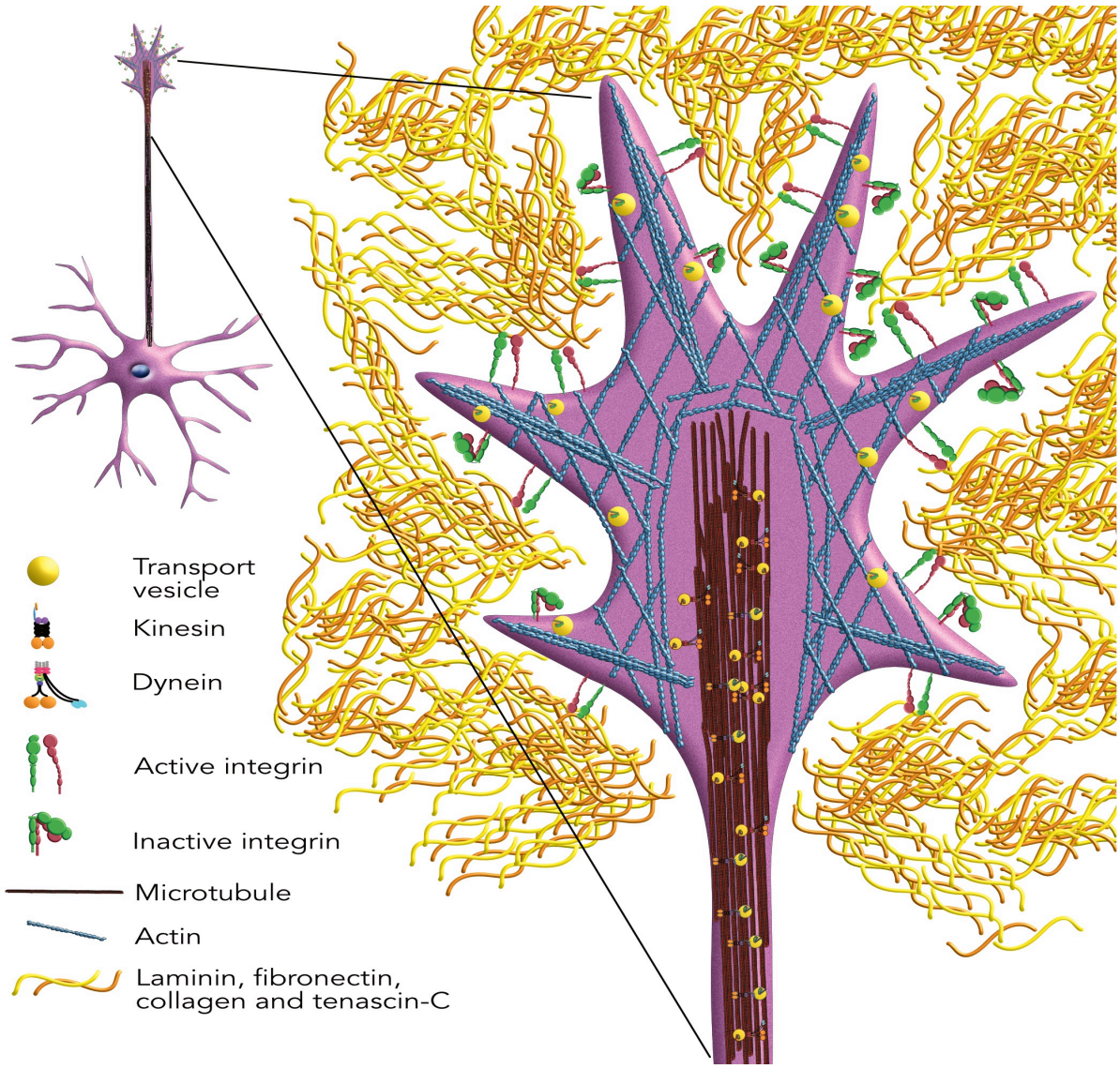

Fig. 1. Integrins are localised to the growth cone of immature and peripheral nervous system neurons. Active and inactive integrins are present on the surface of the neuronal growth cone. However, only active integrins bind molecules of the extracellular matrix.

II. THE LOCALISATION OF INTEGRINS IN THE NERVOUS SYSTEM AND IMPLICATIONS FOR AXONAL REGENERATION

Integrins are expressed by every cell in the body (except red blood cells) which in the CNS includes neurons, astrocytes, microglia, oligodendrocytes, and endothelial cells (reviewed in Milner & Campbell, 2002; Schmid & Anton, 2003). Integrin function depends on the cellular localisation of the receptor. For the purposes of this review, we confine our discussion below to integrin localisation in the nervous system. Various integrins are expressed in particular sets of neurons and glia. There is also specific localisation of integrins within neurons to the somatodendritic and axonal compartments.

(1) mRNA expression

Much of our knowledge of patterns of integrin expression comes from *in situ* hybridization and RT-PCR studies (**Table 1**). In two whole-brain expression studies, differential expression patterns of several integrin subunits were demonstrated in various brain regions. Messenger RNA (mRNA) labelling within CNS neurons varying from relatively low to significantly high levels was detected in layer V of the cortex, hippocampus (CA1, CA3 pyramidal neurons and granule neurons of the dentate gyrus), olfactory bulb, and cerebellar Purkinje neurons for α1, α2, α3, α4, α5, α6, α7, αV, β1, β3, β5, β6, and β7. Furthermore, it has been found that α8 integrin can be detected in the hippocampus and olfactory bulb (Pinkstaff *et al.*, 1999; Chan *et al.*, 2003). In the red nucleus, mRNA of α3, α7, αV and β1 was detected, including an up-regulation in β1 mRNA following axotomy (Plantman *et al.*, 2005). In addition, examination of rat dorsal root ganglia (DRGs) also revealed expression of α5, α6, α7, and β1 integrins (Wallquist *et al.*, 2004; Gardiner *et al.*, 2007; Gonzalez Perez *et al.*, 2016), whereas spinal motor neurons expressed α3, α7, and β1 integrins with α6 expression appearing in these neurons after axotomy (Hammarberg *et al.*, 2000).

Table 1. Integrin mRNA expression in the adult nervous system.

mRNA	α1	α2	α3	α4	α5	α6	α7	α8	αV	β1	β3	β5	β6	β7
Cerebellum	3	3	1, 3	3	1, 3	1, 3	1, 3		1, 3	1, 3	3	1, 3	3	3
Cortex layer V	1, 3	3	1, 3	3	3	3	1, 3		1, 3	3	3	1, 3	3	3
DRGs					6, 7	4	4, 7			4				
Hippocampus	1, 3	3	1, 3	3	1, 3	1, 3	1, 3	1	3	1, 3	3	1, 3	3	3
Olfactory bulb	3	3	1, 3	1, 3	1, 3	1, 3	1, 3	1	1, 3	3	3	1, 3	3	3
Red nucleus			5				5		5	5				
Spinal motor neurons			2			2*	2			2				

Shaded squares indicate that integrin mRNA was detected and they are labelled with the corresponding reference; white squares illustrate that mRNA expression was not tested or not detected. The asterisk (*) indicates that expression was observed only following axotomy. The integrins α9, α10, α11, αD, αE, αL, αM, α2b, αX, β2, β4 and β8 are not included because they were not tested or there was no mRNA detected in any of the cell types analysed. 1, Pinkstaff *et al*. (1999); 2, Hammarberg *et al*. (2000); 3, Chan *et al*. (2003); 4, Wallquist *et al*. (2004); 5, Plantman *et al*. (2005); 6, Gardiner *et al*. (2007); 7, Gonzales-Perez *et al*. (2016). DRGs, dorsal root ganglia.

(2) Subcellular localisation

In order to assess the subcellular localisation of integrin receptors, immunohistochemical approaches or expression of labelled integrins are required. Determining whether integrins are expressed in the axonal or somatodendritic compartment is useful for understanding their potential function. In this regard, numerous studies have examined integrin expression in cultured cells, with fewer studies documenting expression in tissue sections. There are many studies demonstrating integrins in axons during embryonic development, using both immunohistochemistry and staining of cultured embryonic neurons. This is not surprising; integrins are necessary for axon growth during development (reviewed in Gardiner, 2011; Myers *et al.*, 2011). However, in the mature CNS the picture is very different as discussed below.

Integrins have been localised within the somatodendritic compartment of adult layer V pyramidal neurons, CA1 and CA3 hippocampal neurons, granule neurons of the dentate gyrus, and Purkinje cells (Grooms, Terracio, & Jones, 1993; Murase & Hayashi, 1996; Rodriguez *et al.*, 2000; Bi *et al.*, 2001; Schuster *et al.*, 2001; Chan *et al.*, 2003; Kawaguchi & Hirano, 2006; Mortillo *et al.*, 2012; see **Table 2**). Interestingly, certain integrin subunits including α3, α5 and β1 are found in the somatodendritic compartment of diverse neuronal types, which may indicate an important role in dendritic function. Other somatodendritic integrins displayed a more restricted neuron sub-type distribution. For instance, α8 is expressed in layer V pyramidal neurons, olfactory bulb, and hippocampal neurons (Einheber *et al.*, 1996), αV and β8 in cerebellar and hippocampal neurons (Nishimura *et al.*, 1998; Kang *et al.*, 2008) whereas β3 was detected in hippocampal neurons and the inner plexiform layer of the retina in addition to α5 (Kang *et al.*, 2008; Vecino *et al.*, 2015). Additionally, following injury, α7 and β1 subunits were found to be expressed in facial motor neurons (Kloss *et al.*, 1999; Werner *et al.*, 2000). The localisation of integrins in the somatodendritic compartment of adult neurons is summarised in **Table 2**.

The question of whether integrins are found in axons during development and in adulthood is important to understand their function in regeneration. Very few studies however have demonstrated the presence of integrin receptors in the axonal compartment in tissue sections from the mature CNS. This is partly due to the lack of suitable antibodies, but mainly due to the down-regulation of expression of many integrins in the adult CNS in addition to the active exclusion of integrins from most mature CNS axons as discussed below (Section VII). Some studies however have succeeded in localising endogenous integrins specifically (see **Table 3**); for instance α5 integrin has been found within rodent axons of layer V pyramidal neurons and reticular formation (King, McBride, & Priestley, 2001; Bi *et al.*, 2001).

Interestingly, the majority of studies demonstrating axonal localisation of integrins have been in retinal ganglia cells (RGCs) and DRGs, two neuronal subtypes that have been shown experimentally to have increased regenerative capacity relative to many other CNS neuronal subtypes (Richardson & Issa, 1984; Neumann & Woolf, 1999; Leon *et al.*, 2000; Qiu *et al.*, 2002; Monsul *et al.*, 2004). Within adult RGCs, α1, α3, α5, αV, and β1 subunits have been detected in axons (Hernandez, 2000; Vecino *et al.*, 2015). α4, α5, α6, α7 and β1 subunits have been found in both processes of DRGs (Bossy, Bossywetzel, & Reichardt, 1991; Yanagida, Tanaka, & Maruo, 1999; Vogelezang *et al.*, 2001; Schuster *et al.*, 2001; Ekström *et al.*, 2003; Wallquist *et al.*, 2004). Overall, it appears that integrins are present in most axons during embryonic development, but in adulthood they are excluded from many CNS axons but present in retinal and sensory axons. The localisation of integrins in the axonal compartment of adult neurons is summarized in **Table 3**.

Table 2. Integrins localised in the somatodendritic compartment of adult neurons.

Somatodendritic	α3	α5	α7	α8	αV	β1	β3	β8
Cerebellum	10	8			4	3, 10		4
Cortex layer V	6, 10	8		2		10		
Hippocampus	10	8		2	4, 11	1, 9, 10, 12	11	4
Olfactory bulb				2				
RGCs		13					13	
Facial motor neurons			7*			5*, 7*		

Shaded squares indicate that integrin protein levels were detected in the somatodendritic compartment of neurons and they are labelled with the corresponding reference; white squares illustrate that protein expression was not tested or not detected. The asterisk (*) indicates that expression was observed only following axotomy. The integrins, α1, α2, α4, α6, α9, α10, α11, αD, αE, αL, αM, α2b, αX, β2, and β4–β7 are not included because they were not tested or there was no protein detected in the somatodendritic compartment. Dorsal root ganglia are pseudo-unipolar neurons and have therefore been excluded from this somatodendritic compartment analysis. 1, Grooms *et al*. (1993); 2, Einheber *et al*. (1996); 3, Murase & Hiyashi (1996); 4, Nishimura *et al*. (1998); 5, Kloss *et al*. (1999); 6, Rodriguez *et al*. (2000); 7, Werner *et al*. (2000); 8, Bi *et al*. (2001); 9, Schuster *et al*. (2001); 10, Chan *et al*. (2003); 11, Kang *et al*. (2008); 12, Mortillo *et al*. (2012); 13, Vecino *et al*. (2015). RGCs, retinal ganglia cells.

Table 3. Integrins localised in the axonal compartment of adult neurons.

Axon	α1	α3	α4	α5	α6	α7	αV	β1
Cerebellum								1
Cortex layer V				5				
DRGs			7	2	9	4*, 8, 9		2, 4*, 6, 8, 9
RGCs	10	10		10			10	3, 10

Shaded squares indicate that integrin protein levels were detected in the axon compartment of neurons and they are labelled with the corresponding reference; white squares illustrate that protein expression was not tested or not detected. The asterisk (*) indicates that expression was observed only following axotomy. The integrins, α2, α8, α9, α10, α11, αD, αE, αL, αM, α2b, αX, and β2–β8 are not included because these were not tested or there was no protein detected in the axon. Integrins were not detected or analysed in the axonal compartment of the hippocampus and olfactory bulb. We hypothesise that the presence of integrins in the axonal compartment of neurons corresponds with axonal regeneration capacity of the tissue. 1, Murase & Hiyashi (1996); 2, Yanagida *et al*. (1999); 3, Hernandez (2000); 4, Werner *et al*. (2000); 5, King *et al*. (2001); 6, Schuster *et al*. (2001); 7, Vogelezang *et al*. (2001); 8, Ekström *et al*. (2003); 9, Wallquist *et al*. (2004); 10, Vecino *et al*. (2015). DRGs, dorsal root ganglia; RGCs, retinal ganglia cells.

(3) Correlation between integrin localisation and regeneration

The neurons that have been shown to regenerate most readily are also those in which integrins are localised within axons. It is therefore potentially interesting to link the subcellular localisation of integrins to the regenerative ability of the nervous system. As discussed above, DRGs express high levels of integrins in their axons and at least some RGC axons contain integrins (see **Table 3**). Furthermore, it is also known that these neurons have the capacity to regenerate successfully under certain conditions. Mature RGCs project axons through the optic nerve. These cells do not regenerate readily without intervention. However, many groups have demonstrated robust levels of axonal regeneration of RGCs following implantation of a peripheral nerve graft, generation of a lens injury, injection of zymosan (a pro-inflammatory compound), genetic ablation of PTEN or SOCS3, and other interventions (So & Aguayo, 1985; Leon *et al.*, 2000; Yin *et al.*, 2003; Monsul *et al.*, 2004; Park *et al.*, 2008; P. D. Smith *et al.*, 2009b). Likewise, central projections of DRGs readily grow through crushed dorsal roots (Baer, Dawson, & Marshall, 1899), but are prohibited from growing into the spinal cord through the dorsal root entry zone without interventions including implantation of a peripheral nerve graft, a (pre-)conditioning lesion of the sciatic nerve, injection of dibutyryl cyclic AMP, or forced expression of α9 integrin among many others (David & Aguayo, 1981; Richardson & Issa, 1984; Neumann & Woolf, 1999; Qiu *et al.*, 2002; Andrews *et al.*, 2009). We have mentioned above that integrins are localised within the somatodendritic compartments of many cells in the brain (see **Table 2**), but are barely detected in the axons of Purkinje cells or within the corticospinal tract that originates from layer V cortical neurons (see **Table 3**). At the same time adult motor tracts are largely resistant to long-distance regeneration in the mature CNS, presenting a major problem in promoting repair after spinal cord injury (reviewed in Case & Tessier-Lavigne, 2005). Taken together, these data suggest that there is a strong correlation between pathways that have or retain axonal localisation of integrins and those that have the ability (albeit with growth-promoting enhancement) to regenerate over long distances.

(4) Integrins in the somatodendritic compartment

Discussion on the diverse function of integrins in the somatodendritic compartment is beyond the scope of this review but a recent review can be found in Park & Goda, 2016. Furthermore, there is an extensive literature on the role of integrins in dendrites, spines and synapses, including participation in spine dynamics and plasticity (Rohrbough *et al.*, 2000; Shi & Ethell, 2006; McGeachie, Cingolani, & Goda, 2011; Babayan *et al.*, 2012; Levy, Omar, & Koleske, 2014; Heintz, Eva, & Fawcett, 2016).

III. INTEGRINS AND AXONAL REGENERATION IN THE PERIPHERAL NERVOUS SYSTEM

Certain integrins are up-regulated after peripheral nerve injury (Kloss *et al.*, 1999; Werner *et al.*, 2000; Hammarberg *et al.*, 2000; Wallquist *et al.*, 2004; Gardiner *et al.*, 2005; Gonzalez Perez *et al.*, 2016) and can therefore be regarded as regeneration-associated genes (reviewed in Fagoe, van Heest, & Verhaagen, 2014b). After injury of the peripheral nerve, the composition of the ECM changes and collagen, fibronectin and laminin become major components of the basal lamina and the endoneurium of the peripheral nerve stump distal to the lesion (reviewed in Gonzalez Perez, Udina, & Navarro, 2013). Together, this creates an environment that stimulates cell adhesion and axonal regeneration (reviewed in Gardiner, 2011; Jessen, Mirsky, & Arthur-Farraj, 2015). Here, we outline the important role of integrins in promoting axonal regeneration in the injured PNS. Knockout of several integrin subunits have inhibitory effects on peripheral nerve regeneration. It is unclear whether a single knockout will prevent regeneration in the PNS, due to the presence of many integrins in the axons recognizing several ligands.

(1) Laminin-associated integrins

Laminins are secreted by Schwann cells and are a major component of the basal lamina (Wallquist *et al.*, 2002). They consist of α, β and γ chains that form 18 different isoforms (reviewed in Timpl & Brown, 1994; Aumailley *et al.*, 2005; Durbeej, 2010). Many *in vitro* studies have shown that laminin promotes adhesion, migration and regeneration of sensory axons and Schwann cells. The laminin-interacting integrins are α1β1, α2β1, α3β1, α6β1 and α7β1 with each bearing different affinities for the different isoforms of laminin (**Table 4**). The interaction of integrins and laminins was discovered *in vitro* by using function-blocking antibodies as well primary cultures generated from wild type or integrin-knockout mice that were grown on various laminin isoforms.

The high diversity of laminin-associated integrins contributes to the ability of peripheral neurons to grow and regenerate on laminin-rich areas *in vivo*. The laminin-associated integrins α6β1 and α7β1 are up-regulated in various peripheral nerve-injury models (**Table 5**). A causal relationship of laminin-associated integrins promoting regeneration was shown in mice that are deficient in α7, which exhibited reduced facial- (Werner *et al.*, 2000) and sciatic nerve- (Gardiner *et al.*, 2005) regeneration after axotomy. More specifically, depletion of α7 reduced axonal regeneration by 2 millimetres (35%) at 4 days after facial nerve crush and delayed the re-connection of the nerve with the whisker pad compared to wild-type mice (Werner *et al.*, 2000). Gardiner *et al*. (2005) found that fewer axons in α7-

depleted mice regenerated beyond the injury site compared to controls 2 days post-sciatic nerve crush. Another study found that inhibiting α7 and β1 function (using function-blocking antibodies) impaired neurite outgrowth of cultured DRGs following a conditioning lesion *in vivo* (Ekström *et al.*, 2003; Gardiner *et al.*, 2005). Thus, loss of expression or function of laminin-associated integrins results in less-efficient regeneration of peripheral neurons. In addition, the expression of laminin-associated integrins seems to correlate with the regenerative state of neurons. For example, neurons with a poor regenerative capacity including DRGs after a dorsal root injury (Wallquist *et al.*, 2004), red nucleus neurons (Plantman *et al.*, 2005), pyramidal cells and septal neurons (Werner *et al.*, 2000) have unaltered integrin expression after axotomy.

Table 4. Laminin-associated integrins with their laminin ligands.

Integrin receptor	Laminin isoform	References
α1β1	LN-111	Condic, 2001; Desban *et al.*, 2006
	LN-211/221	Colognato *et al.*, 1997
	LN-511	Desban *et al.*, 2006
	LN-521	Desban *et al.*, 2006
α2β1	LN-111	Colognato *et al.*, 1997
	LN-211/221	Colognato *et al.*, 1997
α3β1	LN-111	Ivins *et al.*, 1998; Plantman *et al.*, 2008
	LN-211/221	Tomaselli *et al.*, 1993; Plantman *et al.*, 2008
	LN-332	Gout *et al.*, 2001; Mechai *et al.*, 2005; B. E. Smith *et al.*, 2009a
	LN-511	Kikkawa, Sanzen, & Sekiguchi, 1998; Eble *et al.*, 1998
	LN-521	Kikkawa *et al.*, 1998
α6β1	LN-111	Condic & Letourneau, 1997; Ivins *et al.*, 1998; Schöber *et al.*, 2000
	LN-211/221	Delwel *et al.*, 1994
	LN-332	Gout *et al.*, 2001
	LN-411	Geberhiwot *et al.*, 1999; Plantman *et al.*, 2008
	LN-511	Plantman *et al.*, 2008
α7β1	LN-111	Schöber *et al.*, 2000; Gardiner *et al.*, 2005; Plantman *et al.*, 2008
	LN-211/221	Schöber *et al.*, 2000; Plantman *et al.*, 2008

The laminin (LN) isoforms are shown according to current laminin nomenclature (Aumailley *et al.*, 2005). The isoforms LN-211 and LN-221 were assumed to be identical in the above studies and are therefore labelled LN-211/221

Table 5. Summary of studies that assessed the expression of laminin-associated integrins after peripheral nerve

Integrin	Injury model	Main finding regarding integrin expression	References
α6β1	Ventral root avulsion	Up-regulation of mRNA until 42 days after injury (2.5-fold increase at 7 days post-injury)	Hammarberg *et al.*, 2000
	Sciatic nerve transection	Up-regulation of mRNA until 42 days after injury (2.5-fold increase at 7 days post-injury)	Hammarberg *et al.*, 2000
	Sciatic nerve transection	Up-regulation of mRNA until 14 days after injury (3.0-fold increase at 3 days post-injury)	Wallquist *et al.*, 2004
	Sciatic nerve crush	Protein present in regenerating axons at 3 days after injury	Wallquist *et al.*, 2004
α7β1	Ventral root avulsion	Up-regulation of mRNA until 42 days after injury (6.0-fold increase at 3 days post-injury)	Hammarberg *et al.*, 2000
	Facial nerve transection	Upregulation of protein until 42 days after injury (6.0 fold increase at 7 days-post injury)	Werner *et al.*, 2000
	Sciatic nerve transection	Up-regulation of protein at 4 days after injury (quantification was not performed)	Werner *et al.*, 2000
	Sciatic nerve transection	Up-regulation of mRNA at least 42 days after injury (9-fold increase at 14 and 21 days post-injury)	Hammarberg *et al.*, 2000
	Sciatic nerve transection	Up-regulation of mRNA until 14 days after injury (3.0-fold increase at 3 days post-injury)	Wallquist *et al.*, 2004
	Sciatic nerve transection	Up-regulation of mRNA at 2 days after injury (2.5-fold increase)	Gonzalez Perez *et al.*, 2016
	Sciatic nerve crush	Protein present in regenerating axons at 3 days after injury	Wallquist *et al.*, 2004
	Sciatic nerve crush	Up-regulation of protein for at least 14 days in medium- to large-diameter (NF200 positive) dorsal root ganglion neurons and to a lesser extent in smaller peptidergic neurons. No expression in smaller non-peptidergic neurons	Gardiner *et al.*, 2005

(2) Fibronectin-associated integrins

Fibronectin is another important component of the ECM that stimulates the pro-regenerative state of PNS neurons. Fibronectin is a large glycoprotein that consists of two subunits which form a dimer (reviewed in Singh, Carraher, & Schwarzbauer, 2010; Schwarzbauer & DeSimone, 2011). Fibronectin is secreted mainly by fibroblasts (Zhu *et al.*, 2015) but also by astrocytes and Schwann cells (Baron-Van Evercooren *et al.*, 1986; Egan & Vijayan, 1991; Tom *et al.*, 2004a). Fibronectin is enriched in the injured PNS and contributes to an environment that is permissive for integrin-mediated adhesion and regeneration. Integrins bind to fibronectin *via* an Arg-Gly-Asp (RGD) domain, which is also found on other matrix molecules such as tenascin-C and some laminins.

Fibronectin-associated integrins in adult neurons include α4β1, α5β1, α8β1 and αV integrins. α4β1 binds to fibronectin, however its main role is as a thrombospondin and osteopontin receptor and as a VCAM receptor in inflammatory cells. α4β1 and α5β1 integrins are expressed at high levels in native DRG neurons and growth cones of regenerating neurons (Lefcort *et al.*, 1992; Mathews & ffrench-Constant, 1995; Yanagida *et al.*, 1999; Vogelezang *et al.*, 2001; Hu & Strittmatter, 2008; Saunders *et al.*, 2014). Several studies have shown that the expression of fibronectin-associated integrins is enhanced acutely after injury. α5β1 mRNA expression levels were shown to double in DRGs and spinal cord at 2 days post-sciatic nerve transection (Gonzalez Perez *et al.*, 2016), but were found to remain unaltered 7 days post-sciatic nerve crush (Gardiner *et al.*, 2007). At longer time points after injury, a few studies suggest that there are changes in the localisation of integrins. For instance, the localisation of α5β1 was targeted towards the growth cones favouring neurite elongation of cultured preconditioned DRG neurons (Gardiner *et al.*, 2007). Consistently, α4β1 has been detected at the growth cones *in vivo* while expression levels were unaltered at 4 days after a sciatic nerve injury (Vogelezang *et al.*, 2001).

The pro-regenerative phenotype of fibronectin-associated integrins has been investigated *in vitro*. PC12 cells, that grow poorly on fibronectin, were shown to express α5β1 at low levels and α4β1 not at all (Tomaselli, Damsky, & Reichardt, 1987; Vogelezang *et al.*, 2001). However, cells engineered to express α4β1 showed a 2.5-fold increase in outgrowth on fibronectin compared to controls, indicating that α4β1 expression promotes neurite growth on fibronectin (Vogelezang *et al.*, 2001; 2007). The regenerating effects of α5β1 on a fibronectin substrate was first shown when it was overexpressed *in vitro* in adult DRGs that had a roughly threefold increase in neurite count and length on fibronectin compared to controls (Condic, 2001). Taken together, both α4β1 and α5β1 enhance neurite outgrowth on fibronectin *in vitro*. There are no reports on axonal regeneration experiments in transgenic

mice that lack α4 or α5 because these animals are not viable (Yang, Rayburn, & Hynes, 1993; 1995).

(3) Collagen-associated integrins

Collagen is another ECM molecule that is highly up-regulated after peripheral nerve injury and is synthesised by Schwann cells and fibroblasts (reviewed in Koopmans, Hasse, & Sinis, 2009). The high amount of collagen at the injury site could indicate an important role for axonal integrins that interact with collagen. The collagen-associated integrins expressed by neurons are α1β1 (Ivins, Yurchenco, & Lander, 2000; Vecino *et al.*, 2015), α2β1 (Bradshaw *et al.*, 1995; Emsley *et al.*, 2000; Khalsa *et al.*, 2000), and αVβ8 (Venstrom & Reichardt, 1995; Nishimura *et al.*, 1998). α10β1 and α11β1, two other collagen-associated integrins, are not expressed in the nervous system. The neuronal collagen-associated integrins have been shown to contribute to neurite outgrowth on collagen in cell cultures (Bradshaw *et al.*, 1995; Venstrom *et al.*, 1995; Ivins *et al.*, 2000; Vecino *et al.*, 2015). However, to our knowledge, there are no reports on manipulation of collagen-associated integrins after injury *in vivo*. It would therefore be interesting to explore whether activation or overexpression of the collagen-associated integrins is beneficial for regeneration in the PNS.

In summary, peripheral nerve injury leads to an up-regulation of many ECM molecules including laminin, fibronectin and collagen. Neurons in the PNS express many of the integrins that respond to this post-injury ECM environment, which contributes to the spontaneous regeneration observed after peripheral nerve injury. Thus, studies in the PNS have shown that matching the ECM environment with the appropriate integrin expression pattern promotes axonal regeneration of mature neurons. It is therefore reasonable to try the same approach in the CNS and promote regeneration *via* integrin overexpression.

IV. INTEGRINS THAT BIND TO TENASCIN-C PROMOTE AXONAL REGENERATION IN THE CENTRAL NERVOUS SYSTEM

(1) Tenascin-C-associated integrins

Tenascin-C is a ligand for integrins (reviewed in Tucker & Chiquet-Ehrismann, 2015) and is predominantly expressed in the CNS during development. However, injury results in a steep up-regulation of this ECM glycoprotein by reactive astrocytes (reviewed in Silver & Miller, 2004; Gervasi, Kwok, & Fawcett, 2008; Wiese, Karus, & Faissner, 2012). Tenascin-C is enriched within and surrounding the glial scar after spinal cord injury (Zhang *et al.*, 1997; Tang, Davies, & Davies, 2003; Andrews *et al.*, 2009), and it is expressed at the dorsal root entry zone after a dorsal root injury (Andrews *et al.*, 2009; Cheah *et al.*, 2016). Tenascin-C is expressed not only by astrocytes but also by fibroblasts and spinal neurons among others (Zhang *et al.*, 1995a; 1997; Tang *et al.*, 2003; Zhang *et al.*, 2015). Thus, tenascin-C is enriched at the site of injury which regenerating axons have to penetrate in order to reconnect to their target tissue. Therefore, tenascin-C is a promising target to promote axonal regeneration after CNS trauma.

The tenascin-C-associated integrins include α2β1 (Sriramarao, Mendler, & Bourdon, 1993; Schaff *et al.*, 2011), α7β1 (Mercado *et al.*, 2004), α8β1 (Schnapp *et al.*, 1995; Varnum-Finney *et al.*, 1995; Denda, Reichardt, & Müller, 1998) and α9β1 (Yokosaki *et al.*, 1994; 1998). They are expressed in developing neurons and most of them recognise the fibronectin type 3 repeat domain of tenascin-C through its RGD attachment site. α9β1 is an exception as it recognises a different sequence in this domain, AEIDGIEL (Yokosaki *et al.*, 1998). Tenascin-C-associated integrins have been shown to be required for neurite outgrowth, as assessed in experiments with function-blocking antibodies *in vitro* (Varnum-Finney *et al.*, 1995; Mercado *et al.*, 2004; Andrews *et al.*, 2009). Providing that neurons express an appropriate integrin, tenascin-C is a substrate that favours neurite outgrowth and axonal regeneration (Götz *et al.*, 1996; Rigato *et al.*, 2002; Chen *et al.*, 2009; Liu *et al.*, 2010; Yu *et al.*, 2011), but for neurons lacking the appropriate receptors tenascin-C is inhibitory (reviewed in Faissner, 1997). Adult CNS neurons do not express tenascin-C-binding integrins within their axons, even after injury (Pinkstaff *et al.*, 1999; Andrews *et al.*, 2009). Although glial cell types retain the ability to interact with tenascin-C, it is anti-adhesive to most adult neurons due to their lack of expression of tenascin-C-binding integrins (Zhang *et al.*, 1995b; Golding *et al.*, 1999). Thus, up-regulation of tenascin-C results in an anti-adhesive and growth-inhibiting environment for neurons in the CNS. In the next section, we will discuss experiments that show that tenascin-C is only an axon-regeneration ligand in the

injured adult CNS when neurons are engineered to express an appropriate integrin, such as α9β1.

(2) Viral vector-mediated delivery of α9 integrin in dorsal root ganglia promotes sensory axon regeneration in the central nervous system

We hypothesized that low or absent integrin expression in CNS axons (see **Table 3**) contributes to the poor regenerative capacity of most CNS neurons. To achieve regeneration in the CNS, expression of tenascin-C-binding integrins in neurons might provide a promising tool to overcome the tenascin-C-rich injury site. Viral vector-mediated delivery of α9 into DRGs results in integrin localisation in the axon and could therefore induce integrin-mediated axonal regeneration (Andrews *et al.*, 2009; Cheah *et al.*, 2016; Andrews *et al.*, 2016). Indeed, exogenous expression of α9 allowed cultured adult DRGs to extend neurites on tenascin-C substrates *in vitro*, while neurite outgrowth was largely absent in controls (Andrews *et al.*, 2009). Furthermore, *in vivo* reintroduction of α9 in DRGs improved sensory axonal regeneration into tenascin-C-rich regions after a dorsal root injury or dorsal column crush lesion (Andrews *et al.*, 2009). However, regeneration was limited to the lesion site; there was no axonal growth extending beyond the lesion. Nevertheless, this was enough to result in limited sensory recovery (Andrews *et al.*, 2009). These results demonstrate that tenascin-C-associated integrins such as α9β1 are a viable target to promote axonal regeneration in the CNS. However, this approach should be combined with additional factors, such as integrin activators, to promote long-distance regeneration as well as functional recovery *in vivo*. Section V will demonstrate that integrins become inactivated by stimuli of the extracellular environment, and thus methods that target the activation of the receptor (discussed in Section VI) could enhance axonal regeneration (discussed in Section VI.*c.iii*).

V. INTEGRINS BECOME INACTIVATED AT THE LESION SITE AFTER CENTRAL NERVOUS SYSTEM INJURY

Axon-repulsive molecules at the injury site, such as chondroitin sulphate proteoglycans (CSPGs) (reviewed in Kwok *et al.*, 2011), myelin-derived molecules (reviewed in Schweigreiter & Bandtlow, 2006; Alizadeh, Dyck, & Karimi-Abdolrezaee, 2015; Boghdadi, Teo, & Bourne, 2017) and classical repulsive axon-guidance molecules (reviewed in de Wit & Verhaagen, 2003; Giger, Hollis, & Tuszynski, 2010; Hollis, 2015) have a broad range of functions. Here we highlight that most axon-repulsive molecules initiate inactivation of integrins (see **Fig. 2**).

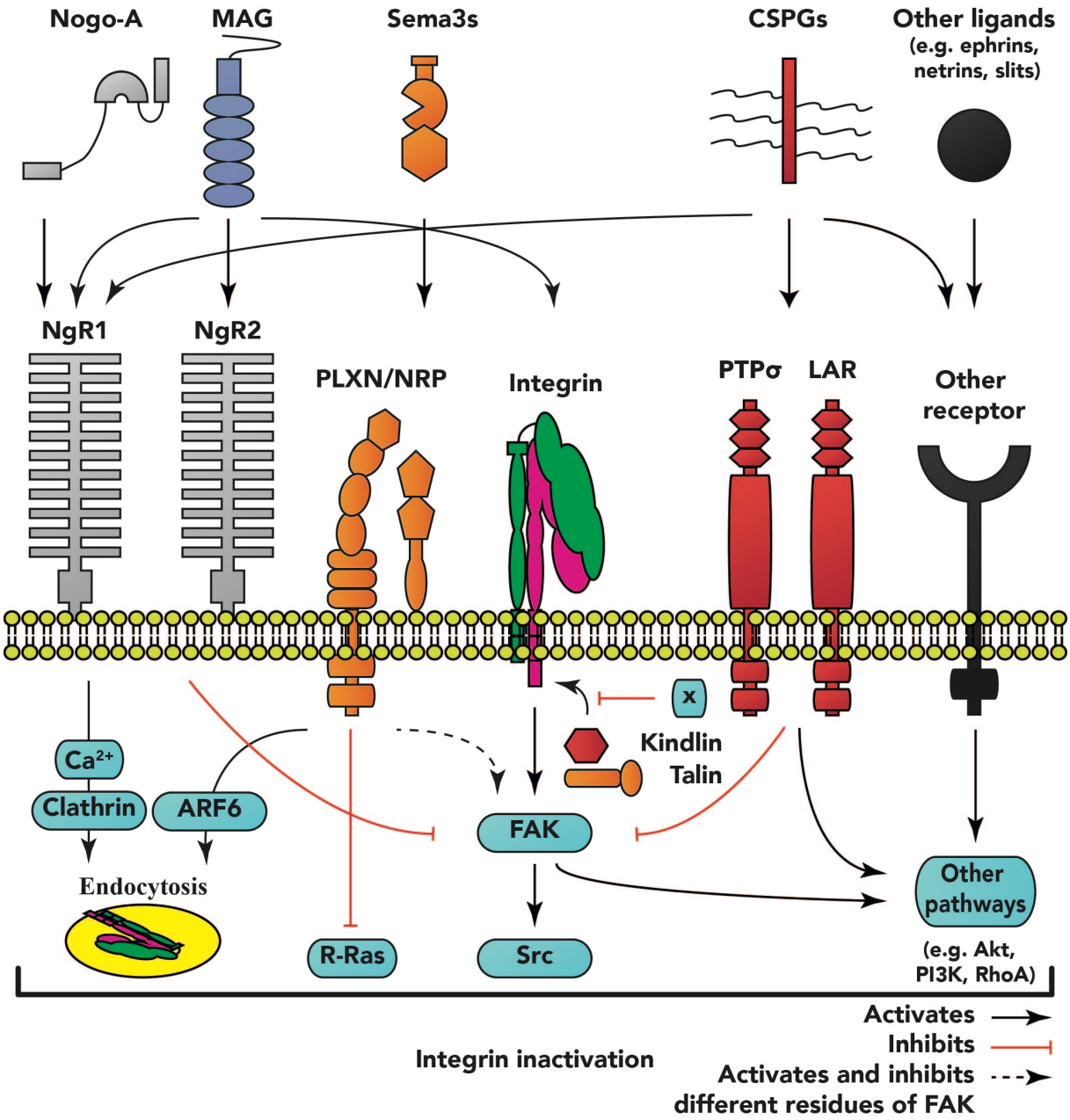

Fig. 2. Molecular mechanisms of integrin inactivation after trauma in the nervous system. Integrins at the growth cones of regenerating axons are exposed to the extracellular environment of the lesion site. Integrins recruit focal adhesion kinases (FAKs) among others, which in turn, activate downstream signalling molecules such as protein kinase B (Akt3), phosphoinositide 3-kinase (PI3K), Ras homolog gene family member A (RhoA), and Src kinase. However, most integrins exist in a bent, inactive state at the cell surface. The lesion site is rich in axon-repulsive molecules, including Nogo-A, myelin-associated glycoprotein (MAG), class III semaphorins (Sema3s), and chondroitin sulphate proteoglycans (CSPGs). These molecules bind to several receptors, such as leukocyte common antigen-related phosphatase (LAR), Nogo receptors (NgR1, NgR2), the plexin/neuropilin (PLXN/NRP) complex and protein tyrosine phosphatase σ (PTPσ), to suppress integrin signalling and axon regeneration. Nogo-A binds to NgR1 and inhibits the phosphorylation of FAK. MAG is a direct ligand for integrins and stimulates integrin signalling. However, MAG also has an opposing effect by NgRs signalling that indirectly elevates intracellular calcium levels and stimulates clathrin-mediated endocytosis of integrins. Most Sema3s mediate signalling *via* the PLXN/NRP receptor complex that results in inactivation of

R-Ras, which in turn interferes with integrin signalling, and activates ADP-ribosylation factor 6 (ARF6) to remove integrins from the cell surface. Sema3A signalling results in the phosphorylation (Tyr397, Tyr576, Tyr577, Tyr925) and de-phosphorylation (Tyr407, Tyr861) of different residues of FAK for Sema3A-mediated axonal remodelling. CSPGs interact with many receptors, including LAR, NgR1 and PTPσ. The CSPG aggrecan has been shown to reduce FAK signalling, but the exact mechanisms remain to be identified. Other ligands such as ephrins, netrins and slits are also known to interfere with integrin signalling. In addition, there is evidence that integrin activation by kindlins and talins is inhibited by various regulatory mechanisms (illustrated as x).

(1) Nogo-A

Nogo-A is a myelin-derived axon repulsive molecule that restricts axonal regeneration after CNS injury (Schnell & Schwab, 1990; Bregman *et al.*, 1995; Brösamle *et al.*, 2000; Kim *et al.*, 2003; Simonen *et al.*, 2003; Zheng *et al.*, 2003; Sicotte *et al.*, 2003; Dimou *et al.*, 2006; Cafferty & Strittmatter, 2006; Lee *et al.*, 2010b; J.-W. Wang *et al.*, 2015a). Nogo receptor 1 (NgR1) is a GPI-linked molecule, and was the first receptor identified for Nogo proteins (Fournier, GrandPre, & Strittmatter, 2001). NgR1 has been shown to transduce Nogo signalling across the plasma membrane by interacting with several other receptors such as Lingo-1, p75, and Troy (Wang *et al.*, 2002; Mi *et al.*, 2004; Park *et al.*, 2005; Shao *et al.*, 2005). Interestingly, Nogo-A has been shown to suppress integrin signalling through integrin inactivation *in vitro* (Hu & Strittmatter, 2008; Tan *et al.*, 2011) and *in vivo* (Huo *et al.*, 2015). Specifically, it has been shown in cell lines that Nogo-A interferes with the function of fibronectin-associated integrins α4β1, α5β1 and αVβ3, but not laminin-associated integrin α6β1 (Hu & Strittmatter, 2008). Nogo-A's attenuation of DRGs neurite outgrowth *in vitro* has been consistently greater on fibronectin than on laminin (Hu & Strittmatter, 2008). Further, it has been shown *in vivo* after an optic nerve crush that Nogo-A down-regulates the expression of αV integrins and thereby reduces integrin signalling, in this case the phosphorylation of FAK (Huo *et al.*, 2015). The same study showed that the expression of another fibronectin-associated integrin, α5, was unaltered by Nogo-A in the injured optic nerve suggesting that Nogo-A has varied effects on different fibronectin-associated integrins, perhaps dependent on the function of the integrin. Taken together, both studies suggest that Nogo-A inhibits specific integrin signalling by inactivation and internalisation (Hu & Strittmatter, 2008; Huo *et al.*, 2015). However, the mechanisms that dictate the interaction between Nogo proteins and integrins require further investigation.

(2) Myelin-associated-glycoprotein

Myelin-associated-glycoprotein (MAG) is another myelin-derived axon-repulsive molecule (Mukhopadhyay *et al.*, 1994; McKerracher *et al.*, 1994; Schäfer *et al.*, 1996). MAG binds to NgR1 (Domeniconi *et al.*, 2002; Wang *et al.*, 2002; Liu *et al.*, 2002; Laurén *et al.*, 2007) and NgR2 (Venkatesh *et al.*, 2005) and many other neuronal receptors (Wong *et al.*, 2002; Atwal *et al.*, 2008; Stiles *et al.*, 2013). It has been known for more than two decades that MAG antagonises integrin signalling and function (Bachmann *et al.*, 1995). More recently, the underlying mechanism became clearer when it was shown that MAG is axon repulsive in cultured postnatal hippocampal neurons and cerebellar granule cells by modulating integrin-signalling independently of NgRs (Goh *et al.*, 2008). This study found that β1 integrin is a direct receptor of MAG and led to increased phosphorylation of FAK. This result is unexpected since FAK signalling is associated with axonal growth. It may therefore be that the signalling is only locally affected and shifts to sites of axon attraction at the growth cone, where new integrin adhesion complexes form to initiate axon guidance. This asymmetrical signalling hypothesis is supported by a study that showed that a local MAG gradient removed integrins at the site of the MAG source only, while untreated neurons had a symmetric distribution of integrins at the growth cone (Hines, Abu-Rub, & Henley, 2010). MAG signalling has also been shown to initiate changes in intracellular Ca^{2+}, thereby inducing clathrin-mediated endocytosis of integrins from the growth cones of *Xenopus laevis* spinal neurons (Hines *et al.*, 2010). Taken together, MAG mediates its axon-repulsive effects by modulating integrin signalling, partly through direct interaction and partly through another signalling complex most likely including NgRs that cause Ca^{2+}-dependent internalisation of integrins.

(3) Aggrecan

Aggrecan is one of the CSPGs produced by neurons and astrocytes, and it is present in the scar tissue that restricts axonal regeneration (Lemons *et al.*, 2003; reviewed in Silver & Miller, 2004). Not surprisingly, adult DRG neurons have restricted neurite outgrowth when cultured on substrates that contain the glycan chains of CSPGs (Tom *et al.*, 2004b; Steinmetz *et al.*, 2005). Aggrecan has been shown to cause a temporary but rapid decrease in integrin-mediated phosphorylation of FAK, and a long-term decrease of Src phosphorylation which is downstream of FAK, leading to inhibition of DRG neurite outgrowth (Tan *et al.*, 2011). The molecular mechanism of how aggrecan inhibits integrin signalling is currently unknown. However, it is known that aggrecan does not affect the number of integrin receptors at the plasma membrane (Tan *et al.*, 2011). Thus, it interferes with integrin signalling independent

of receptor endocytosis. It may interfere indirectly with integrin signalling *via* activation of CSPG receptors such as protein tyrosine phosphatase σ (PTPσ) (Shen *et al.*, 2009; Fry *et al.*, 2010), leukocyte common antigen-related phosphatase (LAR) (Fisher *et al.*, 2011; Xu *et al.*, 2015) or the Nogo receptors NgR1 and NgR3 (Dickendesher *et al.*, 2012).

(4) Class III semaphorins

Class III semaphorins (Sema3s) are classical axon-guidance molecules that are mainly produced by migrating fibroblasts, pericytes and vascular cells in the core of the scar (Pasterkamp, Giger, & Verhaagen, 1998; Pasterkamp *et al.*, 1999; de Winter *et al.*, 2002; Tannemaat *et al.*, 2007; Mire *et al.*, 2008; Minor *et al.*, 2011). It has been shown that Sema3s restrict axonal regeneration after spinal cord injury (Kaneko *et al.*, 2006; Mire *et al.*, 2008; Lee *et al.*, 2010a; Minor *et al.*, 2011; reviewed in Mecollari, Nieuwenhuis, & Verhaagen, 2014). Most Sema3s interact with neuropilins (NRPs), while signal transduction is mediated *via* the plexin (PLXN) co-receptor (reviewed in Sharma, Verhaagen, & Harvey, 2012). The pleiotropic NRPs have also been shown to interact with integrins (Fukasawa, Matsushita, & Korc, 2007; Valdembri *et al.*, 2009) which could suggest that Sema3s affect integrin signalling *via* NRPs. Nonetheless, it has been shown that PLXN signalling leads to rapid disassembly of integrin adhesion at the cell surface and causes actin depolymerisation in various non-neuronal cell lines (Barberis *et al.*, 2004). It has been observed in cultured cortical- and hippocampal neurons that Sema3A-induced collapse of growth cones requires FAK signalling downstream of integrins (Bechara *et al.*, 2008; Chacón, Fernández, & Rico, 2010). More specifically, Sema3A resulted in the phosphorylation (Tyr397, Tyr576, Tyr577, Tyr925) and de-phosphorylation (Tyr407, Tyr861) of different residues of FAK, confirming the central signalling role of this kinase, and this may result in the activation and inhibition of several signalling pathways to induce growth-cone collapse (Chacón *et al.*, 2010). The strongest evidence that Sema3s regulate the activation of integrins originates from studies of angiogenesis. Sema3s, except for Sema3C, inhibit integrin signalling in blood vessels (**Table 6**). Sakurai *et al.*, 2010 highlighted two mechanisms by which Sema3E signalling *via* PLXN reduces the function of integrins in endothelial cells: (1) activation of endosomes that contain ADP-ribosylation factor 6 (ARF6) removes integrins from the cell surface; and (2) inactivation of R-Ras GTPases, which normally activate integrins (Zhang *et al.*, 1996; Keely *et al.*, 1999; Wang *et al.*, 2000; Ivins *et al.*, 2000; Self *et al.*, 2001) *via* the phosphoinositide 3-kinase (PI3K) signalling pathway (Berrier *et al.*, 2000; Oinuma *et al.*, 2010). Sema3s could exert the same and other integrin-mediated mechanisms in neurons resulting in axon repulsion after CNS injuries.

Table 6. Summary of studies in the field of angiogenesis that show that class III semaphorins (Sema3s) modulate integrins.

Sema3s	Main finding regarding integrins after Sema3 overexpression	References
Sema3A	Inhibiting the signalling of αIIbβ3 *in vitro*	Kashiwagi *et al.*, 2005
	Inhibiting the activation of β1 *via* NRP1/PLXN *in vivo*	Serini *et al.*, 2003
Sema3C	Phosphorylation of β1, but not FAK, *via* NRP/PLXN *in vitro*	Banu *et al.*, 2006
Sema3E	Inhibiting the activation of integrins by inactivation of R-Ras *in vitro*	Sakurai *et al.*, 2010
	Endocytosis of integrins by activation of ARF6-postive vesicles *in vitro*	
Sema3F	Inhibiting the activation of β1 *via* NRP1/PLXN *in vivo*	Serini *et al.*, 2003

ARF6, ADP-ribosylation factor 6; FAK, focal adhesion kinase; NRP, neuropilin; PLXN, plexin; R-Ras, Ras-related protein R-Ras.

Taken together, a variety of molecules in the scar and lesion milieu have the ability to regulate integrin function (**Fig. 2**). These molecules affect integrin binding to their ECM ligands and thereby subsequent downstream signalling as well as integrin levels at the cell surface by endocytosis. Integrins are not the only receptors and ligands affecting growth and regeneration. There are other signalling cascades that feed positively or negatively into integrin downstream signalling. For instance, molecules such as Akt, RhoA and PI3K are regulated by many receptors. Finally, another level of control is the pathways that influence integrin activation through kindlins and talin. Studying integrin inhibition has revealed integrin-specific and general mechanisms whereby axonal regeneration fails in adult CNS neurons. Inactivation of integrins in the injured spinal cord also explains the modest axonal regeneration that was observed after forced expression of α9 *in vivo* (Andrews *et al.*, 2009). Expression of an appropriate integrin and overcoming integrin inactivation could therefore be a general approach to promote axonal regeneration in the CNS.

VI. INTEGRIN ACTIVATORS PROMOTE SENSORY AXONAL REGENERATION IN THE SPINAL CORD

Integrins need to be in their active state to interact with components of the ECM and thereby induce an increase in neurite outgrowth and axonal regeneration. Once activated they stimulate FAK and other downstream signalling molecules that are essential for growth cone dynamics and axonal guidance (Robles & Gomez, 2006; reviewed in Mitra, Hanson, & Schlaepfer, 2005). Here we discuss the best-characterised integrin activators with regard to axonal regeneration (see **Fig. 3**).

(1) Manganese

Manganese (Mn^{2+}) is widely used in *in vitro* experiments to enhance the ligand-binding affinity of integrins to the ECM. Divalent cations such as Ca^{2+} and Mn^{2+} interact with metal-ion binding sites of the α integrin subunit and facilitate integrin signalling (Mould, Akiyama, & Humphries, 1995; Oxvig & Springer, 1998). This 'outside-in' activation of integrins by Mn^{2+} has been shown to increase neurite outgrowth in various neuronal cell culture assays (Ivins *et al.*, 2000; Lein *et al.*, 2000; Lemons & Condic, 2006; Tan *et al.*, 2011). Importantly, activation of integrins has been shown to reverse the growth-inhibitory effects of Nogo-A and aggrecan in cultured DRG neurons (Tan *et al.*, 2011). Recently, Mn^{2+} has also been shown to abolish ephrinA3-mediated collapse of proximal dendritic spines in Purkinje cells *via* integrin activation *in vitro* (Heintz *et al.*, 2016). Thus, it is possible to reverse integrin inactivation with Mn^{2+} treatment *in vitro*. However, Mn^{2+} is not suitable for *in vivo* studies because excess and long-term exposure to Mn^{2+} causes neuronal toxicity (reviewed in Guilarte, 2013).

(2) Integrin-activating antibodies

Another classic approach to activate integrins is using antibodies that bind selectively to the ligand-binding region of activated β1 integrin, which can be used both for detecting activated integrins and for maintaining them in the activated state (Takada & Puzon, 1993; Takagi *et al.*, 1997); these antibodies are mostly effective on human integrins. The anti-β1-activating monoclonal antibody TS2/16 interacts with all human integrin heterodimers that contain β1 and less strongly with rodent β1, regardless of the α subunit (Tsuchida *et al.*, 1997). Due to the wide spectrum of integrins that can be targeted, the antibody TS2/16 is particularly interesting and has been used in outgrowth assays. For example, TS2/16-mediated activation of integrins has been shown to reverse the inhibitory effects of Nogo-A on a human T-lymphocyte cell line grown on fibronectin (Hu & Strittmatter, 2008) as well as to inhibit

the effects of aggrecan on axon growth of motor neurons that were derived from human embryonic stem cells (Tan *et al.*, 2011). Thus, the TS2/16 antibody reverses axon-repulsive effects of molecules such as Nogo-A and aggrecan. However, a limitation of applying integrin antibodies is that these need frequent or continuous delivery *in vivo*. In addition, masking of epitopes due to integrin interactions with ECM ligands can reduce the efficiency of integrin-binding antibodies (Mould *et al.*, 2016).

(3) Intracellular proteins

The kindlins and talins are two families of intracellular proteins that bind to the cytoplasmic tail of β integrins and activate the heterodimeric receptor. Integrin activation is ubiquitous throughout the body, but the exact mechanism of the 'inside-out' activation by kindlin and talin is subject to intense debate (reviewed in Moser *et al.*, 2009b; Shattil, Kim, & Ginsberg, 2010; Campbell & Humphries, 2011; Calderwood *et al.*, 2013; Eva & Fawcett, 2014). Despite the limited number of studies investigating the role of these molecules in the nervous system, they have been utilised to enhance integrin-ligand binding and axonal outgrowth of neurons (Tan *et al.*, 2012; 2015; Dingyu *et al.*, 2015; Cheah *et al.*, 2016) as discussed below.

(*a*) *Talins*

Talin isoforms 1 and 2 are expressed in the nervous system (Monkley, Pritchard, & Critchley, 2001; Senetar, Moncman, & McCann, 2007; Debrand *et al.*, 2009; Tan *et al.*, 2015). In nerve growth factor-stimulated PC12 cells, overexpression of the full-length and constitutively activated isoforms of talin has been shown to promote neurite outgrowth in the presence of the repulsive extracellular matrix protein aggrecan (Tan *et al.*, 2015). Dingyu *et al*. (2015) examined the structural tensions of the cytoskeleton in this cell line by fluorescence resonance energy transfer (FRET) imaging and application of genetically encoded optical force probes. They found that CSPGs including aggrecan reduce intracellular structural forces and that overexpression of full-length talin rescued these tensions. In addition, talin decreased the phosphorylation of ROCK1 and increased the activation of ERK and FAK proteins (Dingyu *et al.*, 2015). Based on these results *in vitro*, full-length talin could be a valuable activator of integrins to reverse the effects of the axon-repulsive molecules that are present in the injured spinal cord. However, the large size of the full-length protein presents a challenge for talin expression in neurons. In studies using primary cultures of DRG neurons, only the talin head domain has been overexpressed (Tan *et al.*, 2015). The talin-head domain is required to interact with the cytoplasmic tail of the β integrin subunit and to activate the

heterodimeric receptor (García-Alvarez *et al.*, 2003; Tadokoro *et al.*, 2003; Wegener *et al.*, 2007). However, the talin head domain alone acted as a dominant negative for endogenous talin, and DRG neurite outgrowth on laminin and on aggrecan-laminin substrates was reduced (Tan *et al.*, 2015). Based on these results, the talin head domain alone is not suitable to promote integrin signalling. The limited effect of the talin head is possibly due to the endogenous expression of full-length talins in neurons or because the rod domain is required to link integrins directly with the cytoskeleton. Another disadvantage of talin-targeted experiments and therapeutics is the fact that full-length talins are so large that they are not suitable for an adeno-associated viral vector (AAV)-based gene-delivery approach. The coding sequence for talin is roughly 7500 base pairs, which exceeds the AAV packaging limit of approximately 4700 base pairs. Taken together, talin overexpression would be a promising target to enhance axonal regeneration since it enables integrin signalling directly to the cytoskeleton but is not feasible with the AAV technologies currently available. Talin itself is subject to several regulatory influences, which in turn affect integrin activation and function (reviewed in Ye *et al.*, 2014).

(*b*) *Kindlins*

There are three isoforms of kindlin: kindlin-1, kindlin-2 and kindlin-3. Localisation of the kindlin isoforms in the nervous system is described here. Kindlin-1 is not expressed by cells of the nervous system (Ussar *et al.*, 2006; Tan *et al.*, 2012), but is primarily found in epithelial cells (Lai-Cheong *et al.*, 2008; Ussar *et al.*, 2008). Kindlin-2 is ubiquitously expressed throughout the body (Ussar *et al.*, 2006) and *in situ* hybridisation and RT-PCR studies on whole-brain lysate demonstrated that kindlin-2 mRNA is present in the brain, while kindlin-1 and kindlin-3 were not detected (Ussar *et al.*, 2006; Tan *et al.*, 2012). Immunochemistry on cultured cells confirmed that this isoform is expressed by neurons including DRGs, RGCs, and hippocampal and Purkinje neurons (Tan *et al.*, 2012). In these cultures, kindlin-2 was also found in non-neuronal cells like astrocytes, fibroblasts and Schwann cells (Tan *et al.*, 2012). The latter study demonstrated by short hairpin RNA knockdown that kindlin-2 is required for integrin signalling and axonal growth of neurons. Thus, kindlin-2 is the only isoform endogenously expressed in neurons and plays a role in normal axonal growth. Kindlin-3 is predominantly expressed by cells of the immune system (Malinin *et al.*, 2009; Moser *et al.*, 2009a; Feigelson *et al.*, 2011; Cohen *et al.*, 2013; Moretti *et al.*, 2013) and recently has been discovered in microglia of the brain (Meller *et al.*, 2017).

Kindlin-1 has been used *in vivo* to promote integrin activation and sensory axonal regeneration in rats. Forced expression of kindlin-1 (but not the overexpression of the endogenously present kindlin-2) enhanced the signalling of the integrins that are expressed by DRG neurons. Importantly, kindlin-1 promoted neurite outgrowth on the axon-repulsive substrates aggrecan and Nogo-A (Tan *et al.*, 2012). Furthermore, kindlin-1 counteracted the inhibiting effects of aggrecan on neurite outgrowth of α9 integrin-transfected DRG neurons *in vitro* (Cheah *et al.*, 2016). In accordance with the enhanced outgrowth, the decreased phosphorylation of FAK induced by repulsive substrates was reversed by kindlin-1 (Tan *et al.*, 2012; Cheah *et al.*, 2016). Thus, kindlin-1 overcomes aggrecan- and Nogo-A-mediated inhibition of integrin signalling and restores DRG neurite outgrowth *in vitro*. Furthermore, after a dorsal root crush injury *in vivo*, forced expression of kindlin-1 in the DRG enhanced sensory axonal regeneration. In this study, kindlin-1 treatment using viral vectors resulted in a fairly large number of axons extending towards the spinal cord, while the regenerating axons of the control animals did not pass the axon-repulsive dorsal root entry-zone boundary. Consistent with the improved sensory axonal regeneration, kindlin-1 treatment also improved recovery of thermal sensation after injury (Tan *et al.*, 2012). Thus, kindlin-1 activates integrins that are expressed by DRG neurons and overcomes the inactivation of the axon-repulsive environment to promote sensory axonal regeneration. In other words, kindlin-1 overexpression renders integrins less vulnerable to integrin inactivation and thereby restriction of axonal regeneration. Kindlins are subject to regulation by other pathways, although at present this is not well understood (reviewed in Rognoni *et al.*, 2016).

(*c*) *Kindlin-1 and α9 integrin overexpression*

Integrin-mediated regeneration is most successful when the appropriate integrin is both present and activated. Thus, co-overexpression of kindlin-1 and α9 integrin forms a strong stimulus for axonal regeneration in tenascin-C-rich areas such as the dorsal root entry zone and spinal cord after a dorsal root crush (Cheah *et al.*, 2016). Viral vector-mediated delivery of both molecules to DRGs indeed resulted in a synergistic effect on sensory axonal regeneration. The α9- and kindlin-1-overexpressing axons that reached the spinal cord regenerated from the cervical dorsal root at levels C8 to C5 all the way up into the medulla (Cheah *et al.*, 2016). Mechanical pressure and thermal sensation in the paw as well as limb proprioception improved after injury in animals that had combined α9 and kindlin-1 overexpression. Furthermore, electrophysiological recordings demonstrated that sensory pathways from the paw to the dorsal horn of the spinal cord had regrown following injury and α9/kindlin-1 overexpression. Thus, the combination of α9 and kindlin-1 leads to robust axonal

regeneration of at least 25 mm and partial functional recovery after a dorsal root crush. Furthermore, these results demonstrate that there is a synergistic effect exceeding that of overexpression of α9 (Andrews *et al.*, 2009) or kindlin-1 (Tan *et al.*, 2012) alone. Surprisingly, no severe degree of axonal misguidance occurred in this study, with regenerating axons being found mainly in the dorsal column and terminations in the dorsal horn being predominantly in the correct laminae. These results suggest that when activated integrins encounter an appropriate ECM environment, the remaining structures in the CNS can exert guidance effects on the α9/kindlin-1-overexpressing sensory neurons.

Taken together, there are various approaches to activate integrins, each with a unique mechanism to promote integrin signalling (**Fig. 3**). We have reviewed the evidence that stimulation of integrin signalling in injured neurons is a powerful strategy to boost sensory axon regeneration following CNS injury because it can overcome the repulsive molecules that prevent axonal regeneration in the injured spinal cord. To date, the synergistic effects of kindlin-1 and α9 delivery achieved the longest regeneration observed in the dorsal column pathway by modulating integrin signalling *in vivo* (Cheah *et al.*, 2016). Identifying the integrin adhesome is an active field of research and novel integrin activators are therefore continuously being discovered, such as reelin (Lin *et al.*, 2016), sema7A (Pasterkamp *et al.*, 2003), shank (Lilja *et al.*, 2017) and vimentin (Kim *et al.*, 2016). The identification of new integrin-activating molecules also offers opportunities for future regeneration research.

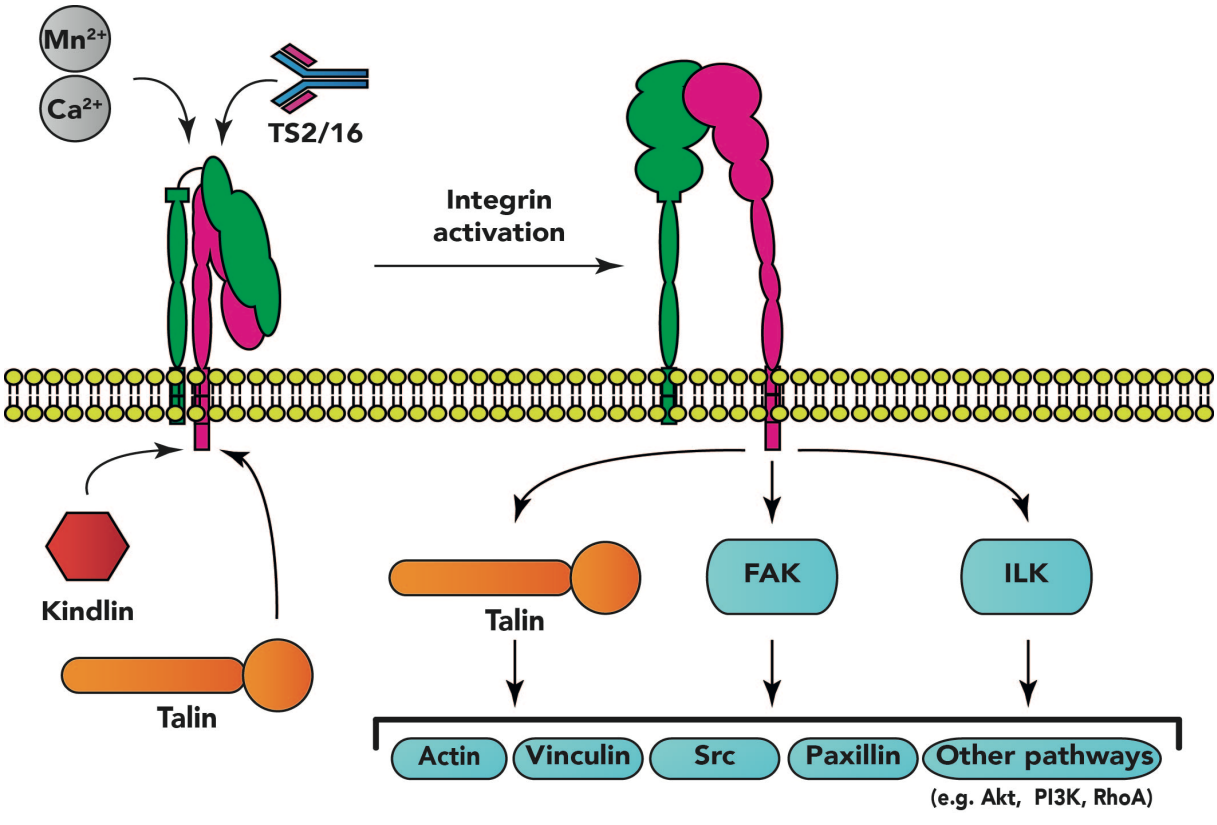

Integrin signalling and cytoskeleton changes

Fig. 3. - previous page - Molecular mechanisms for integrin activation. Integrins exist in two activation states on the cell surface: a bent inactive and a straight active state. There are several ways to activate integrins: (*i*) cations such as Ca2+ and Mn2+ interact with a metal ion-binding site at the ectodomain of the integrin to activate the receptor; (*ii*) kindlins and talins are two families of intracellular proteins that bind to the cytoplasmic tail of β1 integrins to activate the heterodimeric complex; (*iii*) the monoclonal antibody TS2/16 binds to the ectodomain of human β1 integrins to induce a conformational change and receptor activation. Activated integrins have their ectodomain exposed and bind extracellular matrix ligands, which leads to intracellular signalling and changes of the cytoskeleton. Activation of certain integrins can result in cell adhesion and axonal regeneration. FAK, focal adhesion kinase; ILK, integrin-linked kinase; PI3K, phosphoinositide 3-kinase.

VII. DEVELOPMENTAL CHANGES IN NEURONAL INTEGRIN LOCALISATION

(1) Exclusion of integrins from the axon of certain adult central nervous system neurons

Integrins are expressed in developing neurons and have essential roles in the formation of a functional nervous system. They are important for migration (Tate *et al.*, 2004; Andressen *et al.*, 2005; Marchetti *et al.*, 2010), proliferation (Blaess *et al.*, 2004; Leone *et al.*, 2005), adhesion (Tate *et al.*, 2004), differentiation (Tate *et al.*, 2004; Andressen *et al.*, 2005), axon outgrowth (Sakaguchi & Radke, 1996; Harper *et al.*, 2010), axon guidance (Huang *et al.*, 2006; Myers *et al.*, 2011) and lamination (Georges-Labouesse *et al.*, 1998; Marchetti *et al.*, 2010) of neuronal precursor cells of the nervous system. However, during maturation of CNS neurons selective transport mechanisms are set up that send some molecules to dendrites and others to axons (reviewed in Lasiecka & Winckler, 2011; Britt *et al.*, 2016; Bentley & Banker, 2016). This selective polarised transport is essential for giving axons a set of molecules and properties appropriate for their function. As part of this general acquisition of polarity, integrins become excluded from CNS axons (Bi *et al.*, 2001; Franssen *et al.*, 2015). The overall result of these polarity changes is that mature neurons are not able to regenerate, probably due to the absence of various receptors including integrins in their axons.

The distribution of integrins in axons during maturation has been intensively studied, since any treatment involving integrin expression aiming at promoting axon regeneration requires the expressed integrins to reach the axonal compartment and growth cone. By examining localisation of tagged integrins (α6, α9, and β1) *in vivo* in mature and immature sensory, retinal, cortical and red nucleus neurons, a differential ability for integrins to localise within axons became apparent (Andrews *et al.*, 2016). Integrins were transported into the still-developing early postnatal axons of the corticospinal tract, but the investigated α6, α9 and β1 integrins were excluded from mature corticospinal tract and rubrospinal tract axons. High levels of integrins were found in both branches of adult DRG axons and in some RGC

axons (Andrews *et al.*, 2016). It is tempting to correlate this transport with the ability of immature and sensory axons to successfully sprout and regrow following damage (Bregman & Bernsteingoral, 1991; Bates & Stelzner, 1993). In addition and as reviewed earlier, overexpression of α9 integrin in the DRGs indeed stimulated axonal regeneration (Andrews *et al.*, 2009; Cheah *et al.*, 2016). Integrin-driven regeneration in the spinal cord and elsewhere will require an intervention to ensure that the molecules are transported into the axons. However, it is not just integrins that are excluded from axons, but many growth-related molecules, as described below (Section VIII).

(2) Developmental changes in the integrin transport machinery

The exclusion of integrins from the axons of many adult CNS neurons, such as the corticospinal tract, is mediated by the development of selective transport mechanisms that are responsible for neuronal polarity (**Fig. 4**). Studying integrins provides a good tool to study these mechanisms. Integrin trafficking is well studied in cancer cells, where it was found to be transported in recycling endosomes, which are regulated by small GTPases (Powelka *et al.*, 2004). In neurons axonal integrins are mostly transported in Rab11- (Caswell *et al.*, 2008; Eva *et al.*, 2010) and ARF6- (Powelka *et al.*, 2004; Eva *et al.*, 2012) positive recycling endosomes. These GTPases control endosomal targeting and are turned on by GTP exchange factors (GEFs) and turned off by GTP activating proteins (GAPs). Rab11 and ARF6 are responsible for transporting integrins into axons probably as part of a complex with scaffolding molecules, such as the JNK-interacting protein 3 (JIP3) and JIP4 and kinesin- and dynein-motors (Isabet *et al.*, 2009; Suzuki *et al.*, 2010; Montagnac *et al.*, 2011). In immature neurons there exists anterograde integrin transport, but with maturation there is gradually less anterograde and more retrograde integrin transport in the axon, leading to the exclusion of integrins. In cultured cortical neurons from embryonic day 18 rat pups, expression levels of α5, αV and β1 integrins started to decrease after 7 days in culture and were undetectable in the axon after 14 days (Franssen *et al.*, 2015). This exclusion of integrins from the axon coincides with the formation of the axon initial segment (AIS) (Song *et al.*, 2009), which plays a part in the exclusion of integrins since disruption of the AIS increased the amount of integrin within mature axons (Franssen *et al.*, 2015). The AIS exhibits a dense network of proteins including actin, which can restrict access of molecules to axons by acting as a size filter or by supporting retrograde myosin-driven transport (Song *et al.*, 2009; Lewis *et al.*, 2009; Arnold, 2009). There is also a role for actin and modifications of the microtubule cytoskeleton in regulating integrin transport (Franssen *et al.*, 2015). However, the main mechanism for exclusion is the gradual change of the transport direction

during maturation and the establishment of the AIS. The direction of transport is defined by the activation state of ARF6. ARF6 can be inactivated by its GAP ACAP1 and in its inactive state favours anterograde transport (Jackson *et al.*, 2000; Dai *et al.*, 2004). In turn, active ARF6 favours retrograde transport (Eva *et al.*, 2012). Activators of ARF6 are GEFs; two known ARF6 GEFs are ARNO and EFA6 (Sakagami *et al.*, 2006). Importantly, it has been found that during cortical neuronal maturation ARNO and EFA6 are strongly up-regulated (Sakagami *et al.*, 2006) and EFA6 localises to the AIS (Eva *et al.*, 2017). Both, ARNO and EFA6 are important for the exclusion of integrins from axons (Franssen *et al.*, 2015; Eva *et al.*, 2017). Interestingly, it has also been found that Rab11 was largely excluded from mature axons, being present at low levels in axons compared to dendrites in primary cortical neurons grown in culture for more than 14 days (Franssen *et al.*, 2015; Koseki *et al.*, 2017). Overexpression of Rab11 in these neurons permitted integrin transport into the axon and promoted regeneration after laser-induced axotomy *in vitro* (Koseki *et al.*, 2017).

In summary, a developmental switch in the transport of essential growth molecules, such as integrins, results in the exclusion of these molecules from mature CNS axons, likely rendering them unable to regenerate after injury. Interfering with this developmental switch will result in the presence of integrins and other excluded molecules in the axon (Franssen *et al.*, 2015; Koseki *et al.*, 2017). Based on our observations *in vitro*, we further hypothesise that interfering with this developmental transport switch will lead to increased regeneration after injury.

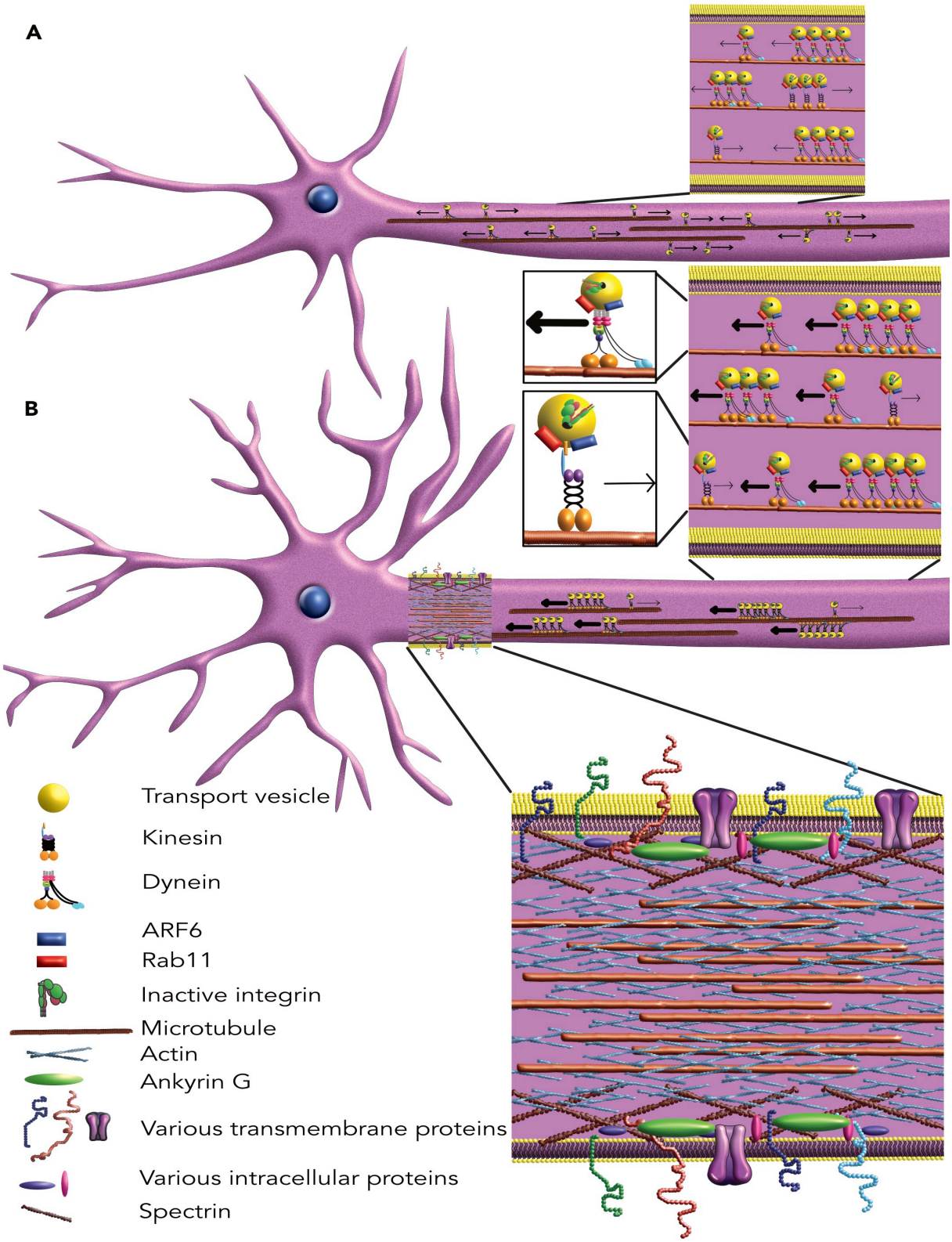

Fig. 4. Comparison of immature and mature central nervous system neurons. (A) Immature neurons do not have a fully developed axon initial segment and their axons have been shown to transport integrins both antero- and retrograde to an equal extent. Vesicles bound to ADP-ribosylation factor 6 (ARF6)- and Ras-associated binding (Rab) protein 11 (Rab11)-GTP are retrograde transported, while vesicles bound to ARF6- and Rab11-GDP move in the anterograde direction. (B) Mature neurons have developed an axon initial segment and are characterised with predominant retrograde axonal transport of integrins.

VIII. THE LOCALIZATION OF OTHER REGENERATION-ASSOCIATED RECEPTORS

Cell surface receptors are promising targets to promote axonal regeneration (reviewed in Cheah & Andrews, 2016). Rab11-positive recycling endosomes contain integrins, but also regulate the transport of other regeneration-associated receptors including tropomyosin receptor kinase receptors (Trks) (Ascaño *et al.*, 2009; Lazo *et al.*, 2013) and insulin-like growth factor receptors (IGFRs) (Romanelli *et al.*, 2007). The observation that Rab11 vesicles are excluded from the axon *in vitro* (Franssen *et al.*, 2015; Koseki *et al.*, 2017) is consistent with an *in vivo* study that observed a somatodendritic distribution of Rab11 in the forebrain, cerebellum, thalamus and brainstem (Sheehan *et al.*, 1996). Here, we discuss that TrkB and insulin-like growth factor 1 receptor (IGF-1R) are also excluded from axons of the adult corticospinal tract and the implications of this for regeneration.

(1) Tropomyosin receptor kinase B

TrkB is a cell-surface receptor that can boost the regenerative response of injured neurons. It binds several neurotrophic factors including brain-derived neurotrophic factor (BDNF), neurotrophin-3, and neurotrophin-4. These neurotrophic factors promote neuronal survival and axonal growth and are involved in synaptic plasticity (reviewed in Minichiello, 2009; Park & Poo, 2013; Harrington & Ginty, 2013). Due to the important role of these factors, it may not be surprising that there is a widespread distribution of TrkB in the adult brain (Yan *et al.*, 1997). Interestingly, adult corticospinal neurons express TrkB in their cell bodies and dendrites, but not in the axon (Yan *et al.*, 1997; Lu, Blesch, & Tuszynski, 2001). Furthermore, TrkB and its other family members, TrkA and TrkC, are not up-regulated after spinal cord contusion (Liebl *et al.*, 2001). Consistent with the absence of TrkB in the corticospinal tract, BDNF-secreting cell grafts in a spinal cord lesion site did not promote axonal regeneration of this motor pathway (Lu *et al.*, 2001). Viral vector-mediated overexpression of TrkB has been shown to result in receptor trafficking into the axon at the level of the subcortical white matter but not further down into the spinal cord (Hollis *et al.*, 2009b). These neurons were able to regenerate into BDNF-secreting cell grafts that were placed into subcortical lesions (Hollis *et al.*, 2009b). However, as elaborated above for integrin receptors, additional interventions would be required to enhance the transport of TrkB into the corticospinal tract to promote substantial regeneration after spinal cord injury. In addition, it had been shown in hippocampal slice cultures that the activation state of TrkB correlates with axonal sprouting (Aungst, England, & Thompson, 2013). The activation state of Trk receptors may therefore influence the regeneration response as well. Taken together,

the absence of TrkB in corticospinal tract axons likely contributes to the restricted axonal regeneration and responsiveness to BDNF treatments after spinal cord injury.

(2) Insulin-like growth factor receptor

IGFR is the transmembrane receptor for insulin-like growth factors (IGFs) and has been shown to promote neuronal survival and outgrowth (reviewed in Sullivan, Kim, & Feldman, 2008). Its mechanism of axonal transport is unknown. IGF-1R has been shown to be essential for the formation of the axon in adult RGCs *in vitro* (Dupraz *et al.*, 2013), highlighting its crucial role in promotion of axonal growth. IGF-1R and insulin receptors were also found to be localized in adult DRGs after injury (Craner *et al.*, 2002; Xu *et al.*, 2004), with their presence likely correlating with the pro-regenerative response of these sensory neurons. IGFs play an important role during the development of the corticospinal tract (Arlotta *et al.*, 2005; Ozdinler & Macklis, 2006), but IGFRs become excluded from axons during maturation of this motor pathway. More specifically, IGF-IR is exclusively localised in the somatodendritic compartment of the neurons in layer V motor cortex (Hollis *et al.*, 2009a). Consistent with the absence of the receptor in the axonal compartment, corticospinal tract axons were not able to regenerate through IGF-secreting cell grafts that were transplanted into the lesion after a spinal cord injury *in vivo* (Hollis *et al.*, 2009a). Interestingly, the latter study showed that the ceruleospinal and raphespinal axons did regenerate into these grafts. We therefore hypothesise that these two descending motor pathways retained IGFRs in their axonal compartments, but the authors did not examine the receptor expression in these neurons. A recent study took an alternative approach and delivered IGF-1 together with osteopontin into the sensorimotor cortex in order to promote corticospinal tract regeneration. Viral vector-mediated delivery of both ligands in the cortex, but not IGF-1 or osteopontin alone, promoted axonal regeneration approximately 1 mm beyond the lesion site after spinal cord hemisection (Liu *et al.*, 2017). The treatment showed the strongest effect on compensatory sprouting from the uninjured side of the spinal cord (Liu *et al.*, 2017). The axonal regeneration and sprouting contributed to the improved hindlimb function of the animals after spinal cord injury. The mechanism by which IGF-1 and osteopontin in the cortex mediate their growth-promoting effect is unclear. It is possible that both ligands activate their receptors in the somatodendritic domain of cortical neurons, which in turn, activate the PI3K/mTOR signal transduction cascade. This is sufficient for robust sprouting in the spinal cord, and short-range regeneration (Liu *et al.*, 2017).

Taken together, like integrins, the deficit of TrkB and IGF-IR in the axons within the corticospinal tract may limit its regeneration. Further investigation is required to determine

whether the exclusion of these receptors in corticospinal tract axons also depends on the presence of the axon initial segment as a barrier and whether the same transport vesicles are involved for their transport as for integrins.

IX. PERSPECTIVES

Integrins are important mediators of axonal regeneration in the injured nervous system. Integrins stimulate axonal regeneration when they are activated and localised at the growth cone to interact with the ECM. In order to use receptors as potential therapeutic targets to promote axonal regeneration, the mechanisms of axonal transport and trafficking need to be better understood. The successful use of activated integrins to promote regeneration of sensory axons leading to recovery of mechano- and temperature sensations *in vivo* (Cheah *et al.*, 2016) indicates that the overall strategy can be successful. Regeneration of the corticospinal pathway is a key event that is necessary to restore motor control after spinal cord injury. If in addition to integrin activation, the integrin trafficking barrier in descending corticospinal motor neurons could be overcome, then motor recovery could be a surmountable obstacle. Strategies to initiate trafficking to the axonal compartment of the corticospinal tract could therefore be based on: (1) overcoming the transport block of the axon initial segment and; (2) stimulation of anterograde transport by modulation of transport vesicles; or (3) adding axonal localisation signals to growth promoting receptors to enter the axon.

X. CONCLUSIONS

(1) Integrins are localised at the growth cone of immature and regenerating neurons and connect the extracellular and intracellular compartments of the neuron.

(2) Matching the extracellular matrix environment with the appropriate integrins promotes limited axonal regeneration of mature neurons.

(3) Presence of integrins in the axon correlates with the regenerative capacity of neuronal pathways.

(4) Integrins participate in spontaneous axonal regeneration after peripheral nerve injuries.

(5) Axon-repulsive molecules at the lesion site of spinal cord injuries inactivate integrins and thereby inhibit axonal regeneration in the central nervous system.

(6) Stimulation of integrin signalling can overcome the repulsive molecules at the site of injury and promote limited sensory axon regeneration in the central nervous system.

(7) Integrins become excluded from the axon during maturation of most central nervous system neurons and this correlates with the loss of the regeneration ability of mature neurons.

(8) Manipulation of the receptor activation state and localisation within axons is not only

important for integrin-mediated axon regeneration, but also for other regeneration-associated receptors such as TrkB and IGF-1R.

CHAPTER II – shRNA and CRISPR-Cas9 to dismantle the axon initial segment in cortical neurons by targeting Ankyrin-G

DECLARATION:

The material in this chapter has not been published. I thank William Hendriks (Harvard Medical School) for sharing his experience regarding the CRISPR-Cas9 technology. This chapter was supervised by James Fawcett and Joost Verhaagen.

I. INTRODUCTION

The axon initial segment (AIS) is a structure located at the proximal part of the axon. It contains a high number of voltage-gated ion channels and many other membrane-bound and cytoskeleton proteins. The AIS is essential for neuronal polarisation (reviewed in Rasband, 2010). It is crucial for action potential propagation and it anatomically forms the border between the somatodendritic- and axonal compartment of multipolar neurons. How the AIS regulates protein trafficking between the sub-cellular compartments of the neuron is not well understood. However, it is clear that the AIS is important for neuronal functioning as mutations affecting the AIS are associated with human diseases (reviewed in Huang & Rasband, 2018). For instance, mutations in the ANK3 gene (encoding the Ankyrin-G protein) are associated with bipolar disorders, epilepsy and intellectual disabilities.

(1) Structure of the axon initial segment

The AIS is approximately 20 to 60 microns long and consists of microtubule bundles and a high-density of proteins (Palay *et al.*, 1968). Proteins found at the AIS include clusters of cell adhesion molecules, cytoskeletal scaffolds, extracellular matrix molecules, and voltage-gated ion channels. The AIS is often visualised by immunochemistry for one of the following proteins: Ankyrin-G (AnkG), βIV spectrin, neurofascin, neuronal cell-adhesion molecule (NrCAM), voltage-gated sodium and potassium channels, or others (reviewed in Ogawa & Rasband, 2008; Rasband, 2010; Leterrier, 2018; Huang & Rasband, 2018). The high number of voltage-gated channels, approximately a 30-fold increase compared to dendrites and distal axon (Kole *et al.*, 2008), is a key characteristic of the AIS.

The cytoskeletal protein AnkG is essential for the AIS as it acts as a so-called 'master scaffolding protein'. All AIS proteins directly or indirectly interact with AnkG, and therefore not surprisingly AnkG consist of many protein interaction sites.

There are two isoforms of the AnkG protein that are 480- and 270 kilodaltons (kDa) in atomic mass. The two isoforms differ in the size of the protein tail structure at the C-terminus. In other words, the 270 kDa isoform has a shorter protein tail than the 480 kDa isoform. The tail consists of multiple SxIP motifs that are important for binding of microtubules (Freal *et al.*, 2016) and a second binding residue to β4-spectrin (Jenkins *et al.*, 2014). The anchoring of microtubules to the AIS is important for axonal protein trafficking (Sobotzik *et al.*, 2009; Nakata *et al.*, 2011; van Beuningen *et al.*, 2015; Kuijpers *et al.*, 2016). The membrane-binding- and spectrin-binding domains of AnkG are both found at the N-terminus of the protein. The membrane-binding domain consists of 24 Ankyrin repeats (Wang *et al.*, 2014) which anchors ion channels and cell-adhesion molecules (CAMs) to the AIS. Examples of CAMs at the AIS are neuronal cell adhesion molecule (NrCAM) and neurofascin (Davis, Lambert, & Bennett, 1996, Hedstrom *et al.*, 2007). The spectrin-binding domain of AnkG recruits actin-spectrin complexes which are important for cytoskeletal stability of the AIS (Yang *et al.*, 2007; Albrecht *et al.*, 2016; Huang *et al.*, 2017a; 2017b).

The formation of the AIS occurs relatively early in the development of multipolar neurons. Our laboratory and others observed that the AIS starts to appear at 3 to 4 days in cultured cortical neurons of rats. The AIS is formed *in vivo* in the time period between embryonic day 13 and postnatal day 1 *in vivo* depending on the brain area and animal species (Galiano *et al.*, 2012; Gutzmann *et al.*, 2014; Le Bras *et al.*, 2014). The intrinsic mechanism of the assembly of the axon initial segment is a topic of intense research.

(2) Removal of scaffolding protein Ankyrin G dismantles the axon initial segment

The many protein interactions by AnkG make this protein crucial to sustain the AIS. This was confirmed by studies using transgenic knockout mice (Jenkins & Bennett, 2001; Pan *et al.*, 2006; Zhou *et al.*, 1998) and short hairpin RNA (shRNA) interference (Hedstrom *et al.*, 2007; Hedstrom, Ogawa, & Rasband, 2008), as removal of this scaffolding protein dismantles the AIS *in vitro* and *in vivo*.

That knockout of AnkG results in dismantling of the AIS was first shown *in vivo* in transgenic mice that lack AnkG in a subset of purkinje cells in the cerebellum (Zhou *et al.*, 1998). Several studies used these mice to identify that AnkG is required for maintenance of the AIS by staining for multiple proteins that are normally found in this important structure (Zhou *et al.*, 1998; Jenkins & Bennett, 2001; Pan *et al.*, 2006; Sobotzik *et al.*, 2009). The purkinje cells that had complete knockout of AnkG failed to concentrate the following proteins at the AIS: voltage-gated sodium channels (Zhou *et al.*, 1998, Jenkins & Bennett, 2001; Pan *et al.*, 2006), voltage-gated potassium channels (Pan *et al.*, 2006), neurofascin

(Zhou *et al.*, 1998, Jenkins *et al.*, 2001), L1 cell adhesion molecule (Jenkins & Bennett, 2001), NrCAM (Jenkins & Bennett, 2001), βIV spectrin (Jenkins & Bennett, 2001), and bundles of microtubules (Sobotzik *et al.*, 2009). All of above studies reported that depletion of the AIS resulted in disturbed firing of action potentials, and the mice developed ataxia.

The importance of AnkG for AIS assembly was also shown in cultured CNS neurons by using shRNA interference (Hedstrom *et al.*, 2007). The latter study delivered the shRNA for AnkG, via a lentivirus, 3 hours after plating of hippocampal neurons and the cells were examined for multiple AIS proteins at 17 DIV. The transfected neurons had knockout of AnkG and as a result the typical AIS structure was not visible anymore by immunofluorescence. In addition to AnkG knockout, the membrane proteins Nav 1.x, βIV spectrin, neurofascin, and NrCAM, failed to localise at the AIS (Hedstrom *et al.*, 2007). In contrast, shRNA interference for neurofascin did not result in disassembly of the AIS (Hedstrom *et al.*, 2007) suggesting that only AnkG is required for upholding of the AIS.

(3) The axon initial segment as a barrier for axonal transport

The AIS is one of the known selective-transport barriers for proteins to enter the axon. Knockout of AnkG not only demolishes the AIS, but also allows proteins from the somatodendritic domain to enter the axon. The studies that observed the mis-trafficking of somatodendritic proteins into the axon will be discussed below.

RNA interference for AnkG in cultured hippocampal neurons resulted in the axonal localisation of cytoplasmic protein microtubule-associated protein-2 (MAP2) and the membrane-associated protein chloride potassium symporter 5 (KCC2) (Hedstrom *et al.*, 2008). Transgenic mice that lack AnkG in purkinje cells had post-synaptic membrane proteins such as metabotropic glutamate receptor 1 in the axon (Sobotzik *et al.*, 2009). Interestingly, both studies observed that loss of the AIS also resulted in axons with characteristics of dendrites such as formation of spines and post-synaptic terminals (Hedstrom *et al.*, 2008; Sobotzik *et al.*, 2009).

The AIS has also been suggested to form a barrier for integrins to enter the axon of polarized CNS neurons. In rat cortical cultures, integrins (α5, αV, β1) are ubiquitously distributed throughout the cell on the first day in culture, but become exclusively localized to the somatodendritic domain when the AIS is matured (Franssen *et al.*, 2015). AAV-mediated delivery of integrins in the corticospinal tract also results in a somatodendritic localisation and the receptors are not found beyond the AIS *in vivo* (Andrews *et al.*, 2016). Both studies suggest a correlation between AIS formation and the sub-cellular distribution of integrins. However, the study by Franssen and colleagues also showed that the AIS contributes to the

exclusion of the axonal integrins via knockdown of AnkG. Lentivirus mediated-shRNA interference allowed endogenous β1-integrin from the somatodendritic domain to enter the axons of transduced cortical neurons *in vitro*. The integrins were detected 400 μm into the axon three days after shRNA application (Franssen *et al.*, 2015). I would consider this as a limited distance of receptors mis-trafficking. Hedstrom *et al.*, 2008 demonstrated in cultured hippocampal neurons that AnkG is a stable protein and successful dismantling of the AIS requires at least two weeks by using the same lentivirus shRNA construct. According to their data, the majority (> 95%) of the transfected neurons still have an AIS at four days post-transduction, and there is only a 40% reduction in the average fluorescent intensity of AnkG. The neurons undergo a complete knockout of AnkG and thereby destruction of the AIS after 14 days of shRNA interference. It is therefore likely that integrins and other regeneration-associated receptors will reach further into the axons by longer time exposure to the shRNA. It is unknown whether dismantling the AIS can promote axonal transport of integrins in CNS neurons *in vivo*.

It is generally accepted that the AIS is important for selective polarized transport. Yet, the intrinsic mechanisms how the AIS regulates protein trafficking remains poorly understood.

(4) Hypothesis 'understanding regenerative failure'

Genetic changes and selective polarised transport contribute to neuronal polarisation, and this correlates with the decline in the intrinsic regeneration capacity of CNS neurons (**Fig. 1**). For instance, Rab11-positive endosomes contain regeneration-associated receptors (reviewed in Nieuwenhuis & Eva, 2018b) are down-regulated and excluded from the axon during maturation which contributes to less efficient axon regeneration (Koseki *et al.*, 2017). In addition, integrins become localised in the somatodendritic domain of matured CNS neurons *in vitro* (Franssen *et al.*, 2015) and *in vivo* (Andrews *et al.*, 2016). The formation of the axon initial segment is one of the important events that contribute to selective polarised transport in multipolar neurons. We hypothesize that dismantling the AIS, via knockout of AnkG, is one approach to overcome the axonal transport block of regeneration associated-receptors and can thereby promote axon regeneration in CNS neurons.

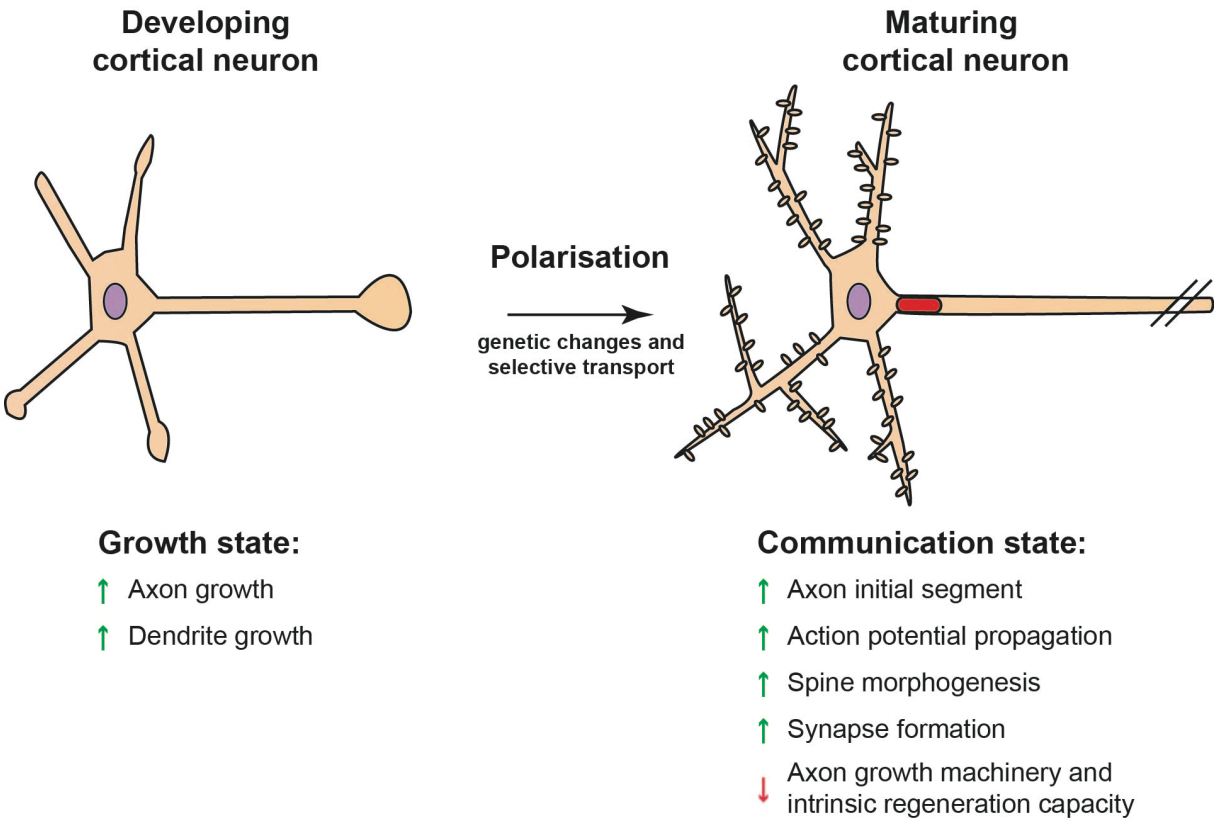

Fig. 1. Polarisation of cultured cortical neurons. Neurons undergo various developmental stages during polarisation. Genetic changes and selective transport of proteins contribute to neuronal polarisation. For simplification purposes, two developmental stages are categorized here. Developing cortical neurons exist in a growth state that promotes axonal and dendritic outgrowth. As neurons mature, there is a decline in their growth capacity as they become geared for neurotransmission. The neurons form an axon initial segment that propagates action potentials and also contributes to polarised membrane protein transport. Mature cortical neurons have a poor intrinsic capacity for axon regeneration. This figure was published in Nieuwenhuis & Eva, 2018b (Small GTPases).

(5) Aim of study

The aim of this study is to make/generate genetic tools to knockout AnkG. The initial approach was to make a plasmid containing shRNA interference for AnkG. During the second year of my PhD, I made a novel plasmid to knockout AnkG based on recent advances in CRISPR-Cas9 technology. This dissertation chapter will be focussed on the generation and characterization of these genetic tools for protein knockout. This chapter also serves as guideline for others that would like to use the CRISPR-Cas9 vector, which is suitable for rAAV production, to knockout their protein of interest. This chapter contains preliminary data in which shRNA interference and CRISPR-Cas9 were tested for their efficiency to knockout AnkG and to dismantle the AIS in cultured cortical neurons. Future research is needed to investigate whether dismantling of the AIS, via AnkG knockout using the tools

created here, enables axonal transport of regeneration-associated receptors in the (injured) corticospinal tract *in vivo*.

(6) Genetic tools to knockout proteins

A common approach to study the function of proteins is by knockout (in addition to overexpression of the corresponding gene, as done in **Chapter III**). There are many protein knockout technologies available including the generation of transgenic knockout mouse. In this chapter, shRNA interference and CRISPR-Cas9 were used as method to knockout AnkG.

(*a*) *shRNA interference*

RNA interference regulates the expression of genes by degrading the messenger RNA after gene transcription. It thereby prevents protein translation in the cell, resulting in protein knockout. This post-transcriptional gene silencing occurs in eukaryotic cells (Agrawal *et al.*, 2003). RNA interference via short interfering RNA (siRNA) and the synthetic shRNA were discovered in the 1990s (Fire *et al.*, 1998). Delivery of siRNA into the cytoplasm results in temporary expression. In contrast, vector-mediated delivery of shRNA results in long-term expression of siRNA-like nucleic acids, because the shRNA is continuously transcribed in the nucleus of the host cell. shRNA interference could therefore result in protein knockout after one single administration.

The mechanism of shRNA interference is described in many reviews and textbooks (Manjunath *et al.*, 2009; Moore *et al.*, 2010); a brief summary is given below. Plasmids containing a RNA promoter and the shRNA sequence can be delivered into cells via transfection, viral vector-mediated delivery, or other molecular techniques. In the cell, the shRNA sequence will be transcribed by class III RNA polymerases when the H1 (or U6) promoter is used. The shRNA will gain a hairpin structure in the nucleus. The structure of the short hairpin is relatively simple as it consists of the following components: 1) a stem region that consist of paired sense and antisense strands and; 2) unpaired nucleotides that form a loop to connect the stem region (see **Tables 1 and 2** for the design of the shRNA sequence, and see **Fig. 2** for a linear schematic illustration). After transcription, a protein complex consisting of Drosha and DGCR9 will release the short hairpin from other transcribed mRNA (Han *et al.*, 2004). This so-called pre-shRNA is transported from the nucleus toward the cytoplasm via an transporter protein called Exportin-5 (Yi *et al.*, 2003). In the cytoplasm, a protein complex containing RNase enzyme Dicer cleaves off the loop structure to generate double-stranded siRNA. Finally, the generated siRNA interacts with the RNA induced silencing complex (RISC), which in turn separates the sequence in two single RNA strands. The so-

called guide strand remains in the RISC complex and binds to the mRNA that was targeted for protein knockout. The guide strand RNA-RISC complex will cleave the targeted mRNA and thereby prevent protein translation of the target gene.

(*b*) *CRISPR-Cas9 interference*

CRISPR-cas9 does not interfere at the mRNA level, but induces a double-strand break (indels) in the DNA. The DNA's repair mechanisms are error prone and thereby likely to induce a point mutation. When a nucleotide deletion of insertion occurs, this can initiate a downstream frameshift to the DNA sequence. The truncated protein, translated from the shifted DNA reading frame, will be degraded by the cell's ubiquitin-proteasome system. Thus, the CRISP-induced indel can therefore ultimately results in protein knockout. In addition to protein knockout, the CRISP-Cas9 system has been suggested for an array of other biological applications (reviewed in Kim & Kim, 2014; Shalem, Sanjana, & Zhang, 2015; Wright, Nuñez, & Doudna, 2016; Lopes, Korkmaz, & Agami, 2016; Barrangou & Doudna, 2016; Barrangou & Horvath, 2017).

CRISPR-Cas has originally been identified as an adaptive immune system by bacteria against infections by bacteriophages (Barrangou *et al.*, 2007; Marraffini & Sontheimer, 2008). Most bacteria store the DNA content from previous phage infections, and when re-infected deploy RNA-guided nucleases for silencing of the nucleotides released by phages (reviewed in Hille *et al.*, 2018). CRISPR stands for **c**lustered **r**egularly **i**nterspaced **s**hort **p**alindrome **r**epeats, and these DNA sequences together with the associated Cas proteins form the bacterial line of defence against foreign DNA.

Part of the bacterial genome consists of identical palindrome DNA sequences (approximately 20 to 40 nucleotides in length) that are frequently repeated, and have spacer DNA in between (e.g. interspaced) (Ishino *et al.*, 1987; Jansen *et al.*, 2002). This spacer DNA is unique and matches with the DNA of phages that was introduced by previous infections (Mojica *et al.*, 2005; Bolotin *et al.*, 2005). The bacterial genome also contains CAS genes that give rise to Cas-protein complexes that consist of helicases and nucleases that can unwind and cleave DNA. The spacer DNA gives rise to CRISPER RNA (crRNA) after transcription that binds to the Cas protein. The Cas proteins interact to short protospacer adjacent motifs (PAM) that are present along the DNA, and are used by Cas proteins as binding sites to unwind double-stranded DNA and to allow the bound crRNA to search for complementary target sequences (Sternberg *et al.*, 2014; Anders *et al.*, 2014). This crRNA-Cas protein complex can therefore specifically interact with infectious phages DNA, while the Cas protein induces a double strand break. The cleavages of the DNA by the crRNA-Cas

protein complex avoids the phage infection and thereby prevents the death of the infected bacteria (reviewed in Hille *et al.*, 2018).

The CRISPR-Cas9 system cannot only target DNA sequences in bacteria, but in any living cell. The CRISPR-Cas9 system can be used to knockout any gene of interest, when the crRNA is replaced by a target sequence of choice and is co-expressed with the CAS protein. The crRNA, also known as the guide RNA, will guide the Cas proteins to cleave complementary DNA in the transduced cells.

II. MATERIALS AND METHODS

(1) Detailed cloning procedures for DNA constructs containing shRNA

The plasmid pSUPER (OligoEngine, VEC-PBS-0002) was used as the vector backbone for the shRNA constructs. Five shRNA constructs were designed: four constructs to knockdown AnkG, and one scrambled shRNA construct that functions as negative control by targeting a non-mammalian (drosophila gnu) gene. This scrambled shRNA sequence was taken from Hedstrom et al., 2007 that used shRNA interference dismantle the AIS. The sequence of AnkG-shRNA1 was taken from studies that successfully interfered with AnkG and the AIS (Hedstrom *et al.*, 2007; 2008; Franssen *et al.*, 2015). This shRNA sequence should therefore result in successful knockout of AnkG and the AIS. The sequences of AnkG-shRNA2, AnkG-shRNA3 and AnkG-shRNA4 were self-designed, by using the online software http://www.invivogen.com/review-sirna-shrna-design, and aimed to target the Ank3 gene in both rat and mice. The four sequences had a 100% score for AnkG specificity and GC ratios of 52.6%, 52.6%, 42.1% and 36.8%, respectively. The designed oligonucleotides (Sigma-Aldrich) were 58 nucleotides in length. Both the forward and reverse oligonucleotides consisted of 19 nucleotides sense and antisense sequences separated by a 9 nucleotides noncomplementary loop sequence. This shRNA sequences were flanked by a 5' mutated BglII restriction overhang (GATCT was mutated in GATCC, which corresponds to BamHI) and a 3' RNA Polymerase III termination signal followed by a HindIII restriction overhang. The forward (**Table 1**) and reverse (**Table 2**) oligonucleotides were ordered from Sigma-Aldrich with a 5' phosphate modification.

Table 1. Forward primers to make shRNA in the 5' to 3' direction

Name	Sticky end BamHI (5 nt)	Stem structure - Sense (19 nt)	Loop (9 nt)	Stem structure – antisense (19 nt)	Term-inal. signal (5 nt)	Sticky end HindIII (1 nt)
AnkG – shRNA1	GATCC	GCCGTCAGTACCATCTTCT	TTCAAGAGA	AGAAGATGGTACTGACGGC	TTTTT	A
AnkG – shRNA2	GATCC	AAGCAGAAGTGGTGCGGT	TTCAAGAGA	TACCGCACCACTTCTGCTT	TTTTT	A
AnkG – shRNA3	GATCC	GAAGAACCAGATGGACATA	TTCAAGAGA	TATGTCCATCTGGTTCTTC	TTTTT	A
AnkG – shRNA4	GATCC	GAAATTATGACCACCACTA	TTCAAGAGA	TAGTGGTGGTCATAATTTC	TTTTT	A
scrambled	GATCC	CTACTGAGAACTAAGAGAG	TTCAAGAGA	CTCTCTTAGTTCTCAGTAG	TTTTT	A

Abbreviation: nt; nucleotides.

Table 2. Reverse primers to make shRNA in the 5' to 3' direction

Name	Sticky end HindIII (5 nt)	Term-inal signal (5 nt)	Stem structure – antisense (19 nt)	Loop (9 nt)	Stem structure – Sense (19 nt)	Sticky end BamHI (1 nt)
AnkG – shRNA1	AGCTT	AAAAA	GCCGTCAGTACCATCTTCT	TCTCTTGAA	AGAAGATGGTACTGACGGC	G
AnkG – shRNA2	AGCTT	AAAAA	AAGCAGAAGTGGTGCGGTA	TCTCTTGAA	TACCGCACCACTTCTGCTT	G
AnkG – shRNA3	AGCTT	AAAAA	GAAGAACCAGATGGACATA	TCTCTTGAA	TATGTCCATCTGGTTCTTC	G
AnkG – shRNA4	AGCTT	AAAAA	GAAATTATGACCACCACTA	TCTCTTGAA	TAGTGGTGGTCATAATTTC	G
Scramb-led shRNA	AGCTT	AAAAA	CTACTGAGAACTAAGAGAG	TCTCTTGAA	CTCTCTTAGTTCTCAGTAG	G

Abbreviation: nt; nucleotides.

(2) Annealing forward and reverse oligonucleotides to generate the shRNA insert

The primers (**Table 1** and **Table 2**) were resuspended in water to a concentration of 3 mg/ml. An equal amount (3 µg, e.g. 1 µl at 3 mg / ml concentration) of each complementary primer was hybridised in sterile annealing buffer that consisted of 100mM NaCl (Sigma-Aldrich) and 50mM HEPES (Gibco, 15630), pH 7.4. A polymerase chain reaction (PCR) machine was utilized to facilitate the annealing. The mixture was incubated at 90°C for 4 min, and was followed by 70°C for 10 minutes, 60°C for 5 minutes, 50°C for 5 minutes, 45°C for 5 minutes, 37°C for 15 minutes, 10°C for 20 minutes, 4°C overnight. The high temperature will undo any secondary structures that were formed at the single stranded primers, the

temperature range near 37°C will promote the DNA-DNA hybridisation, while the lower temperatures are used to store the DNA.

After annealing the primers, the double stranded DNA was isolated and purified. The complete ligation mixture for each shRNA construct was loaded on a 2% agarose gel containing ethidium bromide. A 2% gel was used due to the small size of the annealed oligonucleotides. Agarose gel electrophoresis was performed at 100 millivolt and the reaction was stopped before the DNA loading dye ran out of the gel. After gel electrophoresis, the higher band that contained the double stranded DNA was cut from the gel. The shRNA inserts were isolated from the agarose gel using the Wizard® SV Gel and PCR Clean-up System (Promega, A9282).

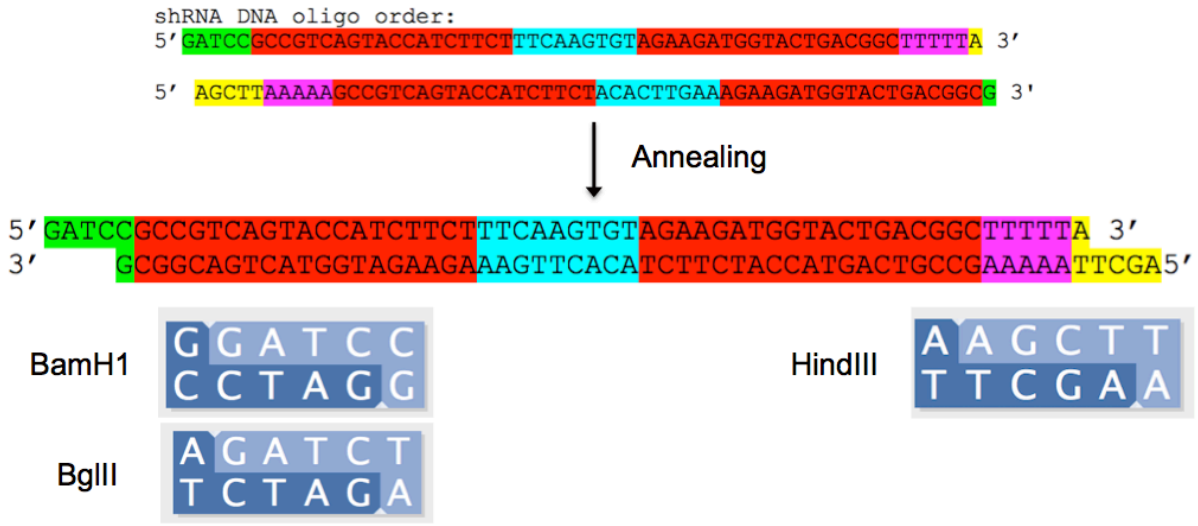

Fig. 2 Schematic illustrating the annealing of the oligonucleotides prior ligation of the shRNA insert downstream of the H1 promoter in plasmid pSUPER. The colours in the shRNA sequences highly the hairpin stem structure (red), the loop structure (cyan blue), the terminal signal (purple) and the flanked mutated restrictions site BglII (green) and HindIII (yellow). This cleavage sites of the restriction enzymes were taken from the software EnzymeX. Lab journal reference: BN-15-14

(3) Linearization of the vector backbone pSUPER

A restriction enzyme digestion was performed to generate overhang ends at the plasmid pSUPER that match the generated shRNA inserts. The restriction enzymes BglII (New England Biolabs, R0144) and HindIII (New England Biolabs, R0104) were used for this purpose. The digestion was performed according to the enzyme supplier instructions. NEBuffer III was chosen as buffer and should result in a HindIII and BglII digestion efficiency of 100% and 50%, respectively. I did not double the amount of HindIII enzyme (due to the 50% digestion efficiency) to avoid unwanted star activity. The restriction enzyme

digestion was performed in a PCR machine for 1 hour at 37°C, and was followed by 80°C for 20 minutes to inactive the HindIII enzyme (BglIII can not be heat inactivated).

The vector backbone was not dephosphorylated using phosphatases, because auto-ligation of the vector backbone should not occur due to the different overhang ends of HindIII and BglII. In addition, the BglII treatment after ligation (Section II.5) eliminates the pSUPER plasmids that do not contain the shRNA insert.

After the digestion, the linearized vector was purified to remove components of the restriction enzyme reaction that may interfere with the ligation of the vector backbone and the shRNA inserts. The mixture was loaded on a 1% agarose gel and standard gel electrophoresis was performed. The linearized vector was isolated from the gel fragments using the Wizard® SV Gel and PCR Clean-up System (Promega, A9282).

(4) Ligation of the shRNA insert into the vector backbone pSUPER

Ligation of the linearized vector backbone and the shRNA insert was achieved using T4 DNA ligase (New England Biolabs, M0202) following the supplier instructions. The ligation was done with a vector backbone to insert ratio of 1:5. An important negative control for ligation to include is the digested vector backbone without (shRNA-) insert. This condition will demonstrate whether auto-ligation of the vector backbone occurred.

(5) BglII digestion to reduce the background levels of shRNA DNA constructs at transformation

After ligation and before transformation of the plasmids in bacteria, a BglII restriction digestion was performed. The ligation mixture was treated with 10 units (1 µl) of BglII in NEBuffer III at 37°C for 30 minutes.

The 'enzyme site mutagenesis' strategy and the BglII restriction digestion will eliminate plasmids that do not contain the shRNA insert. Mutated BglII and HindIII overhang ends flank the shRNA insert and allow the cloning of the shRNA downstream of the H1 promoter at plasmid pSUPER. If the ligation is successful, the BglII restriction site at pSUPER is destroyed and becomes a BamH1 site (mutated BglII overhang) (see **Fig. 2**). The BglII digestion therefore does not digest the plasmids containing the shRNA insert. In contrast, plasmids that did not uptake the shRNA insert will be digested by the BglII enzyme and should therefore not result in bacterial colonies after transformation.

(6) Transformation in bacteria

GT116 Escherichia coli competent cells (InvivoGen, gt116) were used for the transformation of the BglII treated plasmids. GT116 bacteria are engineered to aid the growth of plasmids carrying hairpin structures, the transformation was performed according to the supplier their instructions. The cells were plated on 1.5% ager plates containing ampicillin (1:1000) and kept in a 37°C incubator overnight.

(7) DNA isolation and restriction enzyme digestion to screen for the shRNA insert

Bacterial colonies on the ager plates were picked and grown in lysogeny broth (LB) containing ampicillin (1:1000) and were left overnight in a shaker, 250 rotations per minute (rpm) at 37°C. After incubation, the DNA was isolated using Wizard® Plus SV miniprep DNA purification systems (Promega, A1460).

The isolated DNA was screened for the presence of the shRNA insert. The DNA was digested using Hpy188III in NEB CutSmart buffer and BSA for 1 hour at 37°C. The enzyme was heat inactivated by exposing the mixture to 65°C for 20 minutes. The digested DNA fragments were visualized on a 2% agarose gel according to standard procedures.

The restriction enzyme Hpy188III was selected because it cleaves the plasmid pSUPER and, if present, the loop sequence of the shRNA. Hpy188III treatment in pSUPER results in fragments of the following length: 749 bp, 670 bp, 495 bp, 429 bp, 259 bp, 134 bp, 98bp, 98 bp, 87 bp, 83 bp, and 74 bp. Hpy188III treatment in pSUPER containing the shRNA insert will result in fragments of: 749 bp, 670 bp, 429 bp, 277 bp, 270 bp, 259 bp, 134 bp, 98 bp, 98 bp, 87 bp, 83bp, 74 bp. Thus, the absence of the 495 bp band in the agarose gel will be an indicator for the presence of the shRNA insert in pSUPER.

Plasmids that were screened positive for the shRNA insert were amplified. One ml of LB media containing the plasmid was added into an Erlenmeyer flask containing 100 ml of fresh LB media and the appropriate antibiotics. The medium was incubated on a shaker at 200 rpm for overnight. After incubation, high yields of DNA were obtained using ZymoPURE™ plasmid maxiprep kit (Zymo Research, D4203).

(8) DNA sequencing

DNA sequencing of the shRNA construct was performed by the biochemistry DNA sequencing facility at the University of Cambridge. This desalted oligonucleotide 5’ GTTGTAAAACGACGGCCAGTGAG 3’ is forward primer that binds upstream of the H1 promoter in the pSUPER plasmid. By using this self-designed primer, the sequencing reaction will detect the downstream shRNA sequence during a single sequence reaction. Each

sequencing reaction consisted of 1000 nanogram of DNA plasmid and 10 picomolar of forward sequencing primer, which were diluted in nuclease-free water. The sequencing results were analysed using FinchTV software.

(9) Design of sgRNA sequence for cloning into the plasmid AAV-SYN-SaCas9-HA-hU6-backbone

The design of the sgRNA target sequence for the CRISPR Cas9 technology is relatively simple. In this section, I will describe in six steps how to design an oligonucleotide sequence that contains the sgRNA sequence for Staphylococcus aureus Cas9 (SaCas9) which is flanked with restriction sites for cloning. After the designed oligonucleotides are annealed, they can be inserted into the sgRNA-cloning site of two vector backbones. These vector backbones drive the expression of SaCas9 under the DNA promoters CMV or hSYN, while the expression of the inserted target sequence and sgRNA will be driven by the RNA promoter hU6 (see also **Fig. 3**). These CRISPR-cas9 vector backbones can be found under the following names in both the plasmid databases of the Fawcett and Verhaagen Laboratories: pAAV-CMV-SaCas9-HA-hU6-backbone (sample ID: 697) and pAAV-hSYN-SaCas9-HA-hU6-backbone (sample ID: 698).

1) Find the open reading frame of the gene of interest, derived from the correct animal specie, via NCBI. Also search in the literature whether there are isoform variants of the gene and download these sequences as well. The sequences can be opened in a DNA reading program, such as SerialCloner, and the protein sequences can be aligned using www.uniprot.org/align. Depending on the research question, search for a common sequence area between the gene splice variants to achieve knockout all protein isoforms, or alternatively find a sequence area that is unique for the isoform of interest.

2) Find the PAM sites in the open-reading frame of the gene of interest. The PAM sites for SaCas9 is any variant of 5' NNGRRT 3' (Ran *et al.*, 2015). These nucleotide abbreviations represent: N, any nucleotide; G, Guanine; R, Purine and therefore Adenine or Guanine; or T, Thymine. To achieve a complete protein knockout, select the PAM sites in the exon that is present in all the splice variants. SaCas9 cleavage in the first overlapping exon increase the chances of introducing an early frame-shift mutation and thereby prevention of the translation of a functional protein. Note that the PAM site for the Cas9 nuclease of Streptococcus pyogenes (SpCas9, the common used isoform for CRISPR) is '5 NGG 3' (Ran *et al.*, 2015), and therefore using published sgRNA sequences for this isoform will not work for SaCas9 in

this AAV vector plasmid. I recommend designing multiple target sequences since currently it cannot be predicted how efficient a certain sgRNA for SaCas9 would be.

3) Copy and paste the 21 nucleotides (nt) that are at the 5' end of the selected PAM site. Ran and colleagues showed that sgRNA with a length of 21 nt and 22 nt are the most effective to introduce double strand breaks (Indels) with the SaCas9 isoform (Ran *et al.*, 2015). It was also suggested to avoid guanine-cytosine-rich sequences as sgRNA.

The two-sgRNA sequences that I selected to target the rat ANK3 gene (NM_001033984.1) are:
sgRNA ANK3 - 1: 5' - GCTTCCCAGTTAAAGAAAAAC **- AGGGAT (=PAM)**
sgRNA ANK3 - 2: 5' – AAGAAGCACCGTAAACGGTCC **– CGGGAT (=PAM)**

4) Blast the target sequence at NCBI to check whether your target sequence is specific for your gene of interest in the same animal specie. Blast the target sequences without the PAM site, because SaCas9 can bind to multiple PAM site to introduced indels in potential off-target genes.

5) Add a guanine nucleotide at the 5' end of the target sequence, as this is required to initiate efficient transcription by the U6 promoter.

A guanine nucleotide was added to the 5' end of the two selected target sequences:
sgRNA ANK3 - 1: 5' - GGCTTCCCAGTTAAAGAAAAAC
sgRNA ANK3 - 2: 5' – GAAGAAGCACCGTAAACGGTCC

6) The target sequences can be cloned into the CRISPR-cas9 vector backbones by utilizing the BsaI restriction enzyme (NEB, R0535S). The BsaI enzyme cleave twice downstream of the hU6 promoter in the plasmid. The BsaI overhang ends need to be added to the target sequences in order to assure ligation in the plasmid along with the correct orientation. The insertion of the target sequence in the vector backbone will only succeed with double stranded DNA, and therefore an anti-sense oligonucleotide needs to be made before DNA annealing. The BsaI overhang ends that need to be added to the sense and antisense oligonucleotides are 5' CACC 3' and 5' AAAC 3', respectively. In addition, it is important to order the oligonucleotides with one phosphate group attached to the 5'-end for ligation purposes.

Generation of the antisense oligonucleotide, and addition of the BsaI overhangs which are suitable for cloning into the CRISPR-Cas9 vector backbone:

sgRNA ANK3 – 1

Primer Sense: 5' - *CACC*GGCTTCCCAGTTAAAGAAAAAC 3'

Primer Antisense: 5' – *AAAC*GTTTTTCTTTAACTGGGAAGCC 3'

sgRNA ANK3 – 2

Primer Sense: 5' – *CACC*GAAGAAGCACCGTAAACGGTCC 3'

Primer Antisense: 5' – *AAAC*GGACCGTTTACGGTGCTTCTTC 3'

(10) DNA constructs for CRISPR-Cas9 interference

pX601-AAV-CMV::NLS-SaCas9-NLS-3xHA-bGHpA;U6::BsaI-sgRNA was a gift from Feng Zhang (Addgene plasmid # 61591, renamed as plasmid 697) and was used as vector backbone. The CMV promoter was removed by AgeI (NEB, R0552) and XbaI (NEB, R0145) restriction digestion. The human SYN (hSYN) promoter of pTRUF20B-SEW, which is described in Korecka *et al.*, 2011, was next cloned into the vector backbone to generate pAAV-SYN-SaCas9-hU6-sgRNA (plasmid 698, see **Fig. 3**). The designed target sequences (see section above) were ordered from Sigma-Aldrich as desalted oligonucleotides with a 5' phosphate (**Table 1**) and were annealed in 100mM NaCl, 50mM HEPES, pH 7.4. The annealed oligonucleotides with BsaI overhang ends were next cloned in pAAV-SYN-SaCas9-hU6-sgRNA to generate one plasmid that expresses both SaCas9 and the sgRNA. The successful cloning of the sgRNA was confirmed by DNA sequencing using the primer 5' GCATATACGATACAAGGCTGTTAG 3' that binds in the hU6 promoter.

Table 1 - next page - Oligonucleotides used for the insertion of the sgRNA in pAAV-SYN-SaCas9-hU6-sgRNA. The primers are shown in a 5' to 3' orientation and the G + 21 nucleotides sgRNA are underlined. All target sequences are located in the first exon of the gene of interest, except for Protrudin that targets regions that are unique for the rat gene compared to the human gene, and the corresponding PAM sites are shown. The sense and antisense BsaI overhang ends are CACC and AAAC, respectively. The sgRNA are designed to target rat, expect for EGR-1 and Sema3A that are designed for mouse. Lab journal references: BN-16-20 (ANk3, Memo, Sema3A), BN-16-24 (EFA6), BN-17-52 (Protrudin), BN-18-08 (EGR1), BN-19-07 (NTRK3).

sgRNA	Sense primer	Antisense primer	PAM site (NNGRRT)
Ank3-1	CACCGGCTTCCCAGTTAAAGAAAAAC	AAACGTTTTTCTTTAACTGGGAAGCC	AGGGAT
Ank3-2	CACCGAAGAAGCACCGTAAACGGTCC	AAACGGACCGTTTACGGTGCTTCTTC	CGGGAT
Efa6-1	CACCGCAGCACAGGATCCCTAATACG	AAACCGTATTAGGGATCCTGTGCTGC	ACGAGT
Efa6-2	CACCGGTGGGCCCAGGTCCTCGAGGC	AAACGCCTCGAGGACCTGGGCCCACC	CGGGAT
Efa6-3	CACCGGAGAAGGCCAGTGTGAGGCCA	AAACTGGCCTCACACTGGCCTTCTCC	CTGAAT
EGR1-1	CACCGAGTTTGGGGTAGTTGTCCATG	AAACCATGGACAACTACCCCAAACTC	GTGGGT
EGR1-2	CACCGGCTATTACCGCCGCTGCCCTC	AAACGAGGGCAGCGGCGGTAATAGCC	TGGGGT
EGR1-3	CACCGGTTGTTCGCTCGGCTCCCCTT	AAACAAGGGGAGCCGAGCGAACAACC	GAGGAT
Memo1-1	CACCGGAGCCATCATTGCACCCCATG	AAACCATGGGGTGCAATGATGGCTCC	CAGGAT
Memo1-2	CACCGTACACCGCCTCAGGACCTCAG	AAACCTGAGGTCCTGAGGCGGTGTAC	CTGAAT
NTRK3-1	CACCGCCCAGCCAAGTGTAGTTTCTG	AAACCAGAAACTACACTTGGCTGGGC	GCGGAT
NTRK3-2	CACCGTAGAGCTCCATATCCACAGCA	AAACTGCTGTGGATATGGAGCTCTAC	TTGAGT
NTRK3-3	CACCGTCCTGGCAGCTCTTCCAGACG	AAACCGTCTGGAAGAGCTGCCAGGAC	CTGAGT
Protrudin-1	CACCGATGCAGTCTTCGGATCGGGAC	AAACGTCCCGATCCGAAGACTGCATC	CTGAGT
Protrudin-2	CACCGGTACAGGGCTTGTCTGCAGCG	AAACCGCTGCAGACAAGCCCTGTACC	GCGGAT
Protrudin-3	CACCGGGCGGATGAGCCCCAAGCAGG	AAACCCTGCTTGGGGCTCATCCGCCC	AAGAGT
Sema3A-1	CACCGACTGGGATTGCCTGTCTTTTC	AAACGAAAAGACAGGCAATCCCAGTC	TGGGGT
Sema3A-2	CACCGTCCAGTTACCACACCTTCCTT	AAACAAGGAAGGTGTGGTAACTGGAC	CTGGAT

(11) Cortical neuron cultures and magnetofection

Glass bottom cell culture dishes (Greiner bio-one, 627860) were coated with 2.5 milligrams poly-D-lysine in 0.1M borate buffer (pH 8.5) overnight at room temperature, and were washed in PBS the following day. Primary cortical neuron cultures were prepared from embryonic day 18 Sprague Dawley rat. The embryonic cortex was dissected in Hanks' balanced salt solutions (HBBS) (ThermoFischer Scientific, 14170) using forceps. The neurons were dissociated with 0.1M HEPES (ThermoFischer Scientific, 15630106) in papain (Worthington, LK003176) for 10 minutes at 37°C. They were next briefly rinsed with DNase (Sigma-Aldrich, D5025) and washed with 1mM HEPES in HBSS solution. The neurons were next cultured in neural Q basal medium (Globalstem, gsm9420), supplemented with 2% GS21 (Amsbio, gsm3100) and 1% glutamax (ThermoFischer Scientific, 35050061) on previously coated cell-culture dishes.

The cortical neurons were transfected using oscillating nanomagnetic transfection (magnefect nano system; nanoTherics). The shRNA interference experiment consisted of the following three conditions: 1) 7.5 ug of pAAV-hSYN-eGFP, 2) 3.5 µg of scrambled shRNA and 3.5 µg of pAAV-hSYN-eGFP, and 3) 3.5 µg of Ank3 shRNA1 and 3.5 µg of pAAV-

hSYN-eGFP. These plasmids were transfected 3 days *in vitro* (DIV) and the cortical neurons were fixated on 14 DIV. The CRISPR-Cas9 interference consisted of the following plasmids with each 7.5 µg of DNA: 1) pAAV-SYN-eGFP, 2) pAAV-SYN-SaCas9-HA-Hu6-backbone, 3) pAAV-SYN-SaCas9-HA-hU6-sgRNA-1, 4) pAAV-SYN-SaCas9-HA-hU6-sgRNA-2. The cortical neurons were transfected on either 3- or 7 DIV and were fixated on 14 DIV for immunocytochemistry procedures and image acquisition.

(12) Immunocytochemistry

The cultured cells were fixated with 4% paraformaldehyde (PFA) in PBS for 10 minutes and were washed in PBS. The neurons were permeabilized by applying 0.3% triton (Sigma, X-100) detergent in PBS for five minutes and were afterwards washed in PBS. The cells were afterwards incubated with 3% bovine serum albumin (BSA) (Sigma, A7906) in PBS for 1 hour to prevent nonspecific binding by the primary antibody. The primary antibodies were diluted in 3% BSA and PBS and were added to the cells and kept overnight at 4°C. The primary antibodies used in the shRNA and CRISPR-Cas9 interference studies were anti-Pan-Neurofascin, (A12/18, 1:250, NeuroMab), anti-Ankyrin-G (N106/36, 1:250, NeuroMab or sc-28561, 1:250, Santa Cruz), and anti-HA epitope tag (16B12, 1:1000, Biolegend). Afterwards, the cells were washed and incubated in Alexa Fluor-conjugated secondary antibodies that were diluted in 3% BSA in PBS for 1 hour at room temperature. The secondary antibodies were purchased from ThermoFischer scientific. After secondary antibody incubation, the cells were washed in PBS and mounted in fluorsave reagent (Calbiochem, 345789).

(13) Image acquisition and analysis

The images of the axon initial segments were acquired by using an SP5 confocal with a 40x-oil objective using Leica software. The fluorescent intensities of AnkG and neurofascin were determined using ImageJ by manually drawing a ‘segmented line’ (ROI) over the AIS markers. The average AnkG and neurofascin intensities were calculated by measuring the fluorescence intensity over the ROI and subtracting the intensity in nearby background. The segmented line was approximately 80 µm in length. The raw average florescence intensity is shown in the graphs, or it was normalised to the average AIS intensity of control neurons and next classified as: complete AIS (71-100% AIS), knockdown (20-70% AIS), or knockout.

III. RESULTS

(1) Cellular toxicity following vector-mediated RNA interference

The shRNA plasmids were tested in cortical neurons *in vitro* before adeno-associated virus preparation. The plasmids containing the shRNA sequence for AnkG (Hedstrom *et al.*, 2008), or a scrambled shRNA (Hedstrom *et al.*, 2008), were co-expressed with an eGFP plasmid to highlight neuronal morphology after transfection. The embryonic day 18 cortical neurons were transfected utilizing magnetic nanoparticles on 3 days *in vitro* (DIV) and were examined on 14 DIV. The cultured neurons were stained for AnkG and neurofascin to visualize the axon initial segment. Neurons transfected with eGFP had an AIS and typical 14 DIV neuronal morphology (**Fig. 3 - left**). The axon initial segment of non-transfected neurons were also clearly visible throughout all experimental conditions (**Fig. 3**). However, neurons that were transfected with scrambled shRNA (**Fig. 3 - middle**) and the shRNA targeting AnkG (**Fig. 3 - right**) were dead. This shows that shRNA interference, delivered *via* plasmid transfection, causes cellular toxicity in primary cortical neurons.

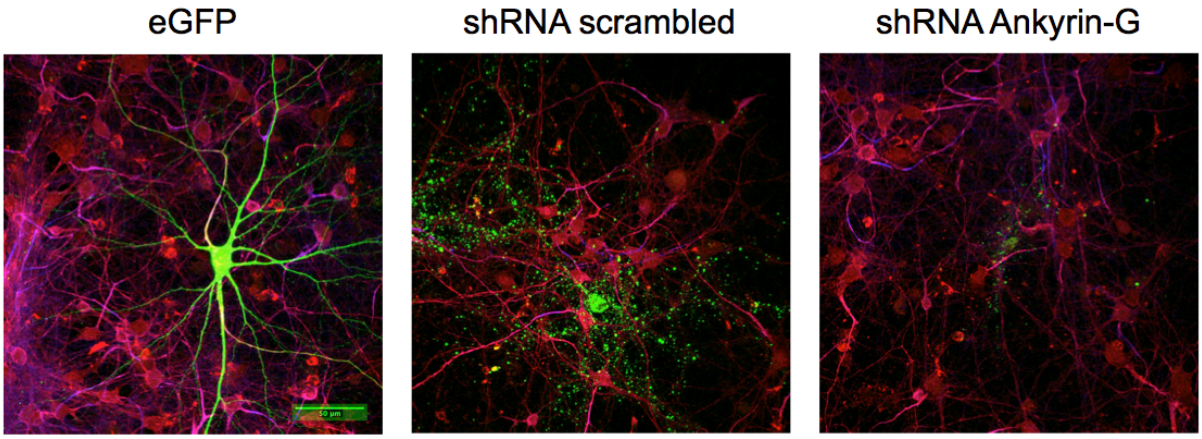

Fig. 3 shRNA interference caused cellular toxicity in primary cortical neurons after 11 days of plasmid transfection. The cells were cultured in high density and stained for AnkG (red) and neurofascin (blue), while the transfected neurons were eGFP-positive (green). Scale bar is 50 µm. Lab journal reference: BN-17-07

(2) Adeno-associated dual promoter construct containing SaCas9 and one sgRNA to target AnkG

After observing that the shRNA interference approach is not suitable for future experiments, we decided to switch to recent advanced technology for knockout of the AIS. The CRISPR-Cas9 technology was getting more accepted and frequency used for knockout of genes as of 2016. At this time, I modified an existing CRISPR-Cas9 plasmid (Addgene plasmid # 61591, Zhang) by swapping the CMV promoter, located upstream of the Cas9 enzyme sequence, for the SYN promoter in order to achieve neuron-specificity (see **Chapter IV**). The optimized plasmid is a dual promoter construct that is suitable for rAAV production. A shorter isoform of Cas9 (Staphylococcus aureus Cas9; SaCas9) is fused to a nuclear localization signal and a 3x HA-tag and is expressed under a hSYN promoter, while the RNA promoter hU6 drives the expression of the guide RNA of interest (**Fig. 4**). The utilization of the short SaCas9 sequence is crucial due to the limited packaging size of rAAVs. Two sgRNA sequences which interact in the first exon of the Ank3 gene (**Fig. 5**) were cloned downstream of the hU6 promoter to generate plasmids that could dismantle the AIS. Future experiments aiming to knockout gene of interests will therefore consist of four conditions: pAAV-SYN-eGFP (vector control), pAAV-SYN-SaCas9-HA-hU6-backbone (control for SaCas9), pAAV-SYN-SaCas9-HA-hU6-sgRNA-1, pAAV-SYN-SaCas9-HA-hU6-sgRNA-2 (experimental groups).

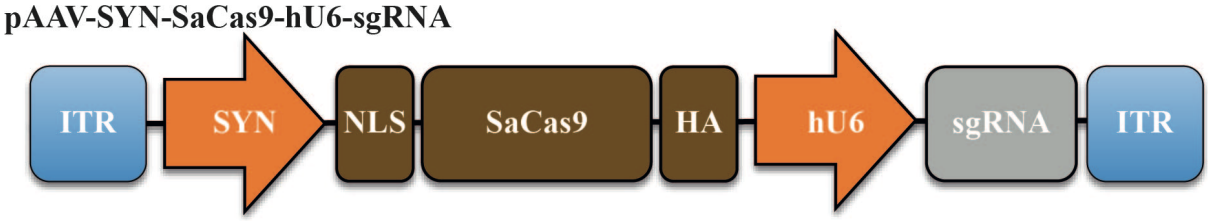

Fig. 4 Schematic representation of the adeno-associated dual promoter construct containing Cas9 from Staphylococcus aureus (SaCas9) and one cloning site for sgRNA insertion. The SYN promoter expresses SaCas9 that is fused to Simian vacuolating virus 40 nuclear localization signal (NLS) and 3x HA tag. The hU6 promoter is upstream of a BsaI cloning site to express any single guide RNA (sgRNA) of interest. The packaging cassette has a total length of 4473 basepairs and are flanked by inverted terminal repeats (ITR). The bovin growth hormone polyadenylation signal (BGHpA) is not shown. Lab journal reference: BN-16-19.

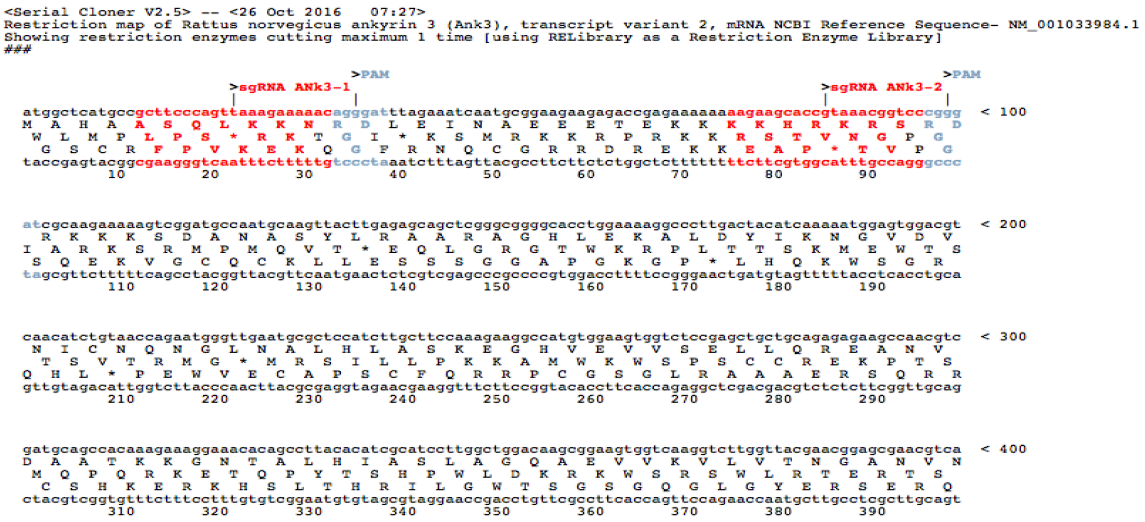

Fig. 5 Schematic showing the beginning 400 nucleotides of the rat ANK3 gene and highlights two target DNA sequences (red) upstream of two PAM sites (NNGRRT) (blue). Annealed DNA oligonucleotides encoding these target sequences were sub-cloned downstream of the hU6 promoter of plasmid pAAV-SYN-SaCas9-HA-hU6-backbone to complete the guide RNA. Lab journal reference: BN-16-20.

(3) SaCas9 alone also does not cause neuronal toxicity nor influences the axon initial segment

To examine whether the CRISPR-Cas9 strategy is viable in primary cortical neurons, the cells were co-transfected on 3 DIV, with the plasmid pAAV-SYN-eGFP and pAAV-SYN-SaCas9-HA-hU6-backbone, and fixated on 14 DIV. The eGFP-transfected neurons had green fluorescence spread throughout the cell, and have an axon initial segment (**Fig. 6A**). The neurons that were transfected with the CRISPR-Cas9 construct were immunelabelled for the HA-tag that is fused to the SaCas9 sequence. In contrast to the eGFP condition, the SaCas9 was mainly localized in the cell body and initial parts of neurites only (**Fig. 6B)**. The 14 DIV neurons that were transfected with SaCas9 without guide RNA were alive and have an axon initial segment (**Fig. 6B**). There was no statistically significantly difference in the fluorescent intensities of AnkG (**Fig. 6C**) and Neurofascin (**Fig. 6D**). The intensities of the AIS markers were measured over the same distance in the axon (**Fig. 6E**). In contrast to the shRNA interference approach, the CRISPR-Cas9 technology is suitable for experiments and does not exhibit any visible toxicity, via plasmid overexpression, in primary neuronal cultures.

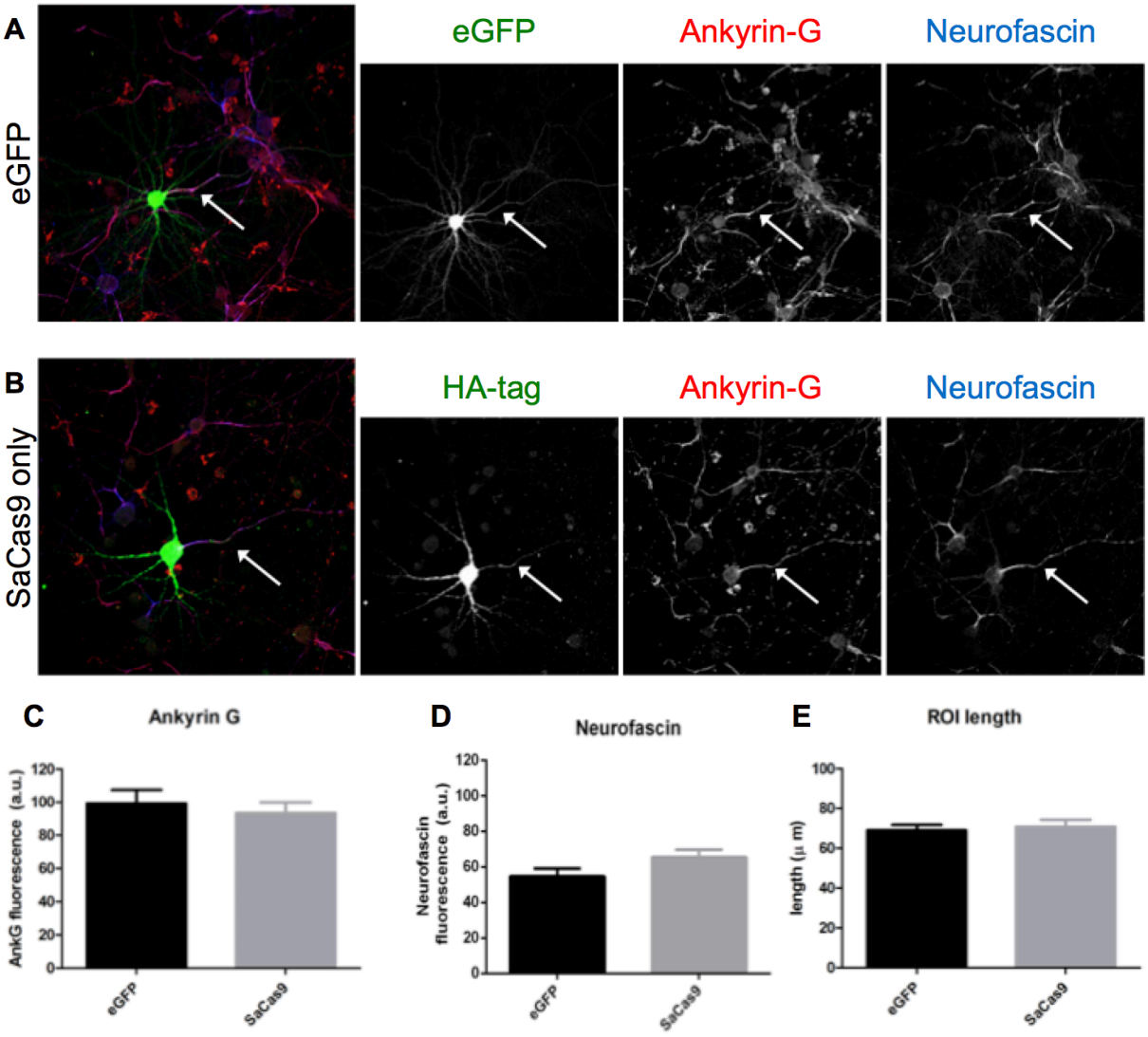

Fig. 6 Validation of the pAAV-SYN-SaCas9-hU6-backbone construct (plasmid 698 in the Cambridge and Amsterdam plasmid databases) in primary cortical neuron cultures. Rat cortical neurons were transfected on 3 DIV with pAAV-SYN-eGFP (A) and pAAV-SYN-SaCas9-hU6-backbone (B), and were stained on 14 DIV for HA-tag (green), Ankyrin-G (red), and Neurofascin (blue). The confocal scanning microscope settings for the red and blue channels were identical; the green intensity setting for exogenous eGFP or the labelled HA-tag differs between the two experimental conditions. (C) Quantification of Ankyrin-G fluorescent intensity ($P > 0.05$, Student's t-test). (C) Quantification of the of Neurofascin fluorescent intensity ($P > 0.05$, Student's t-test). (D) Quantification of the length that was measured as region of interest ($P > 0.05$, Student's t-test). The graphs depict the averages and standard error of the mean. A total of 20 cultured cells were measured for the eGFP condition, and 18 cells for the SaCas9 only condition. Lab journal reference: BN-16-33

(4) Axon initial segment knockout in a proportion of neurons following CRISPR interference after 11 days of transfection

After confirming that SaCas9 itself does not influence the axon initial segment (**Fig. 6**), two CRISPR-cas9 vector plasmids containing sgRNA-targeting AnkG were tested on their potential capacity to dismantle the axon initial segment. The plasmids were transfected on two different time points and fixated on 14 DIV. The half-live time of the AnkG protein in cultured hippocampal neurons was estimated on 14 days in a previous study (Hedstrom *et al.*, 2008).

When the neurons were transfected on 7 DIV and fixated on 14 DIV not a single neuron had a complete knockout of the axon initial segment. There was only a small reduction of the AnkG fluorescent intensity with the sgRNA-2 condition after seven days of transfection (**Fig. 7A**). No difference was found in the average fluorescence intensity of neurofascin (**Fig. 7B**). Thus, seven days is not sufficient to dismantle the axon initial segment after plasmid transfection.

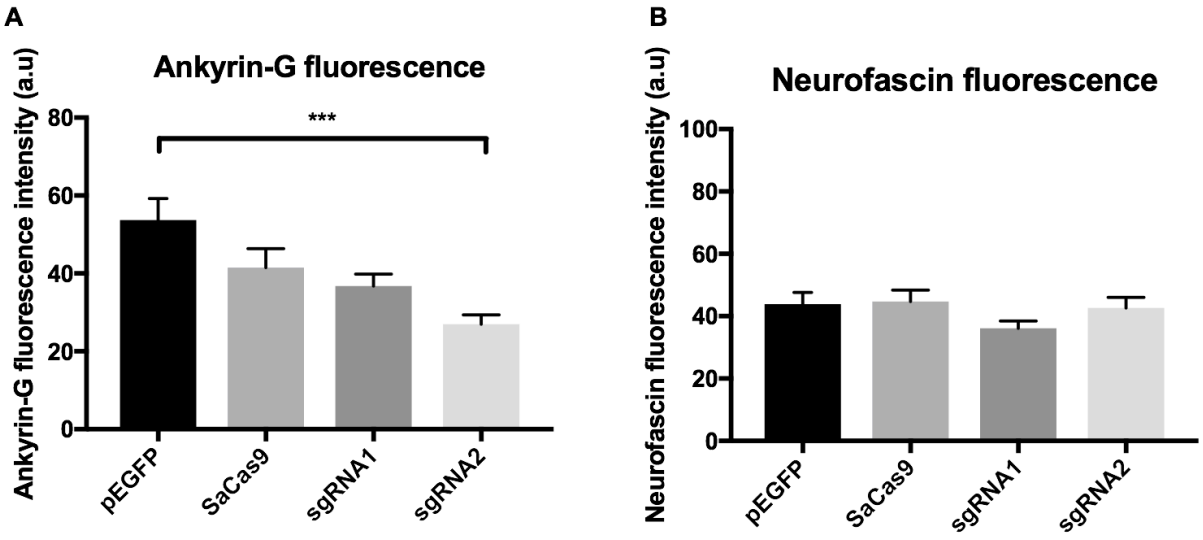

Fig. 7. Seven days of plasmid transfection with sgRNA-1 and sgRNA-2 is not sufficient for complete knockout of the AIS. Quantifications of the protein fluorescent intensities for Ankyrin-G (A) (4 groups and a total of 85 values, K-W=16.8, P<0.001, Kruskal-Wallis test with multiple comparison test) and Neurofascin (B) (df=3(81), F=1.03, P>0.05, ANOVA with Tukey's multiple comparison test). The graphs represent the averages and standard error of the mean. Lab journal reference: BN-16-04

In a follow-up experiment, the neurons were transfected on 3 DIV and kept in the cell culture dish until 14 DIV. As expected, the neurons in the eGFP and the SaCas9 without sgRNA condition all had an axon initial segment (**Fig. 8,** see also **Fig. 6**). **Fig 8A** shows examples of transfected neurons that completely lost their AIS in the sgRNA1 and sgRNA2 experimental conditions. These HA-tagged neurons lost both AIS proteins AnkG and

neurofascin. However, the complete knockout of AnkG (**Fig. 8B**) and the removal of neurofascin (**Fig. 8C**) was observed only in a small proportion of neurons. Knockout of the AIS was observed in 26% and 28% of the neurons that were transfected with the CRISPR-Cas9 constructs containing sgRNA1 and sgRNA2, respectively. Thus, the time period of eleven days after transfection results in dismantling of AIS in a small proportion of neurons using CRISPR interference.

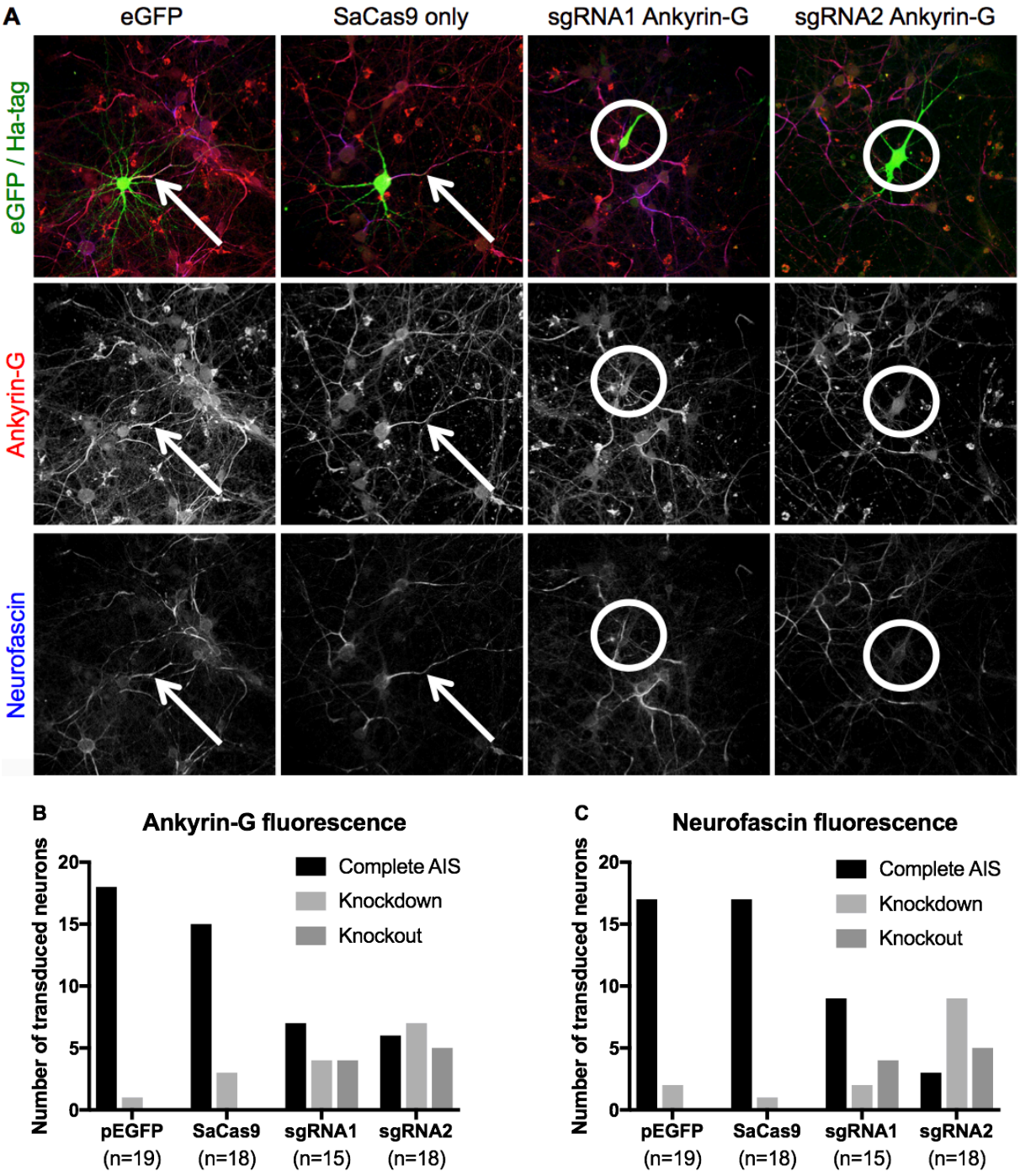

Fig. 8. – previous page - Pilot experiment for the knockout efficiency of the AIS by the CRISPR-cas9 constructs containing sgRNA for AnkG. (A) Examples of neurons that were transfected with the plasmids pAAV-SYN-eGFP, pAAV-SYN-SaCas9-hU6-backbone, pAAV-SYN-SaCas9-hU6-sgRNA-1, pAAV-SYN-SaCas9-hU6-sgRNA-2 on 3 DIV and were fixated on 14 DIV for AIS analysis. (B) Categorization of neurons based on their fluorescent intensity for Ankyrin-G. (C) Categorization of neurons based on their fluorescent intensity for Neurofascin. Complete AIS was classified as 70- till 100% of fluorescence intensity compared to the average normalized intensity of eGFP transfected neurons, knockdown was classified as an fluorescence intensity less than 70% compared to the average of normalized controls, a knockout was classified as complete absence of AIS staining in the transfected neuron. The number of cells for each condition is mentioned in the graphs, this experiment was done once (n=1). Lab journal reference: BN-16-33.

IV. DISCUSSION

This chapter describes plasmids for shRNA interference and CRISPR-Cas9 to knockout AnkG. Both tools for AnkG knockout were tested in cultured cortical neurons and were examined for their ability to dismantle the AIS. The hypothesis whether loss-of function of the AIS can promote axonal transport of integrins *in vivo* has not been investigated yet.

(1) Toxicity in primary cortical neurons by expressing short hairpin RNAs

The cloning of the shRNA plasmid was more difficult than expected. The main challenge that I encountered was the removal or modification of the short hairpin sequence during transformation. The use of the GT116 bacterial strain is crucial for cloning plasmids that contain hairpin structures or ITR repeats. *E.coli* have genes (e.g SbcCD) that encode nucleases that remove hairpin loops from plasmid DNA (Connelly, Kirkham, & Leach, 1998), which make shRNA-containing plasmids instable in most bacteria. The GT116 bacterial strain has these nuclease genes depleted and are therefore more suitable for shRNA cloning. DNA sequencing indeed revealed that the short hairpins were modified (e.g. removed, incomplete, and reversed) when other bacterial strains were used during transformation (data not shown). The BglII restriction digestion prior transformation is also key to increase the number of shRNA-positive colonies (first year report).

This study observed that shRNA interference induced cellular toxicity in primary cortical neuronal cultures. Despite that expression of shRNA has been a popular method to knockout proteins, there are studies that also reported neuronal toxicity (Ulusoy *et al.*, 2009; Ehlert *et al.*, 2010; Khodr *et al.*, 2011; Martin *et al.*, 2011). AAV5-mediated delivery of scrambled-shRNA and shRNA targeting tyrosine hydroxylase in the substantia nigra resulted in neuronal cell loss (Ulusoy *et al.*, 2009). Consistently, delivery of control and shRNA targeting α-synuclein in this brain area, via AAV2, resulted in neuronal degeneration (Khodr *et al.*, 2011). Another study observed cell death in the red nucleus after AAV1-mediated

delivery of scrambled- and shRNA targeting neuropilins (Ehlert *et al.*, 2010). AAV1 was also used to delivery shRNA in the striatum of two mouse lines which also resulted in toxicity and animal illness (Martin *et al.*, 2011). Above studies are consistent with our *in vitro* study, showing that shRNA vectors cause neuronal cell death. Importantly, the cultured neurons that were non-transfected or transfected with eGFP had healthy morphology suggesting that the delivery method is not the reason of toxicity.

Overexpression of the shRNA plasmids possibly overtake the endogenous siRNA machinery in cells (Grimm *et al.*, 2006). The abundance of the H1-promoter driven shRNA can occupy Exportin-5 and thereby prevent the transportation of endogenous RNA into the cytoplasm (Yi *et al.*, 2005, Grimm *et al.*, 2006). The binding competition for this transporter protein also inhibits the efficiency of the RISC complex (Bennasser *et al.*, 2011). The brain may be in particular more vulnerable to this as exportin-5 is expressed in relatively low levels (Yi *et al.*, 2005). The saturation of these key factors in the RNAi machinery may explain observed neuronal cell death.

(2) CRISPR-Cas9 interference for Ankyrin-G

Neurons remained healthy after introducing the CRISPR-Cas9 vector plasmid via transfection. The SaCas9 protein was visualised by staining for the HA-tag and we observed that this DNA endonuclease becomes localised in the soma and proximal parts of neurites. In contrast, transfection of eGFP results in a cytoplasmic expression pattern visualising the entire morphology of the neuron. This validates that the nuclear localization signal attached to the SaCas9 protein is functional. This is an important observation because the SaCas9 needs into the cell nucleus for inducing double strand breaks in DNA. The presence of SaCas9 in the proximal parts of the neurites could be explained by translation of the overexpressed SaCas9 plasmid by cytoplasmic ribosomes in the cell, while this local translated SaCas9 is trafficked towards the nucleus via the nuclear localization tag. Importantly, delivery of the SaCas9 without sgRNA did also not affect the AIS. In summary, the delivery of SaCas9 without sgRNA into cortical neurons does not induce neuronal toxicity and does not induce changes in the axon initial segment. Thus, vector-mediated expression of SaCas9 can be successfully applied *in vitro*.

The two designed target sequences for AnkG do interfere with the AIS. We found that the CRISPR-Cas9 vector plasmid needs to be applied for a long time-period to knockout AnkG. This is most likely due to the long half-live of the AnkG protein. In order to achieve successful AnkG knockout, gene expression needs to be prevented and afterwards the endogenous AnkG protein in the AIS need to be degraded. Hedstrom *et al.*, 2008

demonstrated that the half-live time of endogenously expressed AnkG is at least two weeks in cultured hippocampal neurons. Our study indeed failed to observe a complete AnkG knockout at four- (not shown), and seven days post-transfection. Yet, we observed knockout in a small proportion of neurons after eleven days post-transfection. This is indeed consistent with the suggested stable half-live of AnkG. Yet, we do not know what is the time needed for indel induction by SaCas9. The activity dynamics of SaCas9 could therefore be another rate limiting step for protein knockout. Furthermore, the cultured cortical neurons are heterogeneous population of cells each may have a different axon initial segment fluorescent intensity. Importantly, this study found that neurofascin failed to localise at the AIS as consequence of AnkG knockout as suggested by previous studies (Zhou *et al.*, 1998, Jenkins & Bennett, 2001; Hedstrom *et al.*, 2007). This confirms that AnkG is crucial to sustain the AIS and is a valid target to dismantle this important structure.

The designed sgRNA2 seems more efficient than sgRNA1 to knockdown and knockout AnkG in cortical neurons. I recently found that sgRNA1 targets only the long isoform of Ank3 (see second start codon 'ATG' at position 50 in **Fig. 5**), while sgRNA2 correctly targets both the short and long neuronal isoforms of Ank3.

The CRISPR-interference can be further improved in this study. Firstly, the CRISPR-Cas9 vector plasmid can be applied for a fourteen-day period to match the AnkG half-live time. The earliest time point for a magnetofection reaction that results without neuronal cell death is 2 DIV (Fallini, Bassell, & Rossoll, 2010; see Chapter III, section II.3) and cell cultures can be maintained healthy until 16-18 DIV. This longer time period should enhance the number of cells with successful AnkG knockout. Secondly, the examination of AnkG knockout per transduced neuron can be simplified by co-transfection of an eGFP plasmid, as this visualises the entire neuronal morphology including the proximal part of the axon. Thirdly, the experiment should be repeated, as the current n-number of this study is 1. In addition to examine protein knockout, it will be extremely interesting to perform single-cell DNA sequencing of a transduced neuron and examine whether a double strand break is induced in the target DNA region.

The next important step will be to investigate whether the CRISPR-cas9 interference is functional *in vivo*. Based on the finding of **Chapter IV**, the plasmids can be used for the preparation of recombinant adeno-associated viral vectors with serotype 1 for optimal neuronal transduction in the cortex. The first experiment should be focussed on the detected of SaCas9 in the nucleus of CNS neurons. Daniella Carulli (Netherlands Institute for Neuroscience) tested my CRISPR construct designed for Sema3A in the cerebellum with the AAV1 serotype and found that SaCas9 was localised in the cell body of Purkinje neurons.

She observed that the control vectors without targeting guide RNA were many localised in the cytoplasm of the cell body, while the vectors containing the guide RNA were more frequently found in the nucleus. The second experiment should validate whether the designed sgRNA for Ank3 can dismantle the AIS, by co-staining for the HA-tag, NeuN, AnkG or another AIS protein. I experienced that immunohistochemistry for AnkG can be difficult in cortical tissue *in vivo*. The primary antibodies N106/36 by NeuroMab and sc-28561 by Santa Cruz for AnkG with 1:500 dilution needs to be incubated for three days at four degrees Celsius, or kept overnight at room temperature for successful detection of AnkG in PFA-perfused tissue (Lab journal reference: BN-18-05). The validation of the CRISPR constructs *in vivo* will be crucial for future experiments.

It remains unclear whether the AIS contribute to the axonal transport block of integrins *in vivo*. This research question could be addressed by comparing the following two experimental conditions *in vivo*: 1) co-injection of AAV1-SYN-α9integrin-V5 and AAV1-SYN-SaCas9-HA-hU6-sgRNA-2 2) co-injection of AAV1-SYN-α9integrin-V5 and AAV1-SYN-eGFP. Staining for the V5-epitope fused to integrins will visualize the potential mis-trafficking of integrins into the axon following AnkG knockout.

(3) Dismantling the axon initial segment to stimulate axonal regeneration

Dismantling of the axon initial segment is one strategy to force integrins to enter the axons of the adult CNS neurons. We hypothesize that knockout of AnkG could permit regeneration-associated receptors to travel down the axon of adult CNS neurons *in vivo*. Disadvantages of dismantling the AIS are: 1) the deregulation of action potential propagation and 2) the loss of neuronal polarization. Loss of neuronal polarization and action potential propagation may not necessarily impair the intrinsic axonal regeneration response. However, these functions are essential for neuronal communication and the innervation of target cells after regeneration. Nevertheless, it is essential to demonstrate the proof-of principle that dismantling of the AIS allows integrins into the axons of the corticospinal tract *in vivo* before performing spinal cord injury experiments. If we can first show that dismantling the AIS is indeed essential for successful axon regeneration, a strategy that temporarily dismantle the AIS (namely during the post-lesion period during which axon regeneration takes place) could overcome the above discussed disadvantages.

CHAPTER III - Phosphoinositide 3-kinases promote axon elongation and regeneration of cultured cortical neurons

DECLARATION:

The material in this chapter has not been published at the time of dissertation submission. A shorter version of this chapter will be used for scientific publication after the submission of this dissertation.

I declare that this work was done in collaboration with below scientist, and their contribution is the following:

Joachim Fuchs and Britta Eickholt (Charité University Medicine Berlin) developed the immunocytochemistry procedures to detect PIP_3.

James Fawcett supervised the project.

Richard Eva made Fig. 4 and supervised the project.

I, Bart Nieuwenhuis, made the plasmids, performed the *in vitro* experiments, did the quantifications and analysis of the data, made the figures (except Fig. 4), and wrote the manuscript.

ACKNOWLEDGMENTS:

I would like to acknowledge Veselina Petrova and Elise Laperrousaz for assistance with some of the neuronal cell cultures.

I. INTRODUCTION

The phosphorylation and dephosphorylation of inositol lipids control an orchestra of cellular mechanisms. Inositol lipid signalling is involved in cell growth, differentiation, migration, and survival among other essential functions (reviewed in Falasca & Maffucci, 2012; Hawkins & Stephens, 2016; Backer, 2016). The most evolutionary conserved function of phosphoinositide kinases is the trafficking of vesicles between cellular organelles (Herman, 1990; Backer, 2016). The inositol lipids are also crucial for axon growth and development of the nervous system (reviewed in RodgersTheibert *et al*., 2002; Cosker & Eickholt, 2007; Waite & Eickholt, 2010) Due to the diverse roles of inositol lipid, the signalling pathway is complex and involves many signalling cascades.

(1) Signalling

Phosphatidylinositols (PIPs) are localised at the plasma membrane and have three hydroxyl sites (named 3,4,5) that can be modified by (de-) phosphorylation. These three sites give rise to seven unique phosphoinositides with each being involved in different signalling cascades. Here, we focus will be on phosphatidylinositol 4,5-bisphosphate (PIP_2) and phosphatidylinositol (3,4,5)-trisphosphate (PIP_3) that are modified by the enzymes called phosphatase and tensin homolog (PTEN) and class I Phosphoinositide 3-kinase (PI3K). Importantly, PI3K phosphorylates the 3'-hydroxyl site of PIP_2 to generate PIP_3, while PTEN is a 3'-phosphatase that turns PIP_3 back into PIP_2 (see **Fig. 1**).

There are four class I PI3K isoforms that participate in different signalling pathways: P110α, P110β, P110γ, and P110δ. These isoforms originate from different genes, PIK3CA, PIK3CB, PIK3CG, and PIK3CD, and are expressed in different cell types. Importantly, the activity of the PI3K isoforms depends on upstream cell surface receptor activation. Integrins signalling (Watabe *et al.*, 2011; Niu *et al.*, 2012) *via* FAK (Chen *et al.*, 1996), and other receptors such as TrkB (Tang *et al.*, 2002; Yoshii & Constantine-Paton, 2007) and IGFR-1 (Ou *et al.*, 2014) are known to activate PI3K (see **Fig. 1**). The kinases P110α and P110β are ubiquitously expressed throughout the body, while P110γ, and P110δ are mainly found in immune cells (reviewed in Fruman *et al.*, 2017). A study with LacZ reporter mice highlighted that P110α is ubiquitously expressed in the nervous system, while P110δ is expressed in peripheral nerves, DRGs and the spinal cord of embryonic mice (Eickholt *et al.*, 2007). RNA sequencing data from our laboratory confirmed that P110α is expressed in cultured cortical neurons, while P110β, P110γ and P110δ were expressed in relatively low levels or were not detected (Koseki et al., unpublished; Smith et al., unpublished).

The generated PIP_3 at the inner surface of the plasma membrane is a secondary messenger in many cellular processes. Here, I categorized PIP_3 signalling in three common pathways: (1) neuronal growth and survival; (2) calcium regulation; and (3) cytoskeleton and protein trafficking (see **Fig. 1**). Thus, targeting PI3K influence a wide range of cellular responses including those beneficial for axonal regeneration.

PIP_3 signalling is regulated by negative signalling feedback loops (see **Fig. 1**). The most important and upstream feedback loop is phosphatase PTEN. After PIP_3 is generated, PTEN can immediately end PIP_3 signalling by reversing PIP_3 into PIP_2. A recent study found that S6 Kinase 1 (S6K), which is downstream of mTOR, also acts as a negative regulator of PIP_3 signalling and its mediated neuronal growth (Al-Ali *et al.*, 2017). S6K interact with IRS-1 (Tremblay *et al.*, 2007; Zhang *et al.*, 2008), and this may be one of the mechanisms to attenuate PI3K signalling.

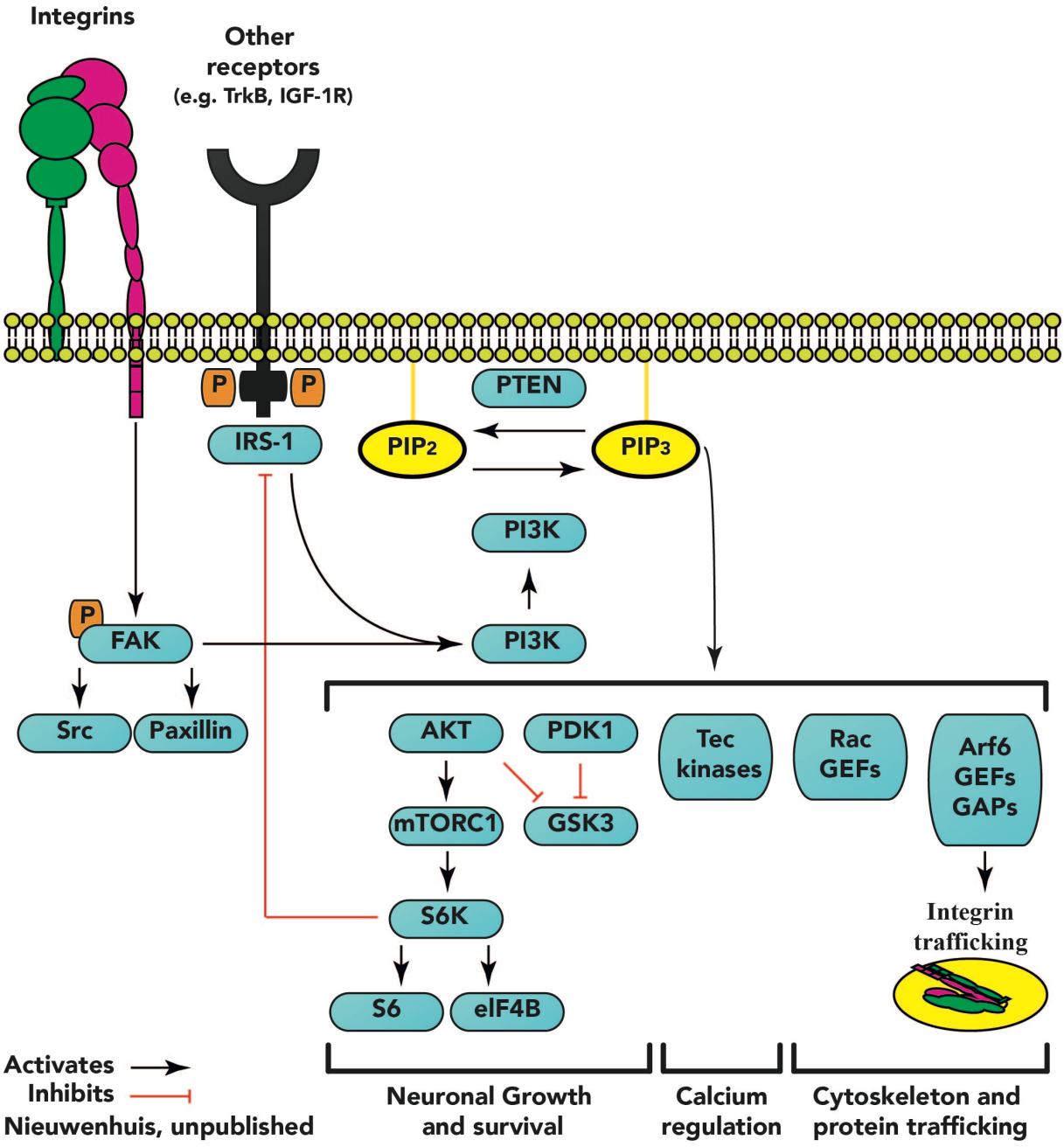

Fig. 1. Schematic of PIP_3 signalling. Ligand binding to cell-surface receptors activates many kinases including phosphoinositide 3-kinase (PI3K). PI3K converts PIP_2 into PIP_3, which in turn, activates a diverse range of cellular functions including neuronal growth and survival, calcium regulation, and cytoskeleton and protein trafficking. PIP_3 signalling is inhibited by negative feedback loops within the pathway. Firstly, phosphatase and tensin homolog (PTEN) dephosphorylates PIP_3 and generates PIP_2. Secondly, S6K1 is a negative regulator of PIP_3 and mediated outgrowth, but the mechanisms remain to be elucidated.

(2) PTEN knockout and axonal regeneration

Many studies aim to boost the intrinsic regeneration response of CNS neurons. That PIP_3 signalling is crucial for axonal regeneration is clearly demonstrated by genetic deletion of PTEN. Removal of PTEN activates the PIP_3 signalling cascade. Conditional PTEN knockout mice resulted in a strong effect on CNS axonal regeneration *in vivo* (Park *et al.*, 2008; Liu *et al.*, 2010). Park et al., (2008) injected AAV2-eGFP or AAV2-Cre two weeks prior optic nerve crush in the conditional PTEN knockout mice to assess whether PTEN is an inhibitor of regeneration. As expected, RGCs injected with AAV2-eGFP were not capable to regenerate their axons beyond the injury site. Genetic deletion of PTEN doubled the survival rate of RGCs and 10% of the RGCs regenerated approximately 3 mm beyond the crush site. The authors confirmed that PTEN deletion enhanced the mTOR pathway by staining for phospho-S6 ribosomal protein (pS6) (see **Fig. 1**), which is a marker for initiation of protein translation. There was an increase of pS6 in the regenerating neurons of PTEN knockout mice (Park *et al.*, 2008). Liu et al., (2010) went a step further and examined the effect of PTEN knockout on corticospinal tract regeneration after spinal cord injury. AAV2-eGFP or AAV2-Cre was injected in the sensorimotor cortex four-week prior (T8) spinal cord crush. Genetic deletion of PTEN resulted in corticospinal tract regeneration into the lesion site and 3 mm beyond the site of injury, while controls did not. Consistent with the study in the optic nerve, the PTEN deletion prevented down-regulation of pS6 in corticospinal neurons after injury (Liu *et al.*, 2010). Surprisingly, the regenerating axons of the PTEN deleted neurons also formed (vGlut1-positive) synapses. Another research group utilized a similar experimental design with the PTEN conditional knockout mice, and found enhanced forelimb motor functional recovery after (C5) spinal cord contusion injury (Danilov & Steward, 2015). Compared to interventions that also successfully enhanced the intrinsic axonal regeneration response of the corticospinal tract, such as overexpression of transcription factors KLF7 (Blackmore *et al.*, 2012) and Sox11 (Wang *et al.*, 2015b), genetic deletion of PTEN is possibly the most successful strategy today. However, studies that interfered with PTEN via AAV-shRNA-PTEN, an approach that is clinically relatively more feasible than genetic deletion, were less successful (Zukor *et al.*, 2013; Lewandowski & Steward, 2014). Nevertheless, the PTEN knockout studies showed that PTEN is an important inhibitor of axonal regeneration. Despite the upregulation of pS6, the exact mechanisms and downstream PIP_3 signalling responsible for the observed axonal regeneration remains poorly understood.

(3) PI3K and axonal regeneration

The known effects of PI3K on axonal regeneration in the peripheral nervous system stems from studies that inhibited the endogenously expressed kinase. After establishing that P110α and P110δ are expressed in the peripheral nervous system (Eickholt et al., 2007; Eva et al., unpublished), their importance for axonal regeneration was examined. Eickholt et al., 2007 used transgenic mice expressing a PIK3CD-inactive mutation (PIK3CD D910A) and performed a sciatic nerve crush. The inactivation of P110δ impaired the initiation of axonal regeneration, as there were less axonal fibers beyond the injury site compared to wild type after three days post-injury. However, there was no significant difference between the transgenic mice and control seven days post-injury, suggesting that other factors such as the ATF3 transcription factor and P110α can still stimulate regeneration in the PNS. Nevertheless, the inactivation of P110δ impaired functional recovery including locomotion and grasping (Eickholt *et al.*, 2007). As expected, the inactivation of P110δ alters the PIP_3 signalling pathway in cultured DRG neurons (after NGF stimulation) and brain extracts. Neurons with inactive P110δ had less phosphorylation of Akt and S6K, while the expression of axon growth inhibitor RhoA was increased (Eickholt *et al.*, 2007).

Eva et al., (unpublished) inhibited various PI3K isoforms in cultured adult DRGs before *in vitro* laser axotomy. Naïve adult DRG had an average regeneration percentage of 70%, and inhibition of certain PI3K isoforms influenced this outcome. DRG neurons inhibited for P110α and P110δ had a regeneration rate of 30%, and 35% respectively. Inhibition of the non-neuronal P110β isoform did not affect the regeneration capacity of DRG neurons.

In summary, the P110α and P110δ isoforms are expressed in the peripheral nervous system and contribute to their regenerative capacity.

(4) Decline of PIP_3 signalling during maturation of CNS neurons

Our laboratory has the hypothesis that the PIP_3 signalling pathway becomes less active in the axon when CNS neurons mature. Here, we discuss three components that we believe that contribute to the developmental decline of axonal PIP_3 signalling: (1) exclusion of regeneration-associated receptors from the axon, (2) down regulation of PI3K, and (3) down regulation of pS6.

We discussed in Chapter I Sections VII and VIII, that growth-associated cell-surface receptors are not localised in the axons of the adult corticospinal tract. The exclusion of integrins (Franssen *et al.*, 2015; Andrews *et al.*, 2016), TrkB (Yan *et al.*, 1997; Lu *et al.*, 2001; Hollis *et al.*, 2009b), and IGF-1R (Hollis *et al.*, 2009a) from the axon has consequences for PIP_3 signalling. These cell-surface receptors are essential for the activation of PI3Ks and therefore PIP_3 signalling. Hence, the exclusion of cell-surface receptors contributes to a decline in PIP_3 signalling and the corresponding poor intrinsic regeneration capacity after injury.

In addition to a decline in the receptor-mediated activation of PI3K, our laboratory has unpublished data showing that PI3K itself is down regulated during maturation of CNS neurons. Koseki et al., (unpublished) performed an RNA sequencing experiment at different time points on cortical neurons that were cultured to maturity (up to 24 days *in vitro*). As expected, the genes PIK3CB and PIK3CG were not expressed in cortical neurons. PIK3CA was expressed in relative high levels at 1 DIV (RNA score: 16) and was drastically decreased in expression levels towards maturity (24 DIV, RNA score: 7). PIK3CD was expressed in low levels throughout polarisation of the neurons (Average RNA score: 6.0). Thus, there is developmental decline in the expression of PI3K in cultured cortical neurons.

When CNS neurons mature, there is also a decline in the phosphorylation of Ribosomal protein (S6), which is downstream in the PIP_3/mTOR pathway (see **Fig. 1**). This developmental decline in pS6 was shown *in vivo* in retinal ganglion cells (Park *et al.*, 2008) and cortical neurons (Liu *et al.*, 2010).

(5) Hypothesis 'understanding regenerative failure'

We hypothesize that the developmental decline in axonal PIP_3 signalling contributes to restricted axonal regeneration in the CNS. In other words, there are insufficient growth and survival molecules in mature CNS axons for successful regeneration: the signalling receptors and PIP_3 levels are sparse.

(6) Aim of study

Because of the importance of PIP_3 signalling in growth and regeneration, we explored whether a gain-of-function approach of PI3K isoforms could promote axonal regeneration of CNS neurons *in vitro*. Because the P110α and P110δ isoforms are important for axonal regeneration in the PNS (see Section I.3), it would be reasonable to expresses or activate these kinases in the CNS to promote regeneration. In addition, we investigated the effect of one PIK3CA-activation mutation, PIK3CA H1047R. This substitution of the histidine (H) to arginine (R) enhances the affinity of P110α towards the plasma membrane (Zhao & Vogt, 2008; Burke *et al.*, 2012; Hon, Berndt, & Williams, 2012) and hyper-activates the PIP_3 signalling pathway (Wu *et al.*, 2014).

II. MATERIALS AND METHODS

(1) DNA constructs

pHR-eGFP and pHR-PI3KCD were a gift from Klaus Okkenhaug (Babraham Institute, Cambridge) and were used for subsequent cloning. pHR-PI3KCA was made by amplifying the PI3KCA sequence from pBabe puro HA PIK3CA, a gift from Jean Zhao (Addgene plasmid # 12522), via the primers 5' GTGTGGATGTGATGAATACTTCC 3' and 5' GGAGGCCAATCTTTTACCAAGC 3' and was cloned into pHR-eGFP between the BamH1 (NEB, R0136) and Not1 (NEB, R0189) digestion site. pHR-PI3KCA H1047R was made by cloning the mutated PI3KCA sequence from pBabe puro HA PIK3CA H1047R, which was a gift from Jean Zhao (Addgene plasmid # 12524), into pHR-eGFP via the same procedures as pHR-PI3KCA. A schematic representation of the four dual promoter plasmids is shown in **Fig. 2**.

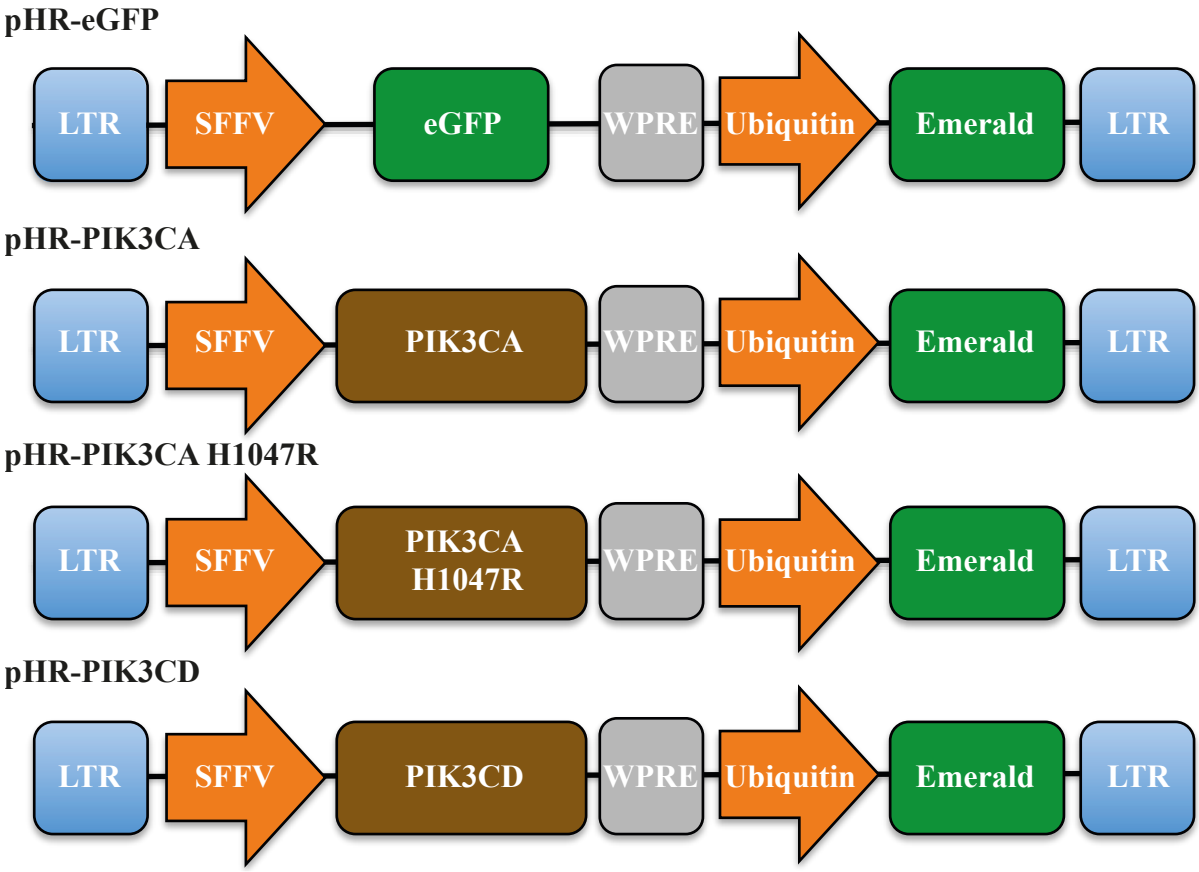

Fig. 2. Schematic representation of lentiviral dual promoter constructs. All constructs express emerald green fluorescent protein (Emerald) under the Ubiquitin promoter. The spleen focus forming virus (SFFV) promoter flanked by a woodchuck hepatitis virus post-transcriptional regulator element (WPRE) drives the expression of enhanced green fluorescent protein (eGFP), PIK3CA, PIK3CA H1047R, or PIK3CD, respectively. The packaging cassettes are flanked by long terminal repeats (LTR). Note: the SFFV promoter had been shown to be capable to successfully drive the expression of transgenes in corticospinal neurons *in vivo* (Yip et al., 2010). Lab journal reference: BN-15-23.

(2) Cortical neuron cultures

Primary cortical neuron cultures were prepared from embryonic day 18 Sprague Dawley rats. Extensive details are described in Chapter II section II.11 and a short summary is below. The neurons were dissociated with papain (Worthington, LK003176) for 10 minutes at 37°C. They were next briefly rinsed with DNase (Sigma, D5025) and washed with HBSS (Gibco, 14170) containing HEPES buffer solution (Gibco, 15630). The neurons were cultured in neural Q basal medium (Globalstem, gsm9420), supplemented with GS21 (Amsbio, gsm3100) and glutamax (Gibco, 35050) and plated on glass bottom cell cultures dishes (Greiner bio-one, 627860) coated with poly-D-lysine in borate buffer.

(3) Magnetofection

The cortical neurons were transfected at 2 days *in vitro* (DIV) or 10 DIV by using oscillating nanomagnetic transfection (magnefect nano system; nanoTherics). The DNA constructs (7 µg per dish) were mixed with 8 µl of magnetic nanoparticles (NeuroMag, NM50200) in 100 µl of culture medium and were incubated for 30 minutes. The culture media was substituted for the transfection mixture, and 900 µl of neuronal media, and afterwards the dishes were placed over a magnetic array, which was moving laterally at 2 Hz and at 0.2 mm amplitude of displacement for 30 minutes at 37°C in a 7% Co_2 incubator. After the transfection, the original culture medium was returned to each well and the neurons were cultured until 4- or 14 DIV.

(4) BDNF stimulation

Cultured pH-eGFP transfected neurons were treated with 400 ng/ml of lyophilized human BDNF protein (RAB0026-1VL-KC) in neural Q basal medium (Globalstem, gsm9420) for 10 minutes before fixation.

(5) Immunocytochemistry

The cultured cortical neurons were fixed with 4% paraformaldehyde (PFA) in PBS for 10 minutes and were washed in PBS. The PFA fixated cells were permeabilized by applying 0.3% triton (Sigma, X-100) detergent in PBS for five minutes and were afterwards washed in PBS. Neurons that were used to stain for α5 integrin were fixed at 14 DIV with cold methanol for 10 minutes. The cells were blocked with 3% bovine serum albumin (BSA) (Sigma, A7906) in PBS for 1 hour. After blocking, the cells were incubated with primary antibodies diluted in 3% BSA in PBS at 4°C overnight. The primary antibodies used were anti-phospho-S6 ribosomal protein (Ser235/236) (4857, 1:200, Cell signaling technology), anti-Rab11 (71-5300, 1:50, ThermoFischer scientific), anti-eGFP (A10262, 1:1000, ThermoFischer scientific), Anti-integrin α5 (AB1928, 1:500, Merck), Anti-Pan-neurofascin (A12/18, 1:200, NeuroMab). Afterwards, the cells were washed and incubated in Alexa Fluor-conjugated secondary antibodies that were diluted in 3% BSA in PBS for 1 hour at room temperature. The secondary antibody used were anti-chicken IgY conjugated to Alexa Fluor 488 (A-11039, 1:1000, ThermoFischer scientific) anti-rabbit IgG conjugated Alexa Fluor 568 (A10042, 1:500, ThermoFischer scientific), anti-mouse IgG conjugated Alexa Fluor 660 (A21055, 1:500, ThermoFischer scientific). The cells were mounted using fluorsave^{tm} reagent (Calbiochem, 345789).

(6) Immunocytochemistry for PIP_3

The procedures to detect PIP_3 were developed by Joachim Fuchs and professor Britta Eickholt (Charité University Medicine Berlin). Low-density cultures were fixated using a pre-warmed (37°C) mixture of 4% PFA and 0.2% glutaraldehyde (GA; G011/3, TAAB Laboratories) in PBS for 15 minutes at room temperature. The GA was added to the PFA because it makes larger crosslinkers than PFA to stabilize lipids in addition to proteins. After fixation, the tissue was washed in 50mM ammonium chloride (NH_4CL) in PBS to remove the fixative and to quench autofluorescence by PFA/GA. The tissue was stored at 4°C until further use, or directly placed on a metal plate with ice for further immunocytochemistry procedures to limit the diffusion of lipids. Pre-chilled blocking (and permeabilisation) solution consisting of 0.2% saponin, 50mM NH_4CL and 3% BSA in PBS was incubated on the cells for 30 minutes at 4°C. The cells were incubated in purified anti-PtdIns(3,4,5)P3 monoclonal antibody (Z-P345b, 1:200, Echelon) in blocking solution for two hours at 4°C. After PIP_3 labeling, the cells were washed in 50mM NH_4CL in PBS for 30 minutes at 4°C. The PIP_3-labbeled cells were post-fixated in 4% PFA in PBS for 5 minutes on ice and 10 minutes are room temperature. After the post-fixation, the cells were washed at room temperature. The cells were permeabilized with blocking solution for 30 minutes at room temperature. After blocking and re-permeabilisation, the secondary antibody anti-mouse IgG conjugated Alexa Fluor 568 (A11004, 1:1000, ThermoFischer scientific) was applied and incubated for 1 hour at room temperature. The cells were washed and afterwards mounted using fluorsave^{tm} reagent.

(7) Neurite outgrowth assay

Cultured cortical neurons were transfected at 2 DIV and immunocytochemistry procedures were done at 4 DIV to enhance the eGFP fluorescence intensity. Images for neuronal morphology were acquired using a fluorescence microscope (BMI-8, Leica) with a 20x light objective using Leica software. The 15 longest neurons for each condition were analysed. Neurons with less than three minor neurites were excluded; hence only polarised neurons were included for image analysis. The neurite lengths were measured using a plugin of the software ImageJ entitled ‘simple neurite tracer’ (Longair, Baker, & Armstrong, 2011).

(8) Morphology analysis of 14 DIV cortical neurons

Images for neuronal morphology of 14 DIV neurons were captured on a fluorescent microscope (DM6000 B, Leica) with a 40×-oil objective using Leica software. For the purpose of sholl analysis, it is crucial that the soma is located in the middle of the acquired image to measure the dendritic branches for 150 μm around the soma. Semi-automated and standardized analysis of neuronal morphology was performed using MATLAB platform version 2017 and the program called SynD (Schmitz *et al.*, 2011). SynD detects the soma by tresholding and component analysis and afterwards detects the neurites by applying steerable filters at the immunofluorescence images. We manually extended neurites that were not completely traced and removed any unwanted crossing of neurites from a different neuron. In addition, we excluded spines that were identified as neurite by SynD. The output of SynD was used for data analysis and includes dendritic length, fluorescent intensities, sholl analysis, and soma size. Prism 7 for Mac OS X was used for statistical analysis.

(9) *In vitro* laser axotomy

In vitro laser axotomy (see **Fig. 3**) was used to study whether overexpression of PI3K promotes axon regeneration in CNS neurons. Cortical neurons were cultured and transfected with pHR-eGFP, pHR-PIK3CA, pHR-PIK3CA H1047R, pHR-PIK3CD on 10 DIV. The four experimental conditions were laser axotomised in a random order on 13 DIV, 14 DIV, 15 DIV, or 16 DIV, and this was repeated for three independent neuronal cultures (**Fig. 3A**). The axon was axotomised at a minimum distance of 1000 μm distal to the soma and on a region that was free from axonal branches. The laser axotomy was done using a 355 nm DPSE laser (Rapp OptoElectronic, Hamburg, Germany) connected to a Leica DMI6000B microscope with Hamamatsu EM CCD C9100 camera. The site of injury was imaged every 30 minutes for 14 hours. The proximal site of the axotomised axon was classified as no regeneration or regeneration (see **Fig. 3B**). Regeneration was defined as the formation of a growth cone followed by axon extension for at least 50 μm. No regeneration was defined as a surviving axon that did not regrow beyond 50 μm. Leica LAS AF software was used to analyse the injured axons for length of axon retraction, initiation time of axon regeneration, and length of axon regeneration. The statistical tests for each experiment are shown in the figure legends.

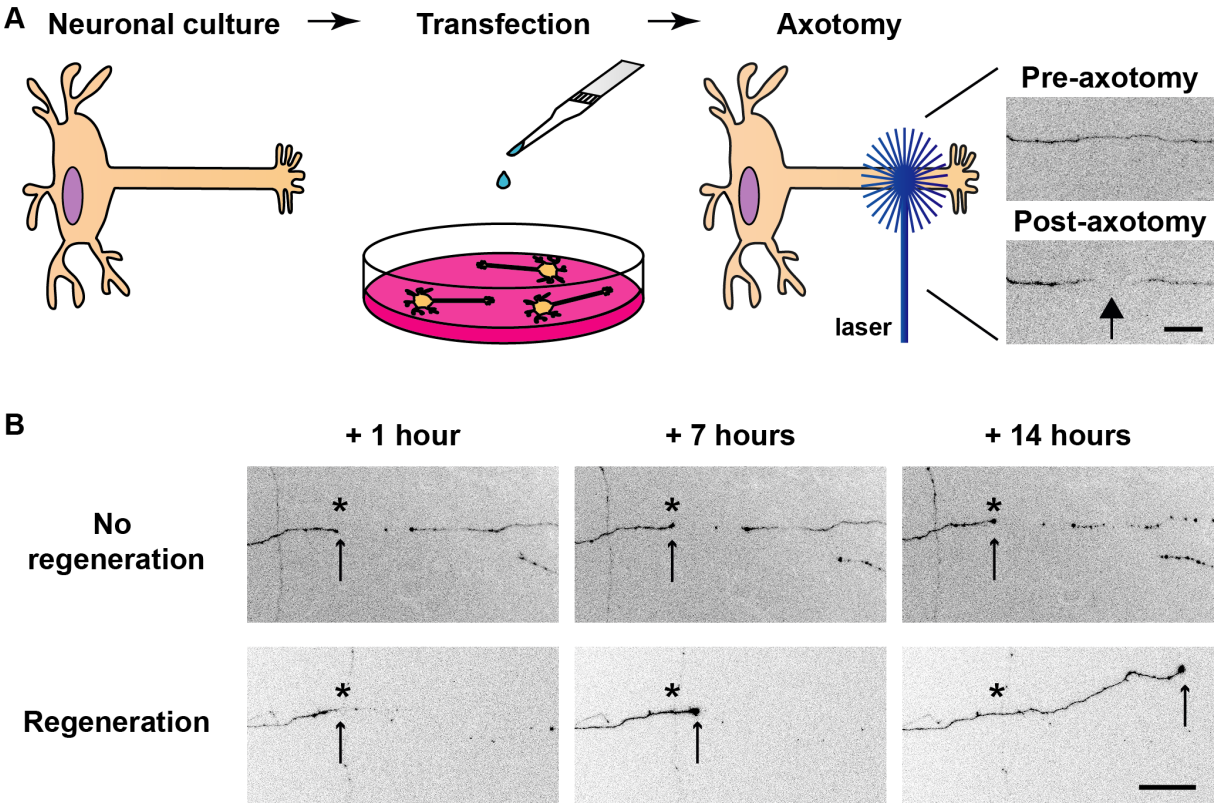

Fig. 3. Cell culture model to study the intrinsic axonal regeneration response. (A) A three-step set-up to investigate axonal regeneration in cultured neurons. In this example, primary cortical neurons were plated on a glass-bottomed imaging dish and were transfected with various DNA plasmids. The axons of the transfected neurons underwent laser axotomy and were video recorded for 14 hours. The arrow shows the site of injury. (B) Representative images of a non-regenerating axon (upper panels) and a regenerating axon (lower panels) from cortical neurons that were cultured for two weeks. The asterisk indicates the location of the proximal stump after one-hour post-axotomy, while the arrow marks the growth cone at indicated time-point. The scale bars are 50 µm. This figure was published in Nieuwenhuis & Eva, 2018a.

(10) Statistical analysis

Statistical analysis was performed by using Graphpad Prism 7 for Mac OS X. All statistical tests and parameters are mentioned in the figure legends. The graphs represent the average for each condition together with the standard error of the mean (SEM), while the individual data points for each investigated cell are illustrated as dots. One-way ANOVA with Tukey's multiple comparison was most frequently used in this chapter as one dependent variable (e.g. neurite length or fluorescent intensity) was examined in four experimental groups. However, if the data distribution breaks the statistical assumption of equal variance in ANOVA (e.g. $P < 0.05$ in the Brown-Forsythe test or Barlett's test) then a Kruskal Wallis with Dunn multiple comparison test was performed. The statistical test for the sholl analysis in **Fig. 6C** was a repeated measure ANOVA followed by Bonferroni multiple comparison tests as an interaction/correlation between the two independent variables 'number of branches' and 'distance from soma' was examined between four experimental groups.

III. RESULTS

(1) Reduction of PIP_3 during maturation of cortical neurons *in vitro*

Neurons lose their intrinsic regeneration capacity in line with maturation. Here, we investigated whether is a decline in PIP_3 during maturation of cortical neurons *in vitro*. Embryonic day 18 cortical neurons were cultured and fixated on 3 DIV and 17 DIV. Specific immunocytochemistry procedures for PIP_3 were performed for both conditions at once. The immunofluorescence intensity is different between 3 DIV and 17 DIV neurons (**Fig. 4**). Developing neurons had relatively high PIP_3 levels, which is mainly localised in the soma and distal end of the axon and the growth cone (**Fig. 4A**). Maturing neurons had relatively low levels of PIP_3 through out the cells (**Fig. 4B**).

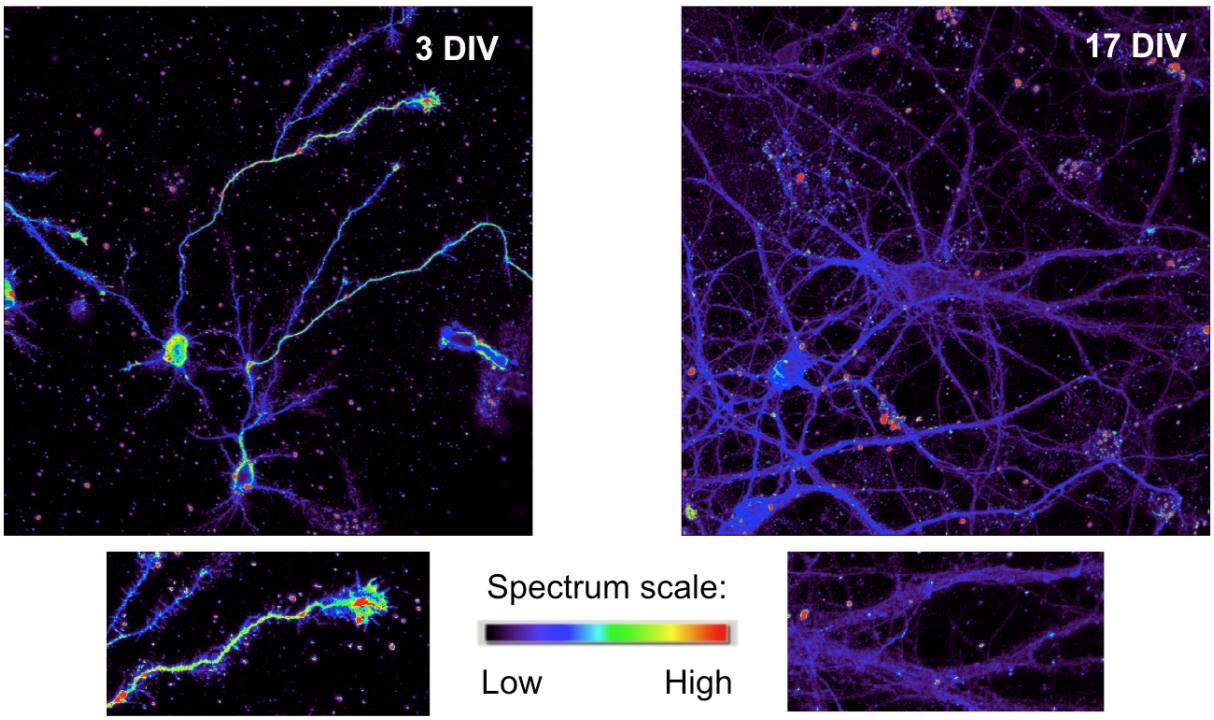

Fig. 4. Immunofluorescence intensities for PIP_3 in cultured cortical neurons at different time points. E18 cortical neurons were cultured and fixated on 3 DIV and 17 DIV. After fixation, the neurons were stained for PIP_3 and the immunofluorescence intensity was compared. (A) Representative 3 DIV neurons with zoom in on the growth cone (B) Representative 17 DIV neurons with a zoom-in on neurites. The images are shown in spectrum scale: blue indicates low fluorescence intensity, red indicates high florescence intensity.

(2) PI3K promotes axon elongation of developing cortical neurons *in vitro*

Before doing axonal regeneration experiments *in vitro*, we investigated whether PI3K overexpression affects axon development. For this purpose, cortical neurons were transfected with pHR-eGFP, pHR-PIK3CA, pHR-PIK3CA H1047R and pHR-PIK3CD on 2 DIV and fixated on 4 DIV for morphological analysis. Neurons expressing pHR-eGFP had an axon (see the longest neurite, black arrows) with a length of approximately 500 μm (**Fig. 5A, 5B**). Gain of PIK3CA function did not affect the axon length, while neurons expressing PIK3CA H1047R and PIK3CD had a twice-longer axon than eGFP and PIK3CA transfected neurons (**Fig. 5A, 5B**). The length of dendrites (see minor neurites, red arrows) was similar between eGFP- and PIK3CA transfected neurons. Expression of PIK3CA H1047R and PIK3CD overexpression lead to a relatively small increase in dendritic growth (**Fig. 5A, 5C**). Overexpression of PI3K approach did not affect neuronal polarization because the axons were clearly visible and approximately 20 times larger than the dendrites in all conditions (**Fig. 5D**).

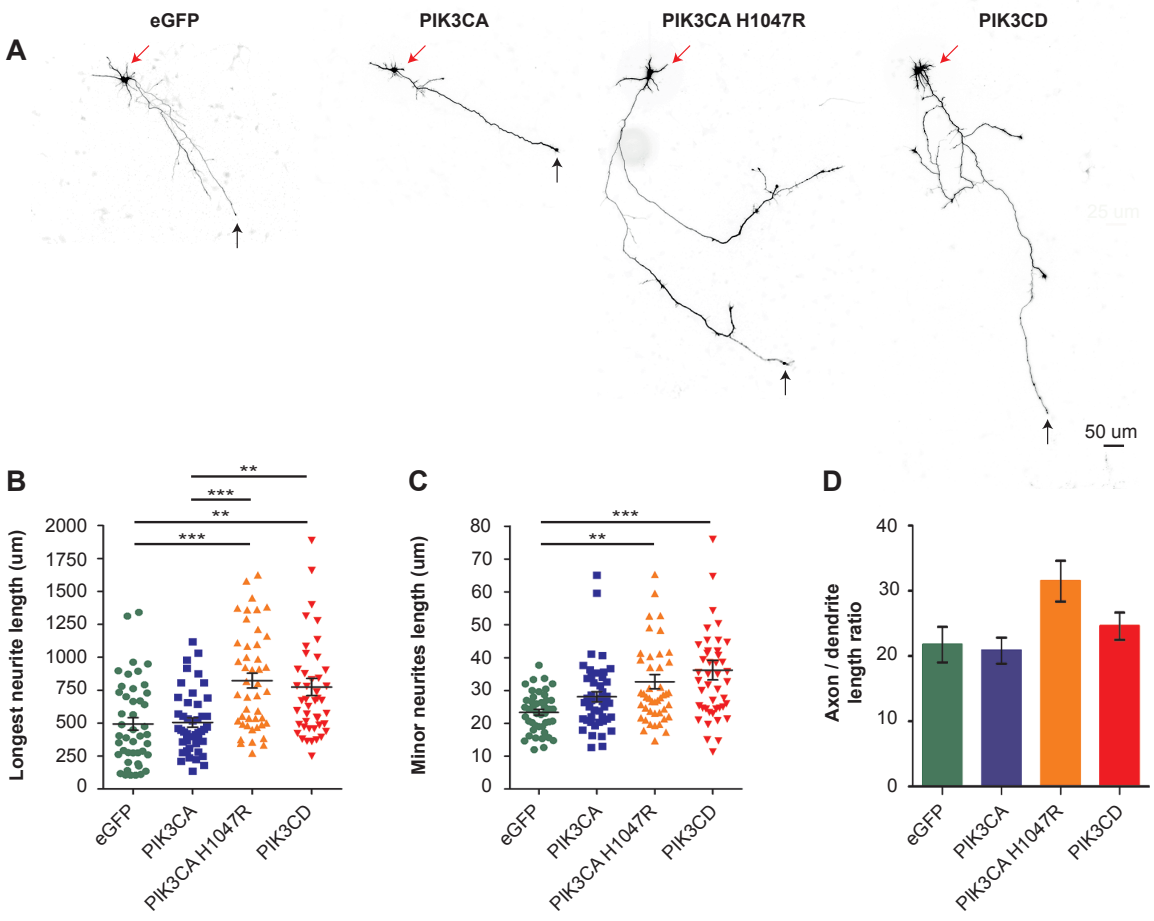

Fig. 5. PIK3CA H1047R and PIK3CD promote axon elongation of developing cortical neurons. E18 cortical neurons were cultured and transfected on 2 DIV. (A) Representative 4 DIV pHR-eGFP, pHR-PIK3CA, pHR-PIK3CA H1047R and pHR-PIK3CD transfected neurons. (B) Quantification of the axon length (back

arrow) ($P < 0.001$, Kruskal-Wallis with Dunn multiple comparison test). (C) Quantification of average dendrites length (red arrow) ($P < 0.001$, Kruskal-Wallis with Dunn multiple comparison test). (D) Quantification of the axon versus dendrite length ratio ($P < 0.05$, Kruskal-Wallis with Dunn multiple comparison test). ** $P<0.01$; ***$P<0.001$. Lab journal references: BN-17-27, BN-17-29, BN-17-30.

(3) PI3K overexpression induces morphology alterations and pS6 signalling in cultured cortical neurons

The effect of PI3K overexpression on neuronal morphology was also studied in more mature cortical neurons *in vitro*. To this aim, cortical neurons were transfected on 10 DIV and analyses were performed on 14 DIV after fixation. Neuronal morphology and pS6 immunofluorescence were analysed using the MATLAB based program SynD (Schmitz *et al.*, 2011). The morphology of the neuron was identified by the expression of emerald green fluorescent protein (Emerald) (**Fig. 6A**) and pS6 was visualised by immunofluorescence (**Fig. 6B**). Sholl analysis showed that the dendritic branching of eGFP and PIK3CA transfected neurons were quite similar, while PIK3CA H1037R and PIK3CD overexpression lead to more highly branched neurons compared to eGFP and PIK3CA (**Fig. 6C**). Consistent with the sholl analysis, the total measured neurite length was different between the four conditions (**Fig. 6D**). The eGFP and PIK3CA transfected neurons had a similar neurite length. The PIK3CA H1047R and PIK3CD neurons had a higher total neurite length than eGFP and PIK3CA neurons. Gain of the PI3K isoforms function also influenced the soma size of the cultured cortical neurons (**Fig. 6E**). Expression of PIK3CA H1047R and PIK3CD enlarged the soma and this increase was statistically significant higher than eGFP and PIK3CA transfected neurons. The soma area of eGFP and PIK3CA were identical. The pS6 intensities were also different between the four conditions (**Fig. 6F**). The eGFP and PIK3CA transfected neurons had similar and relative low pS6 expression levels. Overexpression of PIK3CA H1047R and PIK3CD resulted in an approximately six-fold increase in pS6 intensity compared to eGFP and PIK3CA transfected neurons.

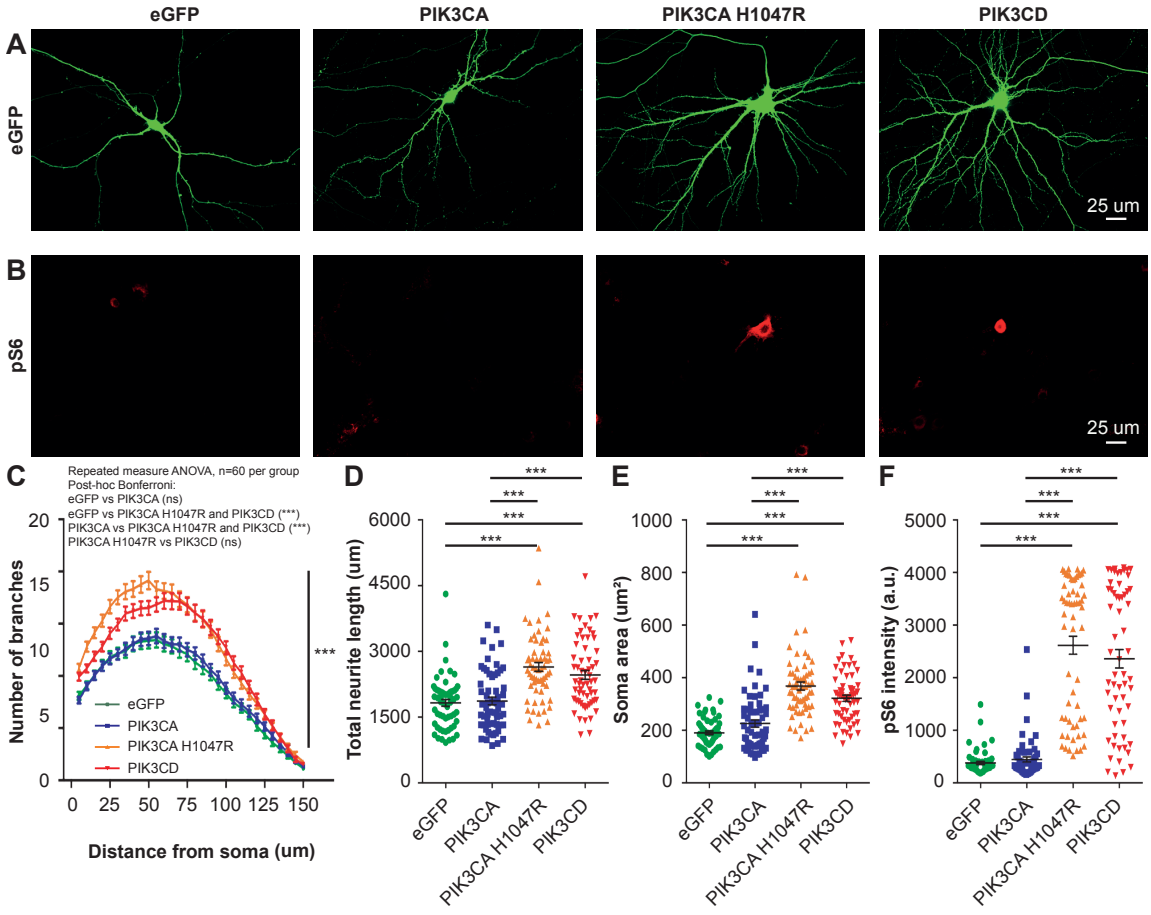

Fig. 6. PIK3CA H1047R and PIK3CD initiate morphological changes and enhance pS6 signalling, PIK3CA does not affect neuronal morphology and pS6 signalling. E18 cortical neurons were cultured and transfected on 10 DIV. Representative 14 DIV pHR-eGFP, pHR-PIK3CA, pHR-PIK3CA H1047R and pHR-PIK3CD transfected neurons with Emerald in (A) and pS6 immunofluorescence in (B). (C) Sholl analysis of neurite branches (df=3(316), F=7.00, P<0.001, Repeated measure ANOVA with Bonferonni's multiple comparison test, n = 80 per group). (D) Quantification of the total neurite length (df=3(236), F=20.7, P<0.001, ANOVA with Tukey's multiple comparison test). (E) Quantification of the soma area (P < 0.001, Kruskal-Wallis with Dunn multiple comparison test, n = 60 per group). (F) Quantification of pS6 immunofluorescence (P < 0.001, Kruskal-Wallis with Dunn multiple comparison test, n = 60 per group). The data shows the average ± SEM. The results are obtained from three independent cultures (n=3) and a total of 60 transfected neurons were analysed for each condition. ***P<0.001. Lab journal references: BN-17-05, BN-17-16, BN-17-42.

(4) Validation of pS6 immunofluorescences

Two control experiments were performed to validate the immunolabelling for pS6. Firstly, application of BDNF to cultured eGFP neurons resulted in an upregulation of pS6 (**Fig. 7A**) Secondly, pS6 immunofluorescence was not detected in PIK3CD transfected neurons that underwent immunocytochemistry procedures lacking the primary antibody for pS6 (**Fig. 7B**). These supplementary experiments demonstrate that the observed pS6 staining is part of the BNDF and PI3K signalling pathway, and the pS6 immunofluorescence is not due to unspecific binding by the secondary antibody.

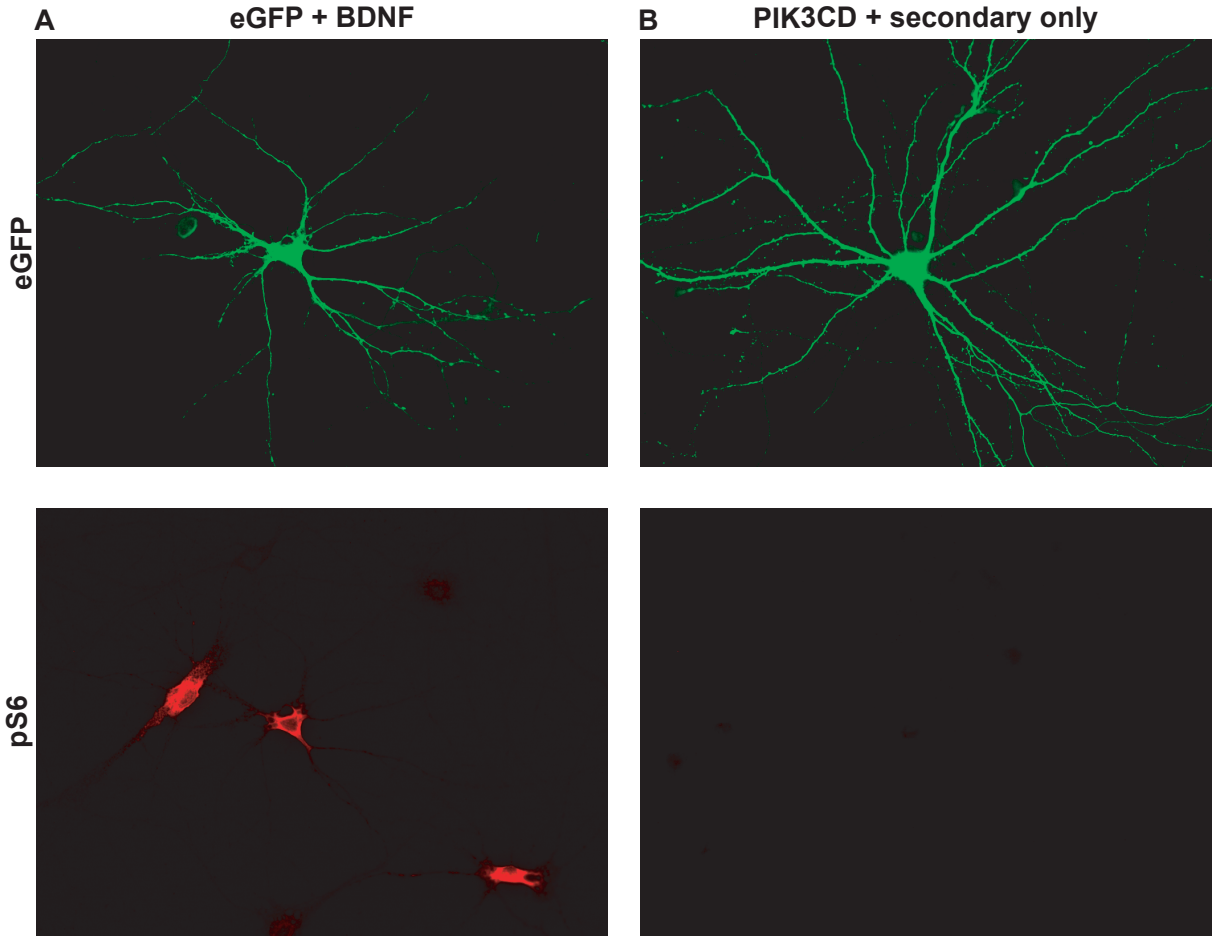

Fig. 7. Validation of pS6 immunofluorescence staining. E18 cortical neurons were cultured and transfected with pHR-eGFP or pHR-PIK3CD on 10 DIV. Exogenous Emerald fluorescence and pS6 staining are shown in the upper and bottom panel, respectively. (A) Representative eGFP transfected neuron that was treated with BDNF before fixation on 14 DIV. (B) Representative 14 DIV PIK3CD transfected neuron that was stained with the secondary antibody only.

(5) PIK3CA H1047R and PIK3CD promote axon regeneration of cortical neurons after in vitro laser axotomy

The effect of PI3K overexpression on axonal regeneration was investigated using *in vitro* laser axotomy (see **Fig. 3**). This method allows precise injury of the axon of individual cultured neurons. Cortical neurons were transfected on 10 DIV and axotomy was performed on 13 – 16 DIV. The axon of transfected neurons was identified based on their morphology. The axon is distinctly detectable at low objective magnification because of its length and absence of spines (**Fig. 7A**). The injured axons were imaged for 14 hour and were analysed for various regenerative indicators within this timeframe. There was a high survival rate of the neurons that underwent axotomy, as only a small proportion of the severed neurons died (**Fig. 8B**). Importantly, the regeneration capacity of the transfected neurons was different between the four conditions (**Fig. 8C**). As expected, eGFP transfected neurons had a poor regenerative capacity (11.9 ± 2.4 %) after two weeks in culture. The PIK3CA transfected neurons also had a low percentage of regenerating axons (22.3 ± 4.6 %), and this percentage was statically similar to eGFP. On the other hand, neurons transfected with PIK3CA H1047R (60.7 ± 4.4 %) and PIK3CD (52.3 ± 4.8 %) had a high percentage of regenerating axons, and this was statistically significant higher the eGFP and PIK3CA. There was no statistically significant difference in the length that the axon regenerated between the four conditions (**Fig. 8D**). However, there is clear trend that PIK3CA H1047R (179 ± 23 μm) and PIK3CD (172 ± 24 μm) transfected neurons regenerated longer distances compared to eGFP (94 ± 31.2 μm) and PIK3CA (101 ± 14 μm). There is small statistical difference in the growth cone size between the groups (**Fig. 7E**). The PIK3CA H1047R (17 ± 1 μm^2) had a slightly bigger growth cone than PIK3CD (13 ± 1.0 μm^2), while the other groups were statically similar. The time taken to form a growth cone and to successfully regenerate was identical between the four groups (**Fig. 8F**), with a minor trend toward quicker initiation of regeneration in the PIK3CA H1047R and PIK3CD groups. The retraction distance of all axotomised neurons was quite similar between the transfected neuron (**Fig. 8G**), however the PIK3CA H1047R (108 ± 8 μm) transfected neurons retracted slightly more than PIK3CA (64 ± 7 μm) transfected neurons.

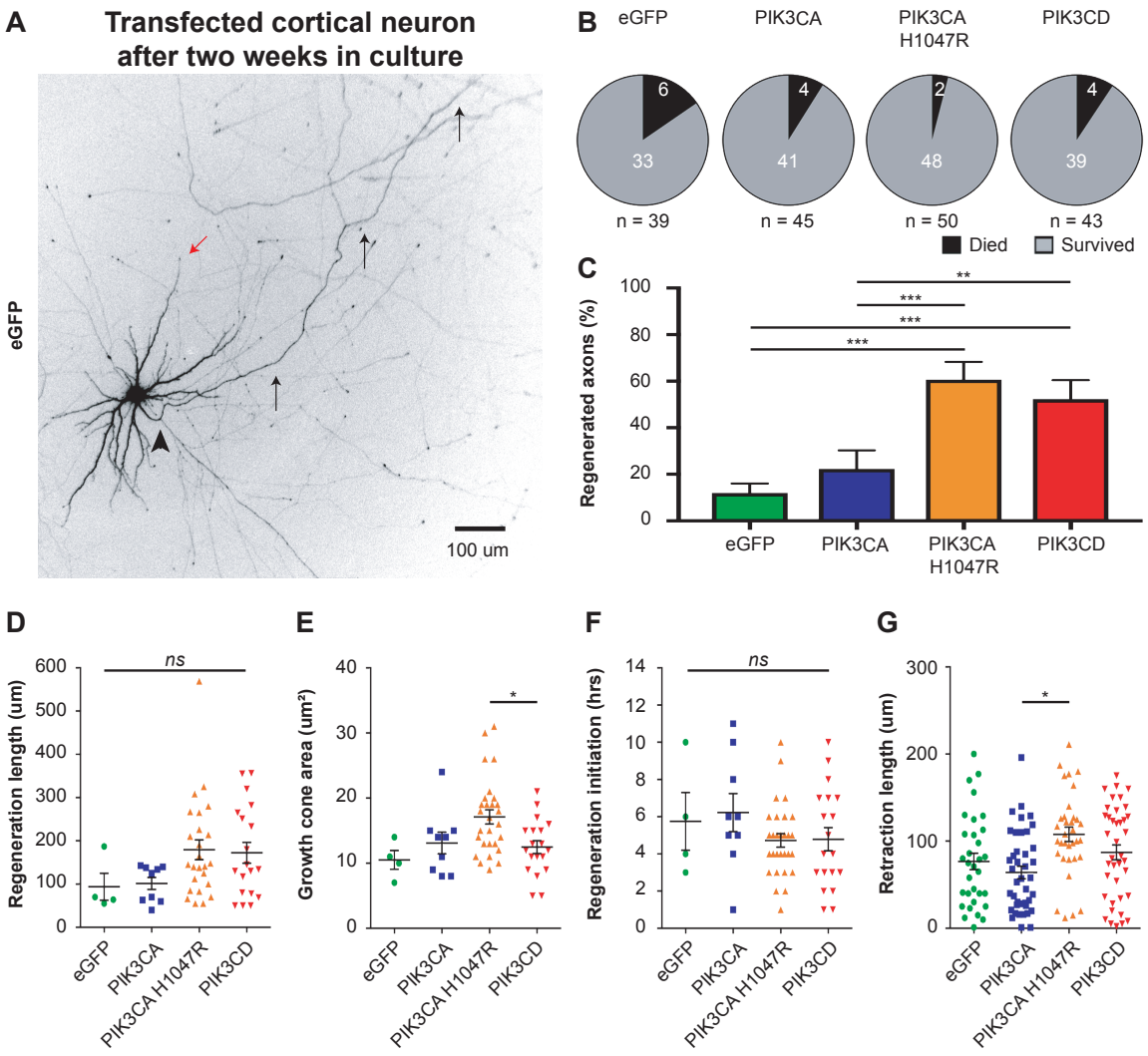

Fig. 8. PIK3CA H1047R and PIK3CD enhance the regenerative capacity of cortical neurons. E18 cortical neurons were cultured and transfected with the dual promoter constructs on 10 DIV. The transfected neurons underwent laser axotomy after two weeks of culture. (A) Axon identification of a cortical neuron on 14 DIV. Transfected neurons were visualised by exogenous emerald fluorescence. There is a clear morphological distinction between the axon and dendrites. The red arrow indicates a dendrite; the arrowhead highlights the axon initial segment; three arrows trace the proximal axon. (B) Total number of axotomised neurons together with their death and survival rates per experimental condition. (C) Percentage of regenerating axons within 14 hours after *in vitro* laser axotomy (df=3(8), F=0.154, P<0.001, ANOVA with Tukey's multiple comparison test). (D) Quantification of axon regeneration length after 14 hours post-axotomy (P > 0.05, Kruskal-Wallis with Dunn multiple comparison test). (E) Quantification of growth cone size (df=3(56), F=1.07, P<0.01, ANOVA with Tukey's multiple comparison test). (F) Quantification of regeneration initiation time (df=3(57), F=1.36, P>0.05, ANOVA with Tukey's multiple comparison test). (G) Quantification of retraction length after axotomy and, if applicable, before initiation a regenerating growth cone (df=3(142), F=1.01, P<0.01, ANOVA with Tukey's multiple comparison test). The data shows the average ± SEM. The results are obtained from three independent cultures (n=3) and the number of neurons analyzed in each group is shown in (B). Ns, not statistically significant; * P<0.05; ** P<0.01; ***P<0.001. Lab journal references: BN-17-32, BN-17-35, BN-17-41, BN-17-55, BN-17-56.

(6) PI3K does not affect endogenous Rab11 and α5 integrin transport in the axon

Previous studies have shown that cortical neurons at 14 DIV lack regeneration-associated receptors in their axon (Franssen *et al.*, 2015; Koseki *et al.*, 2017). As discussed in **Chapter 1**, promoting the transport of regeneration-associated receptors into the axon is one mechanism to enhance axonal regeneration. Here, we explored whether the expression of PI3K can induce mistrafficking of Rab11 vesicles and α5 integrins into the axon. The small GTPase Rab11 is of interest because they mark vesicles containing growth-associated receptors, including α5 integrin (reviewed in Nieuwenhuis & Eva, 2018b). Furthermore, it had been shown previously that axons with more Rab11 vesicles have an enhanced regeneration capacity after *in vitro* laser axotomy (Koseki *et al.*, 2017). As expected, Rab11 vesicles are found in the somatodendritic domain and detected in very low levels in the axons of eGFP-transfected neurons on 14 DIV (**Fig. 9**). Rab11 vesicles were also detected in low levels in the axon of neurons that were transfected with PIK3CA, PIK3CA H1047R or PIK3CD (**Fig. 9**). Consistent with the low levels of axonal Rab11 vesicles, α5 integrin was not detected in the axon and their localisation was limited to the somatodendritic domain in the four experimental conditions (**Fig. 10**). Thus, PI3K overexpression does not affect the distribution of endogenous Rab11 and α5 integrin in 14 DIV cortical neurons.

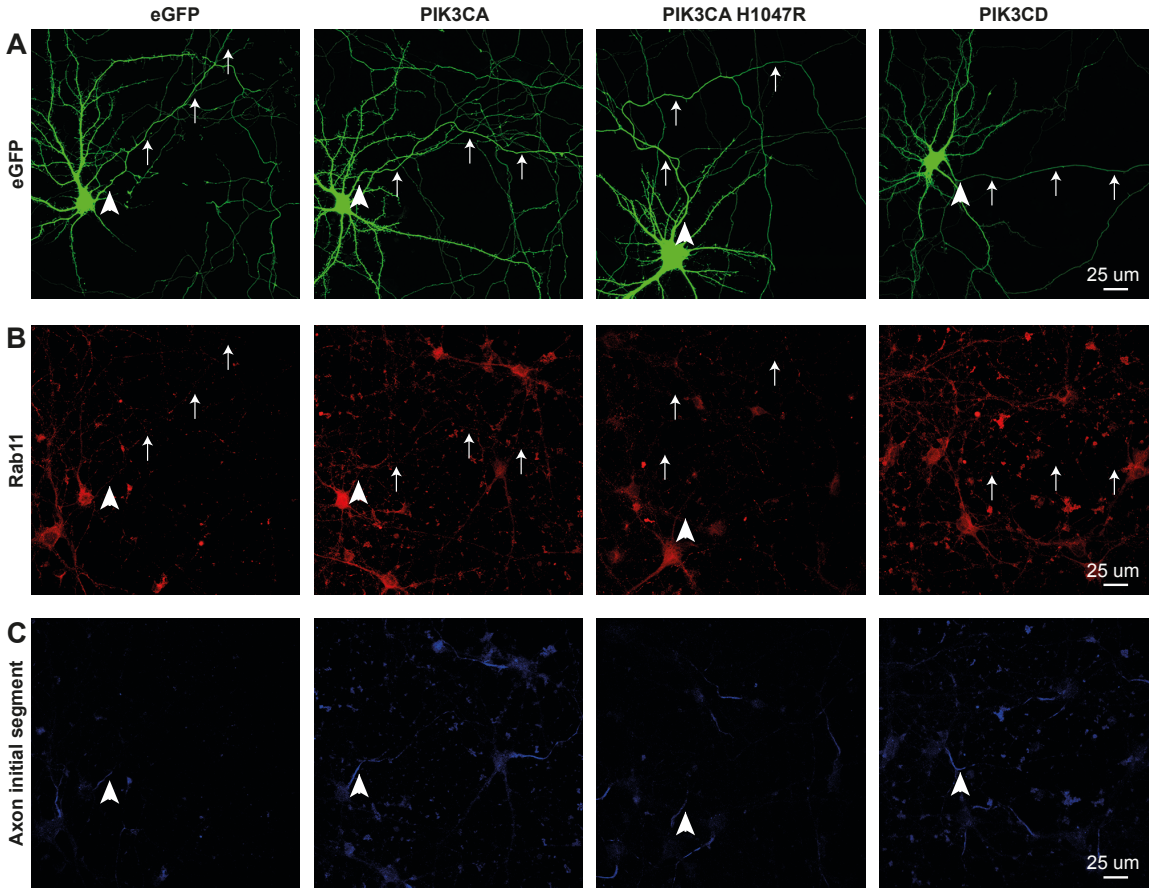

Fig. 9. Distribution of endogenous Rab11 in 14 DIV cortical neurons after PI3K overexpression. Cortical neurons were transfected at 10 DIV with pHR-eGFP, pHR-PIK3CA, pHR-PIK3CA H1047R or pHR-PIK3CD and fixated and stained at 14 DIV. Transfected neurons were detected by exogenous eGFP fluorescence (A), while the cells were co-stained for Rab11 (B) and axon initial segment marker Neurofascin (C). An arrowhead highlights the axon initial segment of a transfected neuron. Three arrows trace the proximal axon. Lab journal reference: BN-17-21.

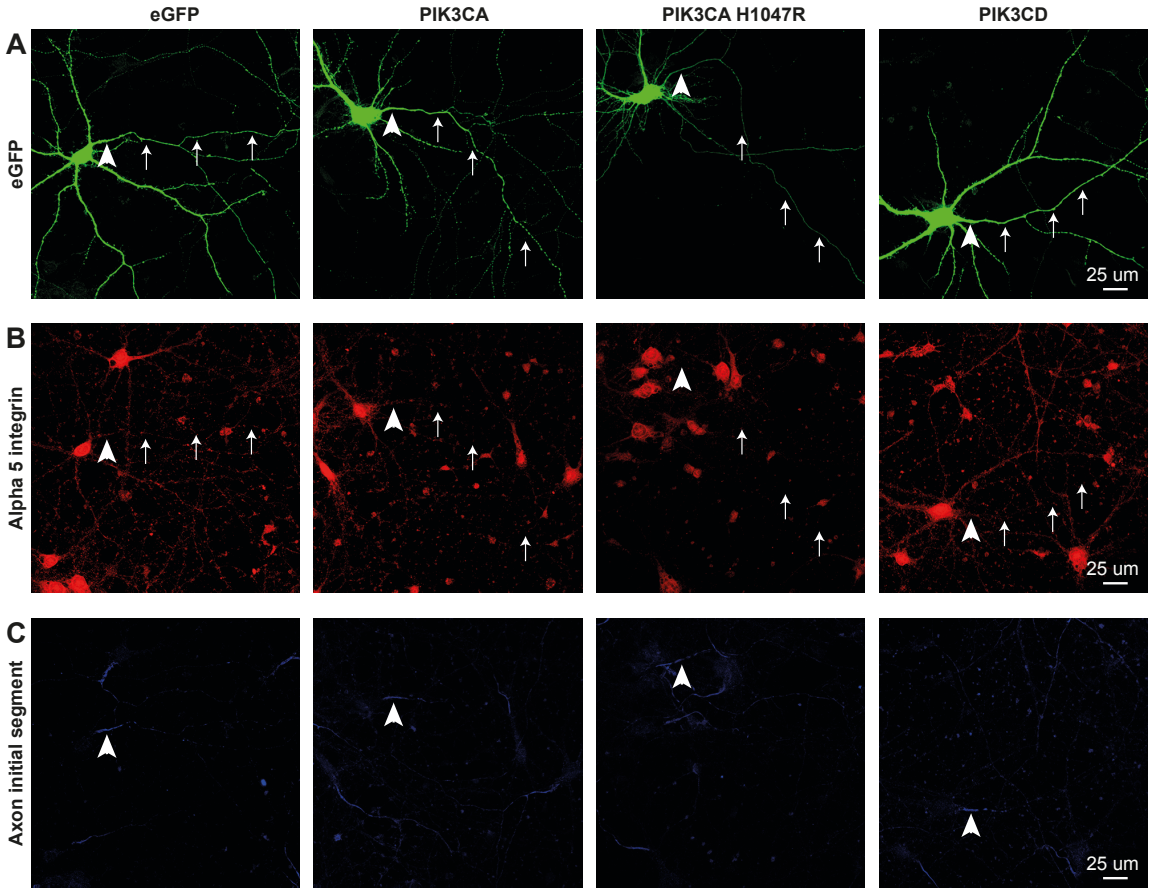

Fig. 10. Distribution of endogenous α5 integrin in 14 DIV cortical neurons after PI3K overexpression. Cortical neurons were transfected at 10 DIV with pHR-eGFP, pHR-PIK3CA, pHR-PIK3CA H1047R or pHR-PIK3CD and fixated and stained at 14 DIV. Transfected neurons were detected by exogenous eGFP fluorescence (A), while the cells were co-stained for α5 integrin (B) and axon initial segment marker Neurofascin (C). An arrowhead highlights the axon initial segment of a transfected neuron. Three arrows trace the proximal axon. Lab journal reference: BN-17-22.

IV. DISCUSSION

This study investigated whether a gain-of-function approach of PI3K isoforms promotes axonal regeneration in CNS neurons. This aim was set because PIP_3 signalling is known to be crucial for growth regeneration, while CNS neurons have a poor regeneration capacity. We examined cultured cortical neurons, instead of hippocampal neurons, because these CNS neurons are largely affected after spinal cord injury or stroke.

(1) PIP_3 signalling and maturation of cortical neurons

The first experiment showed that there is a decline of PIP_3 in cultured cortical neurons in line with maturation. This result supports the hypothesis that neurons have a decline of PIP_3 signalling and that this could contribute to their decreasing regeneration capacity during

maturation. Furthermore, this could suggest that PIP_3 is important during the growth state of cortical neurons. It also validates our strategy to target PI3K to enhance PIP_3 levels to promote axon growth and regeneration in mature cortical neurons.

The claim that PIP_3 signalling is down regulated during maturation of neurons could be strengthen by examining downstream molecules of this signalling pathway. This would also complement the unpublished RNA sequencing data from our laboratory (Koseki et al., unpublished). For instance, the expression of PDK1, phosphorylated Akt, and pS6 could be examined in 1 DIV (neurite extension), 3 DIV (outgrowth), 7 DIV (axon branching) and 14 DIV (maturation and synapse formation) cortical neurons *in vitro*. Previous studies have shown by immunohistochemistry that pS6 is down-regulated when neurons mature *in vivo* (Park *et al.*, 2008; Liu *et al.*, 2010). It will also be interesting to visualise PTEN overtime in cultured cortical neurons. These molecules can also be visualised by western blots in cultured cortical neurons to strengthen the immunofluorescence and RNA sequencing experiments. It is unclear whether it possible to immunolabel for PI3K isoforms in cultured cortical neurons, due to lack of suitable antibodies and low expression levels.

(2) Validation of PIP_3 immunofluorescence

The immunocytochemistry method to visualise PIP_3 is currently being optimised and validated. Researchers from Charité – Universitätsmedizin Berlin and our laboratory in Cambridge are working together on a separate method research article. Recent work by Richard Eva provided the first important evidence that the immunocytochemistry for PIP_3 is specific. He found co-localisation between the PIP_3 antibody and the active signalling areas in cultured fibroblast of transgenic PIP_3 reporter mice (Akt PH domain-GFP). The next validation experiment will be to examine whether the PIP_3 immunofluorescence is a product of PI3K. A comparison in PIP3 immunofluorescence between cortical neurons that are transfected with pHR-EGFP or pHR-PIK3CD will answer this research question. An additional approach to demonstrate the PIP_3 immunofluorescence is a consequence of PI3K, is to apply PI3K inhibitors to cells that express a lot of PIP_3. These PI3K inhibitors should decrease PIP_3 immunofluorescence. Young cortical neurons (see **Fig. 4**) or immortal cell lines would be suitable candidates for this experiment.

In general, the visualisation of PIP_3 at the inner plasma membrane could also be improved by utilizing total internal reflection fluorescence (TIRF) microscopy.

(3) PI3K isoforms and their effect on neuronal morphology of cultured cortical neurons

We investigated whether the PI3K isoforms alter neuronal morphology of cortical neurons *in vitro*. The first experiment examined the effect of PI3K isoforms on neurite outgrowth in immature cortical neurons. Afterwards, the genes were expressed in mature cortical neurons and various morphological markers were analysed. There is a consistent effect of the PI3K isoforms at both time points. Expression of wild PIK3CA does not affect neuronal morphology signalling. The PIK3CA-activation mutation, PIK3CA H1047R, and wild type PIK3CD promote axon outgrowth, dendritic branching, and enlarge the soma. The PIK3CA H1047R and PIK3CD had a very similar effect on neuronal morphology.

Previous studies showed that PIP_3 signalling is important for neurite outgrowth. One of the first evidence was that introducing activated PI3K promotes neurite formation and outgrowth in PC-12 cell lines (Kobayashi *et al.*, 1997; Kita *et al.*, 1998). PI3K signalling after stimulation of BDNF or neurotrophin-3 also promotes axon outgrowth in immature hippocampal neurons (Labelle & Leclerc, 2000; Yoshimura *et al.*, 2005). It was later shown, via PIK3CD kinase-inactive transgenic mice, that P110δ is important for neurite extension in primary cultures of DRG neurons (Eickholt *et al.*, 2007). Consistent with these studies, our experiments show that activated PIK3CA and PIK3D promote neurite outgrowth in immature cortical neurons *in vitro*.

We also observed that that PIK3CA H1047R and PIK3D promote outgrowth in mature cortical neurons, which results a more complex dendritic tree. This is another indication that PI3K promotes neurite outgrowth. The effect on branching of the axon cannot be clarified from the performed sholl analysis, because the method is limited to a single microscopy image and the cell body has to be in the centre of the image. However, the increased dendritic complexity after expression of PI3K is possible an unwanted phenotype for strategies aiming to promote axonal regeneration in the sensorimotor-cortex *in vivo* (as discussed below in Section IV.6).

The enlarged soma and increased pS6 signalling is a known phenomena after enhanced PIP_3 signalling (deletion of PTEN) (Park *et al.*, 2010; Liu *et al.*, 2017). Importantly, the enhanced phosphorylation of ribosomal protein S6 confirms that PIK3CA H1047R and PIK3CD activate the PIP_3/mTOR signalling pathway. The increase soma size could be an indication for new protein synthesis in order to stimulate neuronal growth. However, the current data does not point towards what growth-promoting proteins are being translated.

A key questions remains why expression of wild type PIK3CA does not affect neuronal morphology and stimulation of the PIP_3/mTOR pathway (pS6). We confirmed with

DNA sequencing analysis that all the made dual promoter plasmids, including pHR-PIK3CA, were sound (data now shown). One hypothesis could be that PIK3CA becomes inactivated, while PIK3CA H1047R and PIK3CD are resistant to these post-translational modifications in neurons. A more likely hypothesis could be that PIK3CA requires upstream receptor signalling (by binding a ligand) to become activated and generate PIP_3. Comparing pS6 intensities in neurons treated with BDNF, BDNF and PIK3CA, or PIK3CA alone could test this hypothesis. Our experiments showed that the activating-mutant PIK3CA and PIK3CD stimulate PIP_3 signalling independent of receptor activation. The PIK3CA activation-mutation is indeed known to have enhanced kinase affinity towards the plasma membrane (Zhao & Vogt, 2008; Burke *et al.*, 2012; Hon *et al.*, 2012). That PIK3CA H1047R and PIK3CD alter neuronal morphology in similar extend is consistent with a hypothesis formulated by Dr. Klaus Okkenhaug and his laboratory (Babraham Institute, Cambridge) which is that P110δ is by definition a hyperactive isoform of P110α.

The effect of the PI3K isoforms on synapse formation is beyond the scope of this research. However, PI3K signalling is also known to be important for synapse formation and plasticity (Di Paolo *et al.*, 2004; Arendt *et al.*, 2010; Lee, Huang, & Hsu, 2011). It is possible to investigate synapse formation with the MATLAB programme SynD (Schmitz *et al.*, 2011) because it includes an feature to measure the number of synapses. This detection of synapses requires immunocytochemistry for synaptic markers such as Synaptophysin (synaptic vesicle marker) VAMP2/synaptobrevin (synaptic vesicle marker) or PSD-95 (post-synaptic marker).

(4) PI3K isoforms and axonal regeneration

Deletion of PTEN has been the most important indication that PIP_3 signalling is important for axonal regeneration. As PI3K opposes of PTEN, our experiments demonstrate that expression of PI3K promotes the intrinsic regeneration capacity of CNS neurons.

We confirmed that 14 DIV (eGFP-transfected) neurons have a restricted axon regeneration capacity after *in vitro* laser axotomy (12% of the axotomised neurons did regenerate). The most important finding is that success rate of axonal regeneration is increased in neurons expressing PIK3CA H1047R and PIK3CD. As previously discussed (Section IV.3), the wild type PIK3CA is not capable to active PIP_3 signalling, and therefore it not surprising that it is unable to promote axonal regeneration.

The length of axonal regeneration is another important indication for regeneration. In an *in vivo* situation, it is important to achieve long-distance regeneration to reach the nerve innervation site. Expression of PIK3CA H1047R and PIK3CD seems to stimulate longer

distances of axonal regeneration. However, the reason that this indicator did not reach statistical significance is because there were only four regenerating axons in the eGFP group. In order meet the statistics requirements; more eGFP-transfected neurons could be axotomised.

The importance of growth cone size for axonal regeneration is unclear. The growth cone size depends on many intrinsic and extrinsic factors (reviewed in Hur, Saijilafu, & Zhou, 2012). Koseki *et al.*, 2017 found that cultured cortical neurons have a decline in growth cone size after *in vitro* laser axotomy when neurons mature. This could suggest that a large growth cone (as seen in immature neurons) could be beneficial for axonal regeneration. Eva *et al.*, 2017 found that EFA6 knockout increased the growth size and promote axonal regeneration after *in vitro* laser axotomy. In contrast, Ren & Suter, 2016 found a negative correlation between growth cone size and the speed of growth in cultured (uninjured) bag cell neurons from *Aplysioa californica*. We found that the PI3K isoforms that simulate axonal regeneration had a non-significant effect on the size of growth cone. Consistently, we found no significant effect on the start time of axonal regeneration between the four conditions. Although the initiation of axon regeneration time may become statistically significant quicker, if the n-size for the eGFP group will be increased. Another possibility is that PI3K signalling occurs in the soma area and does not affect the growth cone. One may speculate that nuclear PIP_3 (Kwon *et al.*, 2010; Blind *et al.*, 2014; Wang *et al.*, 2017) affects remodelling of chromatin and regeneration-associated genes become transcribed.

As expected, the axon retraction distance of the axotomised neurons was similar between the four groups. The neurons cultured for two weeks have both short and long retracting axons after laser axotomy. This also validates that the used laser strength for axotomy was the equal in all-experimental conditions.

(5) PI3K isoforms and integrin transport

We hypothesized that expression of PIK3CA H1047R and PIK3CD would stimulate anterograde transport of the integrin machinery toward the growth cone. An increase of integrins in the axon could be one of the mechanisms that promote axonal regeneration. For this purpose, uninjured neurons were plated in low density to avoid that Rab11 and integrin enriched dendrites will cross the axon. However, we did not detect a shift of Rab11 and integrin distribution in uninjured neurons. This could indicate that PI3K signalling does not affect trafficking of integrin receptors in the axon. However, we observed that both PI3K isoforms promote dendritic outgrowth and they may therefore not been moved into the axon. However, it is also possible that the endogenous expression of Rab11 and integrins are too

low to detect in the axon. For this reason, it would be good to include a positive control condition such as 4 DIV cortical neurons. Firstly, this would confirm that there is a relatively reduction of Rab11 and integrins in the axon, compared to dendrites as neurons mature (Koseki *et al.*, 2017). Secondly, this 4 DIV control will make it possible to examine whether expression of PI3K could restore Rab11 and integrins in the axon of 14 DIV neurons similar to young neurons. Once this control condition is included, it is worth to quantify the axon/dendrite immunofluorescence ratio of Rab11 and α5 integrins. We stained for α5 integrin since there are only a few reliable integrin antibodies available. It would also be interesting to explore if PI3K stimulates anterograde transport of integrins, or Trks, when co-expressed. A recent study showed, via siRNA interference, that P110δ is required for the targeting of α2, α5, β1 integrins in the membrane of epithelial cells (Peng *et al.*, 2015). It will be particularly interesting to observe the transport direction in the axon via live cell imaging rather than immunocytochemistry in fixed tissue.

(6) Future research

Our experiments demonstrate that expression of activated PI3Ks enhances the regeneration capacity of CNS neurons in cell culture conditions. The *in vitro* laser axotomy method only examines the intrinsic regeneration response. Koseki et al., 2017 demonstrated this by measuring the regeneration of immature neurons (4 DIV) that were plated on top of mature cultures (25 DIV). The neurons cultured in the 25 DIV environment regenerated their axon as well as neurons plated on PDL, indicating that extrinsic factors do not play a role in this cell culture model. The *in vitro* laser axotomy method therefore identified PIK3CA H1047R and PIK3CD as intrinsic regulators of axonal regeneration. This should be taken forward to study regeneration in animal models of spinal cord injury. It is crucial to examine whether PI3K promotes axonal regeneration and can overcome inhibitory extrinsic factors in scar tissue *in vivo*. It is likely that the PI3K treatment needs to be combined with additional factors, such as α9 integrin that recognises TN-C, to promote long-distance axonal regeneration of CNS neurons.

The mechanisms of PI3K-induced axon regeneration have not been investigated in great detail yet. Similar to the PTEN deletion studies, we only highlighted that the PI3K-Akt-mTOR pathway is beneficial for regeneration. It is important that the mechanism is better understood. A first approach to understand the mechanisms would to visualise whether PI3K (direct immunolabelling) or it's signalling (PIP_3, PGK, Akt) is localised in the axonal or somatodendritic compartment of the neuron. It is most likely that both compartments are required. New growth-promoting proteins are synthesized in the cell body, and afterwards

growth-promoting receptors needs to be transported towards the growth cone of regenerating axons. It will also be interesting to explore weather the PI3K isoforms have a different affinity or activity for PIP_2 or PIP_3 by FRET imaging. Furthermore, it would be interesting to explore a link between PI3K and the small GTPase ARF6. ARF6 is known to be influence by the inositol lipids PIP_2 and PIP_3 (Brown *et al.*, 2001; Li *et al.*, 2005) (see also **Fig. 1**). ARF6 transport integrins (Eva *et al.*, 2012) and is an intrinsic regulator of axonal regeneration (reviewed in Nieuwenhuis & Eva, 2018b, see **Table 1**).

Caution is required if the PI3K strategy is going to be applied to promote axonal regeneration *in vivo*. Because of the diverse roles of inositol lipids, the signalling pathway needs to be strictly controlled and malfunction is associated with many human diseases (reviewed in Fruman *et al.*, 2017), including disorders of the nervous system (reviewed in Gross & Bassell, 2014; Kreis *et al.*, 2014). Enhanced PIP_3 signalling is, for instance, considered as hallmark for cancers. Despite the fact that the tumour suppressor PTEN is expressed in the adult nervous system, it is crucial to specifically target PI3K to layer V cortical neurons and avoid transduction in non-neuronal cells (see Chapter IV). Furthermore, we observed undesired dendritic growth after expression of PI3K and that might cause neurological problems *in vivo*. Identification of downstream molecules may therefore important for precise targeting of axon regeneration, without disturbing other crucial functions in the nervous system. However axonal injury in the CNS is also known to cause neuronal atrophy, in which the soma and dendrites retract, and thus enlargement of soma and neurite growth may therefore not be harmful in that case.

Table 1. ARF6 as an intrinsic regulator of axon growth and regeneration. This table highlights the effects of ARF6 and its associated GAP and GEFs on axon growth and regeneration *in vitro*. Stimulation of anterograde transport of the axonal growth machinery promotes growth, while retrograde transport hinders growth. This table is published in Nieuwenhuis & Eva, 2018b.

ARF6 GEF/GAP	**Main findings regarding axonal growth and regeneration**	**References**
ARF6 (GTPase)	Expression of wild type ARF6 inhibited axon growth by 30% in developing cortical neurons *in vitro*	Suzuki *et al.*, 2010
	Expression of wild type ARF6 or constitutively active ARF6 did not affect axon growth in developing hippocampus neurons *in vitro*	Hernández-Deviez *et al.*, 2004
	Expression of dominant negative ARF6 increased axon growth by 100% in developing hippocampus neurons *in vitro*	Hernández-Deviez *et al.*, 2004
	Expression of dominant negative ARF6 increased axon growth by 67% in developing cortical neurons *in vitro*	Suzuki *et al.*, 2010
ACAP1 (GAP)	Expression promoted axon growth by 25% in adult DRG neurons *in vitro*	Eva *et al.*, 2012
ARNO (GEF)	Expression of wild type ARNO inhibited axon growth by 50% in adult DRG neurons *in vitro*	Eva *et al.*, 2012
	Expression of wild type ARNO did not affect axon growth in developing hippocampus neurons *in vitro*	Hernández-Deviez *et al.*, 2004
	Expression of catalytically inactive ARNO increased axon growth by 500% in developing hippocampus neurons *in vitro*	Hernández-Deviez *et al.*, 2004
	Expression of catalytically inactive ARNO promoted axon growth by 30% in cortical neurons *in vitro*	Franssen *et al.*, 2015
EFA6 (GEF)	Expression inhibited axon growth by 50% in adult DRG neurons *in vitro*	Eva *et al.*, 2012
	Expression inhibited the regeneration capacity of adult DRG neurons by 70% after *in vitro* laser axotomy	Eva *et al.*, 2017
	ShRNA interference increased the regeneration capacity of cortical neurons by 110% after *in vitro* laser axotomy	Eva *et al.*, 2017

CHAPTER IV - Adeno-associated viral vector (AAV)-mediated transduction of the corticospinal tract: comparison of AAV1 and AAV5 and four promoters

DECLARATION:

The material in this chapter has not been published at the time of dissertation submission. A shorter version of this chapter may be made available at the online pre-print server BioRxiv, and will be used for scientific publication after the submission of this dissertation.

I declare that this work was done in collaboration with below scientist, and their contribution is the following:

Barbara Haenzi performed the stereotactic injection of the adeno-associated viruses (AAVs) – shared first authorship.

Sam Hilton provided technical assistance with the perfusions and sectioning of the tissue.

Alejandro Carnicer-Lombarte contributed to the ImageJ macro for semi-automated analysis of images containing brain tissue stained for NeuN and eGFP.

Barbara Hobo contributed by teaching the preparation of recombinant adeno-associated viruses.

Joost Verhaagen supervised the project.

James Fawcett supervised the project.

I, Bart Nieuwenhuis, made the plasmids and recombinant adeno-associated viruses, cut and stained the tissue, took pictures, did the quantifications and analysis of the data, made the figures, and wrote the manuscript.

ACKNOWLEDGMENTS:

We would like to acknowledge Cara Brodie (Cancer Research UK - Cambridge institute) for the fluorescent scanning of the brains stained for NeuN. We also thank Matthew Mason and Fred de Winter (Netherlands Institute for Neuroscience) for advice regarding rAAV production and sending vectors that were used for a pilot experiment, which are not part of this chapter.

I. INTRODUCTION

Gene therapy is a promising strategy for treating genetic and certain acquired disorders including those within the nervous system. Gene therapy could be defined as the delivery of exogenous DNA or RNA into cells with the aim to treat a disease. Gene therapy is especially suitable for conditions in which a single gene and a distinct neuronal subpopulation is affected. Viral vectors are utilized for gene therapy because viruses have naturally evolved to infect other cells and to deliver their genetic contents to the cell nucleus. There are four viruses commonly used for gene delivery in mammalians cells *in vitro* and *in vivo*: retrovirus (including lentivirus), adenovirus, adeno-associated virus (AAV), and herpes simplex virus (HSV). Recombinant adeno-associated viral vectors (rAAVs) are the preferred viral vectors to target the neurons of the central nervous system (CNS), and have been used in clinical trials for several neurological disorders (reviewed in Gray, 2013; Ojala, Amara, & Schaffer, 2015; Naso *et al.*, 2017). Recently, Luxturna® developed by the company Spark Therapeutics, became the first Food and Drug Administration (FDA)-approved gene-therapy for a CNS disorder. Luxturna® consists of a rAAV2 vector containing the RPE65 gene and is directly injected into the eye to reverse retinal dystrophy and blindness in patients with a mutated RPE65 gene. These developments show that rAAV is gaining increasing acceptance as a vector for clinical gene delivery.

(1) The corticospinal tract and spinal cord injury

The corticospinal tract is an important descending motor pathway because it controls the movement of extremities, including arms and legs. Spinal cord injury can lead to damage of the corticospinal tract, among other motor- and sensory tracts, thereby resulting in paralysis. Gene therapy would be an excellent approach to enhance the intrinsic regeneration capacity of the corticospinal tract. The anatomy of the corticospinal tract in humans (reviewed in Blumenfeld *et al.*, 2002) and rodents (reviewed in Ebbesen & Brecht, 2017) will be briefly described below. The corticospinal tract of rat and mice will be described because it is a relevant and widely used model in spinal cord injury research. Mice are chosen because there are many transgenic lines available to study axon regeneration, while rats are often used due to their larger size that makes surgical procedures and behavioural testing easier to perform.

The neurons of the descending corticospinal tract are located in the cerebral motor cortex. The central sulcus is an important hallmark to identify the sensory-motor cortex in humans. The human primary motor cortex is located at the precentral gyrus. The premotor and supplementary motor areas also have axons into the corticospinal tract and are located

anterior of the primary motor cortex (reviewed in Blumenfeld *et al.*, 2002). Rats and mice have a relatively big motor cortex that almost covers their entire frontal cortex (Gioanni & Lamarche, 1985; Neafsey *et al.*, 1986; Brecht *et al.*, 2004). The motor neurons that mainly contribute to the corticospinal tract are pyramidal neurons in layer V of the motor cortex. Therefore, gene therapy for regeneration of the corticospinal tract aims to directly deliver the viral vectors into layer V of the motor cortex.

The axons of the corticospinal tract form synapses on neurons in the grey matter at all levels of the spinal cord. The axons of the corticospinal tract descend via the internal capsule towards the midbrain. Afterwards, the fibers pass the pons towards the pyramid in the rostral medulla. At the pyramidal decussation, the transition between the medulla and spinal cord, a large proportion of the corticospinal tract fibers cross over. In humans, the majority of the fibers cross toward the lateral white matter columns in the spinal cord. After descending in the spinal cord, the axons connect to motor neurons at the anterior horn of the spinal cord. In human fibers that do not cross over at the pyramid in the medulla continue ipsilateral and form the anterior corticospinal tract through the ventral column of the spinal cord, which will terminate on the anterior horn of the spinal cord (reviewed in Blumenfeld *et al.*, 2002). In mouse and rat, the route of the corticospinal tract through the spinal cord differs from humans. Most fibers cross over and will project through the dorsal medial white column of the spinal cord (Miller, 1987). A small proportion of the rodent fibers does not cross and will continue ipsilateral in the ventral- and lateral columns of the spinal cord before terminating at motor neurons in the ventral horn (Brösamle & Schwab, 1997; Steward *et al.*, 2004; Bareyre *et al.*, 2005).

The lower motor neurons located in the ventral horn of the spinal cord can stimulate muscles in the periphery. The anatomy of the spinal cord is different at each spinal level. For instance, the ventral- (descending motor neurons) and dorsal- (ascending sensory neurons) horns have the biggest size at the level of the cervical- and lumbar spinal cord. At the cervical cord, there are motoneurons that are projecting towards the arms. At the lumbar and sacral cord, there are motor neurons projecting towards the legs (reviewed in Blumenfeld *et al.*, 2002).

The severity of the functional consequences of spinal cord injuries depends on the location and the extent of the injury. For instance, a lesion at the cervical level can cause dysfunction of arms and legs, known as tetraplegia. Injury at the level of the thoracic, lumbar, or sacral spinal cord, will have an impact on the legs and is referred to as paraplegia. Due to damage of the corticospinal tract, most spinal cord injury patients are bound to a wheelchair.

(2) Recombinant adeno-associated viral vectors

The biology and structure of AAVs have been described in many reviews and books (reviewed in Agbandje-McKenna & Kleinschmidt, 2011; Murlidharan, Samulski, & Asokan, 2014; Samulski & Muzyczka, 2014; Bedbrook, Deverman, & Gradinaru, 2018). AAVs are non-enveloped (lacking an outer lipid membrane) parvoviruses, which have an icosahedral capsid structure and are approximately 25 nanometers in diameter. AAVs have a linear-single stranded DNA genome that encodes the following proteins: replication (rep) proteins, capsid (cap) proteins, and one assembly activating protein. The genome is approximately 4700 nucleotides long and is flanked by inverted terminal repeats (ITR), which are required for packaging of the AAV genome (Xiao *et al.*, 1997). It is important to note that the genome size determines the maximum packaging capacity of a virus.

Wildtype-AAVs (wtAAV) cannot replicate on their own but require co-infection of adenoviruses or HSVs for their replication. Recombinant adeno-associated viral vectors (rAAV) are produced with the use of helper plasmids that harbour the rep and cap genes that are required for the production of AAV vectors (Xiao, Li, & Samulski, 1998). The development of helper plasmids instead of the use of wtAAV and adenovirus as helper viruses did overcome the problem of contamination of rAAV preparations with these viruses. The rAAV serotypes are produced by a dual- (AAV serotypes 1 to 6) or triple- (AAV serotypes 7 to 9) plasmid transfection in mammalian cells (Grieger, Soltys, & Samulski, 2016; Verhaagen *et al.*, 2018). The transfer plasmid contains a promoter and the transgene of interest, while the helper plasmids contain the rep and cap genes that determine the serotype of the rAAV vector. Thus, production of rAAVs with a serotype specific helper plasmid will result in a rAAV of the desired serotype.

The nine common serotypes are natural variants of AAVs each bearing different cellular tropism. The difference between the serotypes is the capsid that surrounds the AAV genome. The transduction efficiency of the AAVs depends on the ability of the capsids to bind cell surface glycans (reviewed in Huang, Halder, & Agbandje-McKenna, 2014). For instance, AAV1 (Wu *et al.*, 2006) and AAV5 (Kaludov *et al.*, 2001; Seiler *et al.*, 2006) binds α2-3 and α2-6 N-linked sialic acids, while AAV2 interacts with heparin sulfate proteoglycans as their receptor for cell entry (Summerford & Samulski, 1998; Opie *et al.*, 2003; Kern *et al.*, 2003). In addition to the natural AAV serotypes, there are modified AAV variants, e.g. amino acid optimized capsids, to enhance the transduction efficacy in the tissue of interest (Rosario *et al.*, 2016; Chan *et al.*, 2017).

(3) Mechanisms of cell transduction by recombinant adeno-associated viral vectors

Cell transduction is a naturally occurring event of non-pathological AAV virus. This paragraph will briefly describe the mechanisms of cell transduction by AAVs (reviewed in Schultz & Chamberlain, 2008). The capsid of the (r-) AAV vector interacts with receptors on the cell surface of the host cell and passes the plasma membrane *via* endocytosis. The endosome is transported towards the nucleus where the AAV vector genome is released. In human cells the AAV vector genome does integrate into a specific site in chromosome 19 (Samulski *et al.*, 1991), whereas in rat and human cells AAV genomes are also found in episomal DNA in the nucleus of the target cells. An episome is a autonomous double-stranded DNA unit within the nucleus. The transgene (within the newly formed episome) is transcribed by the transcription machinery of the host cell (see Section II.5). The messenger RNA is transferred out of the nucleus and is translated by the host cells' ribosomes into functional proteins.

(4) Comparison of AAV vector serotypes for optimal transduction in the nervous system

To determine what would be the best serotype to transduce specific neuronal populations, several studies compared the transduction efficiency of AAV vector serotypes after direct injection in different parts of the nervous system. AAV1 and AAV5 seem to be most efficient to transduce neurons in general as will be discussed in this section. However, the serotype for transduction of retinal ganglion cells in the eye is AAV2 (Hellström *et al.*, 2009; Nickells *et al.*, 2017). The AAV2 serotype as part of a treatment for human patients with retinal dystrophy caused by an inherited mutation in the RPE65 gene (Bennett *et al.*, 2016a; Russell *et al.*, 2017). The most efficient AAV serotype to transduce primary sensory neurons in the dorsal root ganglia (DRG) is AAV5, closely followed by AAV1 and AAV6 (Mason *et al.*, 2010). Targeting neurons in the substantia nigra and the striatum is relevant for CNS movement disorders such as Parkinson's disease. The most efficient serotypes to target these structures are AAV1, AAV5, and AAV7 depending on the species (McFarland *et al.*, 2009; Markakis *et al.*, 2010; Korecka *et al.*, 2011). The first direct comparison of AAV vector serotypes in the corticospinal tract of rats was done by Hutson *et al.*, 2012. This study found that AAV1, followed by AAV5, are the most efficient to transduce layer V cortical neurons. In a follow-up study, the authors observed that the AAV1 serotype can result in trans-neuronal expression of transgenes in the corticospinal tract following direct injection in the sensorimotor cortex (Hutson, Kathe, & Moon, 2015). The transduction occurs in brain tissue that is directly surrounding the injection site and the transgene was transport in the axon

of the transduced neurons as pyramidotomy prevented transgene expression in the corticospinal axons in the spinal cord (Hutson *et al.*, 2015).

(5) Comparison of promoters for strongest expression of transgenes

The promoter is essential for the transcription of transgenes, turning the DNA template into messenger RNA, before protein translation. The promoter is a regulatory DNA element that is located at the 5' end of a transgene. It consists of a promoter core called the CAAT box, an upstream TATA box that acts as a transcription factor-binding site, and possibly an enhancer or repressor sequence that alters the efficiency of the RNA polymerase. Many transcription factors can bind to the TATA box region of the promoter. In addition to transcription factors binding DNA, they can also interact with each other resulting in protein complexes with different affinities for DNA binding (reviewed in Inukai, Kock, & Bulyk, 2017). The promoter-bound transcription factors initiate the recruitment of RNA polymerase, which will start transcription of the DNA template after ATP hydrolysis.

The promoter also has an important role in the selective expression of transgenes in specific cell types. There are different classes of promoters including, constitutive promoters (activated in many cell types e.g. CMV, full-length PGK and human ubiquitin C promoters), inducible promoters (can be turned on or off by modulators e.g. administration of light or doxycycline), tissue-specific promoters (such as GFAP or SYN) and hybrid promoters (such as CAG which is composed of a chicken beta-actin promoter and a CMV enhancer). The decision which promoter is optimal for AAV-mediated expression of transgenes depends on the experimental requirements, including the target cells that have to be transduced, and the levels and duration of transgene expression. The promoter that result in the strongest expression of layer V neurons is unknown.

(6) Aim of study

Hutson *et al.*, 2012 identified AAV1, followed by AAV5, as optimal serotypes to transduce layer V cortical neurons of the corticospinal tract. Yet, the strongest/best promoter for the expression of transgenes in these CNS neurons is unknown. Here, we aimed to replicate the previous findings for the optimal AAV vector serotype for corticospinal tract transduction. Furthermore, we compared the AAV1 serotype harbouring four different promoters, including the CMV promoter, the mouse PGK (mPGK) promoter, the short-CAG (sCAG) promoter, and the human synapsin (hSYN) promoter. These four promoters were chosen because: (1) this are relatively compact promoters (size range from 470 to 860 bp) thus allowing for the accommodation of relatively large transgenes; (2) these promoters have been used to transduce the nervous system but their activity in the brain has not been studied

in a side by side comparison; and (3) the specific requirement for a strong promoter in the CST due the to the large size of this neuronal pathway. We also examined co-transduction of two viruses (AAV1-hSYN-eGFP and AAV1-hSYN-tdTomato), which is relevant for various experiments that aim to combine multiple transgenes. In addition, we investigated whether the promoters have different selectivity for expression in non-neuronal cells. This promoter comparison study contributes to the optimization of AAV-mediated gene delivery to neurons of corticospinal tract.

II. MATERIALS AND METHODS

(1) AAV vector plasmids

Vector plasmids were designed to investigate the expression potential of different promoters. Therefore, the post-transcriptional regulatory element called woodchuck hepatitis virus posttranscriptional regulatory element (WPRE) was removed of all vector plasmids (**Figure 1**). AAV-CMV-eGFP was a gift from Connie Cepko (Addgene plasmid # 67634). AAV-sCAG-eGFP was provided by the laboratory of Joost Verhaagen and is described in Fagoe *et al.*, 2014a. AAV-mPGK-eGFP was made by utilizing AAV-mPGK-Cre, which was a gift from Patrick Aebischer (Addgene plasmid # 24593), as vector backbone after the Cre sequence was removed via HindIII-HF (NEB, R3104) and EcoRI-HF (NEB, R3101) digestion. The eGFP sequence of AAV-CMV-eGFP was amplified by using the primers 5' GGAATTCATGGTGAGCAAGGGCGAG 3' and 5' AGCGCTTTACTTGTACAGCTCGTCCATG 3', which was next cloned into the digested AAV-mPGK-backbone. Plasmid pTRUF20B-SEW, which was a gift from Deniz Kirik (Lund University) and is described in Korecka *et al.*, 2011, was modified to make AAV-hSYN-eGFP by HincII (NEB, R0103) digestion to remove the WPRE. AAV-hSYN-tdTomato was made by ClaI (NEB, R0197) digestion of AAV-hSYN-tdTomato-WPRE, which was a gift from Hongkui Zeng (Addgene plasmid # 51506).

Fig. 1. – next page - Schematic representation of adeno-associated constructs. (a) Four constructs express enhanced green fluorescent protein (eGFP), which has a length of 720 bp, under different promoters. The CMV promoter has a size of 670 bp and is upstream of a 500 bp b-globin intron (total promoter size: 1170). The mouse PGK (mPGK) promoter has a size of 510 bp and contains a b-globin intron of 500 bp. The short CAG (sCAG) promoter has a size of 860 bp. The shortest promoter is hSYN with a size of 470 bp. One construct expresses tdTomato, which as a length of 1431 bp, under the hSYN promoter. The packaging cassettes are flanked by inverted terminal repeats (ITR). The poly-A signals are not shown.

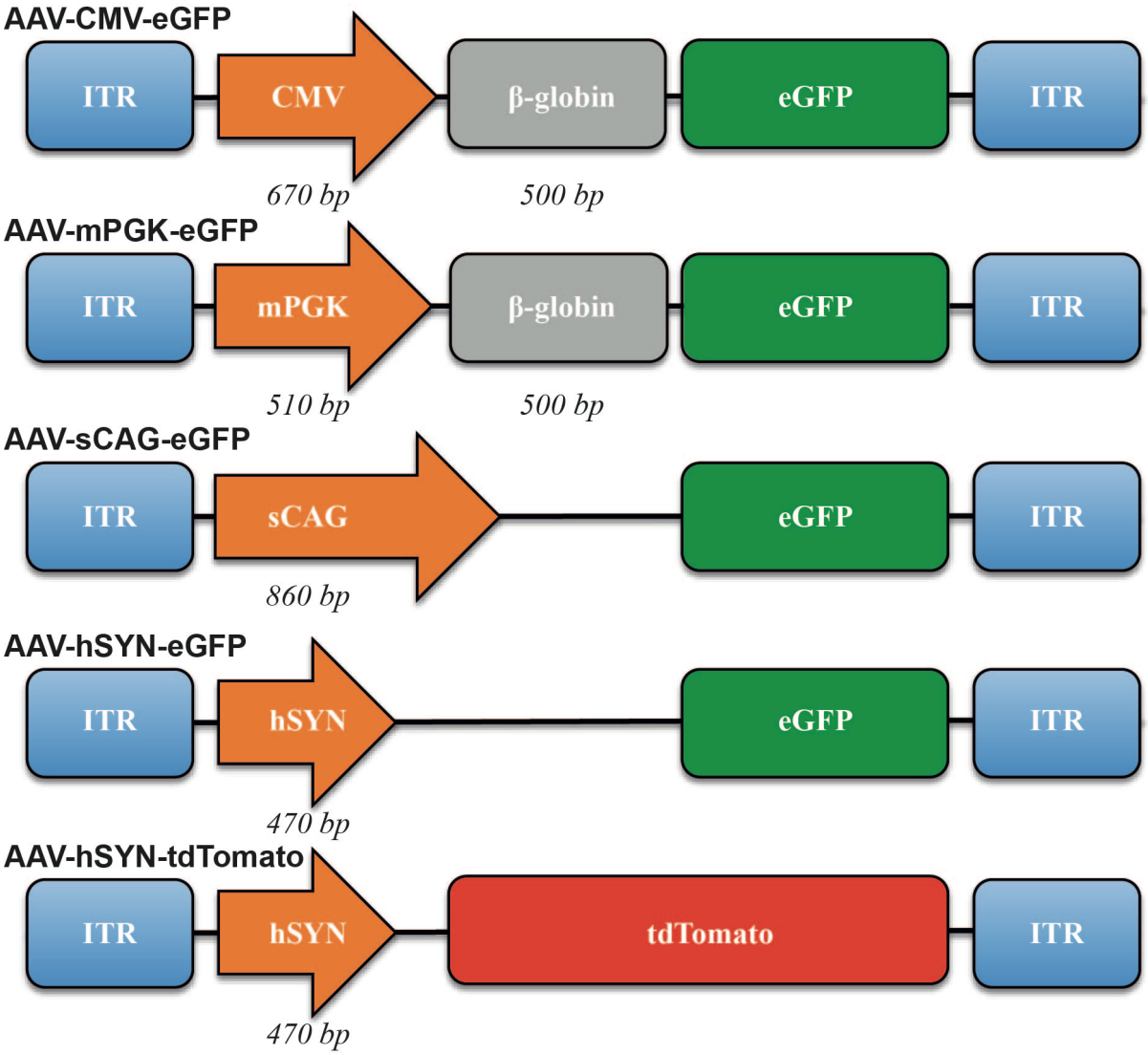

(2) Cortical neuron cultures and magnetofection

The neuronal cultures were prepared as described in Chapter II section II.11. The cortical neurons were transfected at 10 days *in vitro* (DIV) using oscillating nanomagnetic transfection (magnefect nano system; nanoTherics). The vector plasmids (7 µg per dish) were mixed with 8 µl of magnetic nanoparticles (NeuroMag, NM50200) in 100 µl of culture medium and were incubated for 30 minutes. For co-transfection of hSYN-eGFP and hSYN-tdTomato, 3.5 µg of each plasmid were mixed. The culture media was substituted for the transfection mixture and next the dishes were placed over a magnetic array, which was moving laterally at 2 Hz and at 0.2 mm amplitude of displacement for 30 minutes at 37°C in a 7% Co_2 incubator. After the transfection, the original culture medium was returned to each well and the neurons were cultured until 14 DIV when the neurons were fixed with 4% paraformaldehyde (PFA) in PBS for 10 minutes at room temperature and afterwards were washed in PBS. The cells were mounted using fluorsave^{tm} reagent (Calbiochem, 345789).

(3) Image acquisition and analysis of cultured cortical neurons

The images for fluorescent intensity analysis were captured on a fluorescent microscope (DM6000 B, Leica) with a 40x-oil objective. Semi-automated and standardized analysis of the images was performed using MATLAB platform version 2017 and the program called SynD (Schmitz *et al.*, 2011). The following output of SynD was used: (1) the average fluorescence of each neurite within a 100 μm distance from the soma, (2) soma fluorescence intensity, (3) soma area. Prism 7 for Mac OS X was used for statistical analysis. The typical images of cultured cortical neurons were taken using an SP5 confocal with a 40x-oil objective and a 2.5 digital zoom factor using Leica software. The co-transfection rate was determined by manual scoring the acquired confocal images of 100 neurons.

(4) Adeno-associated viruses preparation

The small-scale production of recombinant adeno-associated viral vectors was recently described in detail (Verhaagen *et al.*, 2018). A summary of the performed AAV preparation procedures is described here.

Approximately 12.5 million human embryonic kidney (HEK) 293T cells per virus batch were plated in twelve 15 cm tissue culture plates. The cells were grown in Dulbecco's modified eagle medium (DMEM) (Gibco, 10566) supplemented with 10% fetal calf serum (FCS) and 1% penicillin/streptomycin (PS). The cells were 70% to 80% confluent one day after plating.

The vector plasmids were transfected into the HEK293T cells by utilizing polyethylenimine (PEI). The cationic polymer PEI provides a positive charge to vector plasmids resulting in binding to the negatively charged sugars at the cell-surface and ultimately entrance into the cell via endocytosis (Reed *et al.*, 2006). Two hours prior transfection, culture medium was replaced with Iscove's modified Dulbecco's medium (IMDM) (Gibco, 124400) complemented with 10% FCS / 1% glutamax / 1% PS. A total of 150 μg of vector plasmid and 450 μg helper plasmid (PVD20 and pDP5 for AAV serotype 1 or 5, respectively) (Grimm, Kay, & Kleinschmidt, 2003) were mixed in 12 ml 0.9% sodium chloride (NaCl) for each batch of virus. After vortexing, 1800 μg PEI (PolyScience Inc., 23966) in 12 ml 0.9% NaCl was added and the mixture was incubated for 20 minutes at room temperature (DNA to PEI ratio of 1:3). After incubation, 2 ml of the transfection solution was applied to each plate containing HEK293T cells in IMDM. One day after transfection, the IMDM medium and PEI mixture was removed and replaced with IMDM medium only since long-term exposure to PEI causes cellular toxicity and cell detachment from the tissue culture plates.

Harvesting of the HEK293T cells was performed three days post-transfection. At this time-point, 60% to 80% of the cells should be expressing eGFP or tdTomato (which can be examined by fluorescent microscopy). The cells were harvested by removing the IMDM medium and next Dulbecco's phosphate-buffered saline (D-PBS) (Gibco, 14040) was added followed by collection of the cells with a 28 cm cell scraper (Greiner Bio-One, 541070). A maximum total volume of 17.5 ml was collected. Afterwards, the cells were frozen at -80 °C and thawed in a 37 °C water bath to open the cells and release viral particles. This freeze and thaw procedure was performed three times and the samples were vortexed to break any remaining clumps of cells. 25 µl of 10 mg/ml endonuclease deoxyribonuclease I (DNase I) (Roche, 11284932001) in PBS was added to the cell lysate and was incubated for 1 hour at 37 °C to prevent cell clumping. The cells were stored at -20 °C until the iodixanol gradient procedures the next day.

The cell lysate was thawed and centrifuged at 3200 x g for 30 minutes to yield crude lysate including adeno-associated viruses. The crude lysate was loaded onto a 25 x 89 mm quick-seal polypropylene tube (Beckman, 342414) using a Pasteur pipet. After loading the 17.5 ml crude lysate, a step gradient containing 15% (9 ml), 25% (5 ml), 40% (5 ml) and 60% (3 ml) iodixanol (Axis shield, 1114542) was added using a new Pasteur pipet without air bubbles forming between the layers. The Beckman tube was topped up with D-PBS and sealed using an electric tube topper. Centrifugation of the iodixanol gradient was performed in a 70Ti roter (Beckman Coulter) at 69.000 RPM for 70 minutes. A hole was punctured at the top of the Beckman tube while leaving the needle in place, afterwards a hole was made at the bottom of the tube and the virus was collected at the 40-60% interface (1 ml of 60% and 2 ml of 40% iodixanol layer). The iodixanol fraction that contained the virus was diluted in 12 ml D-PBS and applied to a 100 kDa MWCO Amicon Ultra-15 centrifugal filter device (Millipore, UFC910096) and was next centrifuged at 3200 x g for 15 minutes to concentrate the volume and wash out the iodixanol. The buffer was changed to D-PBS with 5% sucrose using the same Amicon filter and was centrifuged at least three times until 150 µl to 200 µl virus remained in the filter. The produced viruses were stored at -80 °C until use.

The titres of AAVs were determined by quantitative PCR (qPCR). Viral genomic DNA was isolated from 2.2 µl of virus by applying 85.8 µl of 250 µg/mL DNase I in D-PBS (duplicate and 1:40 dilution) and was incubated at 37 °C for 30 minutes. The DNase-treated viruses were next lysed by adding 40 µl 1M sodium hydroxide (NaOH) and were incubated at 50 °C for 15 minutes. After alkaline lysis, the pH was neutralised by applying 40 µl 1M hydrochloric acid (HCL) (1:3 dilution by lysis and neutralisation). After pH neutralisation, 20 µl of the solution was added to 180 milli-Q H_2O (1:10 dilution) and was used as sample for

AAV titration (final work dilution of 1:1200). A calibration curve was made by preparing serial dilutions of a reference plasmid (**Table 1**) ranging from 10^{10} to 10^{3} molecules/ml in milli-Q H_2O. Each qPCR reaction had a total volume of 25 µl and consisted of 12.5 µl SYBR green PCR master mix (Applied biosystems, 4309155), 0.75 µl primer mix (10 µM of forward and reverse primers, **Table 1**), 1.75 µl milli-Q H_2O, and 10 µl AAV titration sample, a plasmid part of the standard calibration curve, or controls such as milli-Q H_2O (negative control), D-PBS with 5% sucrose (negative control), or an AAV titration sample with known titre (positive control). For the reaction, a 96-well PCR plate was used in a qPCR machine (Applied biosystems, 7300) and a thermocycling program as shown in **Table 2** was used. The tires of the AAVs were calculated based on the cycle threshold values using the standard calibration curves. The single AAVs were titre matched to 1.42E+12 gc/ml before stereotactic injections in animals. The co-injection experiment consisted of AAV1-hSYN-eGFP and AAV1-hSYN-tdTomato each with a titre of 1.68 E+11 gc/ml.

Table 1 Reference plasmid and oligonucleotides used for AAV titration

Virus	Reference plasmid	Primer mix name	Forward primer	Reverse primer
AAV1-CMV-eGFP	AAV-hSYN-eGFP	qtitre_eGFP3	GTCTATATCATGGCCGACAA	CTTGAAGTTCACCTTGATGC
AAV1-mPGK-eGFP	AAV-hSYN-eGFP	qtitre_eGFP3	GTCTATATCATGGCCGACAA	CTTGAAGTTCACCTTGATGC
AAV1-sCAG-eGFP	AAV-hSYN-eGFP	qtitre_eGFP3	GTCTATATCATGGCCGACAA	CTTGAAGTTCACCTTGATGC
AAV1-hSYN-eGFP	AAV-hSYN-eGFP	qtiter_hSyn3	GTGCTGAAGCTGGCAGTG	GCAAGTGGGTTTTAGGACCA
AAV5-hSYN-eGFP	AAV-hSYN-eGFP	ncbi4_syn	CCCTGCGTATGAGTGCAAGT	GGTGCTGAAGCTGGCAGT
AAV1-hSYN-tdTomato	AAV-hSYN-eGFP	qtiter_hSyn3	GTGCTGAAGCTGGCAGTG	GCAAGTGGGTTTTAGGACCA

Table 2 Thermocycling conditions for AAV titration

Cycle step	Temperature (°C)	Time (seconds)	Number of cycles
Initial denaturation	50 95	120 600	1
Denaturation Annealing and Extension	95 60	15 60	40
Dissociation stage	95 60 95 60 4	15 60 15 15 Hold	1

(5) Animals and stereotactic injection of adeno-associated viruses in the sensory-motor cortex

A total of 16 adult female rats (Lister Hooded, Charles River Laboratories) and 16 adult female mice (C5BL/6, Charles River Laboratories) were used in this study. The animals were housed in group cages and had access to water and food ad libitum in standard laboratory conditions.

This research has been regulated under the Animals (Scientific Procedures) Act 1986 Amendment Regulations 2012 following ethical review by the University of Cambridge Animal Welfare and Ethical Review Body (AWERB). All procedures were performed using aseptic techniques. Viral vectors were stereotactically injected into the right sensory-motor cortex of mice and rat as described below. The animals were anesthetized with isoflurane (4% isoflurane in O_2 for induction, 2% isoflurane for maintenance) delivered via a facemask and received postoperative analgesia. Body temperature was kept at roughly 36 °C via a heating pad with an anal probe. The head of the animal was shaved and the skin was disinfected. The animal was next placed in the stereotaxic frame (David Kopf Instruments) were a midline incision was made to expose the skull and holes were drilled at coordinates that cover the right sensory-motor cortex (**Figure 2**). A Hamilton syringe with needle was positioned through the generated holes and was lowered into the brain by 0.5 mm for mice and 1.5 mm for rats. Thereafter, 0.5 µl of AAV vector was injected in each hole at a rate of 0.2 µl per minute (total virus volume of 2 µl per mice and 3.5 µl per rat) using a Micro4 micro syringe pump controller. The needle was removed three minutes after injection to allow proper diffusion of the virus and avoid unwanted leaking. Afterwards, the skin was sutured and the animals were recovered at 37 °C before standard housing.

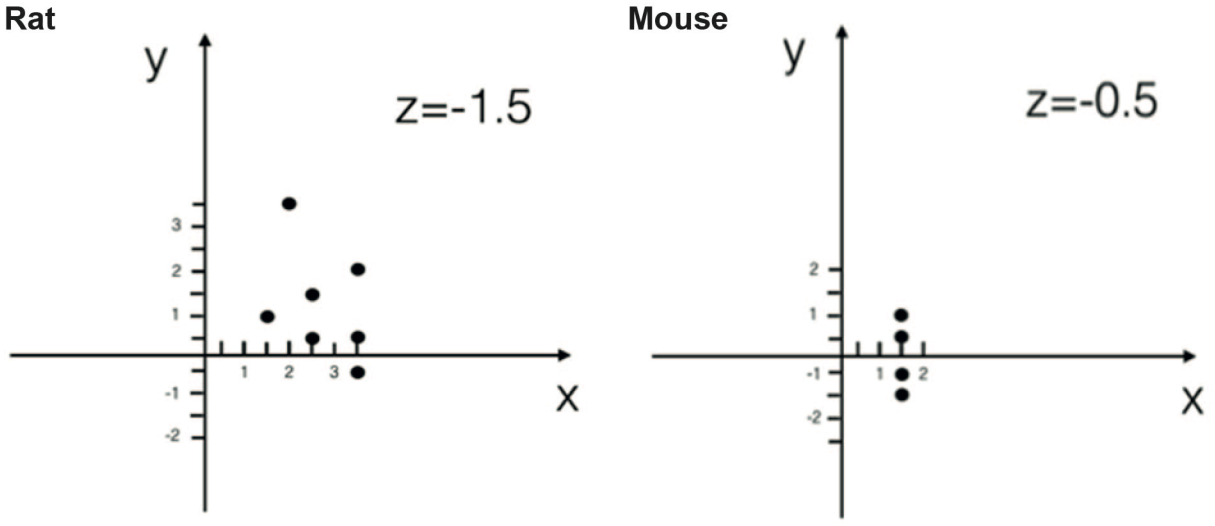

Fig. 2. Injection coordinates for the sensory-motor cortex in the right hemisphere of mice and rat. The 0 point of the XY-graphs represent Bregma and the coordinates were defined by their mediolateral (x) and

anteroposterior (y) position relative to Bregma. (Left) Rats were injected at seven coordinates: +1.5 mm, +1 mm; +2 mm, +3.5 mm; +2.5 mm, + 1.5 mm; +2.5mm, +0.5 mm; + 3.5 mm, +2 mm; + 3.5 mm, + 0.5 mm, +3 mm, -0.5 mm. The virus was injected at a depth of 1.5 mm (z = -1.5 mm). (Right) Mice were injected at four coordinates: +2 mm, +1 mm; +2 mm, +0.5 mm; +2 mm, -0.5 mm; +2 mm, -1 mm. The virus was injected at a depth of 0.5 mm (z = -0.5 mm). Labjournal reference: Barbara Haenzi – experiment 26.

(6) Histology

Six weeks after adeno-associated virus injection, animals were euthanized by injecting an overdose of Euthatal followed by transcardial perfusion with PBS followed by 4% PFA in PBS. The brain and spinal cords were collected and were stored in 4% PFA for 24 hours at 4 °C. Afterwards, the tissue was stored in 30% sucrose in PBS with 0.1% sodium azide at 4 °C until further use. The cerebrum was cut into 40 µm tick coronal sections and the spinal cords were cut in transverse sections with a thickness of 40 µm using a freezing microtome. The tissue was collected in 12 series and was kept in a 24-well plate containing PBS and 0.1% sodium azide.

(7) Immunohistochemistry

The sectioned brains and spinal cords were washed in PBS. After washing, the tissue was permeabilized and blocked by applying 0.3% triton (Sigma, X-100) and 10% goat serum (Sigma-Aldrich, G9023) in PBS for two hours at room temperature. The tissue was next incubated with primary antibodies that were diluted in above-mentioned blocking detergent at 4°C overnight. The primary antibodies used were anti-eGFP (A10262, 1:1000, ThermoFischer scientific or Ab290, 1:1000, Abcam) together with anti-NeuN (ABN91, 1:500, Merck), anti-Glial Fibrillary Acidic protein (Z0334, 1:500, Dako), anti-Iba1 (019-19741, 1:1000, Wako), anti-APC clone CC-1 (OP80, 1:300, Merck), or anti-Olig-2 (AB9610, 1:500, Merck). Afterwards, the cells were washed and incubated in Alexa Fluor-conjugated secondary antibodies that were diluted in 0.3% triton and 10% goat serum in PBS for 2 hour at room temperature. The secondary antibodies used were anti-chicken IgY conjugated to Alexa Fluor 488 (A-11039, 1:500, ThermoFischer scientific), anti-chicken IgY conjugated to Alexa Fluor 568 (A-11041, 1:500, ThermoFischer scientific), anti-rabbit IgG conjugated Alexa Fluor 488 (A-11008, 1:500, ThermoFischer scientific), anti-rabbit IgG conjugated Alexa Fluor 568 (A-11011, 1:500, ThermoFischer scientific), anti-rabbit IgG conjugated Alexa Fluor 647 (A-21245, 1:500, ThermoFischer scientific), anti-mouse IgG2b conjugated Alexa Fluor 568 (A21144, 1:500, ThermoFischer scientific). After washing, the free-floating sections were mounted using fluorsave^{tm} reagent (Calbiochem, 345789) on glass imaging slides.

(8) Microscopy

Cultured cortical neurons were imaged on a fluorescent microscope (DM6000 B, Leica) with a 40x-oil objective using Leica software. Fluorescence slides containing *in vivo* tissue stained for NeuN were scanned on a Zeiss AxioScan Z1 (Histopathology core facility in Cancer Research UK – Cambridge institute) using a 20x light objective. Images containing the regions of interest were exported in TIFF format. All images within an experiment were taken with identical settings. Representative images for astrocytes, microglia, the oligodendrocytes lineage, and the dorsal corticospinal tract were taken using laser-scanning confocal microscopy (Leica, TCS SPE, DMI4000B).

(9) Quantification

Analysis of cultured neurons was performed using MATLAB platform version 2017 and SynD (Schmitz *et al.*, 2011). A detailed description about the morphology analysis of 14 DIV cortical neurons can be found in Chapter III Section II.8.

The mean area of transduction per section was measured in ImageJ by manually outlining the areas that contained eGFP-positive staining. The transduction area reported for each animal is the average taken from two sections with the biggest transduction area.

The number of transduced cortical neurons (eGFP+ NeuN+ cells), and the mean eGFP intensity per transduced neuron was measured using a custom-made ImageJ Macro designed by Alejandro Carnicer-Lombarte (**Fig. 3**) and Microsoft Excel. An excel template that will perform the calculations after inserting the ImageJ output will be uploaded as **supplementary data**. In essence, the ImageJ macro automatically detects the position of all NeuN+ cells in the red channel and afterwards measures the fluorescence intensity within the green channel of each identified cells. After applying the Macro, the number of transduced cortical neurons was determined by counting the detected NeuN+ cells that had a fluorescent intensity that was higher than an arbitrary limit of 30% above the average background intensity of the transduced area. The background intensity was determined by manually outlining the region in-between two transduced neurons, and afterwards taking the average eGFP intensity in three of those regions. Because each brain was cut into series of twelve, the number of eGFP+ NeuN+ cells of each image was multiplied by 12 to obtain the total expected number of transduced neurons per brain section. The mean eGFP intensity per transduced neuron was calculated by taking the average eGFP intensity of the eGFP+ NeuN+ cells and afterwards subtracting the average eGFP intensity of three non-transduced cells within the same section. In general, the numbers reported for each animal is the average taken from two sections with the biggest transduction area.

The number of eGFP-containing axons in the dorsal corticospinal tract was manually counted by using microscope eyepiece reticles (Pyser Optics, NE11A – 01B26210) and a standard fluorescent microscope (DM6000 B, Leica) with 63x-oil objective. The squared grid covered a region of 80x80 µm with this magnification. Axon transduction per ROI for each animal was determined by taking the average number of fluorescent axons in three counting grids. This average number was multiplied by factor 10 or 4 for rats or mice, respectively, to cover the transduced dorsal corticospinal tract at the cervical spinal cord.

One rat (out of the 32 injected animals in total) injected with AAV1-mPGK-eGFP was excluded for corticospinal tract analysis because the stereotactic injections poorly covered the sensory-motor cortex in this animal (**Supplementary figure 1**).

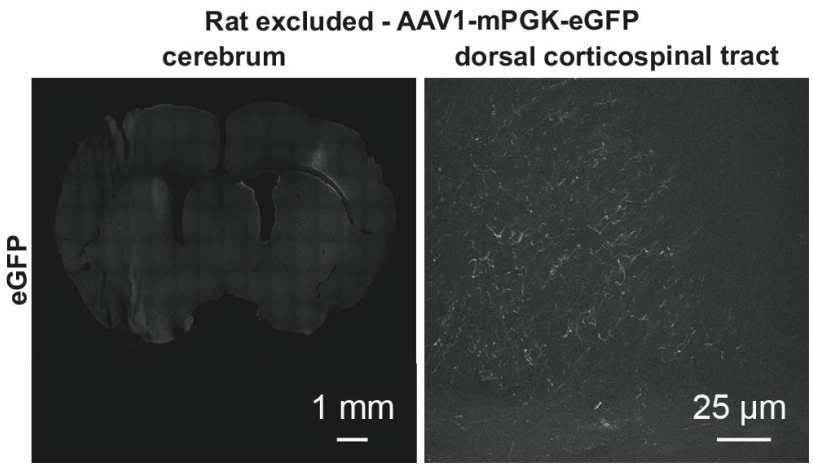

Supplementary figure 1 Rat injected with AAV1-mPGK-eGFP with relative poor transduction coverage of the sensorimotor cortex. Pictures were taken with same fluorescent intensities as **Fig. 11** (mPGK-brain) and **Fig. 13** (mPGK-spinal cord) Lab journal references: BN-18-06 (brain), BN-18-28 (spinal cord).

The number of transduced astrocytes, microglia, and oligodendrocytes were manually counted by using microscope eyepiece reticles (Pyser Optics, NE10A – 01B26208) and a standard fluorescent microscope (DM6000 B, Leica) with 40x-oil objective. The squared grid covered a region of 250x250 µm with this magnification. The transduced cells were visualised by using a filter that permits both green (Alexa 488) and red (Alexa 568) fluorescent light through the eyepiece. The number of transduced cells per ROI for each animal was calculated by taking the average number of eGFP+ cells in three counting grids within one AAV transduced area.

(10) Statistical analysis

Statistical analysis was performed by using Graphpad Prism 7 for Mac OS X. All statistical tests and parameters are mentioned in the figure legends. The graphs represent the average for each condition together with the individual data points for each animal, rather

than error bars (Cumming, Fidler, & Vaux, 2007), because of the relatively small N-numbers per group used in this study.

```
1  //preamble - modify image as appropriate
2  run("Set Scale...", "distance=0 known=0 pixel=1 unit=pixel");
3  waitForUser("draw your RECTANGULAR ONLY area of interest and hit ok");
4  //run("Measure");
5  run("Clear Outside");
6  run("Duplicate...", " ");
7  setRGBWeights(1, 0, 0);
8  run("8-bit");
9  //here goes the code of what you want to get from the red channel
10 setAutoThreshold("Moments dark");
11 setOption("BlackBackground", false);
12 run("Convert to Mask");
13 run("Watershed")
14 run("Size...") //Remember to change the size of your image here to match that of the one you already have
15 run("Make Binary");
16 run("Analyze Particles...", "size=100-3500 circularity=0-1.00 show=Outlines exclude summarize add");
17 close;
18 close;
19 setRGBWeights(0, 1, 0);
20 run("8-bit");
21 run("Size...");
22 roiManager("Show all");
23 roiManager("Select All");
24 waitForUser("happy with the selection?");
25 roiManager("Measure");
26 //here goes the code of what you want to get from the green channel
27 //make sure that at the end the measurement tab is selected
28 saveAs("Results");
29 roiManager("Delete");
30 run("Clear Results");
31 close;
```

Fig. 3. ImageJ macro for automated histological analysis of AAV transduced cortex tissue. The code is highlighted in yellow and purple. The green lines are comments for the user. **Lines 1-2**: the macro begins by removing the scale and therefore all input and output will be in pixels. **Lines 3-6**: Create a region of interest (roi) within the open image. A duplicate is made so that the macro can process any images regardless of the image name. **Lines 7-8**: The macro will open the red channel (e.g. immunofluorescence for cell marker NeuN). **Lines 10-15**: The macro will create a mask on the cells positive for the marker in the red channel using the standard ImageJ thresholding called 'Moments'. Note that the thresholding parameters were manually determined by the user for this experiment, and should be re-determined for each new experiment. Two cells that are close to each other will be separated using the tool watersheding. It is important to manually type the size of the newly drawn region of interest, which was created in lines 3-6, in the pop-up screen (The image size in pixel is written in the top left corner). **Lines 16-18**: The particle analysis is important because it identifies cells based on their size. The current settings will exclude particles from the red channel that are smaller than 100^2 pixels and bigger than 3500^2 pixels. After cell identification, the masks are stored in the roi manager and the red channel gets closed. **Lines 19-27**: The masks, which contain cells that are positive for the marker in the red channel, are moved to the green channel containing eGFP positive cells. The user can view the overlay on the green cells and when satisfied press 'okay' to measure the eGFP intensities. **Lines 28-31**: The output of the ImageJ Macro is the 'number of red cells', the 'area surface of each red cells' and the 'median eGFP intensity of each red cell'. The output can be stored in an excel file and the Macro will be closed. I generated an automated Excel file to determine the number of eGFP+ red channel marker+ cells (see **Fig. 6F** and description in the method quantification section)

III. RESULTS

(1) Mean eGFP intensity of the transfected cortical neurons *in vitro*

The plasmids were validated in cortical neurons *in vitro* before AAV vectors were produced. The plasmids containing the various promoters and the DNA sequences for the fluorescent proteins were transfected into cultured cortical neurons that were derived from embryonic day 18 rats. The neurons were transfected utilizing magnetic beads after culturing them for 10 days *in vitro* (DIV) and were examined on 14 DIV, a time point on which they are considered to be mature. The transfection of all plasmids resulted in eGFP expression (**Fig. 4A**). The strength of the four promoters *in vitro* was determined by measuring the intensity of eGFP in the transfected neurons. After four days of transfection, the eGFP intensity was similar between the CMV, mPGK, sCAG, and hSYN promoters (**Fig. 4B, C**). The eGFP intensity in the neurites was determined by measuring the average fluorescence of each neurite within a 100 μm distance from the soma. The neurite eGFP intensity did not statistically differ between groups and was approximately 1000 arbitrary units (**Fig. 4C**). The eGFP intensity in the soma reached almost saturation levels in each group and was approximately 4000 arbitrary units (**Fig. 4D**). As expected, the soma size of the transfected neurons was not different between the four groups (**Figure 4E**). In addition, sholl analysis of the neurite branches confirmed that the investigated primary cortical neurons had similar morphology for each vector plasmid (**Figure 4F**).

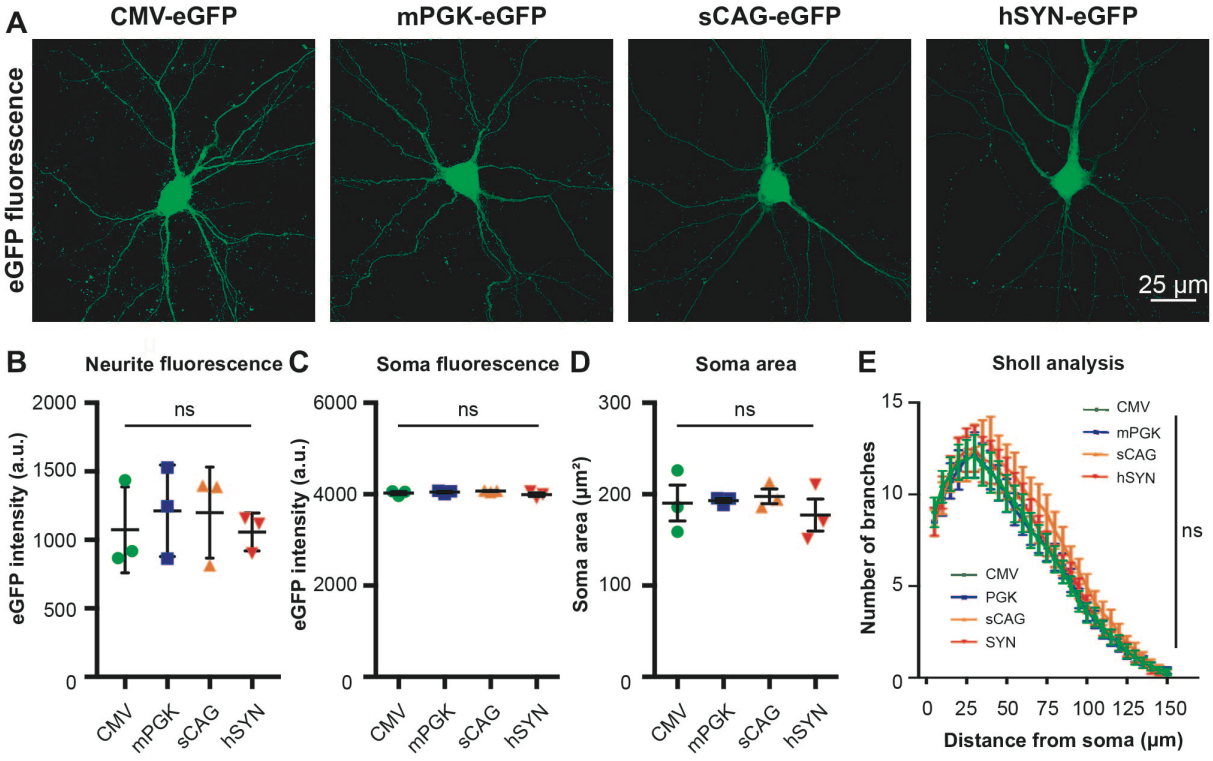

Fig. 4. - previous page - Comparison of four promoters for eGFP expression in cultured cortical neurons after transfection. (A) Representative 14 DIV cortical neurons that were transfected with four different plasmids: CMV-eGFP, mPGK-eGFP, sCAG-eGFP, hSYN-eGFP (B) Quantifications of the mean eGFP intensity in neurites (df=3(8), F=0.23, P>0.05, ANOVA with Tukey's multiple comparison test). (C) Quantification of the mean eGFP intensity in the soma (df=3(8), F=1.39, P>0.05, ANOVA with Tukey's multiple comparison test). (D) Quantification of the soma area (df=3(8), F=0.41, P>0.05, ANOVA with Tukey's multiple comparison test). (E) Sholl analysis of neurite branches (df=3(8), F=0.52, P>0.05, Repeated measure ANOVA, n = 3 per group). The data shows the average ± SEM. The results are obtained from three independent experiments (n=3) and a total of 45 transfected neurons were analyzed for each condition. Ns, not statistically significant. Scale bar: 25 μm. Lab journal references: BN-18-08, BN-18-15, BN-18-16.

(2) Validation of a new ImageJ macro for automated histological analysis of AAV transduced cortex tissue

A custom-made ImageJ macro was made for semi-automated image analysis of fluorescent images (**Fig. 3**) using thresholding, watershedding, particle analysis, and transferring a mask from the red channel (NeuN) to the green channel (eGFP). This novel ImageJ macro can be used to measure: (1) the total number of NeuN+ cells in the region of interest, (2) the number of AAV transduced NeuN+ cells, and (3) the average eGFP intensity of the transduced cells. This ImageJ macro was used to analyse rat and mouse tissue that was stereotactically injected with various AAV serotypes and different promoters in the right sensory-motor cortex. The tissue was perfused six weeks after injection and underwent immunohistochemistry procedures. To examine whether the new ImageJ macro was correctly calibrated, we performed manual analysis of ten random cropped images of AAV transduced cortical tissue and compared this to the output of the ImageJ macro. One cropped fluorescent image of AAV transduced mouse cortical tissue is shown in **Fig. 5A.** The number of NeuN+ cells was manually counted (**Fig. 5B**) and automatically detected by the ImageJ macro (**Fig. 5C**). There was no statistically significant difference between the numbers of NeuN+ cells between the manual (100 ± 0 %) and automated analysis (95.1 ± 4.08 % fraction of normalized cells) (**Fig. 5D**). The eGFP+ NeuN+ cells were also manually counted (**Fig. 5B**) and automatically quantified using the ImageJ macro (**Fig. 5C**). The ImageJ Macro measures the eGFP intensity in all previously detected NeuN+ cells. However, the cells are classified as eGFP+ when the fluorescent intensity passes an arbitrary limit of 30% above the average background intensity (in other words, the intensity has to be above the 1.3 ratio of eGFP to background intensity). There was no statistically significant difference between the numbers of eGFP+ NeuN+ cells between the manual (100 ± 0 %) and automated analysis (112 ± 9.5 % fraction of normalized cells). In addition, the output of the automated analysis can be directly used to calculate the average eGFP intensity per neuron, while manual analysis will require

labour-intensive masking of the NeuN+ cells before measuring the eGFP intensity (not shown).

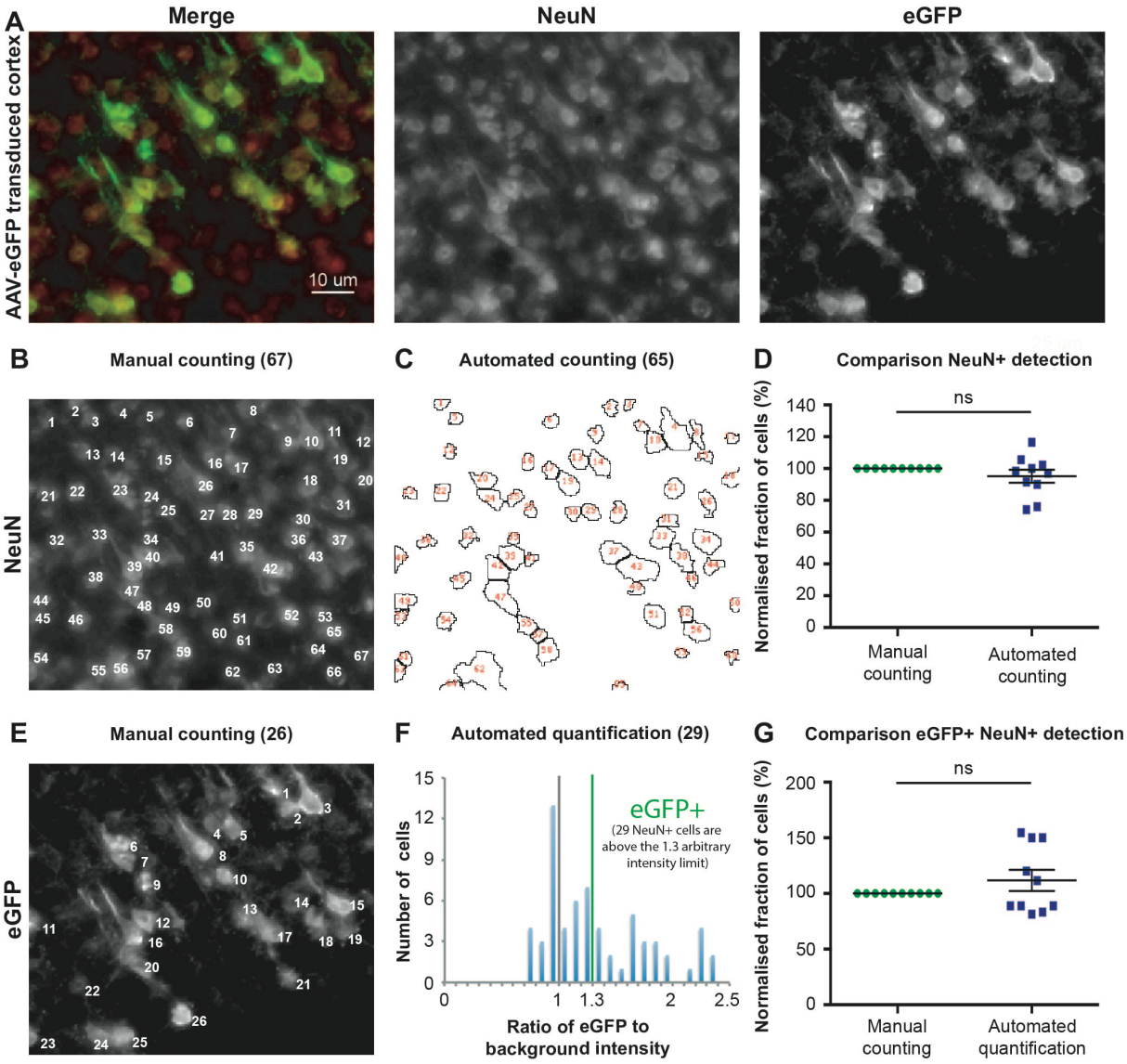

Fig. 5. Detection of NeuN+ and eGFP+ NeuN+ cells in AAV-transduced mouse cortex *via* manual analysis and a new ImageJ macro. Adult mice were stereotactically injected with AAVs expressing eGFP and perfused after six weeks. Immunohistochemistry was performed to visualize NeuN (red) and eGFP (green) in the cortex. A cropped image of an AAV-transduced cortical area is shown in (A). The number of NeuN+ cells was manually counted in (B) and detected by the ImageJ macro in (C). (D) Quantification of the number of NeuN+ cells by manual counting and the ImageJ macro (N=10 per group, Mann-Whitney U=35 P > 0.05, Mann-Whitney test). (E) Manual analysis of the number of eGFP+ NeuN+ cells. (F) Quantification of the number of eGFP+ NeuN+ cells using the ImageJ macro and Excel. The eGFP intensity of all previously detected NeuN+ cells were measured and divided by the intensity of the background within the region of interest to obtain a eGFP/background intensity ratio. The histogram shows the eGFP/background intensity ratio on the X-axis and the frequency (number of cells) on the Y-axis. The grey vertical line represents an eGFP/background ratio of 1 and therefore the number of NeuN+ cells with eGFP intensity similar to the average background intensity (e.g

eGFP- NeuN+ cells). Since measuring fluorescent intensities will follow a normal distribution, it is important to set an arbitrary limit for measuring eGFP+ NeuN+ cells. The green vertical line represents an eGFP/background ratio of 1.3 (e.g. 30% above the average background intensity) and is the decided arbitrary limit to measure eGFP+ NeuN+ cells. (G) Quantification of the number of eGFP+ NeuN+ cells by manual counting and the ImageJ macro (N=10 per group, Mann-Whitney U=50 $P > 0.05$, Mann-Whitney test). The data shows the average ± SEM. Ns, not statistically significant. Images were taken with a Zeiss AxioScan Z1 microscope with 20x objective.

(3) Detection of eGFP in the dorsal corticospinal tract following AAV vector injection in the sensorimotor cortex

The ImageJ macro described above will be useful to quantify the number of transduced neurons in the cortex. A different approach is needed to quantify the number of transduced neurons specifically in the layer V motor cortex, we decided to count the number of axons in the cervical spinal cord that originated from these neurons. A pilot staining on spinal cords was done to confirm that the coordinates used for stereotactic injections indeed target layer V neurons that give rise to the corticospinal tract and whether immunohistochemistry procedures for eGFP are required to visualize axons.

Immunohistochemistry was performed on 40 μm thick, transverse spinal cord sections of one rat that was injected with AAV1-mPGK-eGFP in the right sensory-motor cortex. By using an epifluorescence microscope with 20x objective (**Fig. 6 – upper panels**) the transduced axons in the left dorsal corticospinal tract were clearly visible, while the axons on the contralateral site were not detectable. The image acquisition was done with high intensity power and this resulted in unwanted auto-fluorescence of the grey matter in the 40 μm thick sections (**Fig. 6 – upper panels**). Confocal imaging with a 40x objective resulted in clear visualization of transduced axons and did not result in auto-fluorescence of the grey matter (**Fig. 6 – lower panels**). Axons that were eGFP positive were detectable in both stained for eGFP (**Fig. 6A)** and non-stained sections (**Fig. 6B)**, but the intensity is brighter/higher in stained sections. In summary, this pilot staining showed that the injection coordinates for the right sensory-motor cortex of rats (see **Fig. 2**) targets layer V neurons and that eGFP staining is not required for tissue injected with AAV1-mPGK-eGFP. However, I decided to perform immunohistochemistry procedures for eGFP on future spinal cord tissue in order to enhance the eGFP signal of potentially weaker promoters such as the CMV promoter.

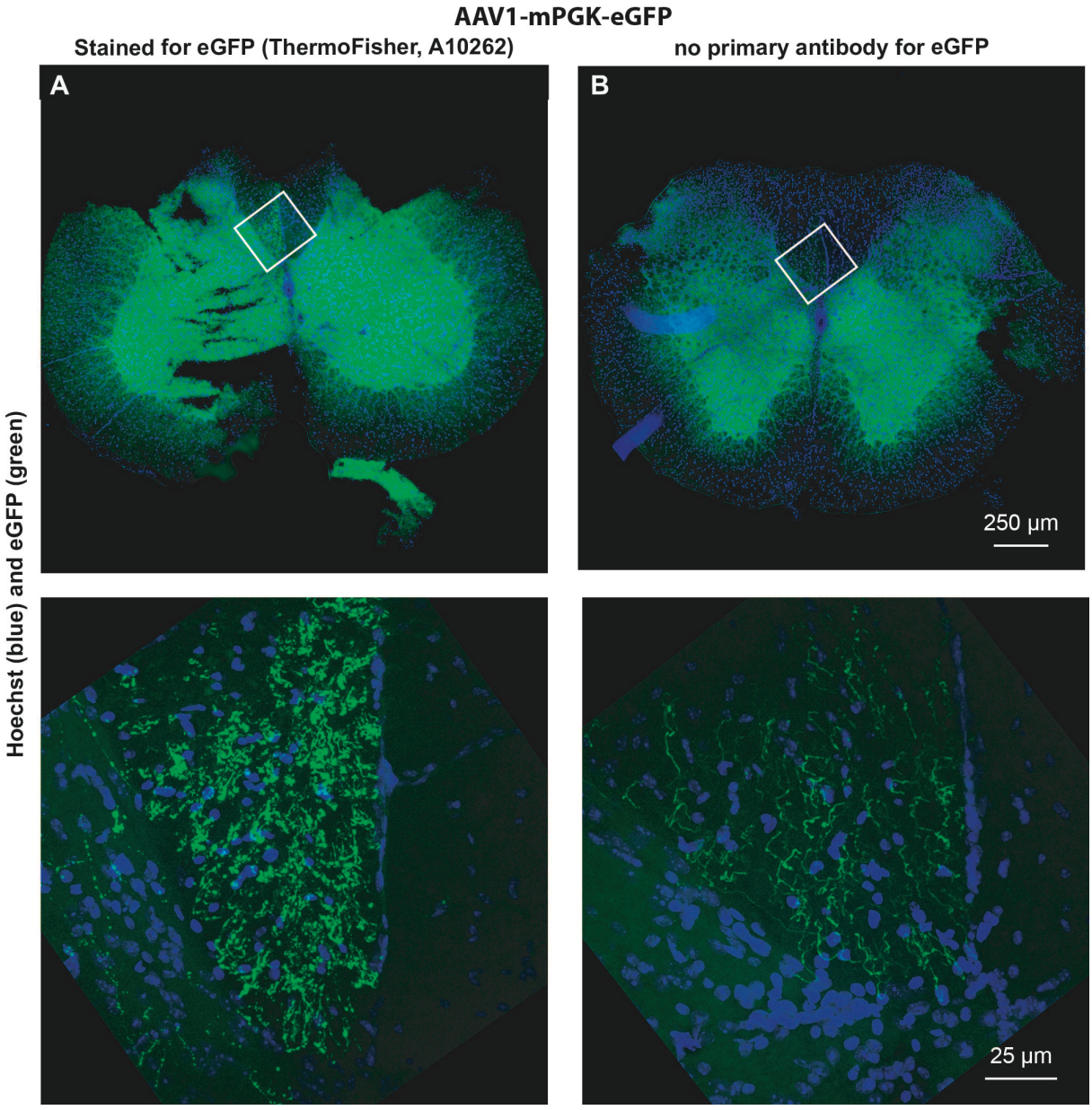

Fig. 6. Detection of eGFP-positive axons in the dCST of a rat injected with AAV1-mPGK-eGFP in the sensory-motor cortex. Transverse sections of the cervical spinal cord that were stained for eGFP by using a 1:1000 dilution of the ThermoFisher A10262 antibody **(A)** or were treated without primary antibody **(B)**. The images in the upper panels are tile-scanned images that were taken with a DMi8 epifluorescence microscope to highlight the entire section. The high signal in grey matter is an artefact caused by the imaging of the 40 µm thick sections using an epifluorescence microscope. The images in the lower panels were taken using a confocal microscope to zoom in on the dCST with high resolution. The artefact in the grey matter disappears and single collaterals become visible when imaged with a confocal microscope. Lab journal reference: BN-18-27.

(4) Efficiency of AAV1 and AAV5 in transducing cortical neurons *in vivo*

AAVs serotypes 1 and 5 with hSYN promoter were injected into the sensory-motor cortex of rats and mice to compare the transduction and gene expression efficiency of these two serotypes in cortical neurons *in vivo*. Six weeks after injection, the animals were perfused and microscopy analyses were performed.

In rats (**Fig. 7A**), the mean area of transduction was not statistically significantly different between AAV1 (1.03 ± 0.17 mm^2) and AAV5 (0.73 ± 0.09 mm^2) (**Fig. 7B**). However, AAV1 (6473 ± 682 NeuN+ cells) transduced two-fold more cortical neurons than AAV5 (3255 ± 377 NeuN+ cells) (**Fig. 7C**). The mean eGFP intensity per transduced neuron was also higher in AAV1 (68.5 ± 2.02 a.u.) compared to AAV5 (28.8 ± 5.45 a.u.) (**Fig. 7D**).

In mice (**Fig. 8A**), the mean area of viral transduction was bigger in AAV1 (1.03 ± 0.10 mm^2) than AAV5 (0.61 ± 0.08 mm^2) injected animals (**Fig. 8B**). The number of transduced cells was almost double in AAV1 (4098 ± 252 NeuN+ cells) compared to AAV5 (2304 ± 291 NeuN+ cells) (**Fig. 8C**). The mean eGFP intensity per transduced neuron was also superior in AAV1 (64.5 ± 2.40 a.u.) than AAV5 (30.0 ± 5.37 a.u.) (**Fig. 8D**).

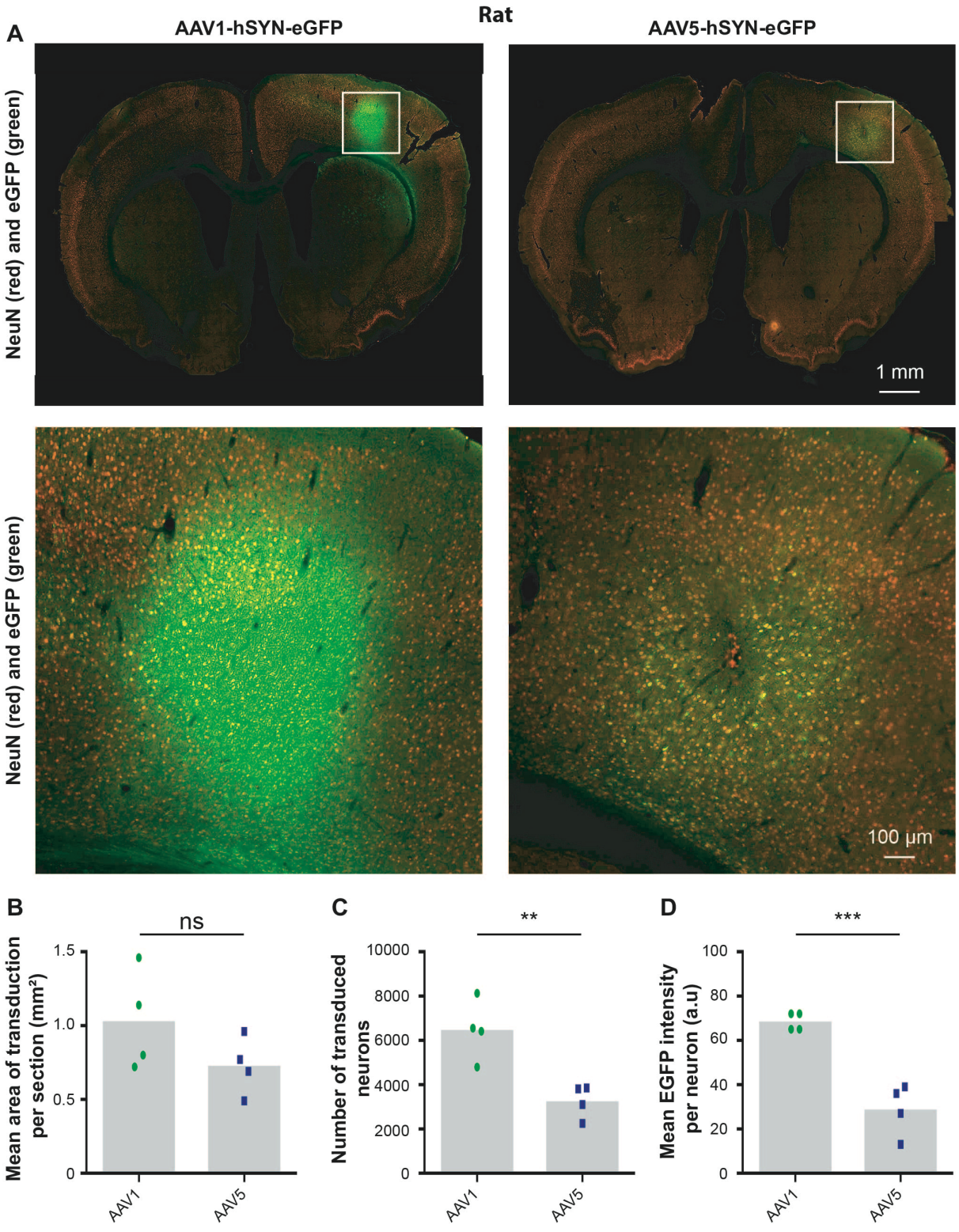

Fig. 7. Transduction of AAV1 and AAV5 harbouring the hSYN-eGFP expression cassette in the sensory-motor cortex of rats. (A) NeuN+ and eGFP staining in the cortex of AAV1-hSYN-eGFP and AAV5-hSYN-eGFP injected rats. (B) Quantification of the mean area of transduction in 40 µm thick sections (df=6, t=1.55, P > 0.05, Student's t-test). (C) Quantification of the number of transduced NeuN+ cells. eGFP+ NeuN+ cells were detected using the ImageJ macro and neurons were considered as transduced when the eGFP intensity was 1.3x higher than the eGFP to background intensity ratio (df=6, t=4.13, P < 0.01, Student's t-test). (D) Quantification of the mean eGFP intensity per transduced neurons (df=6, t=6.44, P < 0.001, Student's t-test). The grey bars

depict the averages and each dot represents the mean value of one animal. A total of 4 rats were analysed for each condition. Ns, not statistically significant; ** P<0.01; *** P<0.001. Lab journal reference: BN-18-06.

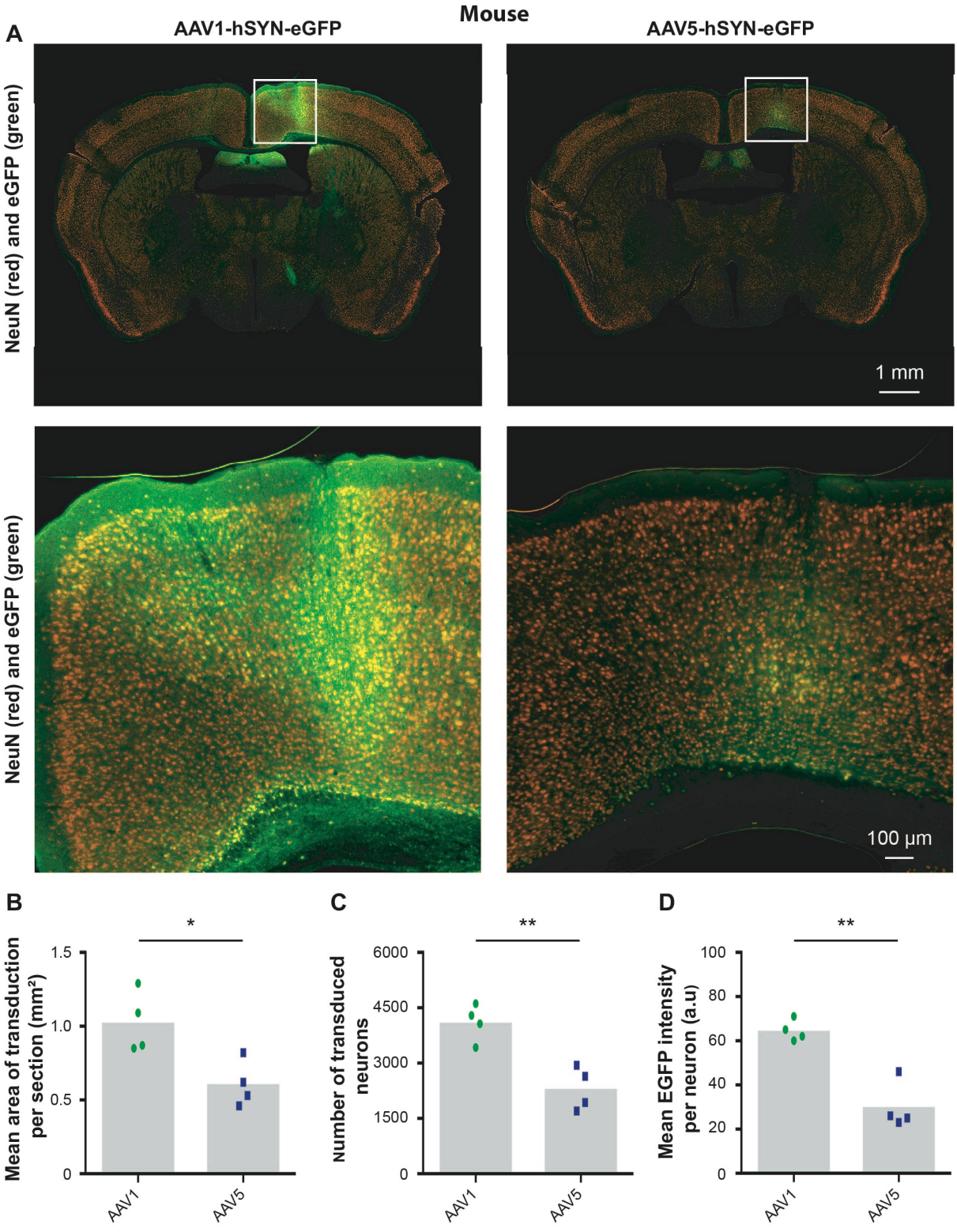

Fig. 8. Transduction of AAV1 and AAV5 harbouring the hSYN-eGFP expression cassette in the sensory-motor cortex of mice. (A) NeuN+ and eGFP staining in the cortex of AAV1-hSYN-eGFP and AAV5-hSYN-eGFP injected mice. (B) Quantification of the mean area of transduction in 40 µm thick sections (df=6, t=3.22, P < 0.05, Student's t-test). (C) Quantification of the number of transduced NeuN+ cells. eGFP+ NeuN+ cells were

detected using the ImageJ macro and neurons were considered as transduced when the eGFP intensity was 1.3x higher than the eGFP to background intensity ratio (df=6, t=4.13, P < 0.01, Student's t-test) (D) Quantification of the mean eGFP intensity per transduced neurons (df=6, t=5.87, P < 0.01, Student's t-test). The grey bars depict the averages and each dot represents the mean value of one animal. A total of 4 mice were analysed for each condition. * P<0.05; ** P<0.01. Lab journal reference: BN-18-12.

(5) Efficiency of AAV1 and AAV5 to transduce layer V corticospinal neurons *in vivo*

The rAAV injection in the sensory-motor cortex resulted in extensive transduction of neurons of the corticospinal tract. eGFP+ fibers were crossing at the pyramidal tract and descended into the left dorsal columns of the spinal cord (**Fig. 9**).

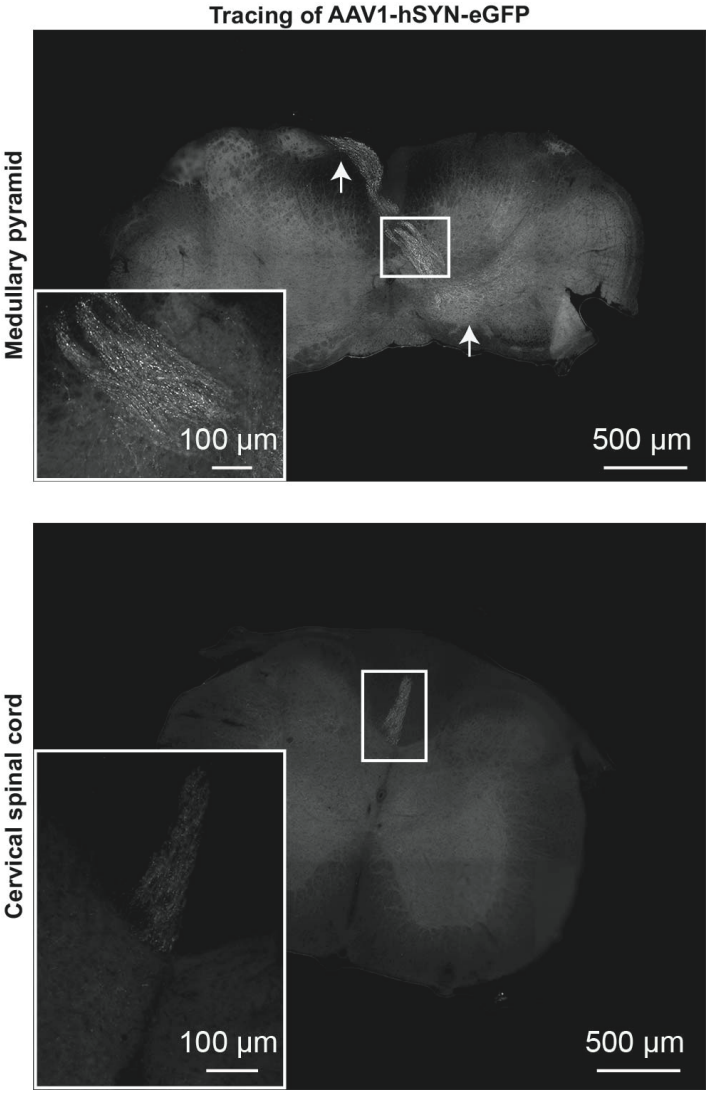

Fig. 9. Transduction of the corticospinal tract in a mouse injected with AAV1-hSYN-eGFP. eGFP-positive fibers are crossing at the level of the medullary pyramid from the right to left brain hemisphere (**upper**), and the axonal fibers are found in the left dorsal columns of the cervical spinal cord (**lower**). The high signal in grey matter is an artefact caused by epifluorescence microscopy of the 40 µm thick sections. The zoom-in figures were taken using a confocal microscope and as a consequence the artefact is reduced. Lab journal references: BN-18-12-typical CST & BN-18-28.

After confirming successful transduction of the corticospinal neurons, we determined the efficiency of the AAV1 and AAV5 serotypes with the hSYN promoter to transduce layer V cortical neurons that give rise to the CST. This was determined by counting the number of transduced axons in the dCST of the spinal cord (**Fig. 10A**). The axons were counted in one transverse section per animal. The number of transduced corticospinal axons was statistically significantly higher in AAV1 than AAV5 in both rats (**Fig. 10B**) and mice (**Fig. 10C**). In the spinal cord of rats, 1305 ± 123 axons were transduced in the AAV1 group, while 838 ± 133 axons were counted in the AAV5 group. In the spinal cord of mice, 484 ± 30 and 250 ± 87 axons were counted for AAV1 and AAV5, respectively. Thus, AAV1 is the superior serotype to transduce layer V neurons in rats and mice. Consistent with the data in the cortex (**Fig. 7** and **Fig. 8**), the eGFP fluorescence intensity was brighter in the AAV1 condition compared to AAV5 (not quantified).

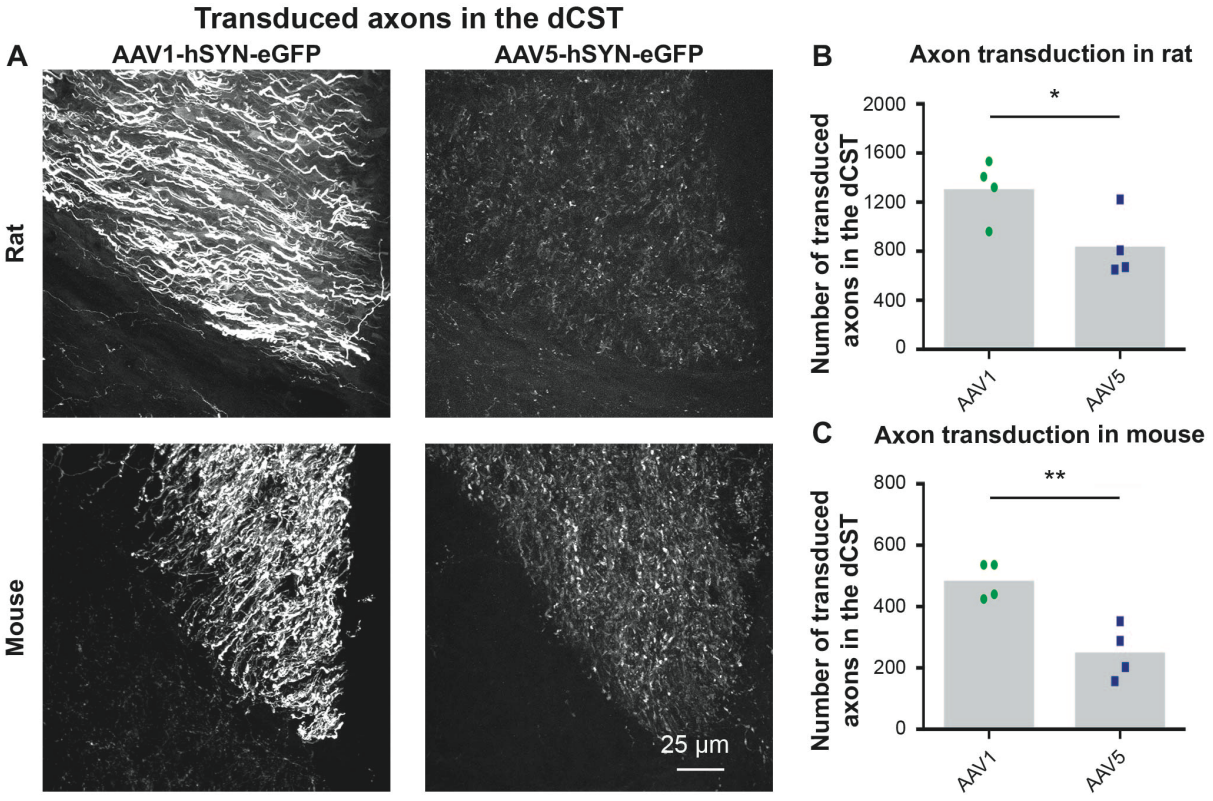

Fig. 10. Transduction of AAV1 and AAV5 in layer V cortical neurons measured by quantifying their axons in the spinal cord. (A) Representative images of transduced axons in the left dorsal column of the spinal cord of AAV1-hSYN-eGFP and AAV5-hSYN-eGFP injected rats and mice. The axons in the AAV1 group were brighter than the AAV5 group (B) Quantification of the number of transduced axons in rat (df=6, t=2.58, $P < 0.05$, Student's t-test). (B) Quantification of the number of transduced axons in mouse (df=6, t=4.43, $P < 0.01$, Student's t-test). The grey bars depict the averages and each dot represents the axon count of one animal. A total of 4 animals were analysed for each condition. * $P<0.05$; ** $P<0.01$. Lab journal reference: BN-18-28.

(6) Efficiency of the four promoters to express eGFP in cortical neurons *in vivo*

After replicating the findings of Hutson *et al.*, 2012 that AAV1 is the superior serotype for corticospinal tract transduction between AAV1 and AAV5, we were interested to determine the optimal promoter for transgene expression in cortical neurons. AAV1-CMV-GFP, AAV1-mPGK-GFP, AAV1-sCAG-GFP, and AAV1-hSYN-GFP were injected into the right sensory-motor cortex of rats and mice for this purpose. The transduction area, the number of transduced cells, and the expression intensity of eGFP was measured 6 weeks after AAV injection.

In rats (**Fig. 11A**), the mean area of transduction was significantly different between the four promoters. The AAV1 vectors with the mPGK and hSYN promoter had an average transduction area of approximately 1 mm^2 (1.24 ± 0.14 mm^2 and 1.03 ± 0.17 mm^2, respectively), whereas the vectors with sCAG and CMV transduced an area of roughly 0.55 mm^2 (0.59 ± 0.09 and 0.55 ± 0.09 mm^2, respectively) (**Fig. 11B**). A difference between the mPGK and hSYN promoter vectors and the sCAG and the CMV promoter vectors was also observed when analysing the number of transduced neurons. The AAV1 vector with mPGK and hSYN promoters transduced on average the highest number of cortical neurons (7950 ± 477 and 6473 ± 682 NeuN+ cells, respectively) followed by sCAG and CMV (2172 ± 189 and 1256 ± 277 NeuN+ cells, respectively) (**Fig. 11C**). Importantly, not only the number of transduced neurons was higher with the mPGK and hSYN promoter but the mPGK and hSYN promoters also displayed significantly higher levels of eGFP expression in cortical neurons (80 ± 6 and 69 ± 3 a.u., respectively) compared to the CMV and sCAG promoters (26 ± 3 and 18 ± 2 a.u., respectively) (**Fig. 11D**).

In mice (**Fig. 12A**), the mean area of transduction was statistically significantly different between the four promoters. The AAV1 vector carrying the hSYN promoter (1.03 ± 0.10 mm^2) had the biggest area of transduction area compared to the other promoters (mPGK, 0.62 ± 0.09 mm^2; sCAG, 0.44 ± 0.11 mm^2; CMV, 0.40 ± 0.07 mm^2) (**Fig. 12B**). The vector with the hSYN promoter transduced the highest number of cortical neurons (4098 ± 252 NeuN+ cells). The vector with the mPGK promoter had the second best mean number of transduced neurons (3464 ± 530 NeuN+ cells) and was followed by CMV and sCAG (1962 ± 387 and 1704 ± 665 NeuN+ cells, respectively) (**Fig. 12C**). Importantly, the eGFP intensity was different between the four promoters. The AAV vectors with the mPGK and hSYN promoters express eGFP with the highest intensity in the neurons (73 ± 10 and 65 ± 2 a.u., respectively). The vectors with the CMV and sCAG promoters had a relatively low eGFP intensity in cortical neurons (42 ± 8 and 28 ± 8 a.u., respectively) (**Fig. 12D**).

In summary, the most efficient promoters for AAV-mediated transgene expression in cortical neurons are mPGK and hSYN in both rats and mice.

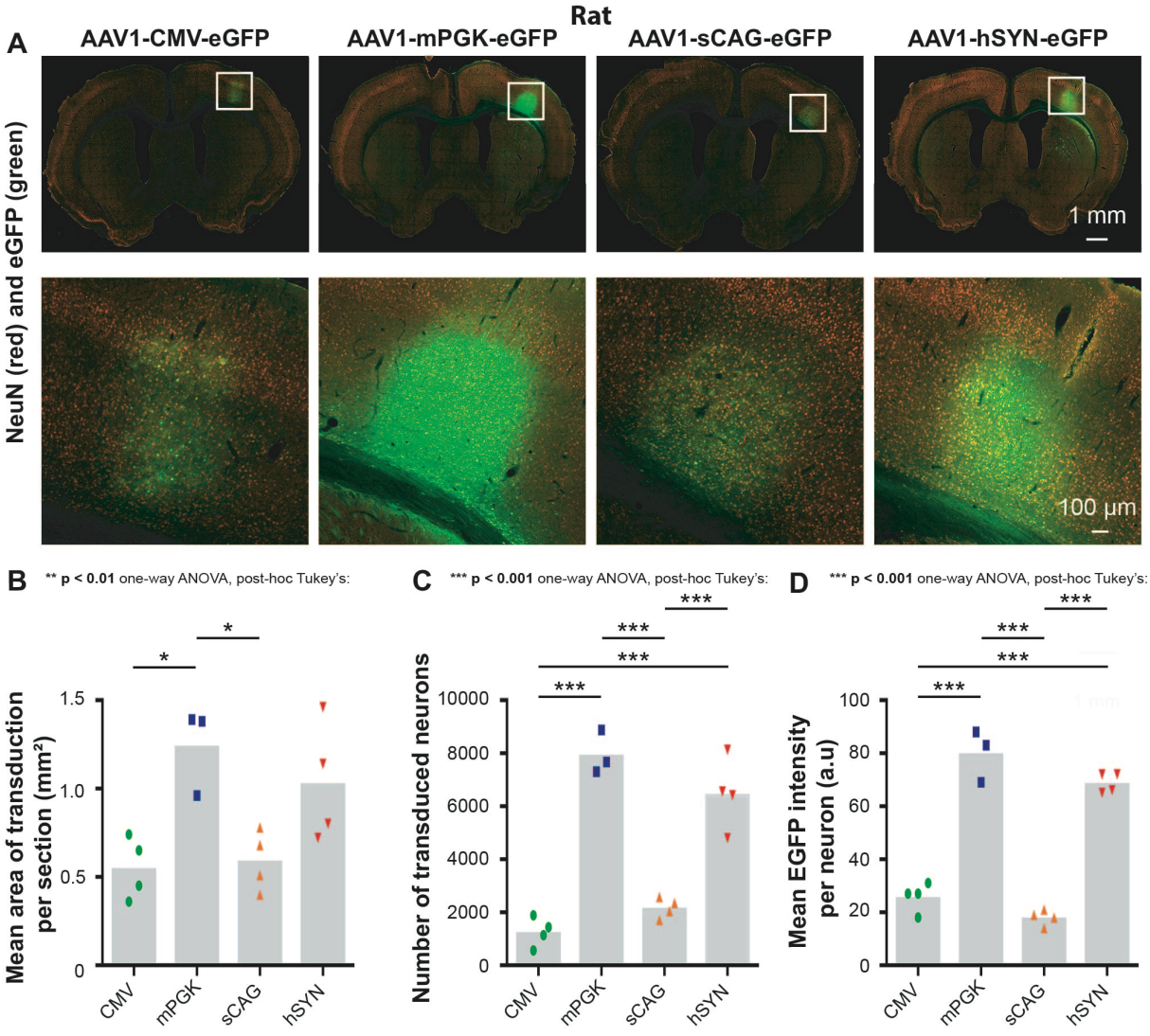

Fig. 11. Neuronal transduction efficiency and mean eGFP intensity of four promoters in the sensory-motor cortex of rats. (A) NeuN+ and eGFP staining in the cortex of AAV1-CMV-eGFP, AAV1-mPGK-eGFP, AAV1-sCAG-eGFP, and AAV1-hSYN-eGFP injected rats. (B) Quantification of the mean area of transduction in 40-micron thick sections (df=3(11), F=6.88, P<0.01, ANOVA with Tukey's multiple comparison test). (C) Quantification of the number of transduced NeuN+ cells. eGFP+ NeuN+ cells were detected using the ImageJ macro and neurons were considered as transduced when the eGFP intensity was 1.3x higher than the eGFP to background intensity ratio (df=3(11), F=50.4, P<0.001, ANOVA with Tukey's multiple comparison test). (D) Quantification of the mean eGFP intensity per transduced neurons (df=3(12), F=107, P<0.001, ANOVA with Tukey's multiple comparison test). The grey bars depict the averages and each dot represents the mean value of one animal. * P<0.05; ** P<0.01; *** P<0.001. Lab journal reference: BN-18-06.

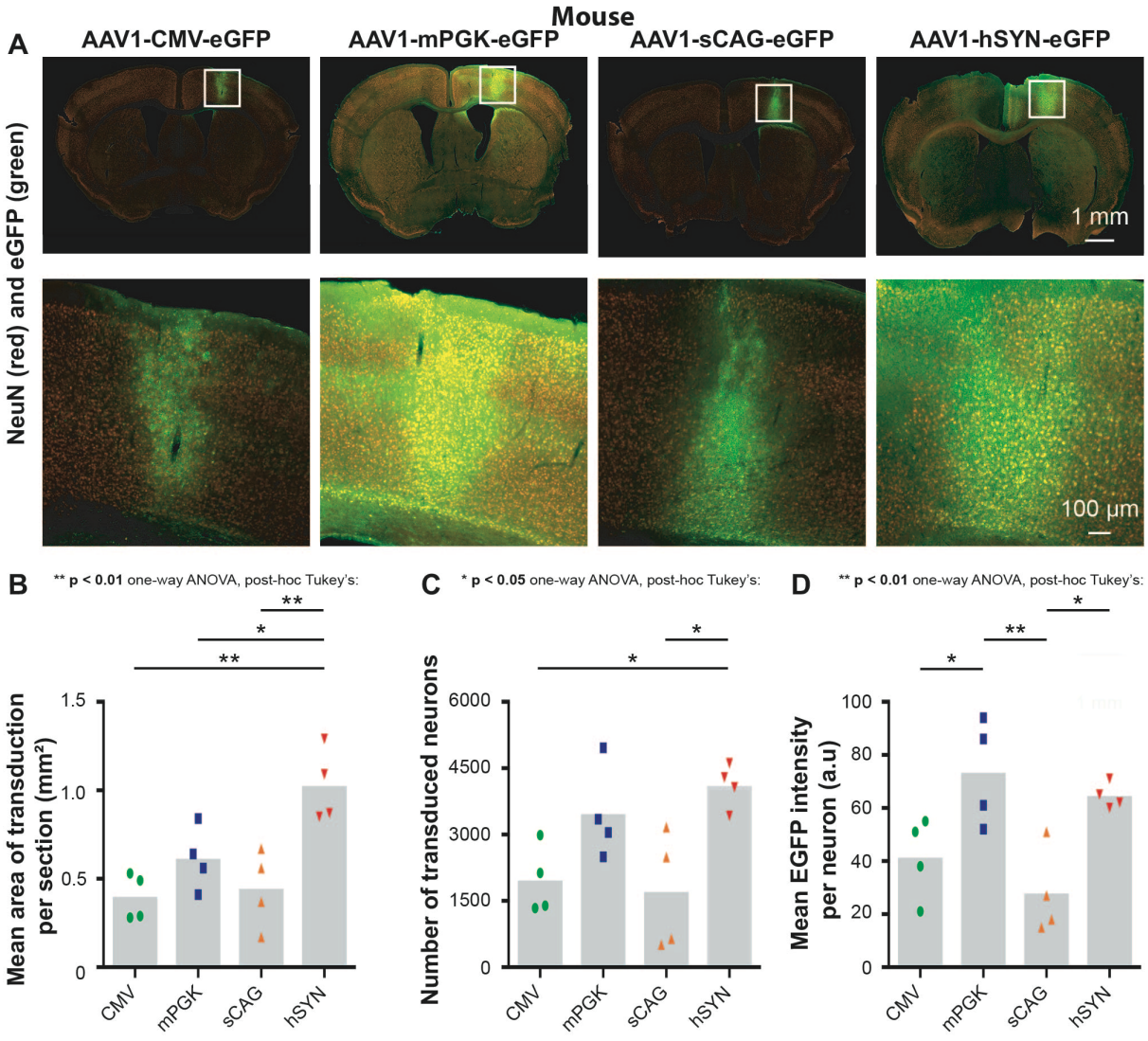

Fig. 12. Neuronal transduction efficiency and mean eGFP intensity of four promoters in the sensory-motor cortex of mice. (A) NeuN+ and eGFP staining in the cortex of AAV1-CMV-eGFP, AAV1-mPGK-eGFP, AAV1-sCAG-eGFP, and AAV1-SYN-eGFP injected mice. (B) Quantification of the mean area of transduction in 40-micron thick sections (df=3(12), F=9.29, P<0.01, ANOVA with Tukey's multiple comparison test). (C) Quantification of the number of transduced NeuN+ cells. eGFP+ NeuN+ cells were detected using the ImageJ macro and neurons were considered as transduced when the eGFP intensity was 1.3x higher than the eGFP to background intensity ratio (df=3(12), F=5.74, P<0.05, ANOVA with Tukey's multiple comparison test). (D) Quantification of the mean eGFP intensity per transduced neurons (df=3(12), F=7.58, P<0.01, ANOVA with Tukey's multiple comparison test). The grey bars depict the averages and each dot represents the mean value of one animal. A total of 4 mice were analysed for each condition. * P<0.05; ** P<0.01. Lab journal reference: BN-18-12.

(7) Efficiency of the four promoters to transduce layer V corticospinal neurons *in vivo*

The number of eGFP-expressing axons that originate from layer V cortical neurons were counted in the dorsal column of the spinal cord. This was done to obtain the transduction efficiency of neurons of the corticospinal tract by AAV1 vectors with different promoters.

In rats (**Fig. 13A, B**), hSYN and mPGK had the best transduction of layer V cortical neuron as 1497 ± 99 and 1305 ± 123 axons were detected in the dorsal column of the cervical spinal cord contralateral to the injected sensory-motor cortex. The sCAG group counted 623 ± 50 green axons, and CMV contained on average 293 ± 49 eGFP-positive fibres in the spinal cord.

In mice (**Fig. 13A, C**), 484 ± 30 and 386 ± 70 axons were visible in the spinal cord in the mPGK and hSYN groups, respectively. The sCAG and CMV promoters had 175 ± 47 and 95 ± 34 axons containing eGFP, respectively.

The transduction efficiency of the AAV1 vector carrying the mPGK and hSYN promoters were not statistically significant different showing that these two promoters are equally strong in both rats and mice. Fewer eGFP-positive axons were observed in the groups that contained the AAV1 vector harbouring the CMV and sCAG promoters indicating that these promoters are less efficient to target the corticospinal tract *in vivo*.

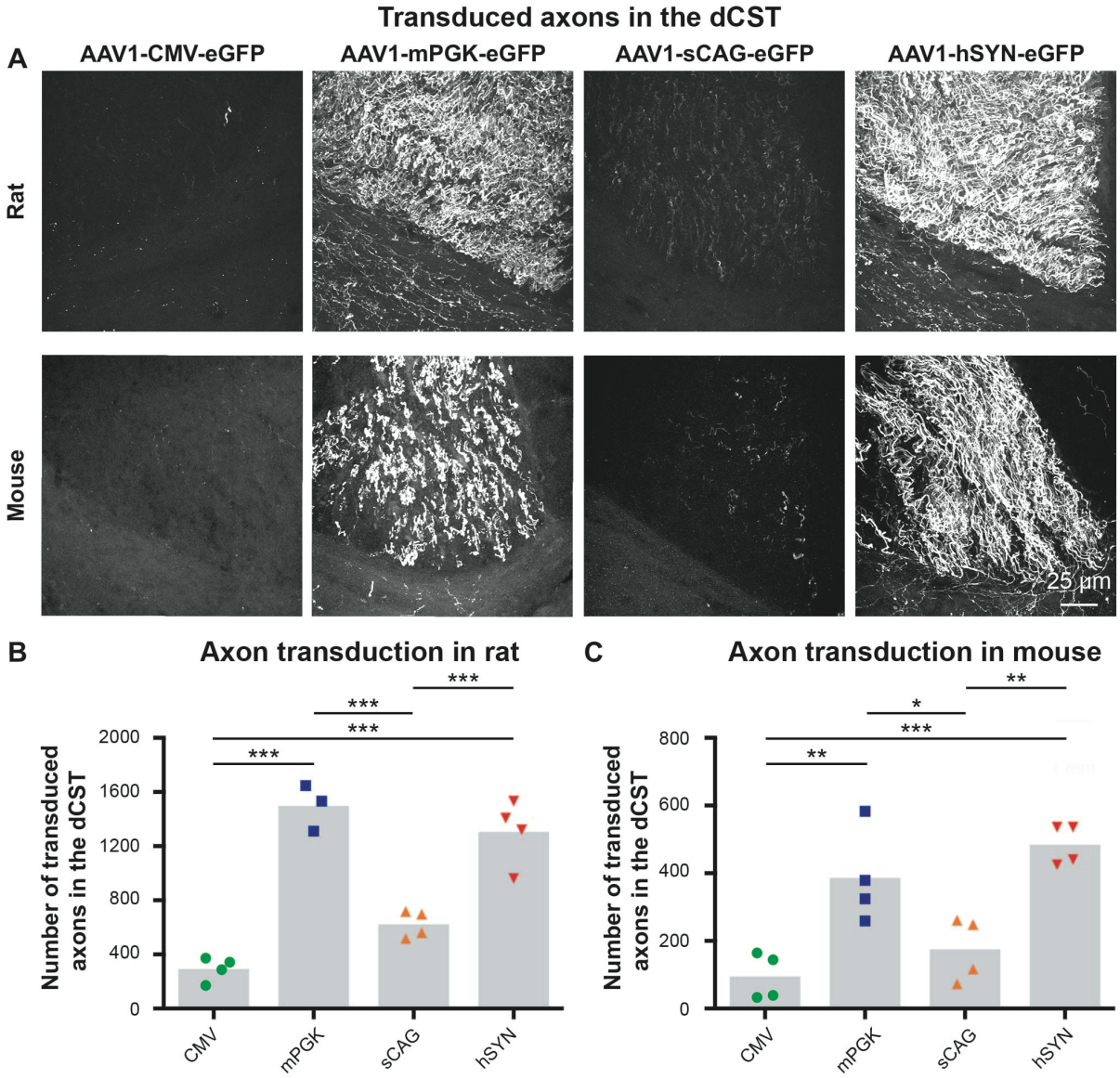

Fig. 13. Transduction efficiency of layer V cortical neurons depending on the choice of promoters CMV, mPGK, sCAG and hSYN measured by eGFP expressing axons in the spinal cord. (A) eGFP positive fibers in the dorsal corticospinal tract of AAV1-CMV-eGFP, AAV1-mPGK-eGFP, AAV1-sCAG-eGFP, and AAV1-hSYN-eGFP injected rats and mice. (B) Quantification of the number of transduced axons in rats (df=3(11), F=43.7, P<0.001, ANOVA with Tukey's multiple comparison test). (B) Quantification of the number of transduced axons in mice (df=3(12), F=14.2, P<0.001, ANOVA with Tukey's multiple comparison test). The grey bars depict the averages and each dot represents the mean value of one animal. * P<0.05; ** P<0.01; *** P<0.001. Lab journal reference: BN-18-28.

(8) Validation of antibodies for detection of non-neuronal cells in the rodent cortex

Antibodies for immunohistochemistry of non-neuronal cells were tested on brain tissue of naïve (non-transduced) animals. The used antibody concentrations were based on the recommendation of the manufacturers or colleagues. The cells of interest are astrocytes, microglia, and oligodendrocytes.

Astrocytes can be detected by the markers aldehyde dehydrogenase I family member L1 (ALDH1L1) and glial fibrillary acidic protein (GFAP) among others. ALDH1L1 is an enzyme found in astrocytes (Cahoy *et al.*, 2008) and GFAP is an intermediate filament found in the processes of astrocytes (reviewed in Hol & Pekny, 2015). The ab87117 antibody for ALDH1L1 resulted in nonspecific staining in PFA perfused mouse cortex (**Fig. 14A, B**). This staining pattern was not the result of unspecific binding by the secondary antibody (**Fig. 14C**). In contrast, the Dako Z033429 antibody for GFAP resulted in strong astrocytic staining throughout the cortex, and a zoom-in image of a single astrocyte is shown in **Fig. 15A, B**. The astrocytes processes were clearly visible with the 1:500 dilution (**Fig. 15A)** and less clearly visible with the 1:1000 dilution (**Fig. 15B**). There was little background staining as a result of unspecific binding by the secondary antibody (**Fig. 15C**). For future experiments, the Dako Z033429 antibody for GFAP with 1:500 dilution was used to detect astrocytes *in vivo*.

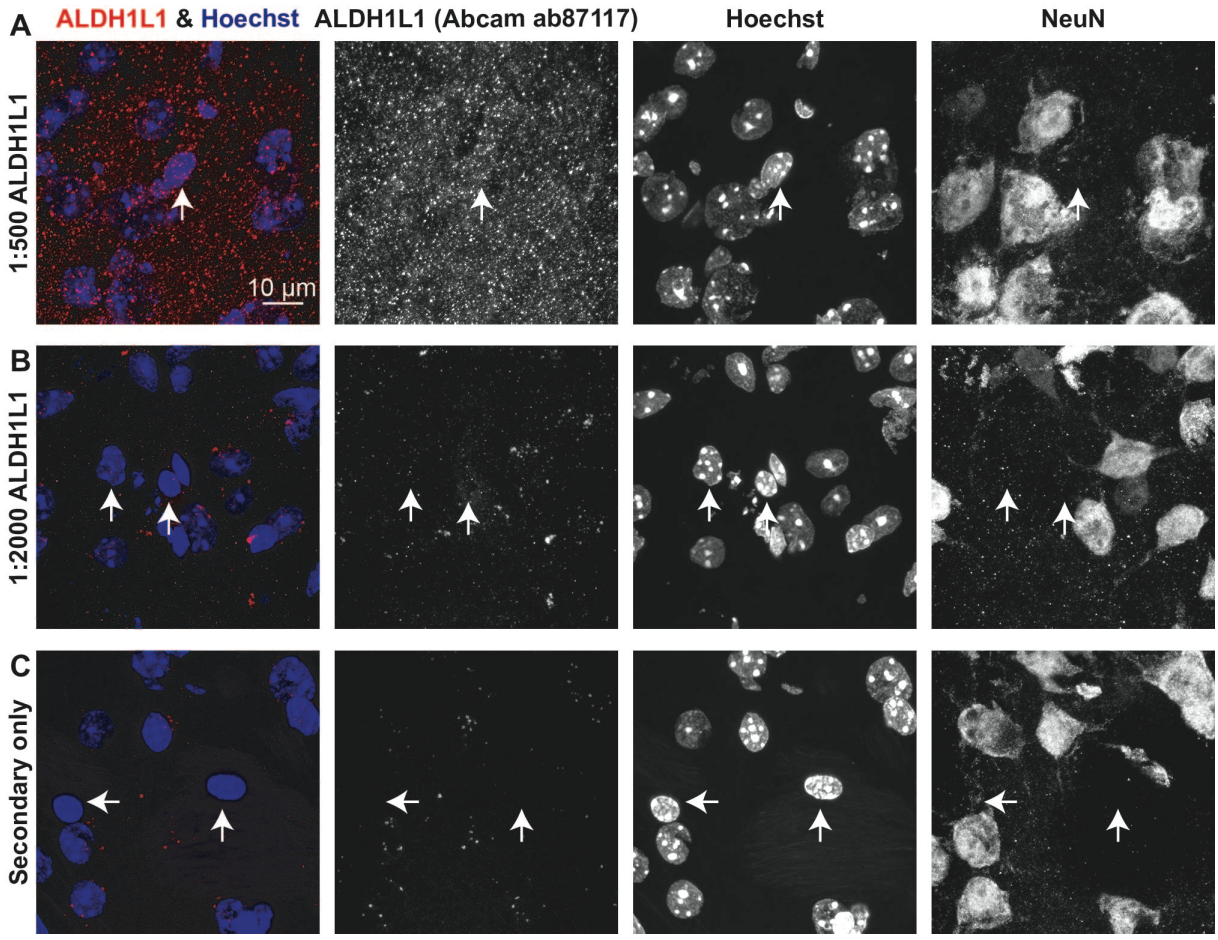

Fig. 14. Dilution range of the ALDH1L1 antibody was unsuccessful to visualize astrocytes in free-floating sections of 4% PFA perfused mouse cortex. 1:500 and 1:2000 dilutions of the Abcam ab87117 antibody are shown in (A) and (B), respectively. One section that was stained without the primary antibody for ALDH1L1 is shown in (C). The arrows highlight nuclei of glial cells, identified by negative NeuN staining. Lab journal reference: BN-18-07.

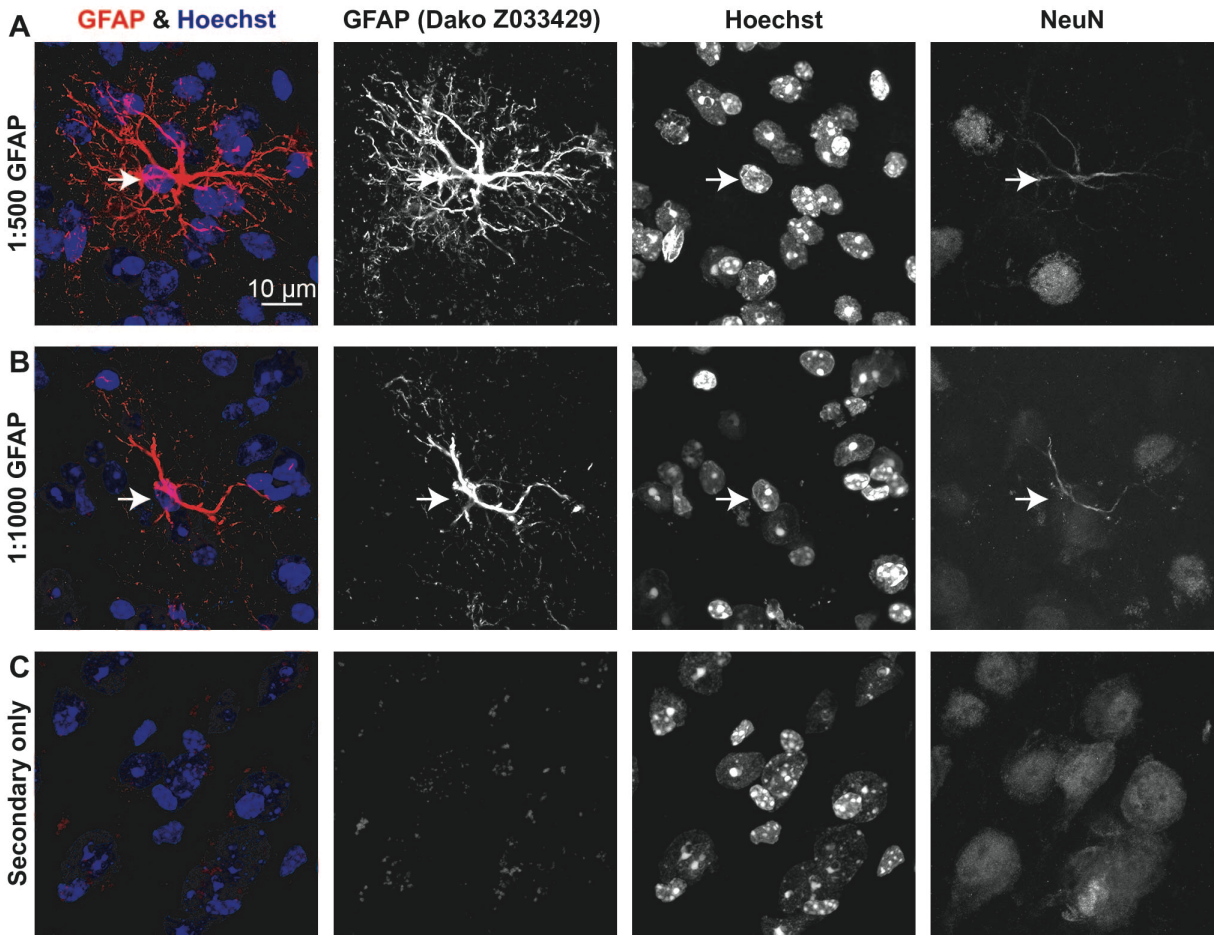

Fig. 15. Validation of the GFAP antibody to detect astrocytes in free-floating sections of 4% PFA perfused mouse cortex. 1:500 and 1:1000 dilutions of the Dako Z033429 antibody is shown in (A) and (B), respectively. One section that was stained without the primary antibody for GFAP is shown in (C). The arrows highlight the nucleus of a GFAP-positive cell. Note: the used confocal laser-scanning settings resulted in bleed through in the NeuN channel, which needs to be prevented in future experiments. Lab journal reference: BN-18-21.

Microglia can be detected by multiple markers including ionized calcium binding adaptor molecule 1 (Iba1) (reviewed in Perry, Nicoll, & Holmes, 2010; Li & Barres, 2018). Iba1, which is also localized in macrophages, is a calcium-binding protein that is important for various calcium-dependent processes such as membrane trafficking and phagocytosis (Ohsawa *et al.*, 2004). The Wako 019-19741 antibody for Iba1 resulted in clear detection of microglia morphology in the PFA-perfused mouse cortex with 1:1000 (**Fig. 16A**) and 1:2000 dilution (**Fig. 16B**) resulted in clear detection of microglia morphology in the PFA perfused mouse cortex. However, the processes were best visible with the dilution of 1:1000 (**Fig. 16A**). The Iba1 immunofluorescence was not due to unspecific binding by the secondary antibody (**Fig. 16C**). For future experiments, a 1:1000 dilution of the Wako 019-19741 antibody for Iba1 was used.

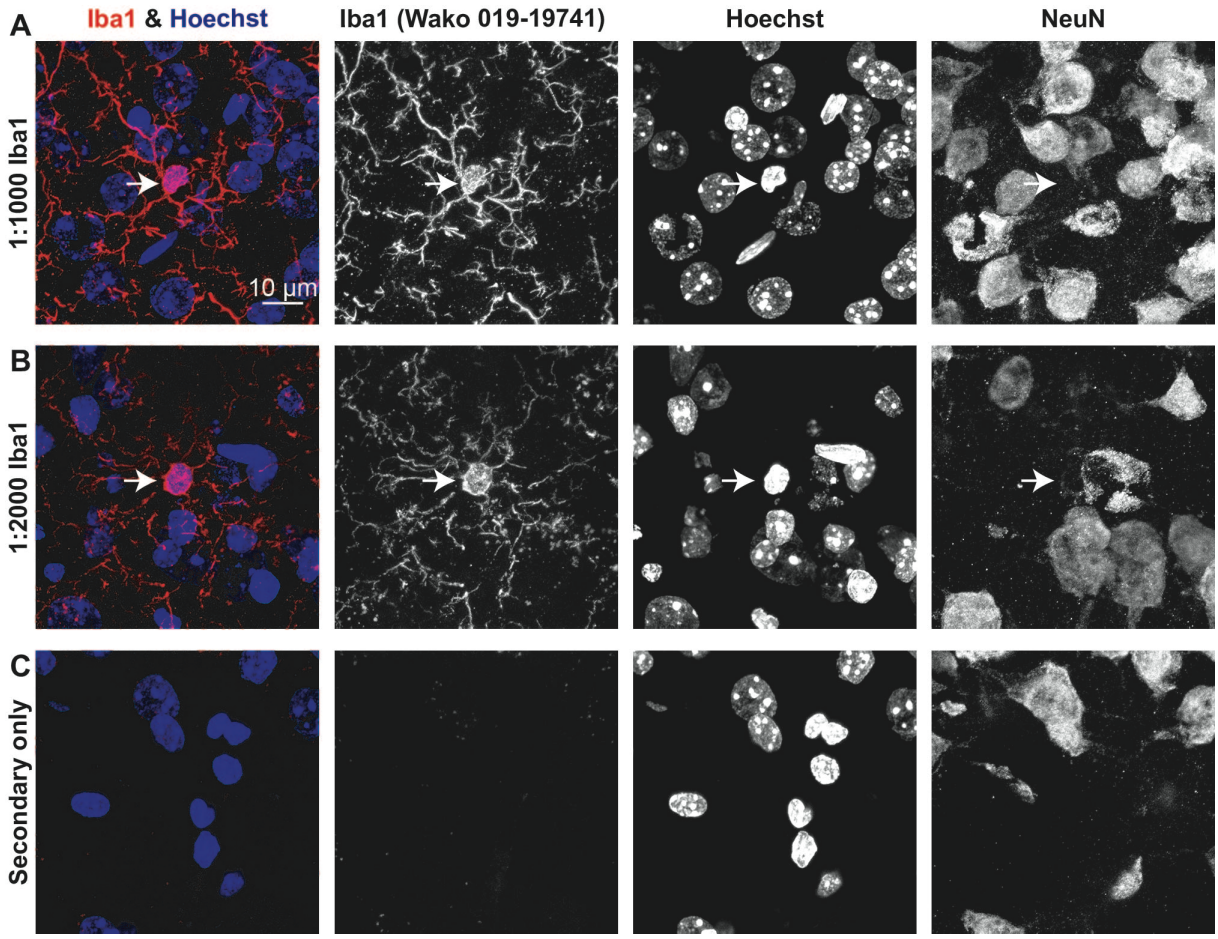

Fig. 16. Validation of the Iba1 antibody to detect microglia in free-floating sections of 4% PFA perfused mouse cortex. 1:1000 and 1:2000 dilutions of the Wako 019-19741 antibody are shown in (A) and (B), respectively. One section that was stained without the primary antibody for Iba1 is shown in (C). The arrows highlight the nucleus of an Iba1-positive cell. Lab journal reference: BN-18-13.

The oligodendrocyte lineage can be visualized by multiple markers (reviewed in Bergles & Richardson, 2016; Franklin & ffrench-Constant, 2017). The oligodendrocyte transcription factor 2 (olig2) is present in the nucleus of both OPC and oligodendrocytes, and I validated the Millipore ab9610 antibody for Olig2 with 1:500 dilution previously (pilot data not shown in dissertation, but see successful staining in **Fig. 22**). Here, we explored the antibodies for chondroitin sulfate proteoglycan 4 (NG2), and adenomatous polyposis coli (APC) clone CC1. NG2 is a hallmark of oligodendrocyte progenitor cells (OPC); the APC clone CC1 recognizes mature oligodendrocytes. Interestingly, in contrast to what the name of the antibody suggests, anti-APC clone CC1 does not bind the antigen for APC but Quaking 7, an RNA binding protein found in myelinating oligodendrocytes (Bin, Harris, & Kennedy, 2016).

The Millipore ab5320 antibody for NG2 resulted in a non-convincing or possibly weak detection of OPC when high antibody concentrations were used in PFA perfused mouse cortex (**Fig. 17A, B**). A limited degree of unspecific binding by the secondary antibody was also detected (**Fig. 17C**), but this does not explain the weak OPC detection.

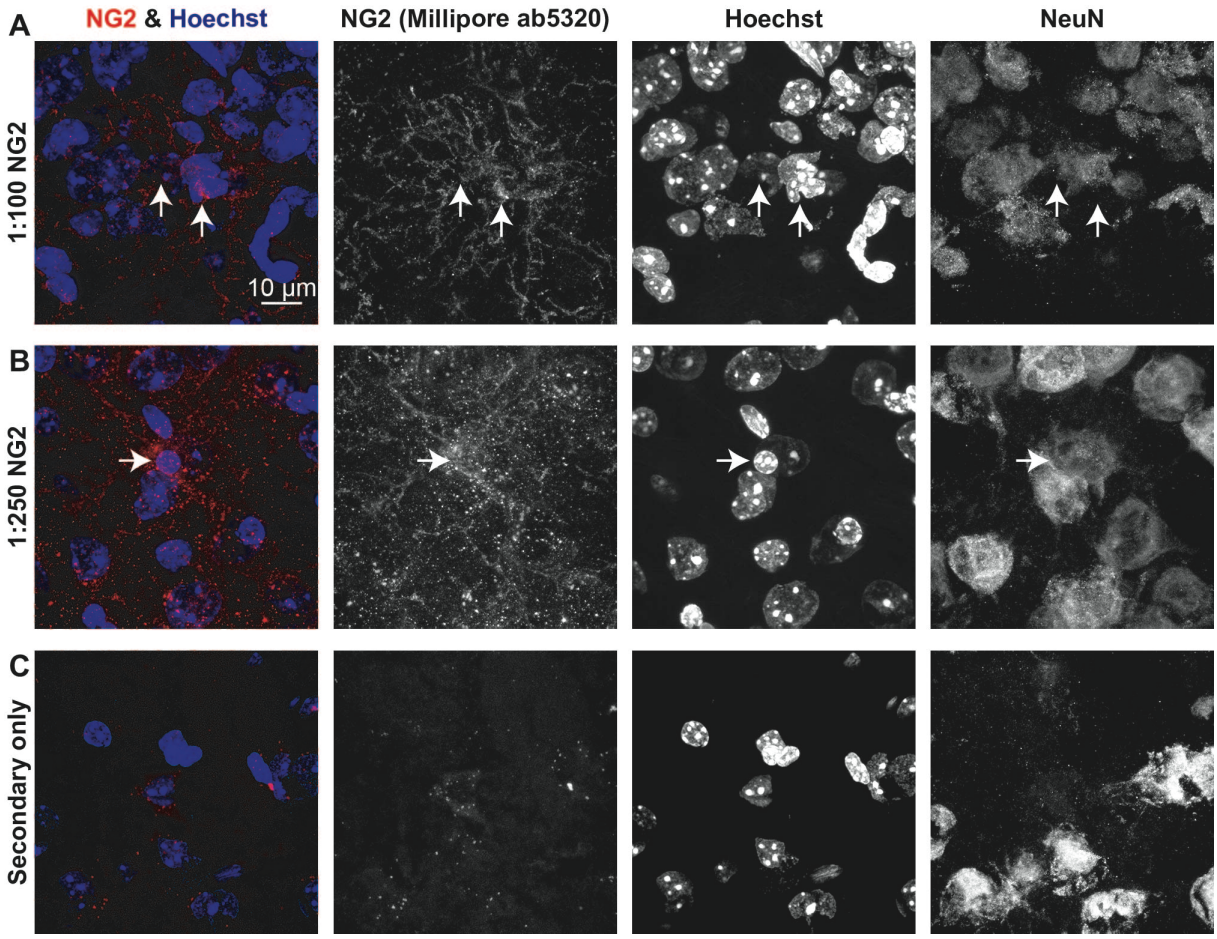

Fig. 17. Dilution range of the NG2 antibody was unsuccessful to detect oligodendrocyte precursor cells in free-floating sections of 4% PFA perfused mouse cortex. 1:100 and 1:250 dilutions of the Millipore ab5320 antibody are shown in (A) and (B), respectively. One section that was stained without the primary antibody for chondroitin sulfate proteoglycan 4 (NG2) is shown in (C). The arrows highlight the nucleus of a possibly NG2-positive cell, but it is not a convincing immunolabelling. Lab journal reference: BN-18-13.

The Millipore OP80 2 antibody for APC did detect cells in the dilution range from 1:100 to 1:500 (**Fig. 18A, B, C**) with a secondary antibody for isotope IgG2a (**Fig. 18D**). Despite that the biggest population of cells was found in and near the corpus callosum area, the detected cells did not display typical oligodendrocyte morphology. The primary antibody is derived from the mouse subclass IgG2b and therefore the wrong secondary antibody (IgG2a) was used for the visualization of the labelled oligodendrocytes in this pilot experiment. Typical oligodendrocyte morphology was detected when the Millipore OP80 2

antibody was used together with the secondary antibody that detects the mouse IgG2b epitope (**Fig. 19A, B, C**). As expected, a majority of oligodendrocytes was detected in and near the corpus callosum. Application of the secondary antibody alone resulted in limited background staining (**Fig. 19D**), and did not result in oligodendrocyte morphology as shown with the primary antibodies. For future experiments, the Millipore OP80 2 clone CC1 antibody with 1:300 dilution was used to detect mature oligodendrocytes *in vivo*.

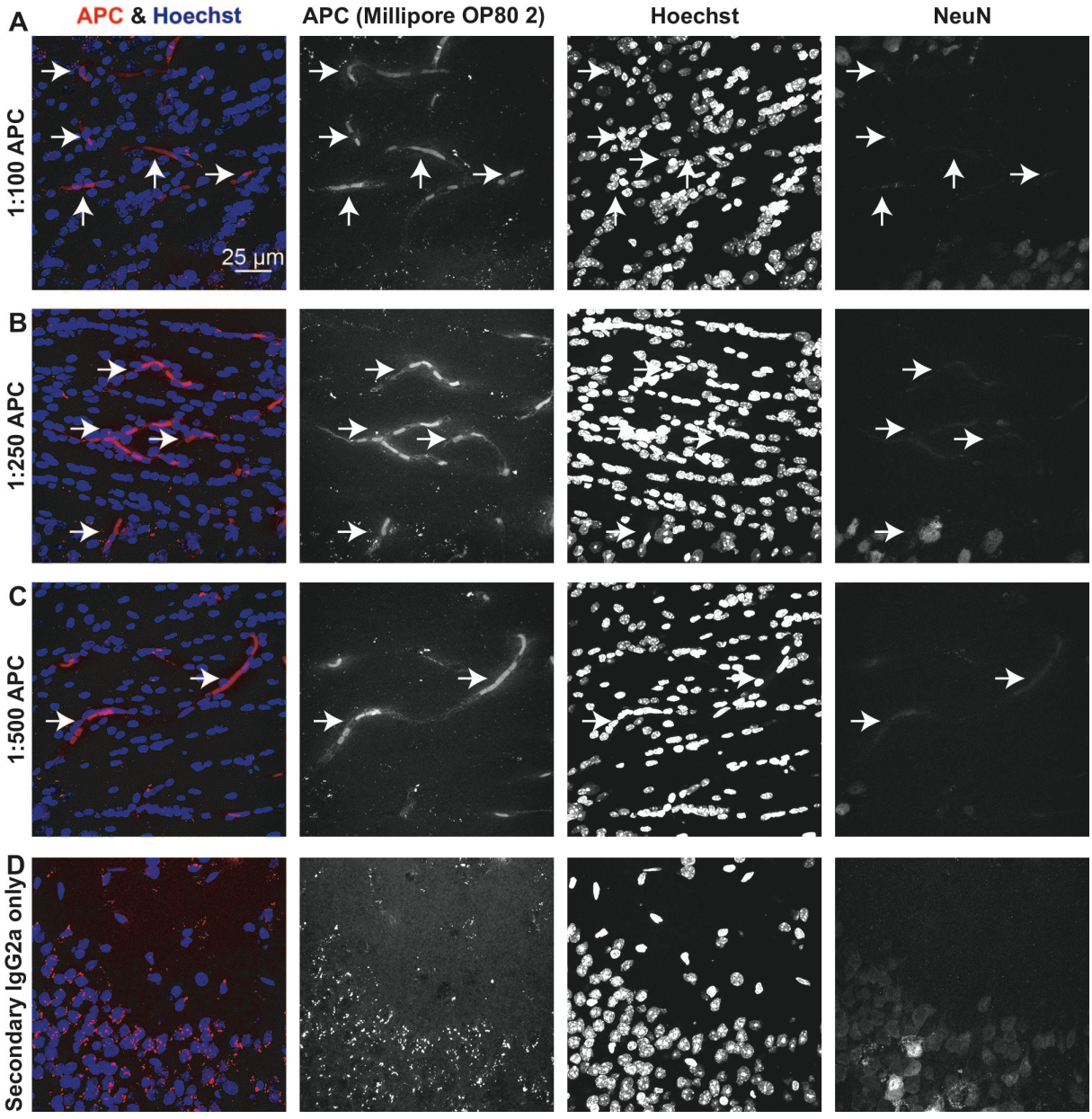

Fig. 18. Dilution range of the anti-APC clone CC1 antibody to detect oligodendrocytes was unsuccessful when combined with secondary IgG2a antibodies in free-floating sections of 4% PFA perfused mouse cortex. Images were taken at the corpus callosum and can be identified by the border of NeuN+ cells. 1:100, 1:250 and 1:500 dilutions of the Millipore OP80 2 antibody is shown in (A), (B), and (C), respectively. One section that was stained with the secondary antibody for the IgG2a isotope only is shown in (D). The arrows

highlight the nucleus of APC-positive cells. Note that the scale bar represents 25 microns, in the other glial stainings the scale bar represented 10 microns. Lab journal reference: BN-18-25.

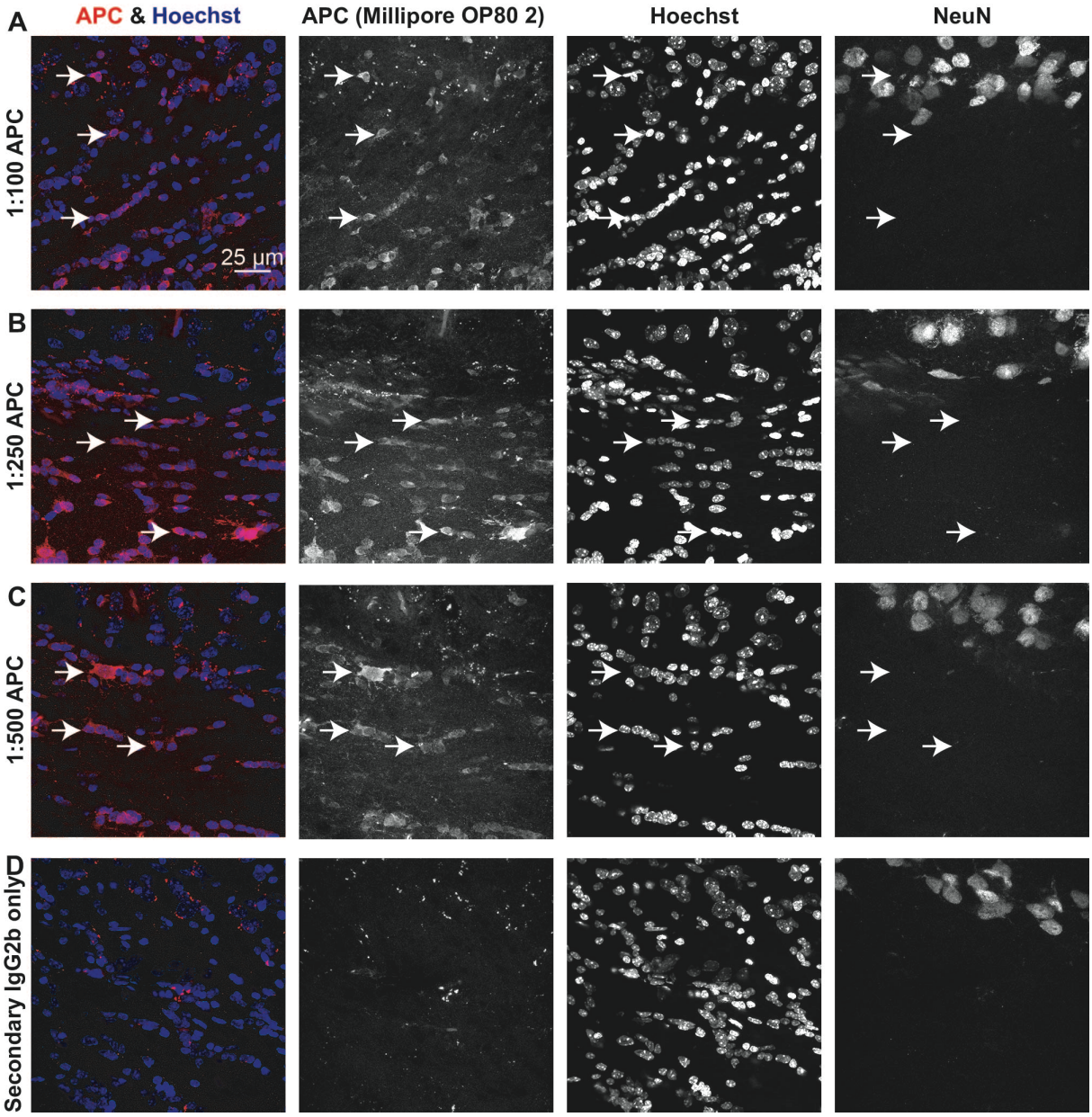

Fig. 19. Validation of the anti-APC clone CC1 antibody to detect oligodendrocytes in free-floating sections of 4% PFA perfused mouse cortex. Images were taken at the corpus callosum and can be identified by the border of NeuN+ cells. 1:100, 1:250 and 1:500 dilutions of the Millipore OP80 2 antibody is shown in (A), (B), and (C), respectively. One section that was stained with the secondary antibody for the IgG2b isotope only is shown in (D). The three arrows highlight the nucleus of APC-positive cells. Note that the scale bar represents 25 microns, in the other glial pilot stainings the scale bar represented 10 microns. Lab journal reference: BN-18-26.

In summary, I tested several antibodies for immunohistochemistry of non-neuronal cells in the mouse cortex. The determination of the optimal dilution to visualize the non-neuronal cells is subjective. Based on above data, I decided to use below antibodies and concentrations for the detection of non-neuronal cells in the AAV transduced tissue (See section II.7): astrocytes, GFAP Dako Z033429 1:500; microglia, Iba1 Wako 019-19741 1:1000; a co-staining for the oligodendrocytes lineage e.g. APC clone CC1, Millipore OP80 2 1:300; and olig2 Millipore ab9610 1:500. The co-staining would, therefore, indicate the following: olig2+ CC1+ cells label mature oligodendrocytes and olig2+ CC1- cells oligodendrocytes precursor cells.

(9) Expression of eGFP in non-neuronal cells depending on the promoter driving eGFP expression

The transduction of astrocytes was determined by counting the number of GFAP-positive cells that expressed eGFP in the cortex. This was determined for the AAV1-CMV-eGFP, AAV1-mPGK-eGFP, AAV1-sCAG-eGFP, and AAV1-hSYN-eGFP transduced brains (**Fig. 20A**). The AAV vectors harbouring the mPGK and hSYN did not result in eGFP expression in astrocytes for both rats (**Fig. 20B**) and mice (**Fig. 20C**). In contrast, the viral vectors containing the CMV (36 ± 5 and 78 ± 11) and sCAG (92 ± 5 and 103 ± 26) promoter did mediate eGFP expression in astrocytes within the injected cerebral hemispheres of rats and mice (**Fig. 20B, C**).

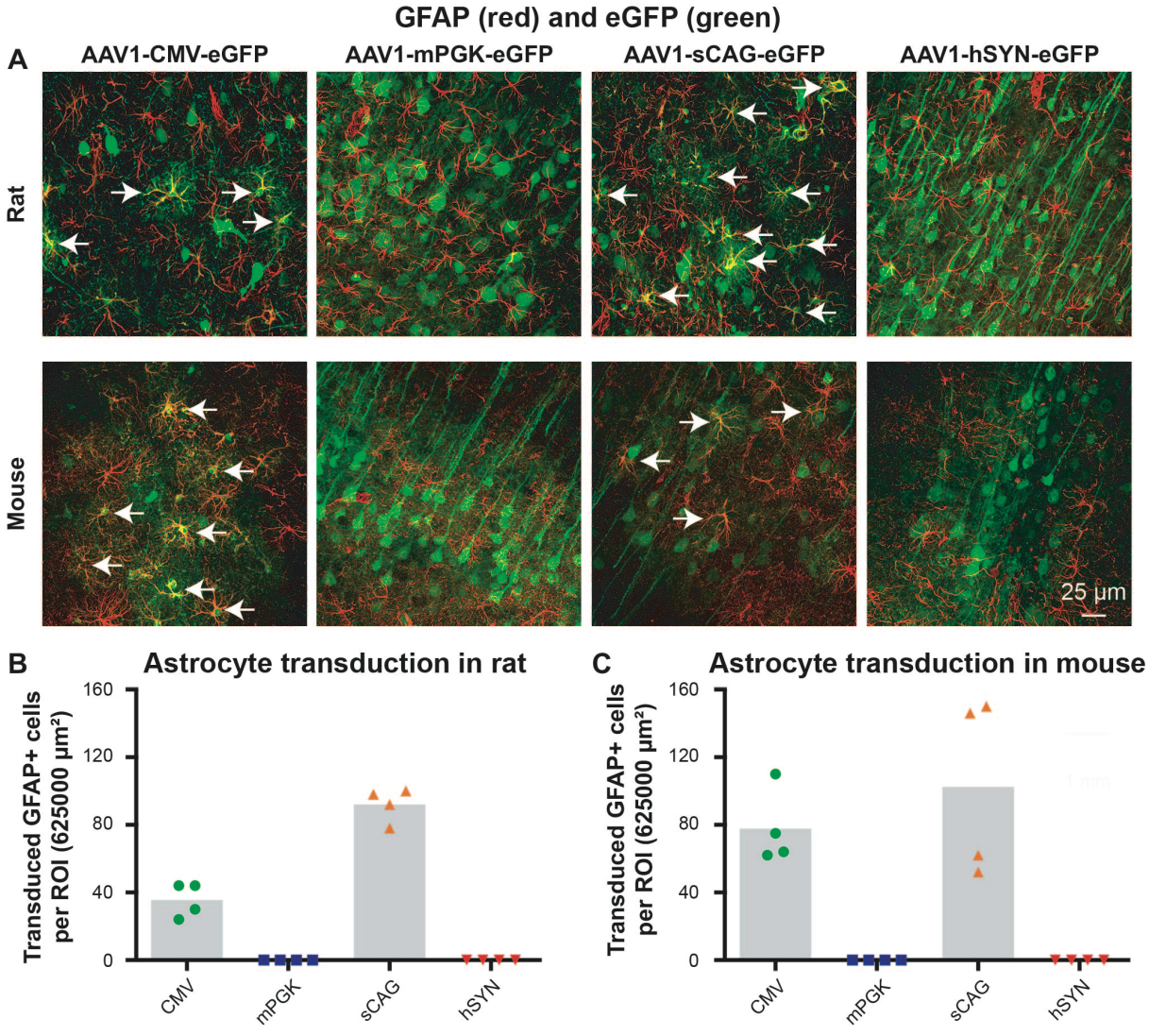

Fig. 20. Expression of eGFP in astrocytes with CMV and sCAG promoters, but not with mPGK and hSYN promoters. (A) GFAP (red) and eGFP (green) staining in the cortex of AAV1-CMV-eGFP, AAV1-PGK-eGFP, AAV1-sCAG-eGFP, and AAV1-hSYN-eGFP injected rats and mice. Quantification of the number of transduced GFAP+ cells in rats (B) and mice (C). The grey bars depict the averages and each dot represents the mean value of one animal, a total of 4 animals were analysed for each condition. Statistical analysis was not

possible because two experimental groups have a mean value of zero transduced astrocytes. Lab journal reference: BN-18-23.

The number of transduced microglia was determined by counting the number of Iba1-positive cells that expressed eGFP in the cerebral cortex that was transduced with AAVs. The AAV viral vector serotype 1 together with the promoters CMV, mPGK, sCAG and hSYN did not result in expression of eGFP in microglia (**Fig. 21A**). No transduced microglia was observed in the investigated 16 rats (**Fig. 21B**) or 16 mice (**Fig. 21C**).

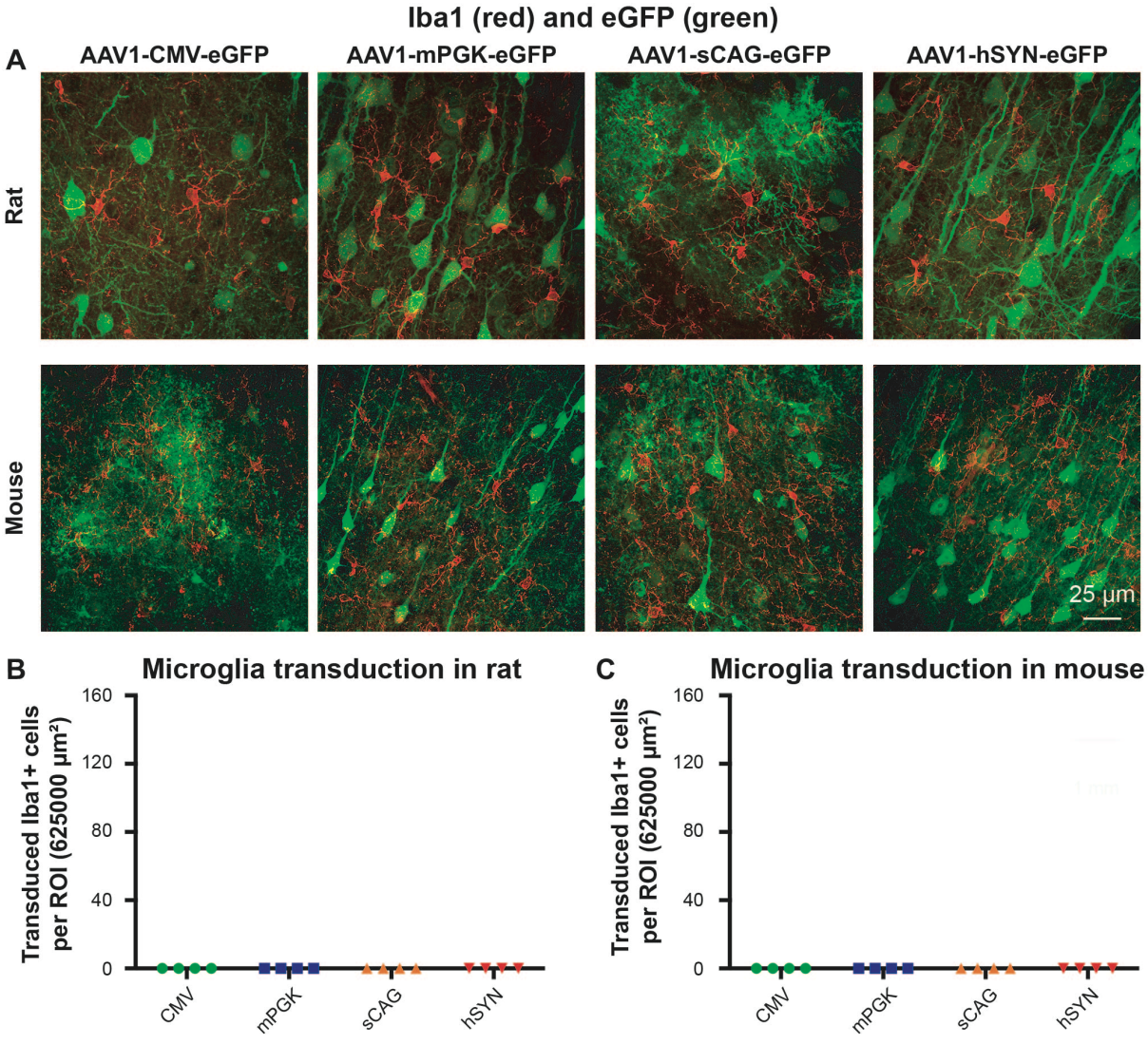

Figure 21 – The recombinant AAVs serotype 1 and the selected four promoters did not have tropism for microglia. (A) Iba1 (red) and eGFP (green) staining in the cortex of AAV1-CMV-eGFP, AAV1-mPGK-eGFP, AAV1-sCAG-eGFP, and AAV1-hSYN-eGFP injected rats and mice. Quantification of the number of transduced Iba+ cells in rats (B) and mice (C). Each dot represents the mean value of one animal, a total of 4 animals were analysed for each condition. Lab journal reference: BN-18-14.

The transduction of oligodendrocytes was also examined in this study. Staining for the oligodendrocyte lineage was performed by using anti-OliG2 and clone CC1 antibodies. We experienced that the CC1 antibody resulted in better visualization of matured oligodendrocytes in mice (**Fig. 22 – right**) than rats (**Fig. 22 – left**). The CMV (**Fig. 22A**) and sCAG (**Fig. 22C**) promoters resulted in several eGFP positive cells in the corpus callosum that did co-label with the oligodendrocytes markers in rats and mice. The corpus callosum of animals transduced with AAV1-mPGK-eGFP consisted mainly of eGFP positive axons and very few transduced oligodendrocytes (**Fig. 22B**). No transduced oligodendrocytes were detected in the corpus callosum of AAV1-hSYN-eGFP injected animals, but clear bundles of eGFP+ axons were visible (**Fig. 22D**).

Fig. 22. - next page - Expression of eGFP in the oligodendrocyte lineage with the AAV1 serotype and the promoters CMV, sCAG, and mPGK, but not with hSYN. The upper panels illustrate an overview of the right cerebral hemisphere that was injected with the rAAV viral vector serotype 1 and four different promoters expressing eGFP. The lower panels are magnification images of the box in the upper panel showing a portion of the corpus callosum. The 40 μm thick brain sections were stained for clone CC1 (red), Olig2 (blue) and eGFP (green) in both rats (left) and mice (right). The experimental conditions were AAV1-CMV-eGFP (A), AAV-mPGK-eGFP (B), AAV-sCAG-eGFP (C), and AAV-hSYN-eGFP (D) injected into the sensory-motor cortex of mice and rats. Lab journal reference: BN-18-29.

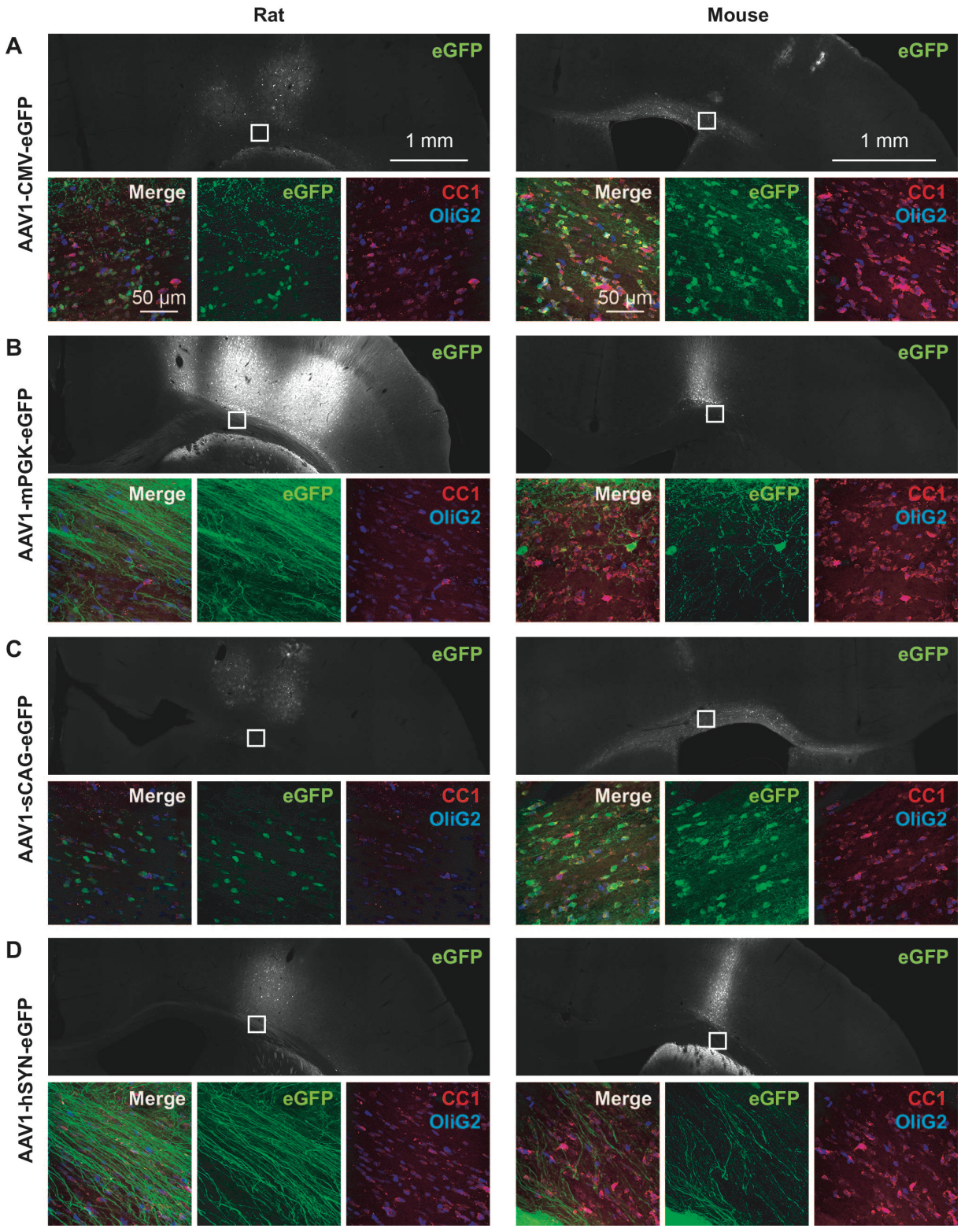
Rat
Mouse
A
AAV1-CMV-eGFP
B
AAV1-mPGK-eGFP
C
AAV1-sCAG-eGFP
D
AAV1-hSYN-eGFP
eGFP
1 mm
Merge
CC1
OliG2
50 µm

(10) Co-transfection efficiency of two plasmids in cortical neurons *in vitro*

Co-transfection of plasmids is a common procedure for various cell culture experiments. Here, we determined the co-transfection rate of plasmids containing hSYN-eGFP and hSYN-tdTomato in cultured cortical neurons by magnetofection. The plasmids hSYN-eGFP and hSYN-tdTomato were mixed in an equal amount and afterwards transfected in cortical neurons on 10 DIV. The number of neurons that expressed both fluorophores, or eGFP-, or tdTomato alone, was counted on 14 DIV. The co-transfection *via* magnetofection resulted only in neurons that were positive for both eGFP and tdTomato (**Fig. 23A, B**) and therefore the co-transfection efficiency was 100%. One control experiment was performed to confirm that the high co-transfection rate was not a result of fluorophores bleed through during image acquisition. Single vector plasmids were transfected into neurons as negative control and images were taken with identical confocal microscope settings. As expected, simultaneous transfection of hSYN-eGFP and hSYN-TdTomato resulted in both green and red fluorescence (**Fig. 23C**). Neurons that were transfected with hSYN-eGFP showed only green fluorescence (**Fig. 23C**), while transfection of hSYN-tdTomato resulted in red fluorescence only (**Fig. 23C**).

Fig. 23. - next page - Co-transfection of hSYN-eGFP and hSYN-tdTomato in cultured cortical neurons *via* magnetofection. Embryonic day 18 cortical neurons from rat were cultured and transfected on 10 DIV with a 1:1 mixture of hSYN-eGFP and hSYN-tdTomato plasmids. (A) Representative image of 14 DIV neurons that were co-transfected. The tile-scan image was taken with a Leica DMi-8 inverted microscope with 20x objective. (B) Quantifications of the number of neurons that expressed eGFP/tdTomato, eGFP, or tdTomato following co-transfection. A total of 100 transfected neurons were imaged with a confocal microscope and analyzed (n = 5, 20 neurons per experiment) (C) Representative images of transfected neurons on 14 DIV. The cells were simultaneously transfected with 3.5 μg hSYN-eGFP and 3.5 μg hSYN-tdTomato, or 7 μg hSYN-eGFP, or 7 μg hSYN-tdTomato plasmid, respectively. Images were taken with an SP5 confocal with 40x objective and 2.5 digital zoom factor. Lab journal reference: BN-18-16.

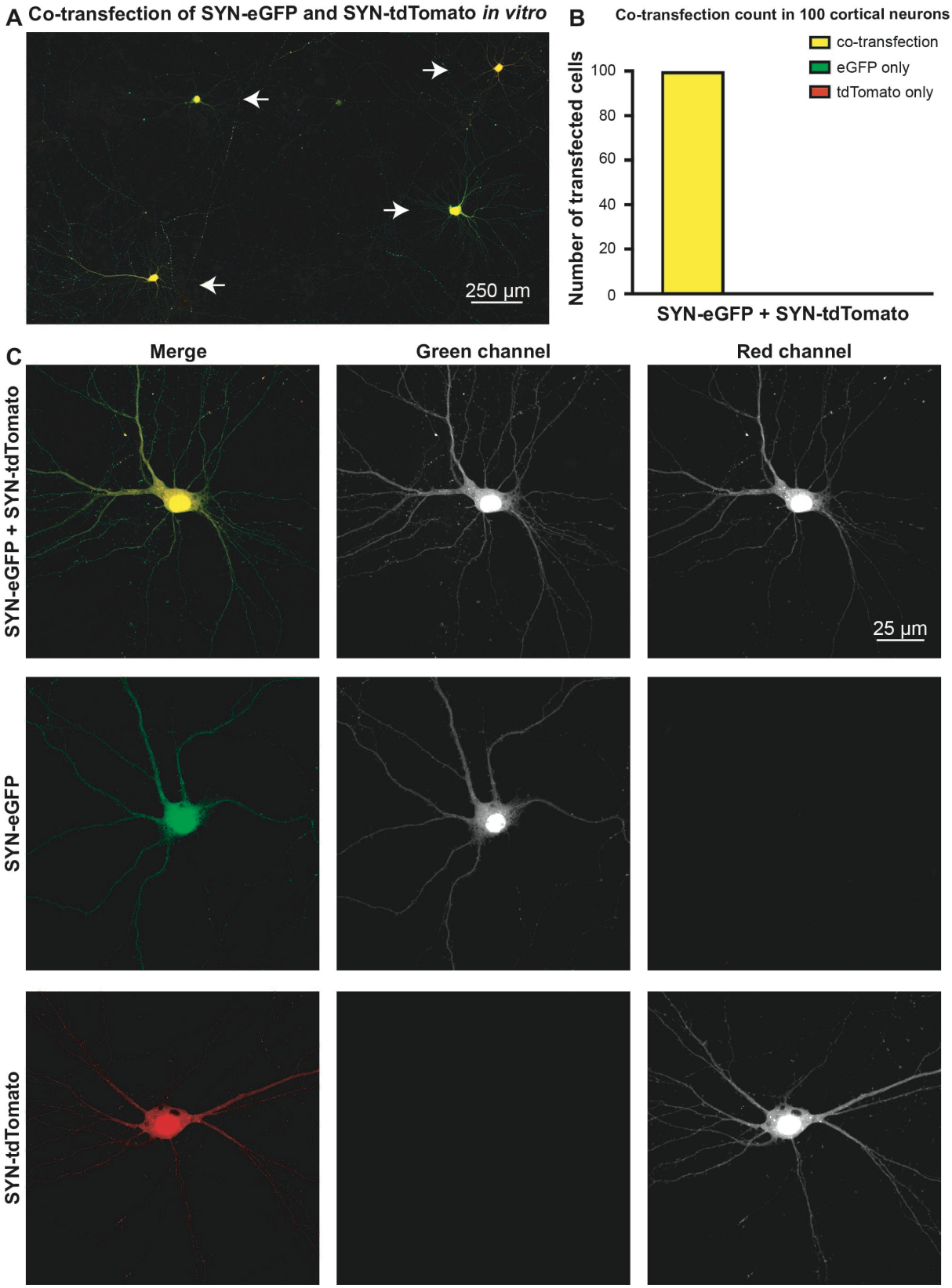
A Co-transfection of SYN-eGFP and SYN-tdTomato *in vitro*
250 µm
B Co-transfection count in 100 cortical neurons
co-transfection
eGFP only
tdTomato only
Number of transfected cells
100
80
60
40
20
0
SYN-eGFP + SYN-tdTomato
C
Merge
Green channel
Red channel
SYN-eGFP + SYN-tdTomato
SYN-eGFP
SYN-tdTomato
25 µm

(11) Co-transduction rate after injecting two viruses in the sensory-motor cortex *in vivo*

Two AAV1 vectors expressing either eGFP or tdTomato under the hSYN promoter were mixed and injected into the right sensory-motor cortex of rats and mice (see **Fig. 2**). AAV1-hSYN-eGFP and AAV-hSYN-tdTomato were titre matched and the mixed vector contained 1.68 E+11 genomic copies of each vector per ml. The aim was to quantify the proportion of double labelling in the corticospinal tract six weeks post-injection. Co-expression of the eGFP and tdTomato fluorophores was observed in a small number of axons in the dorsal column of the spinal cord with this low titre (**Fig 24**). We observed that the eGFP fluorescence was brighter than the tdTomato signal in the axons, yet both had a relatively weak signal. Quantifications were not performed due to the low virus titre, and as a consequence only few neurons were transduced in the brain (not shown). However, this pilot experiment indicates that co-transduction of two viruses by direct mixing before injection is feasible.

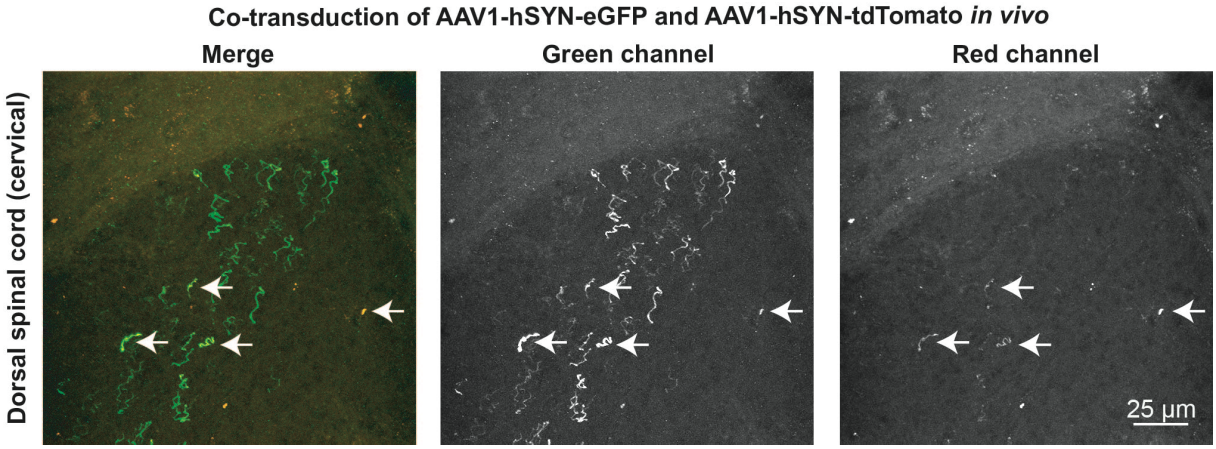

Fig. 24. Co-transduction of two low titre viruses in the corticospinal tract following direct injection in the right sensory-motor cortex. Representative confocal microscope images of one mouse dorsal spinal cord section showing that few axons were (co-) transduced. Lab journal reference: BN-18-28.

IV. DISCUSSION

`The aim of this study was to optimize AAV-mediated transgene expression in cortical spinal neurons of the rat and mouse. We studied the impact of the viral vector serotype and the promoter, two variables that are known to have a significant effect on transduction efficiency of AAV vectors. We first compared the transduction efficiency of AAV serotypes 1 and 5 since these two serotypes have previously been identified as the best and second best for transduction of corticospinal neurons (Hutson *et al.*, 2012). We confirmed that AAV1 is the best serotype for corticospinal neurons. Subsequently, we examined the impact of the promoter by comparing AAV1 vectors harbouring CMV, mPGK, sCAG, or hSYN promoter. The results show that (1) the mPGK and hSYN promoters transduced significantly more neurons than the CMV and sCAG promoters, (2) mPGK and hSYN directed higher levels of transgene expression in individual neurons than the CMV and sCAG promoters, and (3) the hSYN promoter mediated neuron-specific transgene expression, whereas the CMV, sCAG and mPGK promoters directed transgene expression in neurons and non-neuronal cells. These results will be of use for the design of AAV-based gene transfer experiments in corticospinal projection neurons, which form a widely used fiber tract for studies on long-distance axon regeneration in the injured spinal cord.

(1) Comparison of promoters in cultured cortical neurons after transfection

The vector plasmids were transfected into cultured cortical neurons to validate that they were functional before making AAVs. This goal was achieved. We next decided to compare the efficiency of the selected four promoters in cultured cortical neurons after transfection (rather than viral transduction), because this method is commonly used in cell-culture experiments. The time-point of transfection (10 DIV) and analysis (14 DIV) are typically chosen to study mature cortical neurons derived from embryonic day 18 embryos (Eva *et al.*, 2017; Koseki *et al.*, 2017; see also **Chapter II** and **Chapter III**). It is important to note that the plasmid transfection is not a delivery method that is comparable to the AAV-transduction *in vivo*; hence the results *in vitro* are not predictable for the efficiency *in vivo*.

The direct comparison between the plasmid containing the four promoters resulted in no differences in the mean eGFP intensity of the transfected cortical neurons. Four days post-transfection resulted in eGFP intensities close to saturation levels in the soma, were the eGFP protein is synthesized. The soma is therefore not a suitable area to compare the efficiency of transgene expression by different promoters. There was also no difference found in the eGFP intensity in the initial parts of the neurites between the vector plasmids. There was a strong eGFP expression four days after transfection; this relatively long incubation period is the most

likely explanation for observing no differences in the cultured neurons. The eGFP intensity in the distal part of the axon was not analysed, because the cultured neurons form neuronal networks on 14 DIV, which makes it difficult to analyse a single and non-branched transfected axon.

An alternative explanation for the identical eGFP intensities could be due to the fact that the cortical neurons are derived from embryonic rats. I would speculate that the young cortical neurons have a high rate of transcriptional activity that allows the activation of various promoters, while this may become more selective in adult cortical neurons. For instance, the adult cortical neurons may silence the expression of transgenes under non-neuronal promoters.

The data suggest that the choice of promoter may not be important for *in vitro* transfection experiments in order to gain high expression levels. However, the experience from our laboratory is that some promoters e.g. CMV have a low transfection efficiency in cultured neurons when expressing large genes (such as integrins). The number of transduced neurons by each promoter was not determined in this *in vitro* experiment due to the indeed low transfection efficiency by magnetofection (less than 0.1%).

(2) ImageJ macro for semi-automated analysis of NeuN+ and eGFP+ NeuN+ cells in AAV-transduced cortex

The cortex contains an orchestra/plethora of different cell types, including neurons, astrocytes, microglia cells, oligodendrocytes and endothelial cells. Quantifying the number of AAV transduced neurons along with the eGFP fluorescence intensity could therefore be a challenging task. Manual analysis of fluorescent images containing thousands of neurons is time-consuming and prone to human bias and inconsistency. We therefore decided to use a semi-automated quantification by employing a custom-made ImageJ macro, co-developed by a colleague in the lab.

The ImageJ macro automatically detects round cells that are present in the red channel of an image (e.g. NeuN+ cells) and then measures the fluorescent intensity of all marked cells in the green channel (e.g. eGFP). Afterwards, the user has to manually measure the eGFP intensity of three non-transduced cells to set as threshold for the background signal in non-transduced neurons. In addition, the user has to measure a small area in between multiple transduced somata within the region of interest. Based on these background intensity measurements, the number of transduced neurons and the mean eGFP intensity per transduced neuron can be calculated in a Microsoft excel sheet (the excel sheet with automated calculations will be included as **supplementary data** in the paper). The ImageJ parameters to

detect round cells in the red channel (tresholding, watersheding, particle analysis) can be adjusted by the user to fit their experimental needs. For example, the macro can be adjusted to measure the green intensity in larger neuronal cells, including dorsal root ganglion cells or motor neurons.

The Macro was tested on cropped images, to ease and improve the accuracy of the manual counting of the total number of neurons and those that were eGFP-positive, before using the ImageJ macro on the large images from 32 animals. When the correct settings for the identification of round cells were determined, there was no statistically significant difference between the semi-automated and manual counting of neurons in the cropped images. After successful development of the code, the Image J macro was more time-efficient than the manual counting. The code can, therefore, be useful when a large quantity of images is investigated.

The ImageJ macro does have some limitations. The user has to set an arbitrary intensity ratio that will be used to determine whether a round cell is eGFP positive or not. This limit was set to 30% in this study (see **Fig 3F**). This arbitrary limit prevents that eGFP-positive branches (e.g. dendrites or transduced astrocytes) that are overlapping with non-transduced cells will be counted as separate eGFP positive neurons. Nevertheless, we cannot exclude and even deem it likely that transduced non-neuronal cells, especially under the condition of transduction with viruses that have a CMV or sCAG promoter, are incorrectly counted as eGFP-positive neurons (false positives). However, this arbitrary limit allows the eGFP intensity in all transduced neurons above the threshold to be measured. It, therefore, avoids cherry picking of a select number of cells (e.g. n=20 per condition) and manual measurement of the eGFP intensity. In addition, it is difficult for the human eye to identify whether two fluorescent colors do overlap (especially when they are coming from two different fluorescent channels, e.g. NeuN+ in red and eGFP in green), while the computer measures the intensity value consistently. The ImageJ macro is limited to detect round structures only (e.g. nuclear stains such as DAPI or NeuN), and can therefore not be applied to detect more complex morphologies such as microglia or astrocytes.

(3) Comparison of the AAV1 and AAV5 serotypes for transduction of the corticospinal tract

We chose to first compare AAV1 and AAV5 because this were the best and second-best serotypes in an earlier study that compared the transduction of corticospinal tract with seven AAV serotypes (AAV1 to AAV6, and AAV8) harbouring a CMV promoter driving eGFP expression (Hutson *et al.*, 2012).

AAV1 is superior to AAV5 because it transduces almost twice as many corticospinal neurons compared to AAV5 in both mice and rats. This is consistent with the study in rats by Hutson and colleagues in 2012. The transduction efficiency of a specific cell type by an AAV vector is dependent on a number of steps, including interaction of the AAV vector with a cell surface receptor, cellular uptake and subsequent release from endosomes, trafficking to the nucleus and finally transcription and translation of the transgene. The differential transduction efficiency of AAV1 and AAV5 may be due to differential capsid protein – cell surface interactions resulting in more efficient entry of AAV1 in cortical neurons. Although both AAV1 and AAV5 (Kaludov *et al.*, 2001; Seiler *et al.*, 2006) bind to α2-3 and α2-6 N-linked sialic acids (Wu *et al.*, 2006; Mietzsch *et al.*, 2014) Kaludov:2001gv, Seiler:2006fk}, endocytosis may required additional cellular co-receptors. For instance, AAV1 and many other serotypes interact with integrins for efficient transduction while AAV5 does not (Kaminsky *et al.*, 2012). Instead AAV5 utilizes platelet-derived growth factor receptor (PDGFR) as co-receptor for transduction (Di Pasquale *et al.*, 2003). Furthermore, AAV1 and AAV5 bind to different domains of adeno-associated virus receptor (AAVR) on the cell surface to initiate transduction (Pillay *et al.*, 2017). The different patterns of transduction could also be caused by differential endosomal processing of the viral vector particles inside the cell and differential de-capsidation and release of the viral genome into the cell nucleus (Bantel-Schaal, Hub, & Kartenbeck, 2002; Keiser *et al.*, 2011; Aschauer, Kreuz, & Rumpel, 2013).

In contrast to the study of Hutson *et al.*, 2012, we observed that AAV1 directs a significant stronger expression of eGFP in individual neurons compared to AAV5. This difference may be caused by the entry of more copies of the AAV1 than the AAV5 vector into neurons or to the use of different promoters that exhibit different temporal patterns of transcriptional activity. Hutson et al used the viral CMV promoter, whereas we used the strong mammalian SYN promoter. In our hands the CMV promoter is a relatively weak transcriptional activator compared to the SYN promoter (see more discussion below).

The viral vector serotypes AAV1 and AAV5 with the synapsin promoter had both a relatively good spread in the cortex. We did not find a statically significant difference in virus spread between the two serotypes in rats, but the transduction area of AAV1 was slightly bigger in mice.

Other AAV serotypes not investigated by us or Hutson and colleagues, that are commonly used for transduction of CNS neurons are AAV7 (Van der Perren *et al.*, 2011; Gerits *et al.*, 2015) and AAV9 (Aschauer *et al.*, 2013; Schuster *et al.*, 2014; Jackson, Dayton, & Klein, 2015; Markel *et al.*, 2017). AAV7 and 9 have a different mechanism for

transduction compared to AAV1 and AAV5. AAV9 binds Galactose as glycan receptor (Shen *et al.*, 2011; Bell *et al.*, 2012) and is capable to pass the blood-brain-barrier. Interestingly, the receptor for transduction by AAV7 is unknown and was found not to bind in a glycan array that tested 611 different glycans (Mietzsch *et al.*, 2014). Having a widespread transgene expression in the brain, and possibly beyond the blood-brain barrier, can be considered negative for studies aiming to achieve axonal regeneration following an injury of the corticospinal tract. In these particular studies, it is important to achieve a relatively focal expression pattern of regeneration-associated genes into the corticospinal tract only.

(4) Comparison of four promoters for transgene expression in the corticospinal tract

The promoter is a major regulatory element in the viral vector genome that determines both the level and the cell-selectivity of the expression of the transgene in the transduced cell. The size constraints of AAV vectors obviate the need for the use of small promoters. Here we compared four compact promoters for their ability to drive transgene expression in corticospinal neurons. This study found that mPGK and hSYN promoter directed strong neuronal expression in which hSYN was also neuron-specific. The mPGK promoter mainly transduced neurons but also had a rare and weaker expression pattern in oligodendrocytes. The CMV and sCAG resulted in relatively weak transgene expression in neurons as well as non-neuronal cells.

The high levels of neuron-specific transgene expression observed with the human synapsin promoter corroborated previous studies with this promoter (Thiel, Greengard, & Südhof, 1991; Kügler, Kilic, & Bähr, 2003; McLean *et al.*, 2014). Other ubiquitous neuron-specific promoters are the neural protein BM88 and neuronal nicotinic receptor b2 (CHRNβ2) (Pignataro *et al.*, 2017) promoters. The Ca2+/calmodulin-dependent protein kinase II (CaMKII) promoter drives preferably transgene expression in excitatory neurons (Nathanson *et al.*, 2009; Scheyltjens *et al.*, 2015) and the ‘5 tyrosine hydroxylase (TH) promoter is best for dopaminergic neurons (Oh *et al.*, 2009; Stauffer *et al.*, 2016). To our knowledge, there is no promoter available that is specific for layer V pyramidal neurons. Thus, the hSYN promoter is currently the promoter of choice to drive transgene expression in corticospinal neurons, because it is small (allowing large coding sequences to be inserted), strong and neuron specific.

Another important factor for AAV-mediated gene delivery is the size of the chosen promoter because of the approximately 4700 nucleotides packaging capacity of AAVs. All the promoters investigated in this study were relatively small in nucleotide length; sCAG, 860 bp, CMV 670 bp; mPGK 610 bp; hSYN, 470 bp. These DNA regulatory units are therefore

interesting candidates for the delivery of large transgenes, such as regeneration-associated genes like integrins (**Chapter I**) and phosphoinositide 3-kinases (**Chapter III**) via AAV-mediated transduction *in vivo*. However, it is important to note that not only neurons of the corticospinal tract are transduced. The AAV1 and AAV5 serotypes transduced neurons in multiple layers of the cortex. This, for instance, also resulted in axonal fibers crossing over at the corpus callosum.

(5) AAV serotypes and transduction of non-neuronal cells in the cortex

We observed that AAV1 serotype with different promoters induces transgene expression in different cell types. The hSYN promoter was specific for neurons. The promoter mPGK did mainly transduce neurons and had poor cellular tropism for oligodendrocytes. The CMV and sCAG promoters transduced neurons, but also astrocytes and few oligodendrocytes. The transduction of non-neuronal cells can therefore be improved by using different viral serotypes and promoters.

Astrocytes are a common target of interest to be transduced by AAVs. The transduction of astrocytes by the AAV1 serotype with CMV or CAG promoter is not new, as it was previously observed by others (Burger *et al.*, 2004; Hutson *et al.*, 2012; Watakabe *et al.*, 2015). A study by Schober *et al.*, 2016 suggested that the AAV6 serotype (with CMV promoter) has a higher transduction efficiency for astrocytes in rat cortex. One year later, another comparative study with AAV serotypes (with a CMV promoter) suggested that AAV8 was superior to drive transgene expression in astrocytes in the cortex. Koh *et al.*, 2017 utilised the AAV8 serotype combined with the ALDH1L1 promoter and achieved predominantly transduction of astrocytes, and a small number of neurons. Pignataro *et al.*, 2017 also used AAV8, but combined this with truncated forms of the GFAP promoter and achieved high transduction rates of astrocytes, and observed a limited number of transduced oligodendrocytes. Lawlor *et al.*, 2009 achieved targeted transduction of astrocytes in nonhuman primates by using the AAV8 serotype and the GFAP promoter.

Microglia have been proven to be more difficult to transduce with AAVs *in vivo*. The AAV1 serotype together with CMV, mPGK, sCAG, and hSYN, did not transduce microglia in our study. The first transduction of microglia was achieved by using AAV5 in combination with a promoter derived from the macrophage marker F4/80 gene (Cucchiarini *et al.*, 2003). Rosario *et al.*, 2016 characterised that an amino acid optimized AAV6 capsid in combination with the F4/80 or CD68 promoter results in targeted transduction of microglia in the mice brain. It will be interesting to see whether the addition of other microglia specific promoters, e.g. P2ry12 or Tmem119 (Hickman *et al.*, 2013; Bennett *et al.*, 2016b; Satoh *et al.*, 2016),

can improve microglia transduction *in vivo.*

Targeting of the oligodendrocyte lineages by AAVs could be useful for demyelinating disorder studies, among others. We observed that CMV and sCAG had the ability to transduced oligodendrocytes. Consistently, another study also observed that injection of AAV8 with CAG promoter transduces mainly neurons, astrocytes and a small number of oligodendrocytes (Pignataro *et al.*, 2017). In addition, systemic injection of AAV9 with a CMV promoter in the cerebrospinal fluid had been shown to transduce neurons and oligodendrocytes in cats (Bucher *et al.*, 2014). Our study observed that the mPGK promoter had rare transgene activation in oligodendrocytes in the corpus callosum. In general, the transduction of oligodendrocytes can be improved by injecting directly into the corpus callosum or striatum, rather than the injection coordinates that were used to transduce the sensory-motor cortex. The use of a different serotype can also aid the transduction of oligodendrocytes. Hutson and colleagues showed one image that hinted that AAV8 serotype with CMV promoter has a potential oligodendrocyte tropism (Hutson *et al.*, 2012). Another study compared the serotypes AAV1, AAV5, AAV9, and AAV-rh10 with a CMV promoter following intraspinal injection immediately after a spinal cord contusion injury, and found that the AAV-rh10 was most efficient to transduce oligodendrocytes and macrophages/microglia (Petrosyan *et al.*, 2014). An oligotrophic AAV vector called olig001 has been shown to transduce a large proportion of oligodendrocytes in rats and rhesus macaques (Mandel *et al.*, 2017). Examples of promoters that have been implemented in rAAVs and are believed to be specific for the oligodendrocyte lineage are derived from the myelin-associated glycoprotein (MAG) (Jonquieres *et al.*, 2016) and myelin basic protein (MBP) gene (Lawlor *et al.*, 2009; Jonquieres *et al.*, 2013).

However, for overexpression of transgenes in layer V neurons, our study suggest to AAV1 with an hSYN promoter to achieve maximal neuronal targeting and expression.

(6) Co-transduction of two plasmids *in vitro* and viruses *in vivo*

Some gene therapies are based on the combination of multiple genes (e.g. integrin and kindlin). This study examined the co-transfection efficiency of two plasmids in primary cortical neurons and the co-transduction rate of mixing two rAAVs prior to injection in the rat/mouse brain.

Our laboratory prefers the magnetofection method for *in vitro* experiments because of the low neuronal toxicity. Yet, we experience low transfection efficiency by using this method (e.g. 40-150 transduced cells per 200,000 cultured neurons). Magnetofection is a transfection method based on combining plasmid DNA with magnetic nanoparticles that bind

to nucleic acids with high efficiency. The plasmid DNA and magnetic beat complexes are next endocytosed by primary cortical neurons, which have been placed above a magnetic field. We expected high co-transfection efficiency by using this method, but were surprised to find a 100% co-transfection rate (n=5 experiments). We, therefore, speculate that magnetic nanoparticles always bind the DNA of two plasmids during the incubation step prior to the uptake of the molecular complex by the cells. However, the magnetic nanoparticles do not always uptake an even amount of the two plasmids that are mixed in the Eppendorf tube. For instance, when co-transfecting the hSYN-eGFP and hSYN-tdTomato, some neurons were more bright red fluorescent than green and vice versa (data not shown).

We attempted to determine co-transduction *in vivo* by mixing two rAAV viruses. The viral mixture consisted of 50% AAV1-hSYN-eGFP and 50% AAV1-hSYN-tdTomato. In contrast to the transfection methods *in vitro*, the two viral vectors don't form a molecular complex and each viral vector can, therefore, transduce different cells in the brain. Our expectation was that mixing viral vectors does not result in a perfect rate of co-transduction, but yet it remains important to determine how often co-transduction occurs. However, the viral titres that were injected (1.68 E+11 genomic copies per ml) in the brain were too low, and as a consequence only a few transduced axons were observed in the dorsal column of the spinal cord with weak fluorescent intensity. The titre of AAV-hSYN-tdTomato was low due to serum and cell culture issues during the AAV preparation. It is important to repeat this experiment with high enough viral titres, e.g. E+12 or E+13 gc/ml to properly transduce the corticospinal tract. A good co-transduction efficiency of two viral vectors will be crucial for combinatorial gene therapy approaches that aim to achieve axonal regeneration of this motor pathway.

(7) Perspective for spinal cord injury research

It is important for any gene therapy that transgenes are delivered with high cell-specificity and adequate expression levels. This also counts for research in spinal cord injury with loss of motor function; regeneration-associated-genes need to be efficiently delivered into the neurons of the corticospinal tract. High cell-specificity is also crucial because the introduction of regeneration-associated genes into glial cells could lead to unwanted side effects. Based on the data presented in this study, the AAV1 viral vector serotype and the hSYN promoter is the optimal combination for transgene delivery in the corticospinal tract of mice and rats. Viral transduction prior to an injury is common practice for axon regeneration experiments *in vivo*. In the nearby future, it will be interesting to explore whether the AAV1 serotype and promoters will also be functional when applied after a spinal cord injury.

CHAPTER V – Summary and general discussion

Adult neurons of the central nervous system (CNS) have a poor capacity to regenerate their axon after injury. I also observed this in cortical neurons that were cultured for two weeks. Importantly, this dissertation shows that the axon regeneration capacity of CNS neurons can be enhanced using vectors containing phosphoinositide 3-kinases. Furthermore, this dissertation contributed to improved viral transduction of the corticospinal tract in mice and rats. Identification of the superior viral vector serotype and promoter for this motor pathway is crucial for any gene therapy that aims to promote axon regeneration of the CST. This doctoral thesis also investigated whether a novel dual-promoter viral vector containing CRISPR-Cas9 system is suitable for protein knockout in CNS neurons. This final chapter will briefly summarise the findings of this dissertation and place them in perspective to the field of axon regeneration.

Chapter I is a literature review (Nieuwenhuis *et al.*, 2018) highlighting that integrin receptors are an important component of axon regeneration. The review hypothesizes that the absence of integrins in the growth cone, and importantly the subsequent signalling and cytoskeleton changes, is one of the reasons for regenerative failure in adult CNS neurons. Targeting the trafficking of regeneration-associated receptors, such as integrins, TrkB, and IGFR, into the axon is therefore one strategy to promote axon regeneration in the CNS. Furthermore, manipulation of the activation state of receptors could be a promising strategy to promote axon regeneration.

Chapter II is based on the hypothesis that the axon initial segment (AIS) contributes to regenerative failure in adult CNS neurons by forming an axon transport barrier for regeneration-associated receptors such integrins. The aim of this chapter was to knockout cytoskeleton scaffolding protein Ankyrin-G (AnkG) in cortical neurons with the rationale to dismantle the AIS. Short hairpin RNA interference and an approach consisting of viral vector-mediated delivery of CRISPR-associated endonuclease 9 from *Staphylococcus aures* (saCas9) targeting AnkG were made and tested *in vitro*. The data shows that the vector-mediated RNA interference results in cellular toxicity in cultured cortical neurons. Other studies also reported neuronal degeneration in CNS tissue after AAV-mediated delivery of scrambled-shRNA and targeting-shRNA *in vivo* (Ulusoy *et al.*, 2009; Ehlert *et al.*, 2010; Khodr *et al.*, 2011; Martin *et al.*, 2011). For the CRISPR-Cas9 approach, a novel dual promoter AAV viral vector construct was modified resulting in the neuron-specific promoter hSYN to drive the expression of SaCas9 protein and the RNA promoter hU6 to express a single guide RNA. In contrast to shRNA interference, the CRISPR-Cas9 did not result in neuronal cell death *in*

vitro. The SaCas9 protein was found to localise in the soma and importantly knockout of AnkG and dismantling of the AIS was achieved in a small proportion of the cultured cortical neurons. The AnkG knockout efficiency can likely be improved by increasing the duration of the experiment to match the extremely stable half-live time of the AnkG protein (Hedstrom *et al.*, 2008). It is important that future research tests the AAV vector-mediated delivery of SaCas9 *in vivo*. The research-question whether the AIS is a barrier for the entry of integrins in the axon of adult CNS neurons is unanswered. Yet, this chapter achieved the generation of genetic tool that will be useful for other scientist to knockout their protein of interests.

Chapter III explored whether overexpression of phosphoinositide 3-kinases (PI3Ks), which generates PtdIns-3,4,5-P3 (PIP_3), could promote axon regeneration of CNS neurons. Immunohistochemistry for PIP_3 confirmed the hypothesis that there is a decline of PIP_3 levels in the axon in line with maturation. Expression of activated PI3Ks, but not wild type PI3K, in developing neurons resulted in increased axonal growth, and expression in maturing neurons enlarged the soma size and more complex dendritic morphology *in vitro*. Consistently, expression of constitutively activated PI3K enhanced PIP_3 signalling in these neurons. Importantly, the success rate of axon regeneration was increased in cortical neurons that underwent *in vitro* laser axotomy after PI3K overexpression. This chapter highlights that enhancing axonal PIP3 signalling is an important target to promote axon regeneration. Indeed, follow-up experiments in the Keith Martin laboratory showed that AAV-vector mediated delivery of PI3Ks promote axon regeneration in the injured optic nerve *in vivo.* My future research will investigate whether elevated PIP_3 signalling promotes transport of regeneration-associated receptors into the axon as potential mechanism for the observed regeneration.

Chapter IV aimed to optimize AAV-mediated gene transfer to the corticospinal tract *in vivo*. This chapter compared the AAV1 and AAV5 serotypes and the transgene efficiency of four promoters: cytomegalovirus (CMV), mouse phosphoglycerate kinase (mPGK), short CMV early enhancer/chicken β actin (sCAG), and human synapsin (hSYN). The AAVs were injected into the sensorimotor cortex of rats and mice and the transduction was examined by histology after six weeks. Consistent with a previous study (Hutson *et al.*, 2012), we found that that AAV1 is superior to AAV5 to transduce the corticospinal tract. Our study found that the mPGK and hSYN promoters induce the strongest transgene expression in neurons. The AAV1 serotype with the hSYN promoter resulted in neuron-specific expression, while this serotype combined with other promoters also activated transgenes in non-neuronal cells like astrocytes, microglia and oligodendrocytes. This chapter contributes to the optimisation of AAV-mediated delivery of transgenes into corticospinal tract and is therefore beneficial for spinal cord injury research using gene therapy.

This dissertation was focused on axonal growth signalling in CNS neurons, although it is important to note that that intrinsic axon growth is a dynamic process (reviewed in Petrova & Eva, 2018; Fawcett & Verhaagen, 2018). The **general discussion** below briefly highlights that multiple interventions are possible to promote axon regeneration in the CNS.

Successful axon regeneration requires activation of regeneration-associated genes in the nucleus as well as effective growth machinery in the axon. Transcriptional reprogramming is essential in order to synthesize the growth-associated proteins for axon regeneration (reviewed in van Kesteren *et al.*, 2011; Fagoe *et al.*, 2014b). Genetic screenings estimated that approximately 1200 genes, including 50 transcription factors (TFs), are differently regulated in axons that do regenerate compared to adult CNS neurons (Smith & Skene, 1997; Stam *et al.*, 2007; Chandran *et al.*, 2016; Sekine *et al.*, 2018). Current approaches aim to deliver combinations of TFs or pharmaceutical drugs that are able to up-regulate clusters of genes in the regeneration-associated gene program. To date, AAV-mediated delivery of single growth-associated-TFs has lead to restricted axon regeneration in the corticospinal tract (Blackmore *et al.*, 2012; Lang *et al.*, 2013; Z. Wang *et al.*, 2015b). Another hypothesis contributing to regenerative failure is that epigenetic mechanisms block the accessibility of promoters from regeneration associated-genes in adult CNS neurons (Weng *et al.*, 2017; Venkatesh *et al.*, 2018; Oh *et al.*, 2018; reviewed in Danzi *et al.*, 2018). Improving chromatin accessibility is therefore another approach to stimulate axon regeneration in the CNS. Another area of research aims to enhance the intrinsic axon regeneration response by delivering neurotropic factors near the soma (Yu *et al.*, 2011) or near the site of injury (Anderson *et al.*, 2018; Eggers *et al.*, 2019).

In addition to factors within neurons, extrinsic factors play a crucial role in spinal cord injury and axon regeneration. Neuronal cell death, devascularisation, inflammation, demyelination, and astroglial scar formation can restrict axon regeneration. Only the neurons that survive the traumatic insult have the possibility to promote axonal regeneration, and therefore neuroprotective treatments are also important to indirectly stimulate axon regeneration (reviewed in Ulndreaj, Badner, & Fehlings, 2017). The upregulation of axon repulsive molecules at the site of injury are also detrimental for axon regeneration (see Chapter I Section V). Neutralization of myelin-associated growth inhibitors and specifically the inhibitory components of the glial scar are essential in order to permit axon regeneration through the injury site (Kucher *et al.*, 2018; Burnside *et al.*, 2018; reviewed in Quraishe, Forbes, & Andrews, 2018).

There are a number of considerations in order to establish combination therapies for spinal cord injury. It will important to select the most robust treatments to combine, consider

the possible side effects of each treatment, and importantly the combination of treatments should be applied following the progression of spinal cord injury e.g. optimized timing of individual treatments. I would speculate to apply neuroprotective treatments immediately after the injury, followed by anti-scarring and axon regeneration strategies at the sub-acute injury phase. During the more chronic stages, the treatment should consist of long-distance axon guidance and re-myelination treatments. The axons also need to connect and re-innervate the target tissue, which may be aided by electrical stimulation and extensive rehabilitation. Above highlights that the molecular and cellular events after a spinal cord injury are complex and overcoming all these has proven to be difficult to achieve functional recovery. Yet, combination therapies are likely essential to establish long-range axon regeneration and functional recovery after spinal cord injury.

REFERENCES

AGBANDJE-MCKENNA, M. & KLEINSCHMIDT, J.R. (2011) AAV Capsid Structure and Cell Interactions. In *Adeno-Associated Virus* pp. 47–92. Humana Press, Totowa, NJ.

AGRAWAL, N., DASARADHI, P.V.N., MOHMMED, A., MALHOTRA, P., BHATNAGAR, R.K. & MUKHERJEE, S.K. (2003) RNA Interference: Biology, Mechanism, and Applications. *Microbiol. Mol. Biol. Rev.* **67**, 657–685. American Society for Microbiology.

AL-ALI, H., DING, Y., SLEPAK, T., WU, W., SUN, Y., MARTINEZ, Y., XU, X.-M., LEMMON, V.P. & BIXBY, J.L. (2017) The mTOR substrate S6 Kinase 1 (S6K1) is a negative regulator of axon regeneration and a potential drug target for Central Nervous System injury. *The Journal of Neuroscience* **37**, 0931–17–7095. Society for Neuroscience.

ALBRECHT, D., WINTERFLOOD, C.M., SADEGHI, M., TSCHAGER, T., NOÉ, F. & EWERS, H. (2016) Nanoscopic compartmentalization of membrane protein motion at the axon initial segment. *The Journal of Cell Biology* **215**, 37–46. Rockefeller University Press.

ALIZADEH, A., DYCK, S.M. & KARIMI-ABDOLREZAEE, S. (2015) Myelin damage and repair in pathologic CNS: challenges and prospects. *Frontiers in molecular neuroscience* **8**, 35. Frontiers.

ANDERS, C., NIEWOEHNER, O., DUERST, A. & JINEK, M. (2014) Structural basis of PAM-dependent target DNA recognition by the Cas9 endonuclease. *Nature* **513**, 569–573. Nature Publishing Group.

ANDERSON, M.A., BURDA, J.E., REN, Y., AO, Y., O'SHEA, T.M., KAWAGUCHI, R., COPPOLA, G., KHAKH, B.S., DEMING, T.J. & SOFRONIEW, M.V. (2016) Astrocyte scar formation aids central nervous system axon regeneration. *Nature* **532**, 195–200.

ANDERSON, M.A., O'SHEA, T.M., BURDA, J.E., AO, Y., BARLATEY, S.L., BERNSTEIN, A.M., KIM, J.H., JAMES, N.D., ROGERS, A., KATO, B., WOLLENBERG, A.L., KAWAGUCHI, R., COPPOLA, G., WANG, C., DEMING, T.J., HE, Z., COURTINE, G. & SOFRONIEW, M.V. (2018) Required growth facilitators propel axon regeneration across complete spinal cord injury. *Nature* **561**, 396–400. Nature Publishing Group.

ANDRESSEN, C., ADRIAN, S., FÄSSLER, R., ARNHOLD, S. & ADDICKS, K. (2005) The contribution of beta1 integrins to neuronal migration and differentiation depends on extracellular matrix molecules. *European journal of cell biology* **84**, 973–982.

ANDREWS, M.R., CZVITKOVICH, S., DASSIE, E., VOGELAAR, C.F., FAISSNER, A., BLITS, B., GAGE, F.H., FFRENCH-CONSTANT, C. & FAWCETT, J.W. (2009) Alpha9 integrin promotes neurite outgrowth on tenascin-C and enhances sensory axon regeneration. *The Journal of Neuroscience* **29**, 5546–5557. Society for Neuroscience.

ANDREWS, M.R., SOLEMAN, S., CHEAH, M., TUMBARELLO, D.A., MASON, M.R.J., MOLONEY, E., VERHAAGEN, J., BENSADOUN, J.-C., SCHNEIDER, B., AEBISCHER, P. & FAWCETT, J.W. (2016) Axonal localization of integrins in the CNS is neuronal type and age dependent. *eneuro*, ENEURO.0029–16.2016. eneuro.

ARENDT, K.L., ROYO, M., FERNANDEZ-MONREAL, M., KNAFO, S., PETROK, C.N., MARTENS, J.R. & ESTEBAN, J.A. (2010) PIP3 controls synaptic function by maintaining AMPA receptor clustering at the postsynaptic membrane. *Nature neuroscience* **13**, 36–U191. Nature Publishing Group.

ARLOTTA, P., MOLYNEAUX, B.J., CHEN, J., INOUE, J., KOMINAMI, R. & MACKLIS, J.D. (2005) Neuronal subtype-specific genes that control corticospinal motor neuron development in vivo. *Neuron* **45**, 207–221.

ARNAOUT, M.A., GOODMAN, S.L. & XIONG, J.-P. (2007) Structure and mechanics of integrin-based cell adhesion. *Current opinion in cell biology* **19**, 495–507.

ARNOLD, D.B. (2009) Actin and microtubule-based cytoskeletal cues direct polarized targeting of proteins in neurons. *Science signaling* **2**, pe49–pe49. American Association for the Advancement of Science.

ASCAÑO, M., RICHMOND, A., BORDEN, P. & KURUVILLA, R. (2009) Axonal targeting of Trk receptors via transcytosis regulates sensitivity to neurotrophin responses. *The Journal of Neuroscience* **29**, 11674–11685. Society for Neuroscience.

ASCHAUER, D.F., KREUZ, S. & RUMPEL, S. (2013) Analysis of Transduction Efficiency, Tropism and Axonal Transport of AAV Serotypes 1, 2, 5, 6, 8 and 9 in the Mouse Brain. *PloS one* **8**. Public Library of Science.

ATWAL, J.K., PINKSTON-GOSSE, J., SYKEN, J., STAWICKI, S., WU, Y., SHATZ, C. & TESSIER-LAVIGNE, M. (2008) PirB is a functional receptor for myelin inhibitors of axonal regeneration. *Science (New York, N.Y.)* **322**, 967–970. American Association for the Advancement of Science.

AUMAILLEY, M., BRUCKNERTUDERMAN, L., CARTER, W., DEUTZMANN, R., EDGAR, D., EKBLOM, P., ENGEL, J., ENGVALL, E., HOHENESTER, E. & JONES, J. (2005) A simplified laminin nomenclature. *Matrix Biology* **24**, 326–332.

AUNGST, S., ENGLAND, P.M. & THOMPSON, S.M. (2013) Critical role of trkB receptors in reactive axonal sprouting and hyperexcitability after axonal injury. *Journal of neurophysiology* **109**, 813–824. American Physiological Society.

AVRAAMIDES, C.J., GARMY-SUSINI, B. & VARNER, J.A. (2008) Integrins in angiogenesis and lymphangiogenesis. *Nature reviews. Cancer* **8**, 604–617. Nature Publishing Group.

BABAYAN, A.H., KRAMÁR, E.A., BARRETT, R.M., JAFARI, M., HÄETTIG, J., CHEN, L.Y., REX, C.S., LAUTERBORN, J.C., WOOD, M.A., GALL, C.M. & LYNCH, G. (2012) Integrin dynamics produce a delayed stage of long-term potentiation and memory consolidation. *The Journal of Neuroscience* **32**, 12854–12861. Society for Neuroscience.

BACHMANN, M., CONSCIENCE, J.F., PROBSTMEIER, R., CARBONETTO, S. & SCHACHNER, M. (1995) Recognition molecules myelin-associated glycoprotein and tenascin-C inhibit integrin-mediated adhesion of neural cells to collagen. *Journal of neuroscience research* **40**, 458–470. Wiley Subscription Services, Inc., A Wiley Company.

BACKER, J.M. (2016) The intricate regulation and complex functions of the Class III phosphoinositide 3-kinase Vps34. *The Biochemical journal* **473**, 2251–2271. Portland Press Limited.

BAER, W.S., DAWSON, P.M. & MARSHALL, H.T. (1899) REGENERATION OF THE DORSAL ROOT FIBRES OF THE SECOND CERVICAL NERVE WITHIN THE SPINAL CORD. *The Journal of experimental medicine* **4**, 29–45. The Rockefeller University Press.

BANTEL-SCHAAL, U., HUB, B. & KARTENBECK, J. (2002) Endocytosis of adeno-associated virus type 5 leads to accumulation of virus particles in the Golgi compartment. *Journal of virology* **76**, 2340–2349. American Society for Microbiology (ASM).

BANU, N., TEICHMAN, J., DUNLAP-BROWN, M., VILLEGAS, G. & TUFRO, A. (2006) Semaphorin 3C regulates endothelial cell function by increasing integrin activity. *FASEB journal : official publication of the Federation of American Societies for Experimental Biology* **20**, 2150–2152. Federation of American Societies for Experimental Biology.

BARBERIS, D., ARTIGIANI, S., CASAZZA, A., CORSO, S., GIORDANO, S., LOVE, C.A., JONES, E.Y., COMOGLIO, P.M. & TAMAGNONE, L. (2004) Plexin signaling hampers integrin-based adhesion, leading to Rho-kinase independent cell rounding, and inhibiting lamellipodia extension and cell motility. *FASEB journal : official publication of the Federation of American Societies for Experimental Biology* **18**, 592–594. Federation of American Societies for Experimental Biology.

BAREYRE, F.M., KERSCHENSTEINER, M., MISGELD, T. & SANES, J.R. (2005) Transgenic labeling of the corticospinal tract for monitoring axonal responses to spinal cord injury. *Nature medicine* **11**, 1355–1360.

BARON-VAN EVERCOOREN, A., GANSMÜLLER, A., GUMPEL, M., BAUMANN, N. & KLEINMAN, H.K. (1986) Schwann Cell Differentiation in vitro: Extracellular Matrix Deposition and Interaction. *Developmental Neuroscience* **8**, 182–196. Karger Publishers.

BARRANGOU, R. & DOUDNA, J.A. (2016) Applications of CRISPR technologies in research and beyond. *Nature Biotechnology*, 933–941. Nature Research.

BARRANGOU, R. & HORVATH, P. (2017) A decade of discovery: CRISPR functions and applications. *Nature microbiology* **2**, 17092.

BARRANGOU, R., FREMAUX, C., DEVEAU, H., RICHARDS, M., BOYAVAL, P., MOINEAU, S., ROMERO, D.A. & HORVATH, P. (2007) CRISPR provides acquired resistance against viruses in prokaryotes. *Science (New York, N.Y.)* **315**, 1709–1712. American Association for the Advancement of Science.

BATES, C.A. & STELZNER, D.J. (1993) Extension and Regeneration of Corticospinal Axons After Early Spinal-Injury and the Maintenance of Corticospinal Topography. *Experimental neurology* **123**, 106–117.

BECHARA, A., NAWABI, H., MORET, F., YARON, A., WEAVER, E., BOZON, M., ABOUZID, K., GUAN, J.L., LAVIGNE, M.T., LEMMON, V. & CASTELLANI, V. (2008) FAK–MAPK-dependent adhesion disassembly downstream of L1 contributes to semaphorin3A-induced collapse. *The EMBO journal* **27**, 1549–1562. EMBO Press.

BEDBROOK, C.N., DEVERMAN, B.E. & GRADINARU, V. (2018) Viral Strategies for Targeting the Central and Peripheral Nervous Systems. *Annual review of neuroscience* **41**, 323–348. Annual Reviews.

BELL, C.L., GURDA, B.L., VAN VLIET, K., AGBANDJE-MCKENNA, M. & WILSON, J.M. (2012) Identification of the galactose binding domain of the adeno-associated virus serotype 9 capsid. *Journal of virology* **86**, 7326–7333. American Society for Microbiology Journals.

BENNASSER, Y., CHABLE-BESSIA, C., TRIBOULET, R., GIBBINGS, D., GWIZDEK, C., DARGEMONT, C., KREMER, E.J., VOINNET, O. & BENKIRANE, M. (2011) Competition for XPO5 binding between Dicer mRNA, pre-miRNA and viral RNA regulates human Dicer levels. *Nature Structural & Molecular Biology* **18**, 323–U108. Nature Publishing Group.

BENNETT, J., WELLMAN, J., MARSHALL, K.A., MCCAGUE, S., ASHTARI, M., DISTEFANO-PAPPAS, J., ET AL. (2016a) Safety and durability of effect of contralateral-eye administration of AAV2 gene therapy in patients with childhood-onset blindness caused by RPE65 mutations: a follow-on phase 1 trial. *Lancet (London, England)* **388**, 661–672.

BENNETT, M.L., BENNETT, F.C., LIDDELOW, S.A., AJAMI, B., ZAMANIAN, J.L., FERNHOFF, N.B., MULINYAWE, S.B., BOHLEN, C.J., ADIL, A., TUCKER, A., WEISSMAN, I.L., CHANG, E.F., LI, G., GRANT, G.A., GEPHART, M.G.H. & BARRES, B.A. (2016b) New tools for studying microglia in the mouse and human CNS. *Proceedings of the National Academy of Sciences* **113**, E1738–E1746. National Academy of Sciences.

BENTLEY, M. & BANKER, G. (2016) The cellular mechanisms that maintain neuronal polarity. *Nature reviews. Neuroscience* **17**, 611–622.

BERGLES, D.E. & RICHARDSON, W.D. (2016) Oligodendrocyte Development and Plasticity. *Cold Spring Harbor Perspectives in Biology* **8**. Cold Spring Harbor Lab.

BERRIER, A.L., MASTRANGELO, A.M., DOWNWARD, J., GINSBERG, M. & LAFLAMME, S.E. (2000) Activated R-ras, Rac1, PI 3-kinase and PKCepsilon can each restore cell spreading inhibited by isolated integrin beta1 cytoplasmic domains. *Journal of Cell Biology* **151**, 1549–1560. The Rockefeller University Press.

BI, X., LYNCH, G., ZHOU, J. & GALL, C.M. (2001) Polarized distribution of alpha5 integrin in dendrites of hippocampal and cortical neurons. *The Journal of comparative neurology* **435**, 184–193. John Wiley & Sons, Inc.

BIN, J.M., HARRIS, S.N. & KENNEDY, T.E. (2016) The oligodendrocyte-specific antibody 'CC1' binds Quaking 7. *Journal of neurochemistry* **139**, 181–186. John Wiley & Sons, Ltd (10.1111).

BLACKMORE, M.G., WANG, Z., LERCH, J.K., MOTTI, D., ZHANG, Y.P., SHIELDS, C.B., LEE, J.K., GOLDBERG, J.L., LEMMON, V.P. & BIXBY, J.L. (2012) Krüppel-like Factor 7 engineered for transcriptional activation promotes axon regeneration in the adult corticospinal tract. *Proceedings of the National Academy of Sciences of the United States of America* **109**, 7517–7522. National Acad Sciences.

BLAESS, S., GRAUS-PORTA, D., BELVINDRAH, R., RADAKOVITS, R., PONS, S., LITTLEWOOD-EVANS, A., SENFTEN, M., GUO, H., LI, Y., MINER, J.H., REICHARDT, L.F. & MÜLLER, U. (2004) Beta1-integrins are critical for cerebellar granule cell precursor proliferation. *The Journal of Neuroscience* **24**, 3402–3412. Society for Neuroscience.

BLIND, R.D., SABLIN, E.P., KUCHENBECKER, K.M., CHIU, H.-J., DEACON, A.M., DAS, D., FLETTERICK, R.J. & INGRAHAM, H.A. (2014) The signaling phospholipid PIP3 creates a new interaction surface on the nuclear receptor SF-1. *Proceedings of the National Academy of Sciences* **111**, 15054–15059. National Academy of Sciences.

BOGHDADI, A.G., TEO, L. & BOURNE, J.A. (2017) The Involvement of the Myelin-Associated Inhibitors and Their Receptors in CNS Plasticity and Injury. *Molecular neurobiology*, 1–16. Springer US.

BOLOTIN, A., OUINQUIS, B., SOROKIN, A. & EHRLICH, S.D. (2005) Clustered regularly interspaced short palindrome repeats (CRISPRs) have spacers of extrachromosomal origin. *Microbiology-Sgm* **151**, 2551–2561. Microbiology Society.

BOSSY, B., BOSSYWETZEL, E. & REICHARDT, L.F. (1991) Characterization of the Integrin Alpha-8 Subunit - a New Integrin Beta-1-Associated Subunit, Which Is Prominently Expressed on Axons and on Cells in Contact with Basal Laminae in Chick-Embryos. *The EMBO journal* **10**, 2375–2385. European Molecular Biology Organization.

BOUVARD, D., POUWELS, J., DE FRANCESCHI, N. & IVASKA, J. (2013) Integrin inactivators: balancing cellular functions in vitro and in vivo. *Nature Reviews Molecular Cell Biology* **14**, 430–442. Nature Publishing Group.

BRADKE, F., FAWCETT, J.W. & SPIRA, M.E. (2012) Assembly of a new growth cone after axotomy: the precursor to axon regeneration. *Nature reviews. Neuroscience* **13**, 183–193. Nature Publishing Group.

BRADSHAW, A.D., MCNAGNY, K.M., GERVIN, D.B., CANN, G.M., GRAF, T. & CLEGG, D.O. (1995) Integrin alpha 2 beta 1 mediates interactions between developing embryonic retinal cells and collagen. *Development* **121**, 3593–3602. The Company of Biologists Ltd.

BRECHT, M., KRAUSS, A., MUHAMMAD, S., SINAI-ESFAHANI, L., BELLANCA, S. & MARGRIE, T.W. (2004) Organization of rat vibrissa motor cortex and adjacent areas according to cytoarchitectonics, microstimulation, and intracellular stimulation of identified cells. *The Journal of comparative neurology* **479**, 360–373. Wiley-Blackwell.

BREGMAN, B.S. & BERNSTEINGORAL, H. (1991) Both Regenerating and Late-Developing Pathways Contribute to Transplant-Induced Anatomical Plasticity After Spinal-Cord Lesions at Birth. *Experimental neurology* **112**, 49–63.

BREGMAN, B.S., E, K.-B., L, S., HN, D., D, G. & ME, S. (1995) Recovery from spinal cord injury mediated by antibodies to neurite growth inhibitors. *Nature* **378**, 498–501.

BRITT, D.J., FARÍAS, G.G., GUARDIA, C.M. & BONIFACINO, J.S. (2016) Mechanisms of Polarized Organelle Distribution in Neurons. *Frontiers in Cellular Neuroscience* **10**, 88. Frontiers.

BROWN, F.D., ROZELLE, A.L., YIN, H.L., BALLA, T. & DONALDSON, J.G. (2001) Phosphatidylinositol 4,5-bisphosphate and Arf6-regulated membrane traffic. *The Journal of Cell Biology* **154**, 1007–1017. Rockefeller Univ Press.

BRÖSAMLE, C. & SCHWAB, M.E. (1997) Cells of origin, course, and termination patterns of the ventral, uncrossed component of the mature rat corticospinal tract. *The Journal of comparative neurology* **386**, 293–303.

BRÖSAMLE, C., HUBER, A.B., FIEDLER, M., SKERRA, A. & SCHWAB, M.E. (2000) Regeneration of lesioned corticospinal tract fibers in the adult rat induced by a recombinant, humanized IN-1 antibody fragment. *The Journal of Neuroscience* **20**, 8061–8068. Society for Neuroscience.

BUCHER, T., DUBREIL, L., COLLE, M.-A., MAQUIGNEAU, M., DENIAUD, J., LEDEVIN, M., MOULLIER, P. & JOUSSEMET, B. (2014) Intracisternal delivery of AAV9 results in oligodendrocyte and Motor neuron transduction in the whole central nervous system of cats. *Gene therapy* **21**, 522–528. Nature Publishing Group.

BURGER, C., GORBATYUK, O.S., VELARDO, M.J., PEDEN, C.S., WILLIAMS, P., ZOLOTUKHIN, S., REIER, P.J., MANDEL, R.J. & MUZYCZKA, N. (2004) Recombinant AAV viral vectors pseudotyped with viral capsids from serotypes 1, 2, and 5 display differential efficiency and cell tropism after delivery to different regions of the central nervous system. *Molecular therapy : the journal of the American Society of Gene Therapy* **10**, 302–317.

BURKE, J.E., PERISIC, O., MASSON, G.R., VADAS, O. & WILLIAMS, R.L. (2012) Oncogenic mutations mimic and enhance dynamic events in the natural activation of phosphoinositide 3-kinase p110 alpha (PIK3CA). *Proceedings of the National Academy of Sciences* **109**, 15259–15264.

BURNSIDE, E.R., DE WINTER, F., DIDANGELOS, A., JAMES, N.D., ANDREICA, E.-C., LAYARD-HORSFALL, H., MUIR, E.M., VERHAAGEN, J. & BRADBURY, E.J. (2018) Immune-evasive gene switch enables regulated delivery of chondroitinase after spinal cord injury. *Brain : a journal of neurology* **141**, 2362–2381.

CAFFERTY, W.B.J. & STRITTMATTER, S.M. (2006) The Nogo-Nogo receptor pathway limits a spectrum of adult CNS axonal growth. *The Journal of Neuroscience* **26**, 12242–12250. Society for Neuroscience.

CAHOY, J.D., BEN EMERY, KAUSHAL, A., FOO, L.C., ZAMANIAN, J.L., CHRISTOPHERSON, K.S., XING, Y., LUBISCHER, J.L., KRIEG, P.A., KRUPENKO, S.A., THOMPSON, W.J. & BEN A BARRES (2008) A Transcriptome Database for Astrocytes, Neurons, and Oligodendrocytes: A New Resource for Understanding Brain Development and Function. *Journal of Neuroscience* **28**, 264–278. Society for Neuroscience.

CAI, D., QIU, J., CAO, Z., MCATEE, M., BREGMAN, B.S. & FILBIN, M.T. (2001) Neuronal cyclic AMP controls the developmental loss in ability of axons to regenerate. *The Journal of Neuroscience* **21**, 4731–4739.

CALDERWOOD, D.A., CAMPBELL, I.D. & CRITCHLEY, D.R. (2013) Talins and kindlins: partners in integrin-mediated adhesion. *Nature Reviews Molecular Cell Biology* **14**, 503–517. Nature Publishing Group.

CAMPBELL, I.D. & HUMPHRIES, M.J. (2011) Integrin Structure, Activation, and Interactions. *Cold Spring Harbor Perspectives in Biology* **3**, a004994–a004994. Cold Spring Harbor Lab.

CASE, L.C. & TESSIER-LAVIGNE, M. (2005) Regeneration of the adult central nervous system. *Current Biology* **15**, R749–R753.

CASWELL, P.T., CHAN, M., LINDSAY, A.J., MCCAFFREY, M.W., BOETTIGER, D. & NORMAN, J.C. (2008) Rab-coupling protein coordinates recycling of alpha5beta1 integrin and EGFR1 to promote cell migration in 3D microenvironments. *The Journal of Cell Biology* **183**, 143–155. Rockefeller Univ Press.

CHACÓN, M.R., FERNÁNDEZ, G. & RICO, B. (2010) Focal adhesion kinase functions downstream of Sema3A signaling during axonal remodeling. *Molecular and Cellular Neuroscience* **44**, 30–42.

CHAN, C.-S., WEEBER, E.J., KURUP, S., SWEATT, J.D. & DAVIS, R.L. (2003) Integrin requirement for hippocampal synaptic plasticity and spatial memory. *The Journal of Neuroscience* **23**, 7107–7116. Society for Neuroscience.

CHAN, K.Y., JANG, M.J., YOO, B.B., GREENBAUM, A., RAVI, N., WU, W.-L., SÁNCHEZ-GUARDADO, L., LOIS, C., MAZMANIAN, S.K., DEVERMAN, B.E. & GRADINARU, V. (2017) Engineered AAVs for efficient noninvasive gene delivery to the central and peripheral nervous systems. *Nature neuroscience* **20**, 1172–1179. Nature Publishing Group.

CHANDRAN, V., COPPOLA, G., NAWABI, H., OMURA, T., VERSANO, R., HUEBNER, E.A., ET AL. (2016) A Systems-Level Analysis of the Peripheral Nerve Intrinsic Axonal Growth Program. *Neuron* **0**. Elsevier.

CHEAH, M. & ANDREWS, M.R. (2016) Targeting cell surface receptors for axon regeneration in the central nervous system. *Neural regeneration research* **11**, 1884. Medknow Publications.

CHEAH, M., ANDREWS, M.R., CHEW, D.J., MOLONEY, E.B., VERHAAGEN, J., FÄSSLER, R. & FAWCETT, J.W. (2016) Expression of an Activated Integrin Promotes Long-Distance Sensory Axon Regeneration in the Spinal Cord. *The Journal of Neuroscience* **36**, 7283–7297. Society for Neuroscience.

CHEN, H.C., APPEDDU, P.A., ISODA, H. & GUAN, J.L. (1996) Phosphorylation of tyrosine 397 in focal adhesion kinase is required for binding phosphatidylinositol 3-kinase. *The Journal of biological chemistry* **271**, 26329–26334. American Society for Biochemistry and Molecular Biology.

CHEN, J., LEE, H.J., JAKOVCEVSKI, I., SHAH, R., BHAGAT, N., LOERS, G., LIU, H.-Y., MEINERS, S., TASCHENBERGER, G., KÜGLER, S., IRINTCHEV, A. & SCHACHNER, M. (2009) The Extracellular Matrix Glycoprotein Tenascin-C Is Beneficial for Spinal Cord Regeneration. *Molecular therapy : the journal of the American Society of Gene Therapy* **18**, 1769–1777. Nature Publishing Group.

COHEN, S.J., GUREVICH, I., FEIGELSON, S.W., PETROVICH, E., MOSER, M., SHAKHAR, G., FÄSSLER, R. & ALON, R. (2013) The integrin coactivator Kindlin-3 is not required for lymphocyte diapedesis. *Blood* **122**, 2609–2617. American Society of Hematology.

COLOGNATO, H. & TZVETANOVA, I.D. (2011) Glia unglued: how signals from the extracellular matrix regulate the development of myelinating glia. *Developmental neurobiology* **71**, 924–955. Wiley Subscription Services, Inc., A Wiley Company.

COLOGNATO, H., MACCARRICK, M., O'REAR, J.J. & YURCHENCO, P.D. (1997) The laminin alpha2-chain short arm mediates cell adhesion through both the alpha1beta1 and alpha2beta1 integrins. *The Journal of biological chemistry* **272**, 29330–29336.

CONDIC, M.L. (2001) Adult Neuronal Regeneration Induced by Transgenic Integrin Expression. *Journal of Neuroscience* **21**, 4782–4788. Society for Neuroscience.

CONDIC, M.L. & LETOURNEAU, P.C. (1997) Ligand-induced changes in integrin expression regulate neuronal adhesion and neurite outgrowth. *Nature* **389**, 852–856. Nature Publishing Group.

CONNELLY, J.C., KIRKHAM, L.A. & LEACH, D.R. (1998) The SbcCD nuclease of Escherichia coli is a structural maintenance of chromosomes (SMC) family protein that cleaves hairpin DNA. *Proceedings of the National Academy of Sciences* **95**, 7969–7974. National Academy of Sciences.

COSKER, K.E. & EICKHOLT, B.J. (2007) Phosphoinositide 3-kinase signalling events controlling axonal morphogenesis. *Biochemical Society Transactions* **35**, 207–210. Portland Press Limited.

CRANER, M.J., KLEIN, J.P., BLACK, J.A. & WAXMAN, S.G. (2002) Preferential expression of IGF-I in small DRG neurons and down-regulation following injury. *Neuroreport* **13**, 1649–1652.

CUCCHIARINI, M., REN, X.L., PERIDES, G. & TERWILLIGER, E.F. (2003) Selective gene expression in brain microglia mediated via adeno-associated virus type 2 and type 5 vectors. *Gene therapy* **10**, 657–667.

CUMMING, G., FIDLER, F. & VAUX, D.L. (2007) Error bars in experimental biology. *Journal of Cell Biology* **177**, 7–11. Rockefeller University Press.

DAI, J., LI, J., BOS, E., PORCIONATTO, M., PREMONT, R.T., BOURGOIN, S., PETERS, P.J. & HSU, V.W. (2004) ACAP1 promotes endocytic recycling by recognizing recycling sorting signals. *Developmental cell* **7**, 771–776.

DANEN, E.H. & SONNENBERG, A. (2003) Erratum: Integrins in regulation of tissue development and function. J Pathol; 200: 471–480. *The Journal of pathology* **201**, 632–641. John Wiley & Sons, Ltd.

DANILOV, C.A. & STEWARD, O. (2015) Conditional genetic deletion of PTEN after a spinal cord injury enhances regenerative growth of CST axons and motor function recovery in mice. *Experimental neurology* **266**, 147–160. Academic Press.

DANZI, M.C., O'NEILL, N., BIXBY, J.L. & LEMMON, V.P. (2018) Can Chromatin Accessibility be Exploited for Axon Regeneration? *Developmental neurobiology* **78**, 991–997. John Wiley & Sons, Ltd.

DAVID, S. & AGUAYO, A.J. (1981) Axonal Elongation Into Peripheral Nervous-System Bridges After Central Nervous-System Injury in Adult-Rats. *Science (New York, N.Y.)* **214**, 931–933.

DAVIS, J.Q., LAMBERT, S. & BENNETT, V. (1996) Molecular composition of the node of Ranvier: identification of ankyrin-binding cell adhesion molecules neurofascin (mucin+/third FNIII domain-) and NrCAM at nodal axon segments. *Journal of Cell Biology* **135**, 1355–1367. The Rockefeller University Press.

DE WINTER, F., OUDEGA, M., LANKHORST, A.J., HAMERS, F.P., BLITS, B., RUITENBERG, M.J., PASTERKAMP, R.J., GISPEN, W.H. & VERHAAGEN, J. (2002) Injury-induced class 3 semaphorin expression in the rat spinal cord. *Experimental neurology* **175**, 61–75.

DE WIT, J. & VERHAAGEN, J. (2003) Role of semaphorins in the adult nervous system. *Progress in neurobiology* **71**, 249–267.

DEBRAND, E., JAI, EL, Y., SPENCE, L., BATE, N., PRAEKELT, U., PRITCHARD, C.A., MONKLEY, S.J. & CRITCHLEY, D.R. (2009) Talin 2 is a large and complex gene encoding multiple transcripts and protein isoforms. *The FEBS journal* **276**, 1610–1628. Blackwell Publishing Ltd.

DELWEL, G.O., DE MELKER, A.A., HOGERVORST, F., JASPARS, L.H., FLES, D.L., KUIKMAN, I., LINDBLOM, A., PAULSSON, M., TIMPL, R. & SONNENBERG, A. (1994) Distinct and overlapping ligand specificities of the alpha 3A beta 1 and alpha 6A beta 1 integrins: recognition of laminin isoforms. *Molecular biology of the cell* **5**, 203–215. American Society for Cell Biology.

DENDA, S., REICHARDT, L.F. & MÜLLER, U. (1998) Identification of osteopontin as a novel ligand for the integrin alpha8 beta1 and potential roles for this integrin-ligand interaction in kidney morphogenesis. *Molecular biology of the cell* **9**, 1425–1435. American Society for Cell Biology.

DESBAN, N., LISSITZKY, J.-C., ROUSSELLE, P. & DUBAND, J.-L. (2006) α1β1-integrin engagement to distinct laminin-1 domains orchestrates spreading, migration and survival of neural crest cells through independent signaling pathways. *Journal of Cell Science* **119**, 3206–3218. The Company of Biologists Ltd.

DESGROSELLIER, J.S. & CHERESH, D.A. (2010) Integrins in cancer: biological implications and therapeutic opportunities. *Nature reviews. Cancer* **10**, 9–22. Nature Publishing Group.

DI PAOLO, G., MOSKOWITZ, H.S., GIPSON, K., WENK, M.R., VORONOV, S., OBAYASHI, M., FLAVELL, R., FITZSIMONDS, R.M., RYAN, T.A. & DE CAMILLI, P. (2004) Impaired PtdIns(4,5)P2 synthesis in nerve terminals produces defects in synaptic vesicle trafficking. *Nature* **431**, 415–422. Nature Publishing Group.

DI PASQUALE, G., DAVIDSON, B.L., STEIN, C.S., MARTINS, I., SCUDIERO, D., MONKS, A. & CHIORINI, J.A. (2003) Identification of PDGFR as a receptor for AAV-5 transduction. *Nature medicine* **9**, 1306–1312. Nature Publishing Group.

DICKENDESHER, T.L., BALDWIN, K.T., MIRONOVA, Y.A., KORIYAMA, Y., RAIKER, S.J., ASKEW, K.L., WOOD, A., GEOFFROY, C.G., ZHENG, B., LIEPMANN, C.D., KATAGIRI, Y., BENOWITZ, L.I., GELLER, H.M. & GIGER, R.J. (2012) NgR1 and NgR3 are receptors for chondroitin sulfate proteoglycans. *Nature neuroscience* **15**, 703–712. Nature Research.

DIMOU, L., SCHNELL, L., MONTANI, L., DUNCAN, C., SIMONEN, M., SCHNEIDER, R., LIEBSCHER, T., GULLO, M. & SCHWAB, M.E. (2006) Nogo-A-deficient mice reveal strain-dependent differences in axonal regeneration. *The Journal of Neuroscience* **26**, 5591–5603. Society for Neuroscience.

DINGYU, W., FANJIE, M., ZHENGZHENG, D., BAOSHENG, H., CHAO, Y., YI, P., HUIWEN, W., JUN, G. & GANG, H. (2015) Regulation of Intracellular Structural Tension by Talin in the Axon Growth and Regeneration. *Molecular neurobiology*, 1–14. Springer US.

DOMENICONI, M., CAO, Z.U., SPENCER, T., SIVASANKARAN, R., WANG, K.C., NIKULINA, E., KIMURA, N., CAI, H., DENG, K.W., GAO, Y., HE, Z.G. & FILBIN, M.T. (2002) Myelin-associated glycoprotein interacts with the Nogo66 receptor to inhibit neurite outgrowth. *Neuron* **35**, 283–290.

DUPRAZ, S., GRASSI, D., KARNAS, D., NIETO GUIL, A.F., HICKS, D. & QUIROGA, S. (2013) The insulin-like growth factor 1 receptor is essential for axonal regeneration in adult central nervous system neurons. *PloS one* **8**, e54462. Public Library of Science.

DURBEEJ, M. (2010) Laminins. *Cell and tissue research* **339**, 259–268.

EBBESEN, C.L. & BRECHT, M. (2017) Motor cortex - to act or not to act? *Nature reviews. Neuroscience* **18**, 694–705. Nature Publishing Group.

EBLE, J.A., WUCHERPFENNIG, K.W., GAUTHIER, L., DERSCH, P., KRUKONIS, E., ISBERG, R.R. & HEMLER, M.E. (1998) Recombinant soluble human alpha 3 beta 1 integrin: purification, processing, regulation, and specific binding to laminin-5 and invasin in a mutually exclusive manner. *Biochemistry* **37**, 10945–10955. American Chemical Society.

EGAN, R.A. & VIJAYAN, V.K. (1991) Fibronectin immunoreactivity in neural trauma. *Brain research* **568**, 330–334.

EGGERS, R., DE WINTER, F., HOYNG, S.A., HOEBEN, R.C., MALESSY, M.J.A., TANNEMAAT, M.R. & VERHAAGEN, J. (2019) Timed GDNF gene therapy using an immune-evasive gene switch promotes long distance axon regeneration. *Brain : a journal of neurology* **142**, 295–311.

EHLERT, E.M., EGGERS, R., NICLOU, S.P. & VERHAAGEN, J. (2010) Cellular toxicity following application of adeno-associated viral vector-mediated RNA interference in the nervous system. *BMC neuroscience* **11**, 20. BioMed Central Ltd.

EICKHOLT, B.J., AHMED, A.I., DAVIES, M., PAPAKONSTANTI, E.A., PEARCE, W., STARKEY, M.L., BILANCIO, A., NEED, A.C., SMITH, A.J.H., HALL, S.M., HAMERS, F.P., GIESE, K.P., BRADBURY, E.J. & VANHAESEBROECK, B. (2007) Control of axonal growth and regeneration of sensory neurons by the p110delta PI 3-kinase. *PloS one* **2**, e869.

EINHEBER, S., SCHNAPP, L.M., SALZER, J.L., CAPPIELLO, Z.B. & MILNER, T.A. (1996) Regional and ultrastructural distribution of the alpha 8 integrin subunit in developing and adult rat brain suggests a role in synaptic function. *The Journal of comparative neurology* **370**, 105–134.

EKSTRÖM, P.A.R., MAYER, U., PANJWANI, A., POUNTNEY, D., PIZZEY, J. & TONGE, D.A. (2003) Involvement of alpha7beta1 integrin in the conditioning-lesion effect on sensory axon regeneration. *Molecular and cellular neurosciences* **22**, 383–395.

EMSLEY, J., KNIGHT, C.G., FARNDALE, R.W., BARNES, M.J. & LIDDINGTON, R.C. (2000) Structural basis of collagen recognition by integrin alpha2beta1. *Cell* **101**, 47–56. Elsevier.

EVA, R. & FAWCETT, J. (2014) Integrin signalling and traffic during axon growth and regeneration. *Current Opinion in Neurobiology* **27**, 179–185.

EVA, R., CRISP, S., MARLAND, J.R.K., NORMAN, J.C., KANAMARLAPUDI, V., FFRENCH-CONSTANT, C. & FAWCETT, J.W. (2012) ARF6 directs axon transport and traffic of integrins and regulates axon growth in adult DRG neurons. *The Journal of Neuroscience* **32**, 10352–10364. Society for Neuroscience.

EVA, R., DASSIE, E., CASWELL, P.T., DICK, G., FFRENCH-CONSTANT, C., NORMAN, J.C. & FAWCETT, J.W. (2010) Rab11 and its effector Rab coupling protein contribute to the trafficking of beta 1 integrins during axon growth in adult dorsal root ganglion neurons and PC12 cells. *The Journal of Neuroscience* **30**, 11654–11669. Society for Neuroscience.

EVA, R., KOSEKI, H., KANAMARLAPUDI, V. & FAWCETT, J.W. (2017) EFA6 regulates selective polarised transport and axon regeneration from the axon initial segment. *Journal of Cell Science* **130**, 3663–3675. The Company of Biologists Ltd.

FAGOE, N.D., EGGERS, R., VERHAAGEN, J. & MASON, M.R.J. (2014a) A compact dual promoter adeno-associated viral vector for efficient delivery of two genes to dorsal root ganglion neurons. *Gene therapy* **21**, 242–252. Nature Publishing Group.

FAGOE, N.D., VAN HEEST, J. & VERHAAGEN, J. (2014b) Spinal Cord Injury and the Neuron-Intrinsic Regeneration-Associated Gene Program. *NeuroMolecular Medicine*.

FAISSNER, A. (1997) The tenascin gene family in axon growth and guidance. *Cell and tissue research* **290**, 331–341.

FALASCA, M. & MAFFUCCI, T. (2012) Regulation and cellular functions of class II phosphoinositide 3-kinases. *The Biochemical journal* **443**, 587–601. Portland Press Limited.

FALLINI, C., BASSELL, G.J. & ROSSOLL, W. (2010) High-efficiency transfection of cultured primary motor neurons to study protein localization, trafficking, and function. *Molecular neurodegeneration* **5**, 17. BioMed Central.

FAWCETT, J.W. & VERHAAGEN, J. (2018) Intrinsic Determinants of Axon Regeneration. *Developmental neurobiology* **17**, 611. Wiley-Blackwell.

FÄSSLER, R. & MEYER, M. (1995) Consequences of Lack of Beta-1 Integrin Gene-Expression in Mice. *Genes & development* **9**, 1896–1908.

FEIGELSON, S.W., GRABOVSKY, V., MANEVICH-MENDELSON, E., PASVOLSKY, R., SHULMAN, Z., SHINDER, V., KLEIN, E., ETZIONI, A., AKER, M. & ALON, R. (2011) Kindlin-3 is required for the stabilization of TCR-stimulated LFA-1:ICAM-1 bonds critical for lymphocyte arrest and spreading on dendritic cells. *Blood* **117**, 7042–7052. American Society of Hematology.

FIRE, A., XU, S., MONTGOMERY, M.K., KOSTAS, S.A., DRIVER, S.E. & MELLO, C.C. (1998) Potent and specific genetic interference by double-stranded RNA in Caenorhabditis elegans. *Nature* **391**, 806–811. Nature Publishing Group.

FISHER, D., XING, B., DILL, J., LI, H., HOANG, H.H., ZHAO, Z., YANG, X.-L., BACHOO, R., CANNON, S., LONGO, F.M., SHENG, M., SILVER, J. & LI, S. (2011) Leukocyte Common Antigen-Related Phosphatase Is a Functional Receptor for Chondroitin Sulfate Proteoglycan Axon Growth Inhibitors. *Journal of Neuroscience* **31**, 14051–14066. Society for Neuroscience.

FOURNIER, A.E., GRANDPRE, T. & STRITTMATTER, S.M. (2001) Identification of a receptor mediating Nogo-66 inhibition of axonal regeneration. *Nature* **409**, 341–346. Nature Publishing Group.

FRANKLIN, R.J.M. & FFRENCH-CONSTANT, C. (2017) Regenerating CNS myelin - from mechanisms to experimental medicines. *Nature reviews. Neuroscience* **18**, 753–769. Nature Publishing Group.

FRANSSEN, E.H.P., ZHAO, R.-R., KOSEKI, H., KANAMARLAPUDI, V., HOOGENRAAD, C.C., EVA, R. & FAWCETT, J.W. (2015) Exclusion of Integrins from CNS Axons Is Regulated by Arf6 Activation and the AIS. *The Journal of Neuroscience* **35**, 8359–8375. Society for Neuroscience.

FREAL, A., FASSIER, C., LE BRAS, B., BULLIER, E., DE GOIS, S., HAZAN, J., HOOGENRAAD, C.C. & COURAUD, F. (2016) Cooperative Interactions between 480 kDa Ankyrin-G and EB Proteins Assemble the Axon Initial Segment. *The Journal of Neuroscience* **36**, 4421–4433. Society for Neuroscience.

FRUMAN, D.A., CHIU, H., HOPKINS, B.D., BAGRODIA, S., CANTLEY, L.C. & ABRAHAM, R.T. (2017) The PI3K Pathway in Human Disease. *Cell* **170**, 605–635.

FRY, E.J., CHAGNON, M.J., LÓPEZ-VALES, R., TREMBLAY, M.L. & DAVID, S. (2010) Corticospinal tract regeneration after spinal cord injury in receptor protein tyrosine phosphatase sigma deficient mice. *Glia* **58**, 423–433. Wiley Subscription Services, Inc., A Wiley Company.

FUKASAWA, M., MATSUSHITA, A. & KORC, M. (2007) Neuropilin-1 interacts with integrin β1 and modulates pancreatic cancer cell growth, survival and invasion. *Cancer biology & therapy* **6**, 1184–1191. Taylor & Francis.

GALIANO, M.R., JHA, S., HO, T.S.-Y., ZHANG, C., OGAWA, Y., CHANG, K.-J., STANKEWICH, M.C., MOHLER, P.J. & RASBAND, M.N. (2012) A Distal Axonal Cytoskeleton Forms an Intra-Axonal Boundary that Controls Axon Initial Segment Assembly. *Cell* **149**, 1125–1139.

GARCÍA-ALVAREZ, B., DE PEREDA, J.M., CALDERWOOD, D.A., ULMER, T.S., CRITCHLEY, D., CAMPBELL, I.D., GINSBERG, M.H. & LIDDINGTON, R.C. (2003) Structural determinants of integrin recognition by talin. *Molecular cell* **11**, 49–58.

GARDINER, N.J. (2011) Integrins and the extracellular matrix: key mediators of development and regeneration of the sensory nervous system. *Developmental neurobiology* **71**, 1054–1072. Wiley Subscription Services, Inc., A Wiley Company.

GARDINER, N.J., FERNYHOUGH, P., TOMLINSON, D.R., MAYER, U., MARK, VON DER, H. & STREULI, C.H. (2005) Alpha7 integrin mediates neurite outgrowth of distinct populations of adult sensory neurons. *Molecular and cellular neurosciences* **28**, 229–240.

GARDINER, N.J., MOFFATT, S., FERNYHOUGH, P., HUMPHRIES, M.J., STREULI, C.H. & TOMLINSON, D.R. (2007) Preconditioning injury-induced neurite outgrowth of adult rat sensory neurons on fibronectin is mediated by mobilisation of axonal alpha5 integrin. *Molecular and cellular neurosciences* **35**, 249–260.

GAUB, P., JOSHI, Y., WUTTKE, A., NAUMANN, U., SCHNICHELS, S., HEIDUSCHKA, P. & DI GIOVANNI, S. (2011) The histone acetyltransferase p300 promotes intrinsic axonal regeneration. *Brain : a journal of neurology* **134**, 2134–2148.

GEBERHIWOT, T., INGERPUU, S., PEDRAZA, C., NEIRA, M., LEHTO, U., VIRTANEN, I., KORTESMAA, J., TRYGGVASON, K., ENGVALL, E. & PATARROYO, M. (1999) Blood platelets contain and secrete laminin-8 (alpha4beta1gamma1) and adhere to laminin-8 via alpha6beta1 integrin. *Experimental cell research* **253**, 723–732. Academic Press.

GEOFFROY, C.G., HILTON, B.J., TETZLAFF, W. & ZHENG, B. (2016) Evidence for an Age-Dependent Decline in Axon Regeneration in the Adult Mammalian Central Nervous System. *Cell reports* **0**. Elsevier.

GEORGES-LABOUESSE, E., MARK, M., MESSADDEQ, N. & GANSMÜLLER, A. (1998) Essential role of alpha 6 integrins in cortical and retinal lamination. *Current biology : CB* **8**, 983–986.

GERITS, A., VANCRAEYENEST, P., VREYSEN, S., LARAMÉE, M.-E., MICHIELS, A., GIJSBERS, R., VAN DEN HAUTE, C., MOONS, L., DEBYSER, Z., BAEKELANDT, V., ARCKENS, L. & VANDUFFEL, W. (2015) Serotype-dependent transduction efficiencies of recombinant adeno-associated viral vectors in monkey neocortex. *Neurophotonics* **2**, 031209. International Society for Optics and Photonics.

GERVASI, N.M., KWOK, J.C. & FAWCETT, J.W. (2008) Role of extracellular factors in axon regeneration in the CNS: implications for therapy. *Regenerative medicine* **3**, 907–923.

GIGER, R.J., HOLLIS, E.R., II & TUSZYNSKI, M.H. (2010) Guidance Molecules in Axon Regeneration. *Cold Spring Harbor Perspectives in Biology* **2**, a001867–a001867. Cold Spring Harbor Lab.

GIOANNI, Y. & LAMARCHE, M. (1985) A reappraisal of rat motor cortex organization by intracortical microstimulation. *Brain research* **344**, 49–61.

GOH, E.L.K., YOUNG, J.K., KUWAKO, K., TESSIER-LAVIGNE, M., HE, Z., GRIFFIN, J.W. & MING, G.-L. (2008) beta1-integrin mediates myelin-associated glycoprotein signaling in neuronal growth cones. *Molecular brain* **1**, 10. BioMed Central.

GOLDING, J.P., BIRD, C., MCMAHON, S. & COHEN, J. (1999) Behaviour of DRG sensory neurites at the intact and injured adult rat dorsal root entry zone: Postnatal neurites become paralysed, whilst injury improves the growth of embryonic neurites. *Glia* **26**, 309–323. John Wiley & Sons, Inc.

GONZALEZ PEREZ, F., ALÉ, A., SANTOS, D., BARWIG, C., FREIER, T., NAVARRO, X. & UDINA, E. (2016) Substratum preferences of motor and sensory neurons in postnatal and adult rats. *The European journal of neuroscience*, n/a–n/a.

GONZALEZ PEREZ, F., UDINA, E. & NAVARRO, X. (2013) Extracellular matrix components in peripheral nerve regeneration. *International review of neurobiology* **108**, 257–275. Elsevier.

GOUT, S.P., JACQUIER-SARLIN, M.R., ROUARD-TALBOT, L., ROUSSELLE, P. & BLOCK, M.R. (2001) RhoA-dependent switch between alpha2beta1 and alpha3beta1 integrins is induced by laminin-5 during early stage of HT-29 cell differentiation. *Molecular biology of the cell* **12**, 3268–3281. American Society for Cell Biology.

GÖTZ, B., SCHOLZE, A., CLEMENT, A., JOESTER, A., SCHÜTTE, K., WIGGER, F., FRANK, R., SPIESS, E., EKBLOM, P. & FAISSNER, A. (1996) Tenascin-C contains distinct adhesive, anti-adhesive, and neurite outgrowth promoting sites for neurons. *Journal of Cell Biology* **132**, 681–699. The Rockefeller University Press.

GRAUS-PORTA, D., BLAESS, S., SENFTEN, M., LITTLEWOOD EVANS, A., DAMSKY, C., HUANG, Z., ORBAN, P., KLEIN, R., SCHITTNY, J.C. & MÜLLER, U. (2001) Beta1-class integrins regulate the development of laminae and folia in the cerebral and cerebellar cortex. *Neuron* **31**, 367–379.

GRAY, S.J. (2013) Gene therapy and neurodevelopmental disorders. *Neuropharmacology* **68**, 136–142.

GRIEGER, J.C., SOLTYS, S.M. & SAMULSKI, R.J. (2016) Production of Recombinant Adeno-associated Virus Vectors Using Suspension HEK293 Cells and Continuous Harvest of Vector From the Culture Media for GMP FIX and FLT1 Clinical Vector. *Molecular therapy : the journal of the American Society of Gene Therapy* **24**, 287–297.

GRIMM, D., KAY, M.A. & KLEINSCHMIDT, J.A. (2003) Helper virus-free, optically controllable, and two-plasmid-based production of adeno-associated virus vectors of serotypes 1 to 6. *Molecular therapy : the journal of the American Society of Gene Therapy* **7**, 839–850.

GRIMM, D., STREETZ, K.L., JOPLING, C.L., STORM, T.A., PANDEY, K., DAVIS, C.R., MARION, P., SALAZAR, F. & KAY, M.A. (2006) Fatality in mice due to oversaturation of cellular microRNA/short hairpin RNA pathways. *Nature* **441**, 537–541. Nature Publishing Group.

GROOMS, S.Y., TERRACIO, L. & JONES, L.S. (1993) Anatomical localization of beta 1 integrin-like immunoreactivity in rat brain. *Experimental neurology* **122**, 253–259.

GROSS, C. & BASSELL, G.J. (2014) Neuron-specific regulation of class I PI3K catalytic subunits and their dysfunction in brain disorders. *Frontiers in molecular neuroscience* **7**, 12. Frontiers.

GUILARTE, T.R. (2013) Manganese neurotoxicity: new perspectives from behavioral, neuroimaging, and neuropathological studies in humans and non-human primates. *Frontiers in aging neuroscience* **5**, 23. Frontiers.

GUO, W. & GIANCOTTI, F.G. (2004) Integrin signalling during tumour progression. *Nature Reviews Molecular Cell Biology* **5**, 816–826. Nature Publishing Group.

GUTZMANN, A., ERGÜL, N., GROSSMANN, R., SCHULTZ, C., WAHLE, P. & ENGELHARDT, M. (2014) A period of structural plasticity at the axon initial segment in developing visual cortex. *Frontiers in neuroanatomy* **8**, 11. Frontiers.

HAMMARBERG, H., WALLQUIST, W., PIEHL, F., RISLING, M. & CULLHEIM, S. (2000) Regulation of laminin-associated integrin subunit mRNAs in rat spinal motoneurons during postnatal development and after axonal injury. *The Journal of comparative neurology* **428**, 294–304.

HAN, J., LEE, Y., YEOM, K.-H., KIM, Y.-K., JIN, H. & KIM, V.N. (2004) The Drosha-DGCR8 complex in primary microRNA processing. *Genes & development* **18**, 3016–3027. Cold Spring Harbor Lab.

HARBURGER, D.S., BOUAOUINA, M. & CALDERWOOD, D.A. (2009) Kindlin-1 and -2 directly bind the C-terminal region of beta integrin cytoplasmic tails and exert integrin-specific activation effects. *The Journal of biological chemistry* **284**, 11485–11497.

HARPER, M.M., YE, E.-A., BLONG, C.C., JACOBSON, M.L. & SAKAGUCHI, D.S. (2010) Integrins contribute to initial morphological development and process outgrowth in rat adult hippocampal progenitor cells. *Journal of molecular neuroscience : MN* **40**, 269–283.

HARRINGTON, A.W. & GINTY, D.D. (2013) Long-distance retrograde neurotrophic factor signalling in neurons. *Nature reviews. Neuroscience* **14**, 177–187. Nature Publishing Group.

HAWKINS, P.T. & STEPHENS, L.R. (2016) Emerging evidence of signalling roles for PI(3,4)P-2 in Class I and II PI3K-regulated pathways. *Biochemical Society Transactions* **44**, 307–314. Portland Press Limited.

HEDSTROM, K.L., OGAWA, Y. & RASBAND, M.N. (2008) AnkyrinG is required for maintenance of the axon initial segment and neuronal polarity. *The Journal of Cell Biology* **183**, 635–640. Rockefeller Univ Press.

HEDSTROM, K.L., XU, X., OGAWA, Y., FRISCHKNECHT, R., SEIDENBECHER, C.I., SHRAGER, P. & RASBAND, M.N. (2007) Neurofascin assembles a specialized extracellular matrix at the axon initial segment. *The Journal of Cell Biology* **178**, 875–886. Rockefeller Univ Press.

HEINTZ, T.G., EVA, R. & FAWCETT, J.W. (2016) Regional Regulation of Purkinje Cell Dendritic Spines by Integrins and Eph/Ephrins. *PloS one* **11**, e0158558–15. Public Library of Science.

HELLSTRÖM, M., RUITENBERG, M.J., POLLETT, M.A., EHLERT, E.M.E., TWISK, J., VERHAAGEN, J. & HARVEY, A.R. (2009) Cellular tropism and transduction properties of seven adeno-associated viral vector serotypes in adult retina after intravitreal injection. *Gene therapy* **16**, 521–532. Nature Publishing Group.

HERMAN, P.K. (1990) Characterization of Vps34, a Gene Required for Vacuolar Protein Sorting and Vacuole Segregation in Saccharomyces-Cerevisiae. *Molecular and Cellular Biology* **10**, 6742–6754. American Society for Microbiology (ASM).

HERNANDEZ, M.R. (2000) The optic nerve head in glaucoma: Role of astrocytes in tissue remodeling. *Progress in Retinal and Eye Research* **19**, 297–321.

HERNÁNDEZ-DEVIEZ, D.J., ROTH, M.G., CASANOVA, J.E. & WILSON, J.M. (2004) ARNO and ARF6 regulate axonal elongation and branching through downstream activation of phosphatidylinositol 4-phosphate 5-kinase alpha. *Molecular biology of the cell* **15**, 111–120. American Society for Cell Biology.

HICKMAN, S.E., KINGERY, N.D., OHSUMI, T.K., BOROWSKY, M.L., WANG, L.-C., MEANS, T.K. & KHOURY, EL, J. (2013) The microglial sensome revealed by direct RNA sequencing. *Nature neuroscience* **16**, 1896–1905. Nature Publishing Group.

HILLE, F., RICHTER, H., WONG, S.P., BRATOVIČ, M., RESSEL, S. & CHARPENTIER, E. (2018) The Biology of CRISPR-Cas: Backward and Forward. *Cell* **172**, 1239–1259.

HINES, J.H., ABU-RUB, M. & HENLEY, J.R. (2010) Asymmetric endocytosis and remodeling of beta1-integrin adhesions during growth cone chemorepulsion by MAG. *Nature neuroscience* **13**, 829–837.

HOL, E.M. & PEKNY, M. (2015) Glial fibrillary acidic protein (GFAP) and the astrocyte intermediate filament system in diseases of the central nervous system. *Current opinion in cell biology* **32**, 121–130. Elsevier Current Trends.

HOLLIS, E.R. (2015) Axon Guidance Molecules and Neural Circuit Remodeling After Spinal Cord Injury. *Neurotherapeutics : the journal of the American Society for Experimental NeuroTherapeutics*, 1–10. Springer US.

HOLLIS, E.R., II, LU, P., BLESCH, A. & TUSZYNSKI, M.H. (2009a) IGF-I gene delivery promotes corticospinal neuronal survival but not regeneration after adult CNS injury. *Experimental neurology* **215**, 53–59.

HOLLIS, E.R., JAMSHIDI, P., LÖW, K., BLESCH, A. & TUSZYNSKI, M.H. (2009b) Induction of corticospinal regeneration by lentiviral trkB-induced Erk activation. *Proceedings of the National Academy of Sciences of the United States of America* **106**, 7215–7220. National Acad Sciences.

HON, W.-C., BERNDT, A. & WILLIAMS, R.L. (2012) Regulation of lipid binding underlies the activation mechanism of class IA PI3-kinases. *Oncogene* **31**, 3655–3666. Nature Publishing Group.

HORTON, E.R., BYRON, A., ASKARI, J.A., NG, D.H.J., MILLON-FRÉMILLON, A., ROBERTSON, J., KOPER, E.J., PAUL, N.R., WARWOOD, S., KNIGHT, D., HUMPHRIES, J.D. & HUMPHRIES, M.J. (2015) Definition of a consensus integrin adhesome and its dynamics during adhesion complex assembly and disassembly. *Nature cell biology* **17**, 1577–1587. Nature Publishing Group.

HU, F. & STRITTMATTER, S.M. (2008) The N-terminal domain of Nogo-A inhibits cell adhesion and axonal outgrowth by an integrin-specific mechanism. *The Journal of Neuroscience* **28**, 1262–1269. Society for Neuroscience.

HU, P. & LUO, B.-H. (2013) Integrin bi-directional signaling across the plasma membrane. *Journal of cellular physiology* **228**, 306–312. Wiley Subscription Services, Inc., A Wiley Company.

HUANG, C.Y.-M. & RASBAND, M.N. (2018) Axon initial segments: structure, function, and disease. *Annals of the New York Academy of Sciences* **38**, 193. Wiley/Blackwell (10.1111).

HUANG, C.Y.-M., ZHANG, C., HO, T.S.-Y., OSES-PRIETO, J., BURLINGAME, A.L., LALONDE, J., NOEBELS, J.L., LETERRIER, C. & RASBAND, M.N. (2017a) αII spectrin forms a periodic cytoskeleton at the axon initial segment and is required for nervous system function. *The Journal of Neuroscience*, 2112–2117. Society for Neuroscience.

HUANG, C.Y.-M., ZHANG, C., ZOLLINGER, D.R., LETERRIER, C. & RASBAND, M.N. (2017b) An αII spectrin based cytoskeleton protects large diameter Myelinated axons from degeneration. *The Journal of Neuroscience*, 2113–2117. Society for Neuroscience.

HUANG, L.-Y., HALDER, S. & AGBANDJE-MCKENNA, M. (2014) Parvovirus glycan interactions. *Current opinion in virology* **7**, 108–118.

HUANG, Z., SHIMAZU, K., WOO, N.H., ZANG, K., MÜLLER, U., LU, B. & REICHARDT, L.F. (2006) Distinct roles of the beta 1-class integrins at the developing and the mature hippocampal excitatory synapse. *The Journal of Neuroscience* **26**, 11208–11219. Society for Neuroscience.

HUMPHRIES, J.D. (2006) Integrin ligands at a glance. *Journal of Cell Science* **119**, 3901–3903. The Company of Biologists Ltd.

HUMPHRIES, J.D., PAUL, N.R., HUMPHRIES, M.J. & MORGAN, M.R. (2015) Emerging properties of adhesion complexes: what are they and what do they do? *Trends in Cell Biology* **25**, 388–397.

HUO, Y., YIN, X.-L., JI, S.-X., ZOU, H., LANG, M., ZHENG, Z., CAI, X.-F., LIU, W., CHEN, C.-L., ZHOU, Y.-G., YUAN, R.-D. & YE, J. (2015) Amino-Nogo Inhibits Optic Nerve Regeneration and Functional Recovery via the Integrin αv Signaling Pathway in Rats. *Cellular Physiology and Biochemistry* **35**, 616–626. Karger Publishers.

HUR, E.-M., SAIJILAFU & ZHOU, F.-Q. (2012) Growing the growth cone: remodeling the cytoskeleton to promote axon regeneration. *Trends in neurosciences* **35**, 164–174.

HUTSON, T.H., KATHE, C. & MOON, L.D.F. (2015) Trans-neuronal transduction of spinal neurons following cortical injection and anterograde axonal transport of a bicistronic AAV1 vector. *Gene therapy*, 1–6.

HUTSON, T.H., VERHAAGEN, J., YÁÑEZ-MUÑOZ, R.J. & MOON, L.D.F. (2012) Corticospinal tract transduction: a comparison of seven adeno-associated viral vector serotypes and a non-integrating lentiviral vector. *Gene therapy* **19**, 49–60. Nature Publishing Group.

HYNES, R.O. (2002) Integrins: bidirectional, allosteric signaling machines. *Cell* **110**, 673–687.

INUKAI, S., KOCK, K.H. & BULYK, M.L. (2017) Transcription factor-DNA binding: beyond binding site motifs. **43**, 110–119.

ISABET, T., MONTAGNAC, G., REGAZZONI, K., RAYNAL, B., KHADALI, EL, F., ENGLAND, P., FRANCO, M., CHAVRIER, P., HOUDUSSE, A. & MÉNÉTREY, J. (2009) The structural basis of Arf effector specificity: the crystal structure of ARF6 in a complex with JIP4. *The EMBO journal* **28**, 2835–2845.

ISHINO, Y., SHINAGAWA, H., MAKINO, K., AMEMURA, M. & NAKATA, A. (1987) Nucleotide sequence of the iap gene, responsible for alkaline phosphatase isozyme conversion in Escherichia coli, and identification of the gene product. *Journal of bacteriology* **169**, 5429–5433. American Society for Microbiology (ASM).

IVINS, J.K., COLOGNATO, H., KREIDBERG, J.A., YURCHENCO, P.D. & LANDER, A.D. (1998) Neuronal receptors mediating responses to antibodyactivated laminin-1. *Journal of Neuroscience* **18**, 9703–9715. Society for Neuroscience.

IVINS, J.K., YURCHENCO, P.D. & LANDER, A.D. (2000) Regulation of neurite outgrowth by integrin activation. *Journal of Neuroscience* **20**, 6551–6560. Society for Neuroscience.

JACKSON, K.L., DAYTON, R.D. & KLEIN, R.L. (2015) AAV9 supports wide-scale transduction of the CNS and TDP-43 disease modeling in adult rats. *Molecular therapy. Methods & clinical development* **2**.

JACKSON, T.R., BROWN, F.D., NIE, Z.Z., MIURA, K., FORONI, L., SUN, J.L., HSU, V.W., DONALDSON, J.G. & RANDAZZO, P.A. (2000) ACAPs are Arf6 GTPase-activating proteins that function in the cell periphery. *Journal of Cell Biology* **151**, 627–638. The Rockefeller University Press.

JANSEN, R., VAN EMBDEN, J., GAASTRA, W. & SCHOULS, L.M. (2002) Identification of genes that are associated with DNA repeats in prokaryotes. *Molecular Microbiology* **43**, 1565–1575.

JENKINS, P.M., KIM, N., JONES, S.L., TSENG, W.C., SVITKINA, T.M., YIN, H.H. & BENNETT, V. (2014) Giant ankyrin-G: A critical innovation in vertebrate evolution of fast and integrated neuronal signaling. *Proceedings of the National Academy of Sciences of the United States of America*, 201416544. National Acad Sciences.

JENKINS, S.M. & BENNETT, V. (2001) Ankyrin-G coordinates assembly of the spectrin-based membrane skeleton, voltage-gated sodium channels, and L1 CAMs at Purkinje neuron initial segments. *The Journal of Cell Biology* **155**, 739–746. Rockefeller Univ Press.

JESSEN, K.R., MIRSKY, R. & ARTHUR-FARRAJ, P. (2015) The Role of Cell Plasticity in Tissue Repair: Adaptive Cellular Reprogramming. *Developmental cell* **34**, 613–620.

JONQUIERES, VON, G., FROHLICH, D., KLUGMANN, C.B., WEN, X., HARASTA, A.E., RAMKUMAR, R., SPENCER, Z.H.T., HOUSLEY, G.D. & KLUGMANN, M. (2016) Recombinant Human Myelin-Associated Glycoprotein Promoter Drives Selective AAV-Mediated Transgene Expression in Oligodendrocytes. *Frontiers in molecular neuroscience* **9**, 2136. Frontiers.

JONQUIERES, VON, G., MERSMANN, N., KLUGMANN, C.B., HARASTA, A.E., LUTZ, B., TEAHAN, O., HOUSLEY, G.D., FROHLICH, D., KRAMER-ALBERS, E.-M. & KLUGMANN, M. (2013) Glial Promoter Selectivity following AAV-Delivery to the Immature Brain. *PloS one* **8**. Public Library of Science.

KALUDOV, N., BROWN, K.E., WALTERS, R.W., ZABNER, J. & CHIORINI, J.A. (2001) Adeno-associated virus serotype 4 (AAV4) and AAV5 both require sialic acid binding for hemagglutination and efficient transduction but differ in sialic acid linkage specificity. *Journal of virology* **75**, 6884–6893. American Society for Microbiology.

KAMINSKY, P.M., KEISER, N.W., YAN, Z., LEI-BUTTERS, D.C.M. & ENGELHARDT, J.F. (2012) Directing integrin-linked endocytosis of recombinant AAV enhances productive FAK-dependent transduction. *Molecular therapy : the journal of the American Society of Gene Therapy* **20**, 972–983.

KANEKO, S., IWANAMI, A., NAKAMURA, M., KISHINO, A., KIKUCHI, K., SHIBATA, S., ET AL. (2006) A selective Sema3A inhibitor enhances regenerative responses and functional recovery of the injured spinal cord. *Nature medicine* **12**, 1380–1389.

KANG, W.-S., CHOI, J.-S., SHIN, Y.-J., KIM, H.-Y., CHA, J.-H., LEE, J.-Y., CHUN, M.-H. & LEE, M.-Y. (2008) Differential regulation of osteopontin receptors, CD44 and the alpha(v) and beta(3) integrin subunits, in the rat hippocampus following transient forebrain ischemia. *Brain research* **1228**, 208–216.

KASHIWAGI, H., SHIRAGA, M., KATO, H., KAMAE, T., YAMAMOTO, N., TADOKORO, S., KURATA, Y., TOMIYAMA, Y. & KANAKURA, Y. (2005) Negative regulation of platelet function by a secreted cell repulsive protein, semaphorin 3A. *Blood* **106**, 913–921.

KAWAGUCHI, S.-Y. & HIRANO, T. (2006) Integrin alpha3beta1 suppresses long-term potentiation at inhibitory synapses on the cerebellar Purkinje neuron. *Molecular and cellular neurosciences* **31**, 416–426.

KAZANIS, I. & FFRENCH-CONSTANT, C. (2011) Extracellular matrix and the neural stem cell niche. *Developmental neurobiology* **71**, 1006–1017. Wiley Subscription Services, Inc., A Wiley Company.

KEELY, P.J., RUSYN, E.V., COX, A.D. & PARISE, L.V. (1999) R-Ras signals through specific integrin alpha cytoplasmic domains to promote migration and invasion of breast epithelial cells. *Journal of Cell Biology* **145**, 1077–1088. Rockefeller Univ Press.

KEISER, N.W., YAN, Z., ZHANG, Y., LEI-BUTTERS, D.C.M. & ENGELHARDT, J.F. (2011) Unique characteristics of AAV1, 2, and 5 viral entry, intracellular trafficking, and nuclear import define transduction efficiency in HeLa cells. *Human Gene Therapy* **22**, 1433–1444. Mary Ann Liebert, Inc. 140 Huguenot Street, 3rd Floor New Rochelle, NY 10801 USA.

KERN, A., SCHMIDT, K., LEDER, C., MÜLLER, O.J., WOBUS, C.E., BETTINGER, K., LIETH, VON DER, C.W., KING, J.A. & KLEINSCHMIDT, J.A. (2003) Identification of a heparin-binding motif on adeno-associated virus type 2 capsids. *Journal of virology* **77**, 11072–11081. American Society for Microbiology (ASM).

KHALSA, P.S., ZHANG, C., SOMMERFELDT, D. & HADJIARGYROU, M. (2000) Expression of integrin alpha2beta1 in axons and receptive endings of neurons in rat, hairy skin. *Neuroscience Letters* **293**, 13–16.

KHODR, C.E., SAPRU, M.K., PEDAPATI, J., HAN, Y., WEST, N.C., KELLS, A.P., BANKIEWICZ, K.S. & BOHN, M.C. (2011) An α-synuclein AAV gene silencing vector ameliorates a behavioral deficit in a rat model of Parkinson's disease, but displays toxicity in dopamine neurons. *Brain research* **1395**, 94–107.

KIKKAWA, Y., SANZEN, N. & SEKIGUCHI, K. (1998) Isolation and characterization of laminin-10/11 secreted by human lung carcinoma cells. laminin-10/11 mediates cell adhesion through integrin alpha3 beta1. *The Journal of biological chemistry* **273**, 15854–15859. American Society for Biochemistry and Molecular Biology.

KIM, H. & KIM, J.-S. (2014) A guide to genome engineering with programmable nucleases. *Nature Reviews Genetics* **15**, 321–334. Nature Publishing Group.

KIM, J., YANG, C., KIM, E.J., JANG, J., KIM, S.-J., KANG, S.M., KIM, M.G., JUNG, H., PARK, D. & KIM, C. (2016) Vimentin filaments regulate integrin-ligand interactions by binding to the cytoplasmic tail of integrin β3. *Journal of Cell Science*, jcs.180315. The Company of Biologists Ltd.

KIM, J.-E., LI, S., GRANDPRÉ, T., QIU, D. & STRITTMATTER, S.M. (2003) Axon Regeneration in Young Adult Mice Lacking Nogo-A/B. *Neuron* **38**, 187–199.

KING, V.R., MCBRIDE, A. & PRIESTLEY, J.V. (2001) Immunohistochemical expression of the alpha 5 integrin subunit in the normal adult rat central nervous system. *Journal of neurocytology* **30**, 243–252. Kluwer Academic Publishers.

KITA, Y., KIMURA, K.D., KOBAYASHI, M., IHARA, S., KAIBUCHI, K., KURODA, S., UI, M., IBA, H., KONISHI, H., KIKKAWA, U., NAGATA, S. & FUKUI, Y. (1998) Microinjection of activated phosphatidylinositol-3 kinase induces process outgrowth in rat PC12 cells through the Rac-JNK signal transduction pathway. *Journal of Cell Science* **111**, 907–915.

KLOSS, C.U.A., WERNER, A., KLEIN, M.A., SHEN, J., MENUZ, K., PROBST, J.C., KREUTZBERG, G.W. & RAIVICH, G. (1999) Integrin family of cell adhesion molecules in the injured brain: Regulation and cellular localization in the normal and regenerating mouse facial motor nucleus. *Journal of Comparative Neurology* **411**, 162–178. John Wiley & Sons, Inc.

KOBAYASHI, M., NAGATA, S., KITA, Y., NAKATSU, N., IHARA, S., KAIBUCHI, K., KURODA, S., UI, M., IBA, H., KONISHI, H., KIKKAWA, U., SAITOH, I. & FUKUI, Y. (1997) Expression of a Constitutively Active Phosphatidylinositol 3-Kinase Induces Process Formation in Rat PC12 Cells USE OF Cre/loxP RECOMBINATION SYSTEM. *The Journal of biological chemistry* **272**, 16089–16092. American Society for Biochemistry and Molecular Biology.

KOH, W., PARK, Y.M., LEE, S.E. & LEE, C.J. (2017) AAV-Mediated Astrocyte-Specific Gene Expression under Human ALDH1L1 Promoter in Mouse Thalamus. *Experimental Neurobiology* **26**, 350–361.

KOLE, M.H.P., ILSCHNER, S.U., KAMPA, B.M., WILLIAMS, S.R., RUBEN, P.C. & STUART, G.J. (2008) Action potential generation requires a high sodium channel density in the axon initial segment. *Nature neuroscience* **11**, 178–186. Nature Publishing Group.

KOOPMANS, G., HASSE, B. & SINIS, N. (2009) Chapter 19 The Role of Collagen in Peripheral Nerve Repair. In pp. 363–379. Elsevier.

KORECKA, J., ULUSOY, A., VERHAAGEN, J. & BOSSERS, K. (2011) *Comparison of AAV serotypes for gene delivery to dopaminergic neurons in the substantia nigra*.

KOSEKI, H., DONEGÁ, M., LAM, B.Y., PETROVA, V., VAN ERP, S., YEO, G.S., KWOK, J.C., FFRENCH-CONSTANT, C., EVA, R. & FAWCETT, J. (2017) Selective Rab11 transport and the intrinsic regenerative ability of CNS axons. *eLife* **6**, e26956. eLife Sciences Publications Limited.

KREIS, P., LEONDARITIS, G., LIEBERAM, I. & EICKHOLT, B.J. (2014) Subcellular targeting and dynamic regulation of PTEN: implications for neuronal cells and neurological disorders. *Frontiers in molecular neuroscience* **7**, 23. Frontiers.

KUCHER, K., JOHNS, D., MAIER, D., ABEL, R., BADKE, A., BARON, H., THIETJE, R., CASHA, S., MEINDL, R., GOMEZ-MANCILLA, B., PFISTER, C., RUPP, R., WEIDNER, N., MIR, A., SCHWAB, M.E. & CURT, A. (2018) First-in-Man Intrathecal Application of Neurite Growth-Promoting Anti-Nogo-A Antibodies in Acute Spinal Cord Injury. *Neurorehabilitation and neural repair* **32**, 578–589. SAGE PublicationsSage CA: Los Angeles, CA.

KUIJPERS, M., VAN DE WILLIGE, D., FREAL, A., CHAZEAU, A., FRANKER, M.A., HOFENK, J., RODRIGUES, R.J.C., KAPITEIN, L.C., AKHMANOVA, A., JAARSMA, D. & HOOGENRAAD, C.C. (2016) Dynein Regulator NDEL1 Controls Polarized Cargo Transport at the Axon Initial Segment. *Neuron* **89**, 461–471. Elsevier Ltd.

KÜGLER, S., KILIC, E. & BÄHR, M. (2003) Human synapsin 1 gene promoter confers highly neuron-specific long-term transgene expression from an adenoviral vector in the adult rat brain depending on the transduced area. *Gene therapy* **10**, 337–347. Nature Publishing Group.

KWOK, J.C.F., DICK, G., WANG, D. & FAWCETT, J.W. (2011) Extracellular matrix and perineuronal nets in CNS repair. *Developmental neurobiology* **71**, 1073–1089. Wiley Subscription Services, Inc., A Wiley Company.

KWON, I.-S., LEE, K.-H., CHOI, J.W. & AHN, J.-Y. (2010) PI(3,4,5)P3 regulates the interaction between Akt and B23 in the nucleus. *BMB reports* **43**, 127–132.

LABELLE, C. & LECLERC, N. (2000) Exogenous BDNF, NT-3 and NT-4 differentially regulate neurite outgrowth in cultured hippocampal neurons. *Brain research. Developmental brain research* **123**, 1–11.

LAI-CHEONG, J.E., USSAR, S., ARITA, K., HART, I.R. & MCGRATH, J.A. (2008) Colocalization of kindlin-1, kindlin-2, and migfilin at keratinocyte focal adhesion and relevance to the pathophysiology of Kindler syndrome. *The Journal of investigative dermatology* **128**, 2156–2165.

LANG, C., BRADLEY, P.M., JACOBI, A., KERSCHENSTEINER, M. & BAREYRE, F.M. (2013) STAT3 promotes corticospinal remodelling and functional recovery after spinal cord injury. *EMBO reports* **14**, 931–937. EMBO Press.

LASIECKA, Z.M. & WINCKLER, B. (2011) Mechanisms of polarized membrane trafficking in neurons — Focusing in on endosomes. *Molecular and Cellular Neuroscience* **48**, 278–287.

LAURÉN, J., HU, F., CHIN, J., LIAO, J., AIRAKSINEN, M.S. & STRITTMATTER, S.M. (2007) Characterization of myelin ligand complexes with neuronal Nogo-66 receptor family members. *The Journal of biological chemistry* **282**, 5715–5725. American Society for Biochemistry and Molecular Biology.

LAWLOR, P.A., BLAND, R.J., MOURAVLEV, A., YOUNG, D. & DURING, M.J. (2009) Efficient Gene Delivery and Selective Transduction of Glial Cells in the Mammalian Brain by AAV Serotypes Isolated From Nonhuman Primates. *Molecular therapy : the journal of the American Society of Gene Therapy* **17**, 1692–1702.

LAZO, O.M., GONZALEZ, A., ASCAÑO, M., KURUVILLA, R., COUVE, A. & BRONFMAN, F.C. (2013) BDNF Regulates Rab11-Mediated Recycling Endosome Dynamics to Induce Dendritic Branching. *Journal of Neuroscience* **33**, 6112–6122. Society for Neuroscience.

LE BRAS, B., FREAL, A., CZARNECKI, A., LEGENDRE, P., BULLIER, E., KOMADA, M., BROPHY, P.J., DAVENNE, M. & COURAUD, F. (2014) In vivo assembly of the axon initial segment in motor neurons. *Brain structure & function* **219**, 1433–1450. Springer Berlin Heidelberg.

LEE, C.-C., HUANG, C.-C. & HSU, K.-S. (2011) Insulin promotes dendritic spine and synapse formation by the PI3K/Akt/mTOR and Rac1 signaling pathways. *Neuropharmacology* **61**, 867–879.

LEE, J.K., CHOW, R., XIE, F., CHOW, S.Y., TOLENTINO, K.E. & ZHENG, B. (2010a) Combined genetic attenuation of myelin and semaphorin-mediated growth inhibition is insufficient to promote serotonergic axon regeneration. *The Journal of Neuroscience* **30**, 10899–10904. Society for Neuroscience.

LEE, J.K., GEOFFROY, C.G., CHAN, A.F., TOLENTINO, K.E., CRAWFORD, M.J., LEAL, M.A., KANG, B. & ZHENG, B. (2010b) Assessing spinal axon regeneration and sprouting in Nogo-, MAG-, and OMgp-deficient mice. *Neuron* **66**, 663–670. Elsevier.

LEFCORT, F., VENSTROM, K., MCDONALD, J.A. & REICHARDT, L.F. (1992) Regulation of expression of fibronectin and its receptor, alpha 5 beta 1, during development and regeneration of peripheral nerve. *Development* **116**, 767–782. NIH Public Access.

LEIN, P., GALLAGHER, P.J., AMODEO, J., HOWIE, H. & ROTH, J.A. (2000) Manganese induces neurite outgrowth in PC12 cells via upregulation of αv integrins. *Brain research* **885**, 220–230.

LEMONS, M.L. & CONDIC, M.L. (2006) Combined integrin activation and intracellular cAMP cause Rho GTPase dependent growth cone collapse on laminin-1. *Experimental neurology* **202**, 324–335.

LEMONS, M.L., SANDY, J.D., ANDERSON, D.K. & HOWLAND, D.R. (2003) Intact aggrecan and chondroitin sulfate-depleted aggrecan core glycoprotein inhibit axon growth in the adult rat spinal cord. *Experimental neurology* **184**, 981–990.

LEON, S., YIN, Y.Q., NGUYEN, J., IRWIN, N. & BENOWITZ, L.I. (2000) Lens injury stimulates axon regeneration in the mature rat optic nerve. *Journal of Neuroscience* **20**, 4615–4626.

LEONE, D.P., RELVAS, J.B., CAMPOS, L.S., HEMMI, S., BRAKEBUSCH, C., FÄSSLER, R., FFRENCH-CONSTANT, C. & SUTER, U. (2005) Regulation of neural progenitor proliferation and survival by beta1 integrins. *Journal of Cell Science* **118**, 2589–2599. The Company of Biologists Ltd.

LETERRIER, C. (2018) The Axon Initial Segment: An Updated Viewpoint. *The Journal of Neuroscience* **38**, 2135–2145. Society for Neuroscience.

LEVY, A.D., OMAR, M.H. & KOLESKE, A.J. (2014) Extracellular matrix control of dendritic spine and synapse structure and plasticity in adulthood. *Frontiers in neuroanatomy* **8**, 116. Frontiers.

LEWANDOWSKI, G. & STEWARD, O. (2014) AAVshRNA-Mediated Suppression of PTEN in Adult Rats in Combination with Salmon Fibrin Administration Enables Regenerative Growth of Corticospinal Axons and Enhances Recovery of Voluntary Motor Function after Cervical Spinal Cord Injury. *Journal of Neuroscience* **34**, 9951–9962. Society for Neuroscience.

LEWIS, T.L.J., MAO, T., SVOBODA, K. & ARNOLD, D.B. (2009) Myosin-dependent targeting of transmembrane proteins to neuronal dendrites. *Nature neuroscience* **12**, 568–576. Nature Publishing Group.

LI, J., BALLIF, B.A., POWELKA, A.M., DAI, J., GYGI, S.P. & HSU, V.W. (2005) Phosphorylation of ACAP1 by Akt regulates the stimulation-dependent recycling of integrin beta1 to control cell migration. *Developmental cell* **9**, 663–673.

LI, Q. & BARRES, B.A. (2018) Microglia and macrophages in brain homeostasis and disease. *Nature reviews. Immunology* **18**, 225–242. Nature Publishing Group.

LIEBL, D.J., HUANG, W., YOUNG, W. & PARADA, L.F. (2001) Regulation of Trk receptors following contusion of the rat spinal cord. *Experimental neurology* **167**, 15–26.

LILJA, J., ZACHARCHENKO, T., GEORGIADOU, M., JACQUEMET, G., FRANCESCHI, N.D., PEUHU, E., HAMIDI, H., POUWELS, J., MARTENS, V., NIA, F.H., BEIFUSS, M., BOECKERS, T., KREIENKAMP, H.-J., BARSUKOV, I.L. & IVASKA, J. (2017) SHANK proteins limit integrin activation by directly interacting with Rap1 and R-Ras. *Nature cell biology* **14**, 430. Nature Research.

LIN, L., YAN, F., ZHAO, D., LV, M., LIANG, X., DAI, H., QIN, X., ZHANG, Y., HAO, J., SUN, X., YIN, Y., HUANG, X., ZHANG, J., LU, J. & GE, Q. (2016) Reelin promotes the adhesion and drug resistance of multiple myeloma cells via integrin β1 signaling and STAT3. *Oncotarget* **5**. Impact Journals.

LIU, B.P., FOURNIER, A., GRANDPRÉ, T. & STRITTMATTER, S.M. (2002) Myelin-associated glycoprotein as a functional ligand for the Nogo-66 receptor. *Science (New York, N.Y.)* **297**, 1190–1193. American Association for the Advancement of Science.

LIU, K., LU, Y., LEE, J.K., SAMARA, R., WILLENBERG, R., SEARS-KRAXBERGER, I., TEDESCHI, A., PARK, K.K., JIN, D., CAI, B., XU, B., CONNOLLY, L., STEWARD, O., ZHENG, B. & HE, Z. (2010) PTEN deletion enhances the regenerative ability of adult corticospinal neurons. *Nature neuroscience* **13**, 1075–1081. Nature Publishing Group.

LIU, K., TEDESCHI, A., PARK, K.K. & HE, Z. (2011) Neuronal intrinsic mechanisms of axon regeneration. *Annual review of neuroscience* **34**, 131–152. Annual Reviews.

LIU, Y., WANG, X., LI, W., ZHANG, Q., LI, Y., ZHANG, Z., ZHU, J., CHEN, B., WILLIAMS, P.R., ZHANG, Y., YU, B., GU, X. & HE, Z. (2017) A Sensitized IGF1 Treatment Restores Corticospinal Axon-Dependent Functions. *Neuron* **95**, 817–833.e4.

LONGAIR, M.H., BAKER, D.A. & ARMSTRONG, J.D. (2011) Simple Neurite Tracer: open source software for reconstruction, visualization and analysis of neuronal processes. *Bioinformatics* **27**, 2453–2454.

LOPES, R., KORKMAZ, G. & AGAMI, R. (2016) Applying CRISPR-Cas9 tools to identify and characterize transcriptional enhancers. *Nature Reviews Molecular Cell Biology*. Nature Publishing Group.

LU, P., BLESCH, A. & TUSZYNSKI, M.H. (2001) Neurotrophism without neurotropism: BDNF promotes survival but not growth of lesioned corticospinal neurons. *The Journal of comparative neurology* **436**, 456–470.

MALININ, N.L., ZHANG, L., CHOI, J., CIOCEA, A., RAZORENOVA, O., MA, Y.-Q., PODREZ, E.A., TOSI, M., LENNON, D.P., CAPLAN, A.I., SHURIN, S.B., PLOW, E.F. & BYZOVA, T.V. (2009) A point mutation in KINDLIN3 ablates activation of three integrin subfamilies in humans. *Nature medicine* **15**, 313–318. Nature Publishing Group.

MANDEL, R.J., MARMION, D.J., KIRIK, D., CHU, Y., HEINDEL, C., MCCOWN, T., GRAY, S.J. & KORDOWER, J.H. (2017) Novel oligodendroglial alpha synuclein viral vector models of multiple system atrophy: studies in rodents and nonhuman primates. *Acta neuropathologica communications* **5**. BioMed Central.

MANJUNATH, N., WU, H., SUBRAMANYA, S. & SHANKAR, P. (2009) Lentiviral delivery of short hairpin RNAs. *Advanced drug delivery reviews* **61**, 732–745. Elsevier.

MARCHETTI, G., DE ARCANGELIS, A., PFISTER, V. & GEORGES-LABOUESSE, E. (2013) α6 integrin subunit regulates cerebellar development. *Cell Adhesion & Migration* **7**, 325–332. Taylor & Francis.

MARCHETTI, G., ESCUIN, S., VAN DER FLIER, A., DE ARCANGELIS, A., HYNES, R.O. & GEORGES-LABOUESSE, E. (2010) Integrin alpha5beta1 is necessary for regulation of radial migration of cortical neurons during mouse brain development. *The European journal of neuroscience* **31**, 399–409. Blackwell Publishing Ltd.

MARKAKIS, E.A., VIVES, K.P., BOBER, J., LEICHTLE, S., LERANTH, C., BEECHAM, J., ELSWORTH, J.D., ROTH, R.H., SAMULSKI, R.J. & REDMOND, D.E. (2010) Comparative transduction efficiency of AAV vector serotypes 1-6 in the substantia nigra and striatum of the primate brain. *Molecular therapy : the journal of the American Society of Gene Therapy* **18**, 588–593.

MARKEL, S.F., ANDREWS, A.M., LUTTON, E.M., MU, D., HUDRY, E., HYMAN, B.T., MAGUIRE, C.A. & RAMIREZ, S.H. (2017) Trafficking of adeno-associated virus vectors across a model of the blood-brain barrier; a comparative study of transcytosis and transduction using primary human brain endothelial cells. *Journal of neurochemistry* **140**, 216–230. John Wiley & Sons, Ltd (10.1111).

MARRAFFINI, L.A. & SONTHEIMER, E.J. (2008) CRISPR interference limits horizontal gene transfer in staphylococci by targeting DNA. *Science (New York, N.Y.)* **322**, 1843–1845. American Association for the Advancement of Science.

MARTIN, J.N., WOLKEN, N., BROWN, T., DAUER, W.T., EHRLICH, M.E. & GONZALEZ-ALEGRE, P. (2011) Lethal toxicity caused by expression of shRNA in the mouse striatum: implications for therapeutic design. *Gene therapy* **18**, 666–673. Nature Publishing Group.

MASON, M.R.J., EHLERT, E.M.E., EGGERS, R., POOL, C.W., HERMENING, S., HUSEINOVIC, A., TIMMERMANS, E., BLITS, B. & VERHAAGEN, J. (2010) Comparison of AAV Serotypes for Gene Delivery to Dorsal Root Ganglion Neurons. *Molecular therapy : the journal of the American Society of Gene Therapy* **18**, 715–724. Nature Publishing Group.

MATHEWS, G.A. & FFRENCH-CONSTANT, C. (1995) Embryonic fibronectins are up-regulated following peripheral nerve injury in rats. *Journal of neurobiology* **26**, 171–188. Wiley Subscription Services, Inc., A Wiley Company.

MCCARTY, J.H., LACY-HULBERT, A., CHAREST, A., BRONSON, R.T., CROWLEY, D., HOUSMAN, D., SAVILL, J., ROES, J. & HYNES, R.O. (2005) Selective ablation of alpha v integrins in the central nervous system leads to cerebral hemorrhage, seizures, axonal degeneration and premature death. *Development* **132**, 165–176. The Company of Biologists Ltd.

MCFARLAND, N.R., LEE, J.-S., HYMAN, B.T. & MCLEAN, P.J. (2009) Comparison of transduction efficiency of recombinant AAV serotypes 1, 2, 5, and 8 in the rat nigrostriatal system. *Journal of neurochemistry* **109**, 838–845. Wiley/Blackwell (10.1111).

McGeachie, A.B., Cingolani, L.A. & Goda, Y. (2011) Stabilising influence: integrins in regulation of synaptic plasticity. *Neuroscience research* **70**, 24–29.

McKerracher, L., David, S., Jackson, D.L., Kottis, V., Dunn, R.J. & Braun, P.E. (1994) Identification of myelin-associated glycoprotein as a major myelin-derived inhibitor of neurite growth. *Neuron* **13**, 805–811.

McLean, J.R., Smith, G.A., Rocha, E.M., Hayes, M.A., Beagan, J.A., Hallett, P.J. & Isacson, O. (2014) Widespread neuron-specific transgene expression in brain and spinal cord following synapsin promoter-driven AAV9 neonatal intracerebroventricular injection. *Neuroscience Letters* **576**, 73–78. Elsevier Ireland Ltd.

Means, T.K. & Luster, A.D. (2010) Integrins limit the Toll. *Nature immunology* **11**, 691–693. Nature Publishing Group.

Mechai, N., Wenzel, M., Koch, M., Lucka, L., Horstkorte, R., Reutter, W. & Danker, K. (2005) The cytoplasmic tail of the alpha3 integrin subunit promotes neurite outgrowth in PC12 cells. *Journal of neuroscience research* **82**, 753–761. Wiley Subscription Services, Inc., A Wiley Company.

Mecollari, V., **Nieuwenhuis, B**. & Verhaagen, J. (2014) A perspective on the role of class III semaphorin signaling in central nervous system trauma, 1–17.

Meller, J., Chen, Z., Dudiki, T., Cull, R.M., Murtazina, R., Bal, S.K., Pluskota, E., Stefl, S., Plow, E.F., Trapp, B.D. & Byzova, T.V. (2017) Integrin-Kindlin3 requirements for microglial motility in vivo are distinct from those for macrophages. *JCI insight* **2**. American Society for Clinical Investigation.

Mercado, M.L.T., Nur-e-Kamal, A., Liu, H.-Y., Gross, S.R., Movahed, R. & Meiners, S. (2004) Neurite outgrowth by the alternatively spliced region of human tenascin-C is mediated by neuronal alpha7beta1 integrin. *The Journal of Neuroscience* **24**, 238–247. Society for Neuroscience.

Mi, S., Lee, X., Shao, Z., Thill, G., Ji, B., Relton, J., Levesque, M., Allaire, N., Perrin, S., Sands, B., Crowell, T., Cate, R.L., McCoy, J.M. & Pepinsky, R.B. (2004) LINGO-1 is a component of the Nogo-66 receptor/p75 signaling complex. *Nature neuroscience* **7**, 221–228. Nature Publishing Group.

Mietzsch, M., Broecker, F., Reinhardt, A., Seeberger, P.H. & Heilbronn, R. (2014) Differential adeno-associated virus serotype-specific interaction patterns with synthetic heparins and other glycans. *Journal of virology* **88**, 2991–3003. American Society for Microbiology Journals.

Miller, M.W. (1987) The origin of corticospinal projection neurons in rat. *Experimental brain research* **67**, 339–351.

Milner, R. & Campbell, I.L. (2002) The integrin family of cell adhesion molecules has multiple functions within the CNS. *Journal of neuroscience research* **69**, 286–291. Wiley Subscription Services, Inc., A Wiley Company.

Minichiello, L. (2009) TrkB signalling pathways in LTP and learning. *Nature reviews. Neuroscience* **10**, 850–860. Nature Publishing Group.

MINOR, K.H., BOURNAT, J.C., TOSCANO, N., GIGER, R.J. & DAVIES, S.J.A. (2011) Decorin, erythroblastic leukaemia viral oncogene homologue B4 and signal transducer and activator of transcription 3 regulation of semaphorin 3A in central nervous system scar tissue. *Brain : a journal of neurology* **134**, 1140–1155. Oxford University Press.

MIRE, E., THOMASSET, N., JAKEMAN, L.B. & ROUGON, G. (2008) Modulating Sema3A signal with a L1 mimetic peptide is not sufficient to promote motor recovery and axon regeneration after spinal cord injury. *Molecular and cellular neurosciences* **37**, 222–235.

MITRA, S.K., HANSON, D.A. & SCHLAEPFER, D.D. (2005) Focal adhesion kinase: in command and control of cell motility. *Nature Reviews Molecular Cell Biology* **6**, 56–68. Nature Publishing Group.

MOJICA, F., DIEZ-VILLASENOR, C., GARCIA-MARTINEZ, J. & SORIA, E. (2005) Intervening sequences of regularly spaced prokaryotic repeats derive from foreign genetic elements. *Journal of Molecular Evolution* **60**, 174–182. Springer-Verlag.

MONKLEY, S.J., PRITCHARD, C.A. & CRITCHLEY, D.R. (2001) Analysis of the mammalian talin2 gene TLN2. *Biochemical and biophysical research communications* **286**, 880–885.

MONSUL, N.T., GEISENDORFER, A.R., HAN, P.J., BANIK, R., PEASE, M.E., SKOLASKY, R.L. & HOFFMAN, P.N. (2004) Intraocular injection of dibutyryl cyclic AMP promotes axon regeneration in rat optic nerve. *Experimental neurology* **186**, 124–133.

MONTAGNAC, G., DE FORGES, H., SMYTHE, E., GUEUDRY, C., ROMAO, M., SALAMERO, J. & CHAVRIER, P. (2011) Decoupling of activation and effector binding underlies ARF6 priming of fast endocytic recycling. *Current biology : CB* **21**, 574–579. Elsevier.

MOORE, C.B., GUTHRIE, E.H., HUANG, M.T.-H. & TAXMAN, D.J. (2010) Short hairpin RNA (shRNA): design, delivery, and assessment of gene knockdown. *Methods in molecular biology (Clifton, N.J.)* **629**, 141–158. Humana Press, Totowa, NJ.

MORETTI, F.A., MOSER, M., LYCK, R., ABADIER, M., RUPPERT, R., ENGELHARDT, B. & FÄSSLER, R. (2013) Kindlin-3 regulates integrin activation and adhesion reinforcement of effector T cells. *Proceedings of the National Academy of Sciences of the United States of America* **110**, 17005–17010. National Acad Sciences.

MORTILLO, S., ELSTE, A., GE, Y., PATIL, S.B., HSIAO, K., HUNTLEY, G.W., DAVIS, R.L. & BENSON, D.L. (2012) Compensatory redistribution of neuroligins and N-cadherin following deletion of synaptic β1-integrin. *The Journal of comparative neurology* **520**, 2041–2052. Wiley Subscription Services, Inc., A Wiley Company.

MOSER, M., BAUER, M., SCHMID, S., RUPPERT, R., SCHMIDT, S., SIXT, M., WANG, H.-V., SPERANDIO, M. & FÄSSLER, R. (2009a) Kindlin-3 is required for beta2 integrin-mediated leukocyte adhesion to endothelial cells. *Nature medicine* **15**, 300–305. Nature Publishing Group.

MOSER, M., LEGATE, K.R., ZENT, R. & FÄSSLER, R. (2009b) The tail of integrins, talin, and kindlins. *Science (New York, N.Y.)* **324**, 895–899. American Association for the Advancement of Science.

MOSER, M., NIESWANDT, B., USSAR, S., POZGAJOVA, M. & FÄSSLER, R. (2008) Kindlin-3 is essential for integrin activation and platelet aggregation. *Nature medicine* **14**, 325–330. Nature Publishing Group.

MOULD, A.P., AKIYAMA, S.K. & HUMPHRIES, M.J. (1995) Regulation of integrin alpha 5 beta 1-fibronectin interactions by divalent cations. Evidence for distinct classes of binding sites for Mn2+, Mg2+, and Ca2+. *The Journal of biological chemistry* **270**, 26270–26277.

MOULD, A.P., ASKARI, J.A., BYRON, A., TAKADA, Y., JOWITT, T.A. & HUMPHRIES, M.J. (2016) Ligand-induced Epitope Masking: DISSOCIATION OF INTEGRIN α5β1-FIBRONECTIN COMPLEXES ONLY BY MONOCLONAL ANTIBODIES WITH AN ALLOSTERIC MODE OF ACTION. *The Journal of biological chemistry* **291**, 20993–21007. American Society for Biochemistry and Molecular Biology.

MUKHOPADHYAY, G., DOHERTY, P., WALSH, F.S., CROCKER, P.R. & FILBIN, M.T. (1994) A novel role for myelin-associated glycoprotein as an inhibitor of axonal regeneration. *Neuron* **13**, 757–767.

MURASE, S. & HAYASHI, Y. (1996) Expression pattern of integrin beta 1 subunit in Purkinje cells of rat and cerebellar mutant mice. *The Journal of comparative neurology* **375**, 225–237.

MURLIDHARAN, G., SAMULSKI, R.J. & ASOKAN, A. (2014) Biology of adeno-associated viral vectors in the central nervous system. *Frontiers in molecular neuroscience* **7**, 76. Frontiers.

MYERS, J.P., SANTIAGO MEDINA, M. & GOMEZ, T.M. (2011) Regulation of axonal outgrowth and pathfinding by integrin–ecm interactions. *Developmental neurobiology* **71**, 901–923. Wiley Subscription Services, Inc., A Wiley Company.

NAKATA, T., NIWA, S., OKADA, Y., PEREZ, F. & HIROKAWA, N. (2011) Preferential binding of a kinesin-1 motor to GTP-tubulin-rich microtubules underlies polarized vesicle transport. *The Journal of Cell Biology* **194**, 245–255. Rockefeller Univ Press.

NASO, M.F., TOMKOWICZ, B., PERRY, W.L.I. & STROHL, W.R. (2017) Adeno-Associated Virus (AAV) as a Vector for Gene Therapy. *Biodrugs* **31**, 317–334. Springer International Publishing.

NATHANSON, J.L., YANAGAWA, Y., OBATA, K. & CALLAWAY, E.M. (2009) Preferential labeling of inhibitory and excitatory cortical neurons by endogenous tropism of adeno-associated virus and lentivirus vectors. *Neuroscience* **161**, 441–450.

NEAFSEY, E.J., BOLD, E.L., HAAS, G., HURLEY-GIUS, K.M., QUIRK, G., SIEVERT, C.F. & TERREBERRY, R.R. (1986) The organization of the rat motor cortex: a microstimulation mapping study. *Brain research* **396**, 77–96.

NEUMANN, S. & WOOLF, C.J. (1999) Regeneration of dorsal column fibers into and beyond the lesion site following adult spinal cord injury. *Neuron* **23**, 83–91.

NICKELLS, R.W., SCHMITT, H.M., MAES, M.E. & SCHLAMP, C.L. (2017) AAV2-Mediated Transduction of the Mouse Retina After Optic Nerve Injury. *Investigative ophthalmology & visual science* **58**, 6091–6104.

NIEUWENHUIS, B. & EVA, R. (2018a) Linking axon transport to regeneration using in vitro laser axotomy. *Neural regeneration research* **13**, 410–412. Medknow Publications.

NIEUWENHUIS, B. & EVA, R. (2018b) ARF6 and Rab11 as intrinsic regulators of axon regeneration. *Small GTPases*, 1–10. Taylor & Francis.

NIEUWENHUIS, B., HAENZI, B., ANDREWS, M.R., VERHAAGEN, J. & FAWCETT, J.W. (2018) Integrins promote axonal regeneration after injury of the nervous system. *Biological Reviews* **93**, 1339–1362. Wiley/Blackwell (10.1111).

NISHIMURA, S.L., BOYLEN, K.P., EINHEBER, S., MILNER, T.A., RAMOS, D.M. & PYTELA, R. (1998) Synaptic and glial localization of the integrin alphavbeta8 in mouse and rat brain. *Brain research* **791**, 271–282.

NIU, H., CHEN, X., GRUPPO, R.A., LI, D., WANG, Y., ZHANG, L., WANG, K., CHAI, W., SUN, Y., DING, Z., GARTNER, T.K. & LIU, J. (2012) Integrin αIIb-mediated PI3K/Akt activation in platelets. *PloS one* **7**, e47356. Public Library of Science.

OGAWA, Y. & RASBAND, M.N. (2008) The functional organization and assembly of the axon initial segment. *Current Opinion in Neurobiology* **18**, 307–313.

OH, M.S., HONG, S.J., HUH, Y. & KIM, K.-S. (2009) Expression of transgenes in midbrain dopamine neurons using the tyrosine hydroxylase promoter. *Gene therapy* **16**, 437–440. Nature Publishing Group.

OH, Y.M., MAHAR, M., EWAN, E.E., LEAHY, K.M., ZHAO, G. & CAVALLI, V. (2018) Epigenetic regulator UHRF1 inactivates REST and growth suppressor gene expression via DNA methylation to promote axon regeneration. *Proceedings of the National Academy of Sciences of the United States of America* **19**, 201812518–E12426. National Academy of Sciences.

OHSAWA, K., IMAI, Y., SASAKI, Y. & KOHSAKA, S. (2004) Microglia/macrophage-specific protein Iba1 binds to fimbrin and enhances its actin-bundling activity. *Journal of neurochemistry* **88**, 844–856.

OINUMA, I., ITO, Y., KATOH, H. & NEGISHI, M. (2010) Semaphorin 4D/Plexin-B1 stimulates PTEN activity through R-Ras GTPase-activating protein activity, inducing growth cone collapse in hippocampal neurons. *The Journal of biological chemistry* **285**, 28200–28209. American Society for Biochemistry and Molecular Biology.

OJALA, D.S., AMARA, D.P. & SCHAFFER, D.V. (2015) Adeno-associated virus vectors and neurological gene therapy. *The Neuroscientist : a review journal bringing neurobiology, neurology and psychiatry* **21**, 84–98. SAGE Publications.

OPIE, S.R., WARRINGTON, K.H., AGBANDJE-MCKENNA, M., ZOLOTUKHIN, S. & MUZYCZKA, N. (2003) Identification of amino acid residues in the capsid proteins of adeno-associated virus type 2 that contribute to heparan sulfate proteoglycan binding. *Journal of virology* **77**, 6995–7006. American Society for Microbiology (ASM).

OU, D.-L., LEE, B.-S., LIN, L.-I., LIOU, J.-Y., LIAO, S.-C., HSU, C. & CHENG, A.-L. (2014) Vertical blockade of the IGFR-PI3K/Akt/mTOR pathway for the treatment of hepatocellular carcinoma: the role of survivin. *Molecular Cancer* **13**. BioMed Central.

OUDEGA, M. (2012) MOLECULAR AND CELLULAR MECHANISMS UNDERLYING THE ROLE OF BLOOD VESSELS IN SPINAL CORD INJURY AND REPAIR. *CELL AND TISSUE RESEARCH* **349**, 269–288. SPRINGER-VERLAG.

OXVIG, C. & SPRINGER, T.A. (1998) Experimental support for a beta-propeller domain in integrin alpha-subunits and a calcium binding site on its lower surface. *Proceedings of the National Academy of Sciences* **95**, 4870–4875.

OZDINLER, P.H. & MACKLIS, J.D. (2006) IGF-I specifically enhances axon outgrowth of corticospinal motor neurons. *Nature neuroscience* **9**, 1371–1381. Nature Publishing Group.

PALAY, S.L., SOTELO, C., PETERS, A. & ORKAND, P.M. (1968) THE AXON HILLOCK AND THE INITIAL SEGMENT. *Journal of Cell Biology* **38**, 193–201. Rockefeller University Press.

PAN, Z., KAO, T., HORVATH, Z., LEMOS, J., SUL, J.-Y., CRANSTOUN, S.D., BENNETT, V., SCHERER, S.S. & COOPER, E.C. (2006) A common ankyrin-G-based mechanism retains KCNQ and NaV channels at electrically active domains of the axon. *The Journal of Neuroscience* **26**, 2599–2613. Society for Neuroscience.

PAOLILLO, M., SERRA, M. & SCHINELLI, S. (2016) Integrins in glioblastoma: still an attractive target? *Pharmacological research*.

PARK, H. & POO, M.-M. (2013) Neurotrophin regulation of neural circuit development and function. *Nature reviews. Neuroscience* **14**, 7–23. Nature Publishing Group.

PARK, J.B., YIU, G., KANEKO, S., WANG, J., CHANG, J.F. & HE, Z.G. (2005) A TNF receptor family member, TROY, is a coreceptor with Nogo receptor in mediating the inhibitory activity of myelin inhibitors. *Neuron* **45**, 345–351. Elsevier.

PARK, K.K., LIU, K., HU, Y., KANTER, J.L. & HE, Z. (2010) PTEN/mTOR and axon regeneration. *Experimental neurology* **223**, 45–50.

PARK, K.K., LIU, K., HU, Y., SMITH, P.D., WANG, C., CAI, B., XU, B., CONNOLLY, L., KRAMVIS, I., SAHIN, M. & HE, Z. (2008) Promoting axon regeneration in the adult CNS by modulation of the PTEN/mTOR pathway. *Science (New York, N.Y.)* **322**, 963–966. American Association for the Advancement of Science.

PARK, Y.K. & GODA, Y. (2016) Integrins in synapse regulation. *Nature reviews. Neuroscience*. Nature Research.

PASTERKAMP, R.J., GIGER, R.J. & VERHAAGEN, J. (1998) Regulation of semaphorin III/collapsin-1 gene expression during peripheral nerve regeneration. *Experimental neurology* **153**, 313–327.

PASTERKAMP, R.J., GIGER, R.J., RUITENBERG, M.J., HOLTMAAT, A.J., DE WIT, J., DE WINTER, F. & VERHAAGEN, J. (1999) Expression of the gene encoding the chemorepellent semaphorin III is induced in the fibroblast component of neural scar tissue formed following injuries of adult but not neonatal CNS. *Molecular and cellular neurosciences* **13**, 143–166.

PASTERKAMP, R.J., PESCHON, J.J., SPRIGGS, M.K. & KOLODKIN, A.L. (2003) Semaphorin 7A promotes axon outgrowth through integrins and MAPKs. *Nature* **424**, 398–405.

PENG, J., AWAD, A., SAR, S., KOMAIHA, O.H., MOYANO, R., RAYAL, A., SAMUEL, D., SHEWAN, A., VANHAESEBROECK, B., MOSTOV, K. & GASSAMA-DIAGNE, A. (2015) Phosphoinositide 3-kinase p110δ promotes lumen formation through the enhancement of apico-basal polarity and basal membrane organization. *Nature communications* **6**, 5937. Nature Publishing Group.

PERRY, V.H., NICOLL, J.A.R. & HOLMES, C. (2010) Microglia in neurodegenerative disease. *Nature reviews. Neurology* **6**, 193–201.

PETROSYAN, H.A., ALESSI, V., SINGH, V., HUNANYAN, A.S., LEVINE, J.M. & ARVANIAN, V.L. (2014) Transduction efficiency of neurons and glial cells by AAV-1, -5, -9, -rh10 and -hu11 serotypes in rat spinal cord following contusion injury. *Gene therapy* **21**, 991–1000. Nature Publishing Group.

PETROVA, V. & EVA, R. (2018) The Virtuous Cycle of Axon Growth: Axonal Transport of Growth-Promoting Machinery as an Intrinsic Determinant of Axon Regeneration. *Developmental neurobiology* **78**, 898–925.

PIGNATARO, D., SUCUNZA, D., VANRELL, L., LOPEZ-FRANCO, E., DOPESO-REYES, I.G., VALES, A., HOMMEL, M., RICO, A.J., LANCIEGO, J.L. & GONZALEZ-ASEGUINOLAZA, G. (2017) Adeno-Associated Viral Vectors Serotype 8 for Cell-Specific Delivery of Therapeutic Genes in the Central Nervous System. *Frontiers in neuroanatomy* **11**.

PILLAY, S., ZOU, W., CHENG, F., PUSCHNIK, A.S., MEYER, N.L., GANAIE, S.S., DENG, X., WOSEN, J.E., DAVULCU, O., YAN, Z., ENGELHARDT, J.F., BROWN, K.E., CHAPMAN, M.S., QIU, J. & CARETTE, J.E. (2017) AAV serotypes have distinctive interactions with domains of the cellular receptor AAVR. *Journal of virology* **91**, 1239. American Society for Microbiology Journals.

PINKSTAFF, J.K., DETTERICH, J., LYNCH, G. & GALL, C. (1999) Integrin subunit gene expression is regionally differentiated in adult brain. *Journal of Neuroscience* **19**, 1541–1556. Society for Neuroscience.

PLANTMAN, S., NOVIKOVA, L., NOVIKOV, L., HAMMARBERG, H., WALLQUIST, W., KELLERTH, J.-O. & CULLHEIM, S. (2005) Integrin messenger RNAs in the red nucleus after axotomy and neurotrophic administration. *Neuroreport* **16**, 709–713.

PLANTMAN, S., PATARROYO, M., FRIED, K., DOMOGATSKAYA, A., TRYGGVASON, K., HAMMARBERG, H. & CULLHEIM, S. (2008) Integrin-laminin interactions controlling neurite outgrowth from adult DRG neurons in vitro. *Molecular and cellular neurosciences* **39**, 50–62.

POWELKA, A.M., SUN, J., LI, J., GAO, M., SHAW, L.M., SONNENBERG, A. & HSU, V.W. (2004) Stimulation-dependent recycling of integrin beta1 regulated by ARF6 and Rab11. *Traffic (Copenhagen, Denmark)* **5**, 20–36.

QIU, J., CAI, D., DAI, H., MCATEE, M., HOFFMAN, P.N., BREGMAN, B.S. & FILBIN, M.T. (2002) Spinal axon regeneration induced by elevation of cyclic AMP. *Neuron* **34**, 895–903.

QURAISHE, S., FORBES, L.H. & ANDREWS, M.R. (2018) The Extracellular Environment of the CNS: Influence on Plasticity, Sprouting, and Axonal Regeneration after Spinal Cord Injury. *Neural Plasticity* **2018**, –18. Hindawi.

RAN, F.A., CONG, L., YAN, W.X., SCOTT, D.A., GOOTENBERG, J.S., KRIZ, A.J., ZETSCHE, B., SHALEM, O., WU, X., MAKAROVA, K.S., KOONIN, E.V., SHARP, P.A. & ZHANG, F. (2015) In vivo genome editing using Staphylococcus aureus Cas9. *Nature* **520**, 186–191.

RASBAND, M.N. (2010) The axon initial segment and themaintenance of neuronal polarity, 1–11. Nature Publishing Group.

REED, S.E., STALEY, E.M., MAYGINNES, J.P., PINTEL, D.J. & TULLIS, G.E. (2006) Transfection of mammalian cells using linear polyethylenimine is a simple and effective means of producing recombinant adeno-associated virus vectors. *Journal of virological methods* **138**, 85–98.

REN, Y. & SUTER, D.M. (2016) Increase in Growth Cone Size Correlates with Decrease in Neurite Growth Rate. *Neural Plasticity* **2016**, –13. Hindawi.

RICHARDSON, P.M. & ISSA, V.M. (1984) Peripheral injury enhances central regeneration of primary sensory neurones. *Nature* **309**, 791–793.

RIGATO, F., GARWOOD, J., CALCO, V., HECK, N., FAIVRE-SARRAILH, C. & FAISSNER, A. (2002) Tenascin-C promotes neurite outgrowth of embryonic hippocampal neurons through the alternatively spliced fibronectin type IIIBD domains via activation of the cell adhesion molecule F3/contactin. *Journal of Neuroscience* **22**, 6596–6609.

ROBERTSON, J., JACQUEMET, G., BYRON, A., JONES, M.C., WARWOOD, S., SELLEY, J.N., KNIGHT, D., HUMPHRIES, J.D. & HUMPHRIES, M.J. (2015) Defining the phospho-adhesome through the phosphoproteomic analysis of integrin signalling. *Nature communications* **6**, 6265. Nature Publishing Group.

ROBLES, E. & GOMEZ, T.M. (2006) Focal adhesion kinase signaling at sites of integrin-mediated adhesion controls axon pathfinding. *Nature neuroscience* **9**, 1274–1283.

RODGERS, E.E.THEIBERT, AB (2002) Functions of PI 3-kinase in development of the nervous system. *International journal of developmental neuroscience : the official journal of the International Society for Developmental Neuroscience* **20**, 187–197.

RODRIGUEZ, M.A., PESOLD, C., LIU, W.S., KRIHO, V., GUIDOTTI, A., PAPPAS, G.D. & COSTA, E. (2000) Colocalization of integrin receptors and reelin in dendritic spine postsynaptic densities of adult nonhuman primate cortex. *Proceedings of the National Academy of Sciences* **97**, 3550–3555. National Acad Sciences.

ROGNONI, E., RUPPERT, R. & FÄSSLER, R. (2016) The kindlin family: functions, signaling properties and implications for human disease. *Journal of Cell Science* **129**, 17–27. The Company of Biologists Ltd.

ROHRBOUGH, J., GROTEWIEL, M.S., DAVIS, R.L. & BROADIE, K. (2000) Integrin-mediated regulation of synaptic morphology, transmission, and plasticity. *Journal of Neuroscience* **20**, 6868–6878. Society for Neuroscience.

ROMANELLI, R.J., LEBEAU, A.P., FULMER, C.G., LAZZARINO, D.A., HOCHBERG, A. & WOOD, T.L. (2007) Insulin-like growth factor type-I receptor internalization and recycling mediate the sustained phosphorylation of Akt. *The Journal of biological chemistry* **282**, 22513–22524. American Society for Biochemistry and Molecular Biology.

ROSARIO, A.M., CRUZ, P.E., CEBALLOS-DIAZ, C., STRICKLAND, M.R., SIEMIENSKI, Z., PARDO, M., SCHOB, K.-L., LI, A., ASLANIDI, G.V., SRIVASTAVA, A., GOLDE, T.E. & CHAKRABARTY, P. (2016) Microglia-specific targeting by novel capsid- modified AAV6 vectors. *Molecular therapy. Methods & clinical development* **3**.

RUSSELL, S., BENNETT, J., WELLMAN, J.A., CHUNG, D.C., YU, Z.-F., TILLMAN, A., ET AL. (2017) Efficacy and safety of voretigene neparvovec (AAV2-hRPE65v2) in patients with RPE65-mediated inherited retinal dystrophy: a randomised, controlled, open-label, phase 3 trial. *Lancet (London, England)* **390**, 849–860.

SAKAGAMI, H., SUZUKI, H., KAMATA, A., OWADA, Y., FUKUNAGA, K., MAYANAGI, H. & KONDO, H. (2006) Distinct spatiotemporal expression of EFA6D, a guanine nucleotide exchange factor for ARF6, among the EFA6 family in mouse brain. *Brain research* **1093**, 1–11.

SAKAGUCHI, D.S. & RADKE, K. (1996) Beta 1 integrins regulate axon outgrowth and glial cell spreading on a glial-derived extracellular matrix during development and regeneration. *Brain research. Developmental brain research* **97**, 235–250.

SAKURAI, A., GAVARD, J., ANNAS-LINHARES, Y., BASILE, J.R., AMORNPHIMOLTHAM, P., PALMBY, T.R., YAGI, H., ZHANG, F., RANDAZZO, P.A., LI, X., WEIGERT, R. & GUTKIND, J.S. (2010) Semaphorin 3E initiates antiangiogenic signaling through plexin D1 by regulating Arf6 and R-Ras. *Molecular and Cellular Biology* **30**, 3086–3098. American Society for Microbiology.

SAMULSKI, R.J. & MUZYCZKA, N. (2014) AAV-Mediated Gene Therapy for Research and Therapeutic Purposes. *Annual review of virology* **1**, 427–451.

SAMULSKI, R.J., ZHU, X., XIAO, X., BROOK, J.D., HOUSMAN, D.E., EPSTEIN, N. & HUNTER, L.A. (1991) Targeted integration of adeno-associated virus (AAV) into human chromosome 19. *The EMBO journal* **10**, 3941–3950. John Wiley & Sons, Ltd.

SATOH, J.-I., KINO, Y., ASAHINA, N., TAKITANI, M., MIYOSHI, J., ISHIDA, T. & SAITO, Y. (2016) TMEM119 marks a subset of microglia in the human brain. *Neuropathology* **36**, 39–49. John Wiley & Sons, Ltd (10.1111).

SAUNDERS, N.R., NOOR, N.M., DZIEGIELEWSKA, K.M., WHEATON, B.J., LIDDELOW, S.A., STEER, D.L., EK, C.J., HABGOOD, M.D., WAKEFIELD, M.J., LINDSAY, H., TRUETTNER, J., MILLER, R.D., SMITH, A.I. & DIETRICH, W.D. (2014) Age-dependent transcriptome and proteome following transection of neonatal spinal cord of Monodelphis domestica (South American grey short-tailed opossum). *PloS one* **9**, e99080. Public Library of Science.

SCHAFF, M., RECEVEUR, N., BOURDON, C., WURTZ, V., DENIS, C.V., OREND, G., GACHET, C., LANZA, F. & MANGIN, P.H. (2011) Novel function of tenascin-C, a matrix protein relevant to atherosclerosis, in platelet recruitment and activation under flow. *Arteriosclerosis, thrombosis, and vascular biology* **31**, 117–124. Lippincott Williams & Wilkins.

SCHÄFER, M., FRUTTIGER, M., MONTAG, D., SCHACHNER, M. & MARTINI, R. (1996) Disruption of the gene for the myelin-associated glycoprotein improves axonal regrowth along myelin in C57BL/Wlds mice. *Neuron* **16**, 1107–1113.

SCHEYLTJENS, I., LARAMÉE, M.-E., VAN DEN HAUTE, C., GIJSBERS, R., DEBYSER, Z., BAEKELANDT, V., VREYSEN, S. & ARCKENS, L. (2015) Evaluation of the expression pattern of rAAV2/1, 2/5, 2/7, 2/8, and 2/9 serotypes with different promoters in the mouse visual cortex. *Journal of Comparative Neurology* **523**, 2019–2042. John Wiley & Sons, Ltd.

SCHITTENHELM, J., TABATABAI, G. & SIPOS, B. (2016) The role of integrins in primary and secondary brain tumors. *Histology and histopathology*, 117741.

SCHMID, R.S. & ANTON, E.S. (2003) Role of integrins in the development of the cerebral cortex. *Cerebral Cortex* **13**, 219–224.

SCHMITZ, S.K., HJORTH, J.J.J., JOEMAI, R.M.S., WIJNTJES, R., EIJGENRAAM, S., DE BRUIJN, P., GEORGIOU, C., DE JONG, A.P.H., VAN OOYEN, A., VERHAGE, M., CORNELISSE, L.N., TOONEN, R.F. & VELDKAMP, W. (2011) Automated analysis of neuronal morphology, synapse number and synaptic recruitment. *Journal of Neuroscience Methods* **195**, 185–193. Elsevier B.V.

SCHNAPP, L.M., HATCH, N., RAMOS, D.M., KLIMANSKAYA, I.V., SHEPPARD, D. & PYTELA, R. (1995) The Human Integrin Alpha-8-Beta-1 Functions as a Receptor for Tenascin, Fibronectin, and Vitronectin. *The Journal of biological chemistry* **270**, 23196–23202.

SCHNELL, L. & SCHWAB, M.E. (1990) Axonal regeneration in the rat spinal cord produced by an antibody against myelin-associated neurite growth inhibitors. *Nature* **343**, 269–272.

SCHOBER, A.L., GAGARKIN, D.A., CHEN, Y., GAO, G., JACOBSON, L. & MONGIN, A.A. (2016) Recombinant Adeno-Associated Virus Serotype 6 (rAAV6) Potently and Preferentially Transduces Rat Astrocytes In vitro and In vivo. *Frontiers in Cellular Neuroscience* **10**.

SCHÖBER, S., MIELENZ, D., ECHTERMEYER, F., HAPKE, S., PÖSCHL, E., MARK, VON DER, H., MOCH, H. & MARK, VON DER, K. (2000) The Role of Extracellular and Cytoplasmic Splice Domains of α7-Integrin in Cell Adhesion and Migration on Laminins. *Experimental cell research* **255**, 303–313. Academic Press.

SCHULTZ, B.R. & CHAMBERLAIN, J.S. (2008) Recombinant adeno-associated virus transduction and integration. *Molecular therapy : the journal of the American Society of Gene Therapy* **16**, 1189–1199.

SCHUSTER, D.J., DYKSTRA, J.A., RIEDL, M.S., KITTO, K.F., BELUR, L.R., MCIVOR, R.S., ELDE, R.P., FAIRBANKS, C.A. & VULCHANOVA, L. (2014) Biodistribution of adeno-associated virus serotype 9 (AAV9) vector after intrathecal and intravenous delivery in mouse. *Frontiers in neuroanatomy* **8**. Frontiers.

SCHUSTER, T., KRUG, M., STALDER, M., HACKEL, N., GERARDY SCHAHN, R. & SCHACHNER, M. (2001) Immunoelectron microscopic localization of the neural recognition molecules L1, NCAM, and its isoform NCAM180, the NCAM-associated polysialic acid, beta1 integrin and the extracellular matrix molecule tenascin-R in synapses of the adult rat hippocampus. *Journal of neurobiology* **49**, 142–158. John Wiley & Sons, Inc.

SCHWARZBAUER, J.E. & DESIMONE, D.W. (2011) Fibronectins, their fibrillogenesis, and in vivo functions. *Cold Spring Harbor Perspectives in Biology* **3**, a005041–a005041. Cold Spring Harbor Lab.

SCHWEIGREITER, R. & BANDTLOW, D.C.E. (2006) Nogo in the Injured Spinal Cord. *dx.doi.org* **23**, 384–396. Mary Ann Liebert, Inc. 2 Madison Avenue Larchmont, NY 10538 USA.

SEILER, M.P., MILLER, A.D., ZABNER, J. & HALBERT, C.L. (2006) Adeno-associated virus types 5 and 6 use distinct receptors for cell entry. *Human Gene Therapy* **17**, 10–19. Mary Ann Liebert, Inc. 2 Madison Avenue Larchmont, NY 10538 USA.

SEKINE, Y., LIN-MOORE, A., CHENETTE, D.M., WANG, X., JIANG, Z., CAFFERTY, W.B., HAMMARLUND, M. & STRITTMATTER, S.M. (2018) Functional Genome-wide Screen Identifies Pathways Restricting Central Nervous System Axonal Regeneration. *Cell reports* **24**, 269.

SELF, A.J., CARON, E., PATERSON, H.F. & HALL, A. (2001) Analysis of R-Ras signalling pathways. *Journal of Cell Science* **114**, 1357–1366.

SENETAR, M.A., MONCMAN, C.L. & MCCANN, R.O. (2007) Talin2 is induced during striated muscle differentiation and is targeted to stable adhesion complexes in mature muscle. *Cell motility and the cytoskeleton* **64**, 157–173. Wiley Subscription Services, Inc., A Wiley Company.

SERINI, G., VALDEMBRI, D., ZANIVAN, S., MORTERRA, G., BURKHARDT, C., CACCAVARI, F., ZAMMATARO, L., PRIMO, L., TAMAGNONE, L., LOGAN, M., TESSSIER-LAVIGNE, M., TANIGUCHI, M., PUSCHEL, A.W. & BUSSOLINO, F. (2003) Class 3 semaphorins control vascular morphogenesis by inhibiting integrin function. *Nature* **424**, 391–397. Nature Publishing Group.

SHALEM, O., SANJANA, N.E. & ZHANG, F. (2015) High-throughput functional genomics using CRISPR-Cas9. *Nature Reviews Genetics* **16**, 299–311. Nature Publishing Group.

SHAO, Z., BROWNING, J.L., LEE, X., SCOTT, M.L., SHULGA-MORSKAYA, S., ALLAIRE, N., THILL, G., LEVESQUE, M., SAH, D., MCCOY, J.M., MURRAY, B., JUNG, V., PEPINSKY, R.B. & MI, S. (2005) TAJ/TROY, an Orphan TNF Receptor Family Member, Binds Nogo-66 Receptor 1 and Regulates Axonal Regeneration. *Neuron* **45**, 353–359.

SHARMA, A., VERHAAGEN, J. & HARVEY, A.R. (2012) Receptor complexes for each of the Class 3 Semaphorins. *Frontiers in Cellular Neuroscience* **6**, 28. Frontiers.

SHATTIL, S.J., KIM, C. & GINSBERG, M.H. (2010) The final steps of integrin activation: the end game. *Nature Reviews Molecular Cell Biology* **11**, 288–300. Nature Publishing Group.

SHEEHAN, D., RAY, G.S., CALHOUN, B.C. & GOLDENRING, J.R. (1996) A somatodendritic distribution of Rab11 in rabbit brain neurons. *Neuroreport* **7**, 1297–1300.

SHEN, S., BRYANT, K.D., BROWN, S.M., RANDELL, S.H. & ASOKAN, A. (2011) Terminal N-linked galactose is the primary receptor for adeno-associated virus 9. *The Journal of biological chemistry* **286**, 13532–13540. American Society for Biochemistry and Molecular Biology.

SHEN, Y., TENNEY, A.P., BUSCH, S.A., HORN, K.P., CUASCUT, F.X., LIU, K., HE, Z., SILVER, J. & FLANAGAN, J.G. (2009) PTPsigma is a receptor for chondroitin sulfate proteoglycan, an inhibitor of neural regeneration. *Science (New York, N.Y.)* **326**, 592–596. American Association for the Advancement of Science.

SHI, Y. & ETHELL, I.M. (2006) Integrins control dendritic spine plasticity in hippocampal neurons through NMDA receptor and Ca2+/calmodulin-dependent protein kinase II-mediated actin reorganization. *Journal of Neuroscience* **26**, 1813–1822. Society for Neuroscience.

SICOTTE, M., TSATAS, O., JEONG, S.Y., CAI, C.-Q., HE, Z. & DAVID, S. (2003) Immunization with myelin or recombinant Nogo-66/MAG in alum promotes axon regeneration and sprouting after corticospinal tract lesions in the spinal cord. *Molecular and Cellular Neuroscience* **23**, 251–263.

SILVER, J. & MILLER, J.H. (2004) Regeneration beyond the glial scar. *Nature reviews. Neuroscience* **5**, 146–156. Nature Publishing Group.

SIMONEN, M., PEDERSEN, V., WEINMANN, O., SCHNELL, L., BUSS, A., LEDERMANN, B., CHRIST, F., SANSIG, G., VAN DER PUTTEN, H. & SCHWAB, M.E. (2003) Systemic Deletion of the Myelin-Associated Outgrowth Inhibitor Nogo-A Improves Regenerative and Plastic Responses after Spinal Cord Injury. *Neuron* **38**, 201–211.

SINGH, P., CARRAHER, C. & SCHWARZBAUER, J.E. (2010) Assembly of Fibronectin Extracellular Matrix. *Annual review of cell and developmental biology* **26**, 397–419. NIH Public Access.

SMITH, B.E., BRADSHAW, A.D., CHOI, E.S.H., ROUSELLE, P., WAYNER, E.A. & CLEGG, D.O. (2009a) Human SY5Y Neuroblastoma Cell Interactions with Laminin Isoforms: Neurite Outgrowth on Laminin-5 Is Mediated by Integrin α3β1. *Cell Communication & Adhesion* **3**, 451–462. Taylor & Francis.

SMITH, D.S. & SKENE, J.H. (1997) A transcription-dependent switch controls competence of adult neurons for distinct modes of axon growth. *Journal of Neuroscience* **17**, 646–658.

SMITH, P.D., SUN, F., PARK, K.K., CAI, B., WANG, C., KUWAKO, K., MARTINEZ-CARRASCO, I., CONNOLLY, L. & HE, Z. (2009b) SOCS3 deletion promotes optic nerve regeneration in vivo. *Neuron* **64**, 617–623.

SO, K.F. & AGUAYO, A.J. (1985) Lengthy Regrowth of Cut Axons From Ganglion-Cells After Peripheral-Nerve Transplantation Into the Retina of Adult-Rats. *Brain research* **328**, 349–354.

SOBOTZIK, J.-M., SIE, J.M., POLITI, C., DEL TURCO, D., BENNETT, V., DELLER, T. & SCHULTZ, C. (2009) AnkyrinG is required to maintain axo-dendritic polarity in vivo. *Proceedings of the National Academy of Sciences of the United States of America* **106**, 17564–17569. National Acad Sciences.

SONG, A.-H., WANG, D., CHEN, G., LI, Y., LUO, J., DUAN, S. & POO, M.-M. (2009) A Selective Filter for Cytoplasmic Transport at the Axon Initial Segment. *Cell* **136**, 1148–1160.

SRIRAMARAO, P., MENDLER, M. & BOURDON, M.A. (1993) Endothelial-Cell Attachment and Spreading on Human Tenascin Is Mediated by Alpha-2-Beta-1 and Alpha-v-Beta-3 Integrins. *Journal of Cell Science* **105**, 1001–1012. The Company of Biologists Ltd.

STAM, F.J., MACGILLAVRY, H.D., ARMSTRONG, N.J., DE GUNST, M.C.M., ZHANG, Y., VAN KESTEREN, R.E., SMIT, A.B. & VERHAAGEN, J. (2007) Identification of candidate transcriptional modulators involved in successful regeneration after nerve injury. *The European journal of neuroscience* **25**, 3629–3637. Blackwell Publishing Ltd.

STAUFFER, W.R., LAK, A., YANG, A., BOREL, M., PAULSEN, O., BOYDEN, E.S. & SCHULTZ, W. (2016) Dopamine Neuron-Specific Optogenetic Stimulation in Rhesus Macaques. *Cell* **166**, 1564–.

STEINMETZ, M.P., HORN, K.P., TOM, V.J., MILLER, J.H., BUSCH, S.A., NAIR, D., SILVER, D.J. & SILVER, J. (2005) Chronic enhancement of the intrinsic growth capacity of sensory neurons combined with the degradation of inhibitory proteoglycans allows functional regeneration of sensory axons through the dorsal root entry zone in the mammalian spinal cord. *The Journal of Neuroscience* **25**, 8066–8076. Society for Neuroscience.

STERNBERG, S.H., REDDING, S., JINEK, M., GREENE, E.C. & DOUDNA, J.A. (2014) DNA Interrogation by the CRISPR RNA-Guided Endonuclease Cas9. *Biophysical Journal* **106**, 695A–695A.

STEWARD, O., ZHENG, B., HO, C., ANDERSON, K. & TESSIER-LAVIGNE, M. (2004) The dorsolateral corticospinal tract in mice: an alternative route for corticospinal input to caudal segments following dorsal column lesions. *The Journal of comparative neurology* **472**, 463–477. Wiley-Blackwell.

STILES, T.L., DICKENDESHER, T.L., GAULTIER, A., FERNANDEZ-CASTANEDA, A., MANTUANO, E., GIGER, R.J. & GONIAS, S.L. (2013) LDL receptor-related protein-1 is a sialic-acid-independent receptor for myelin-associated glycoprotein that functions in neurite outgrowth inhibition by MAG and CNS myelin. *Journal of Cell Science* **126**, 209–220. The Company of Biologists Ltd.

SULLIVAN, K.A., KIM, B. & FELDMAN, E.L. (2008) Insulin-like growth factors in the peripheral nervous system. *Endocrinology* **149**, 5963–5971. Endocrine Society.

SUMMERFORD, C. & SAMULSKI, R.J. (1998) Membrane-associated heparan sulfate proteoglycan is a receptor for adeno-associated virus type 2 virions. *Journal of virology* **72**, 1438–1445. American Society for Microbiology (ASM).

SUZUKI, A., ARIKAWA, C., KUWAHARA, Y., ITOH, K., WATANABE, M., WATANABE, H., SUZUKI, T., FUNAKOSHI, Y., HASEGAWA, H. & KANAHO, Y. (2010) The scaffold protein JIP3 functions as a downstream effector of the small GTPase ARF6 to regulate neurite morphogenesis of cortical neurons. *FEBS letters* **584**, 2801–2806. Elsevier.

TADOKORO, S., SHATTIL, S.J., ETO, K., TAI, V., LIDDINGTON, R.C., DE PEREDA, J.M., GINSBERG, M.H. & CALDERWOOD, D.A. (2003) Talin binding to integrin beta tails: a final common step in integrin activation. *Science (New York, N.Y.)* **302**, 103–106. American Association for the Advancement of Science.

TAKADA, Y. & PUZON, W. (1993) Identification of a regulatory region of integrin beta 1 subunit using activating and inhibiting antibodies. *The Journal of biological chemistry* **268**, 17597–17601. American Society for Biochemistry and Molecular Biology.

TAKADA, Y., YE, X. & SIMON, S. (2007) The integrins. *Genome Biol*.

TAKAGI, J., ISOBE, T., TAKADA, Y. & SAITO, Y. (1997) Structural interlock between ligand-binding site and stalk-like region of beta1 integrin revealed by a monoclonal antibody recognizing conformation-dependent epitope. *Journal of biochemistry* **121**, 914–921. Oxford University Press.

TAN, C.L., ANDREWS, M.R., KWOK, J.C.F., HEINTZ, T.G.P., GUMY, L.F., FÄSSLER, R. & FAWCETT, J.W. (2012) Kindlin-1 enhances axon growth on inhibitory chondroitin sulfate proteoglycans and promotes sensory axon regeneration. *The Journal of Neuroscience* **32**, 7325–7335. Society for Neuroscience.

TAN, C.L., KWOK, J.C.F., HELLER, J.P.D., ZHAO, R., EVA, R. & FAWCETT, J.W. (2015) Full length talin stimulates integrin activation and axon regeneration. *Molecular and cellular neurosciences* **68**, 1–8.

TAN, C.L., KWOK, J.C.F., PATANI, R., FFRENCH-CONSTANT, C., CHANDRAN, S. & FAWCETT, J.W. (2011) Integrin activation promotes axon growth on inhibitory chondroitin sulfate proteoglycans by enhancing integrin signaling. *The Journal of Neuroscience* **31**, 6289–6295. Society for Neuroscience.

TANG, S.-J., REIS, G., KANG, H., GINGRAS, A.-C., SONENBERG, N. & SCHUMAN, E.M. (2002) A rapamycin-sensitive signaling pathway contributes to long-term synaptic plasticity in the hippocampus. *Proceedings of the National Academy of Sciences* **99**, 467–472. National Acad Sciences.

TANG, X., DAVIES, J.E. & DAVIES, S.J.A. (2003) Changes in distribution, cell associations, and protein expression levels of NG2, neurocan, phosphacan, brevican, versican V2, and tenascin-C during acute to chronic maturation of spinal cord scar tissue. *Journal of neuroscience research* **71**, 427–444. Wiley Subscription Services, Inc., A Wiley Company.

TANNEMAAT, M.R., KORECKA, J., EHLERT, E.M.E., MASON, M.R.J., VAN DUINEN, S.G., BOER, G.J., MALESSY, M.J.A. & VERHAAGEN, J. (2007) Human neuroma contains increased levels of semaphorin 3A, which surrounds nerve fibers and reduces neurite extension in vitro. *The Journal of Neuroscience* **27**, 14260–14264. Society for Neuroscience.

TATE, M.C., GARCÍA, A.J., KESELOWSKY, B.G., SCHUMM, M.A., ARCHER, D.R. & LAPLACA, M.C. (2004) Specific beta1 integrins mediate adhesion, migration, and differentiation of neural progenitors derived from the embryonic striatum. *Molecular and cellular neurosciences* **27**, 22–31.

THIEL, G., GREENGARD, P. & SÜDHOF, T.C. (1991) Characterization of tissue-specific transcription by the human synapsin I gene promoter. *Proceedings of the National Academy of Sciences* **88**, 3431–3435. National Academy of Sciences.

TIMPL, R. & BROWN, J.C. (1994) The laminins. *Matrix Biology* **14**, 275–281. Elsevier.

TOM, V.J., DOLLER, C.M., MALOUF, A.T. & SILVER, J. (2004a) Astrocyte-associated fibronectin is critical for axonal regeneration in adult white matter. *The Journal of Neuroscience* **24**, 9282–9290. Society for Neuroscience.

TOM, V.J., STEINMETZ, M.P., MILLER, J.H., DOLLER, C.M. & SILVER, J. (2004b) Studies on the development and behavior of the dystrophic growth cone, the hallmark of regeneration failure, in an in vitro model of the glial scar and after spinal cord injury. *The Journal of Neuroscience* **24**, 6531–6539. Society for Neuroscience.

TOMASELLI, K.J., DAMSKY, C.H. & REICHARDT, L.F. (1987) Interactions of a neuronal cell line (PC12) with laminin, collagen IV, and fibronectin: identification of integrin-related glycoproteins involved in attachment and process outgrowth. *Journal of Cell Biology* **105**, 2347–2358. Rockefeller Univ Press.

TOMASELLI, K.J., DOHERTY, P., EMMETT, C.J., DAMSKY, C.H., WALSH, F.S. & REICHARDT, L.F. (1993) Expression of beta 1 integrins in sensory neurons of the dorsal root ganglion and their functions in neurite outgrowth on two laminin isoforms. *Journal of Neuroscience* **13**, 4880–4888. Society for Neuroscience.

TREMBLAY, F., BRULE, S., UM, S.H., LI, Y., MASUDA, K., RODEN, M., SUN, X.J., KREBS, M., POLAKIEWICZ, R.D., THOMAS, G. & MARETTE, A. (2007) Identification of IRS-1 Ser-1101 as a target of S6K1 in nutrient- and obesity-induced insulin resistance. *Proceedings of the National Academy of Sciences* **104**, 14056–14061. National Acad Sciences.

TSUCHIDA, J., UEKI, S., SAITO, Y. & TAKAGI, J. (1997) Classification of 'activation' antibodies against integrin beta1 chain. *FEBS letters* **416**, 212–216.

TUCKER, R.P. & CHIQUET-EHRISMANN, R. (2015) Tenascin-C: Its functions as an integrin ligand. *International Journal of Biochemistry & Cell Biology* **65**, 165–168.

TYZACK, G.E., SITNIKOV, S., BARSON, D., ADAMS-CARR, K.L., LAU, N.K., KWOK, J.C., ZHAO, C., FRANKLIN, R.J.M., KARADOTTIR, R.T., FAWCETT, J.W. & LAKATOS, A. (2014) Astrocyte response to motor neuron injury promotes structural synaptic plasticity via STAT3-regulated TSP-1 expression. *Nature communications* **5**, 4294. Nature Publishing Group.

ULNDREAJ, A., BADNER, A. & FEHLINGS, M.G. (2017) Promising neuroprotective strategies for traumatic spinal cord injury with a focus on the differential effects among anatomical levels of injury. *F1000Research* **6**, 1907.

ULUSOY, A., SAHIN, G., BJÖRKLUND, T., AEBISCHER, P. & KIRIK, D. (2009) Dose optimization for long-term rAAV-mediated RNA interference in the nigrostriatal projection neurons. *Molecular therapy : the journal of the American Society of Gene Therapy* **17**, 1574–1584.

USSAR, S., MOSER, M., WIDMAIER, M., ROGNONI, E., HARRER, C., GENZEL-BOROVICZENY, O. & FÄSSLER, R. (2008) Loss of Kindlin-1 Causes Skin Atrophy and Lethal Neonatal Intestinal Epithelial Dysfunction. *PLOS Genetics* **4**, e1000289. Public Library of Science.

USSAR, S., WANG, H.-V., LINDER, S., FÄSSLER, R. & MOSER, M. (2006) The Kindlins: subcellular localization and expression during murine development. *Experimental cell research* **312**, 3142–3151.

VALDEMBRI, D., CASWELL, P.T., ANDERSON, K.I., SCHWARZ, J.P., KÖNIG, I., ASTANINA, E., CACCAVARI, F., NORMAN, J.C., HUMPHRIES, M.J., BUSSOLINO, F. & SERINI, G. (2009) Neuropilin-1/GIPC1 signaling regulates alpha5beta1 integrin traffic and function in endothelial cells. *PLoS biology* **7**, e25. Public Library of Science.

VAN BEUNINGEN, S.F.B., WILL, L., HARTERINK, M., CHAZEAU, A., VAN BATTUM, E.Y., FRIAS, C.P., ET AL. (2015) TRIM46 Controls Neuronal Polarity and Axon Specification by Driving the Formation of Parallel Microtubule Arrays. *Neuron* **88**, 1208–1226. Elsevier.

VAN DER FLIER, A. & SONNENBERG, A. (2001) Function and interactions of integrins. *Cell and tissue research* **305**, 285–298. Springer-Verlag.

VAN DER PERREN, A., TOELEN, J., CARLON, M., VAN DEN HAUTE, C., COUN, F., HEEMAN, B., REUMERS, V., VANDENBERGHE, L.H., WILSON, J.M., DEBYSER, Z. & BAEKELANDT, V. (2011) Efficient and stable transduction of dopaminergic neurons in rat substantia nigra by rAAV 2/1, 2/2, 2/5, 2/6.2, 2/7, 2/8 and 2/9. *Gene therapy* **18**, 517–527. Nature Publishing Group.

VAN KESTEREN, R.E., MASON, M.R.J., MACGILLAVRY, H.D., SMIT, A.B. & VERHAAGEN, J. (2011) A gene network perspective on axonal regeneration. *Frontiers in molecular neuroscience* **4**, 46. Frontiers.

VARNUM-FINNEY, B., VENSTROM, K., MÜLLER, U., KYPTA, R., BACKUS, C., CHIQUET, M. & REICHARDT, L.F. (1995) The integrin receptor alpha 8 beta 1 mediates interactions of embryonic chick motor and sensory neurons with tenascin-C. *Neuron* **14**, 1213–1222. NIH Public Access.

VECINO, E., HELLER, J.P., VEIGA-CRESPO, P., MARTIN, K.R. & FAWCETT, J.W. (2015) Influence of extracellular matrix components on the expression of integrins and regeneration of adult retinal ganglion cells. *PloS one* **10**, e0125250.

VENKATESH, I., MEHRA, V., WANG, Z., CALIFF, B. & BLACKMORE, M.G. (2018) Developmental Chromatin Restriction of Pro-Growth Gene Networks Acts as an Epigenetic Barrier to Axon Regeneration in Cortical Neurons. *Developmental neurobiology* **78**, 960–977. John Wiley & Sons, Ltd.

VENKATESH, K., CHIVATAKARN, O., LEE, H., JOSHI, P.S., KANTOR, D.B., NEWMAN, B.A., MAGE, R., RADER, C. & GIGER, R.J. (2005) The Nogo-66 receptor homolog NgR2 is a sialic acid-dependent receptor selective for myelin-associated glycoprotein. *The Journal of Neuroscience* **25**, 808–822. Society for Neuroscience.

VENSTROM, K. & REICHARDT, L. (1995) Beta 8 integrins mediate interactions of chick sensory neurons with laminin-1, collagen IV, and fibronectin. *Molecular biology of the cell* **6**, 419–431. American Society for Cell Biology.

VERHAAGEN, J., HOBO, B., EHLERT, E.M.E., EGGERS, R., KORECKA, J.A., HOYNG, S.A., ATTWELL, C.L., HARVEY, A.R. & MASON, M.R.J. (2018) Small Scale Production of Recombinant Adeno-Associated Viral Vectors for Gene Delivery to the Nervous System. *Methods in molecular biology (Clifton, N.J.)* **1715**, 3–17. Springer New York, New York, NY.

VOGELEZANG, M., FORSTER, U.B., HAN, J., GINSBERG, M.H. & FFRENCH-CONSTANT, C. (2007) Neurite outgrowth on a fibronectin isoform expressed during peripheral nerve regeneration is mediated by the interaction of paxillin with α4β1 integrins. *BMC neuroscience* **8**, 1. BioMed Central.

VOGELEZANG, M.G., LIU, Z., RELVAS, J.B., RAIVICH, G., SCHERER, S.S. & FFRENCH-CONSTANT, C. (2001) Alpha4 integrin is expressed during peripheral nerve regeneration and enhances neurite outgrowth. *The Journal of Neuroscience* **21**, 6732–6744.

WAITE, K. & EICKHOLT, B.J. (2010) The neurodevelopmental implications of PI3K signaling. *Current topics in microbiology and immunology* **346**, 245–265. Springer Berlin Heidelberg, Berlin, Heidelberg.

WALLQUIST, W., PATARROYO, M., THAMS, S., CARLSTEDT, T., STARK, B., CULLHEIM, S. & HAMMARBERG, H. (2002) Laminin chains in rat and human peripheral nerve: Distribution and regulation during development and after axonal injury. *Journal of Comparative Neurology* **454**, 284–293. Wiley Subscription Services, Inc., A Wiley Company.

WALLQUIST, W., ZELANO, J., PLANTMAN, S., KAUFMAN, S.J., CULLHEIM, S. & HAMMARBERG, H. (2004) Dorsal root ganglion neurons up-regulate the expression of laminin-associated integrins after peripheral but not central axotomy. *The Journal of comparative neurology* **480**, 162–169. Wiley Subscription Services, Inc., A Wiley Company.

WANG, B., ZOU, J.X., EK-RYLANDER, B. & RUOSLAHTI, E. (2000) R-Ras contains a proline-rich site that binds to SH3 domains and is required for integrin activation by R-Ras. *The Journal of biological chemistry* **275**, 5222–5227.

WANG, C., WEI, Z., CHEN, K., YE, F., YU, C., BENNETT, V. & ZHANG, M. (2014) Structural basis of diverse membrane target recognitions by ankyrins. *eLife* **3**.

WANG, J.-W., YANG, J.-F., MA, Y., HUA, Z., GUO, Y., GU, X.-L. & ZHANG, Y.-F. (2015a) Nogo-A expression dynamically varies after spinal cord injury. *Neural regeneration research* **10**, 225–229. Medknow Publications.

WANG, K.C., KIM, J.A., SIVASANKARAN, R., SEGAL, R. & HE, Z.G. (2002) p75 interacts with the Nogo receptor as a co-receptor for Nogo, MAG and OMgp. *Nature* **420**, 74–78. Nature Publishing Group.

WANG, Y.-H., HARIHARAN, A., BASTIANELLO, G., TOYAMA, Y., SHIVASHANKAR, G.V., FOIANI, M. & SHEETZ, M.P. (2017) DNA damage causes rapid accumulation of phosphoinositides for ATR signaling. *Nature communications* **8**, 2118. Nature Publishing Group.

WANG, Z., REYNOLDS, A., KIRRY, A., NIENHAUS, C. & BLACKMORE, M.G. (2015b) Overexpression of sox11 promotes corticospinal tract regeneration after spinal injury while interfering with functional recovery. *The Journal of Neuroscience* **35**, 3139–3145. Society for Neuroscience.

WATABE, H., FURUHAMA, T., TANI-ISHII, N. & MIKUNI-TAKAGAKI, Y. (2011) Mechanotransduction activates $\alpha_5\beta_1$ integrin and PI3K/Akt signaling pathways in mandibular osteoblasts. *Experimental cell research* **317**, 2642–2649.

WATAKABE, A., OHTSUKA, M., KINOSHITA, M., TAKAJI, M., ISA, K., MIZUKAMI, H., OZAWA, K., ISA, T. & YAMAMORI, T. (2015) Comparative analyses of adeno-associated viral vector serotypes 1, 2, 5, 8 and 9 in marmoset, mouse and macaque cerebral cortex. *Neuroscience research* **93**, 144–157.

WEGENER, K.L., PARTRIDGE, A.W., HAN, J., PICKFORD, A.R., LIDDINGTON, R.C., GINSBERG, M.H. & CAMPBELL, I.D. (2007) Structural basis of integrin activation by talin. *Cell* **128**, 171–182.

WENG, Y.-L., AN, R., CASSIN, J., JOSEPH, J., MI, R., WANG, C., ZHONG, C., JIN, S.-G., PFEIFER, G.P., BELLACOSA, A., DONG, X., HOKE, A., HE, Z., SONG, H. & MING, G.-L. (2017) An Intrinsic Epigenetic Barrier for Functional Axon Regeneration. *Neuron* **94**, 337–346.e6. Elsevier.

WERNER, A., WILLEM, M., JONES, L.L., KREUTZBERG, G.W., MAYER, U. & RAIVICH, G. (2000) Impaired axonal regeneration in alpha7 integrin-deficient mice. *The Journal of Neuroscience* **20**, 1822–1830. Society for Neuroscience.

WIESE, S., KARUS, M. & FAISSNER, A. (2012) Astrocytes as a source for extracellular matrix molecules and cytokines. *Frontiers in pharmacology* **3**, 120. Frontiers.

WINOGRAD-KATZ, S.E., FÄSSLER, R., GEIGER, B. & LEGATE, K.R. (2014) The integrin adhesome: from genes and proteins to human disease. *Nature Reviews Molecular Cell Biology* **15**, 273–288. Nature Research.

WONG, S.T., HENLEY, J.R., KANNING, K.C., HUANG, K.-H., BOTHWELL, M. & POO, M.-M. (2002) A p75NTR and Nogo receptor complex mediates repulsive signaling by myelin-associated glycoprotein. *Nature neuroscience* **5**, 1302–1308. Nature Publishing Group.

WRIGHT, A.V., NUÑEZ, J.K. & DOUDNA, J.A. (2016) Biology and Applications of CRISPR Systems: Harnessing Nature's Toolbox for Genome Engineering. *Cell* **164**, 29–44.

WU, X., RENUSE, S., SAHASRABUDDHE, N.A., ZAHARI, M.S., CHAERKADY, R., KIM, M.-S., ET AL. (2014) Activation of diverse signalling pathways by oncogenic PIK3CA mutations. *Nature communications* **5**. Nature Publishing Group.

WU, Z., MILLER, E., AGBANDJE-MCKENNA, M. & SAMULSKI, R.J. (2006) Alpha2,3 and alpha2,6 N-linked sialic acids facilitate efficient binding and transduction by adeno-associated virus types 1 and 6. *Journal of virology* **80**, 9093–9103. American Society for Microbiology.

XIAO, X., LI, J. & SAMULSKI, R.J. (1998) Production of high-titer recombinant adeno-associated virus vectors in the absence of helper adenovirus. *Journal of virology* **72**, 2224–2232.

XIAO, X., XIAO, W.D., LI, J. & SAMULSKI, R.J. (1997) A novel 165-base-pair terminal repeat sequence is the sole cis requirement for the adeno-associated virus life cycle. *Journal of virology* **71**, 941–948. American Society for Microbiology (ASM).

XU, B., PARK, D., OHTAKE, Y., LI, H., HAYAT, U., LIU, J., SELZER, M.E., LONGO, F.M. & LI, S. (2015) Role of CSPG receptor LAR phosphatase in restricting axon regeneration after CNS injury. *Neurobiology of disease* **73**, 36–48.

XU, Q.G., LI, X.Q., KOTECHA, S.A., CHENG, C., SUN, H.S. & ZOCHODNE, D.W. (2004) Insulin as an in vivo growth factor. *Experimental neurology* **188**, 43–51.

YAN, Q., RADEKE, M.J., MATHESON, C.R., TALVENHEIMO, J., WELCHER, A.A. & FEINSTEIN, S.C. (1997) Immunocytochemical localization of TrkB in the central nervous system of the adult rat. *The Journal of comparative neurology* **378**, 135–157.

YANAGIDA, H., TANAKA, J. & MARUO, S. (1999) Immunocytochemical localization of a cell adhesion molecule, integrin α5β1, in nerve growth cones. *Journal of orthopaedic science : official journal of the Japanese Orthopaedic Association* **4**, 353–360. Springer-Verlag.

YANG, J.T., RAYBURN, H. & HYNES, R.O. (1993) Embryonic mesodermal defects in alpha 5 integrin-deficient mice. *Development* **119**, 1093–1105.

YANG, J.T., RAYBURN, H. & HYNES, R.O. (1995) Cell adhesion events mediated by alpha 4 integrins are essential in placental and cardiac development. *Development* **121**, 549–560.

YANG, Y., OGAWA, Y., HEDSTROM, K.L. & RASBAND, M.N. (2007) betaIV spectrin is recruited to axon initial segments and nodes of Ranvier by ankyrinG. *Journal of Cell Biology* **176**, 509–519. Rockefeller University Press.

YE, F., LAGARRIGUE, F. & GINSBERG, M.H. (2014) SnapShot: talin and the modular nature of the integrin adhesome. *Cell* **156**, 1340–1340.e1341.

YI, R., DOEHLE, B.P., QIN, Y., MACARA, I.G. & CULLEN, B.R. (2005) Overexpression of Exportin 5 enhances RNA interference mediated by short hairpin RNAs and microRNAs. *Rna* **11**, 220–226. Cold Spring Harbor Lab.

YI, R., QIN, Y., MACARA, I.G. & CULLEN, B.R. (2003) Exportin-5 mediates the nuclear export of pre-microRNAs and short hairpin RNAs. *Genes & development* **17**, 3011–3016. Cold Spring Harbor Lab.

YIN, Y., CUI, Q., LI, Y., IRWIN, N., FISCHER, D., HARVEY, A.R. & BENOWITZ, L.I. (2003) Macrophage-derived factors stimulate optic nerve regeneration. *The Journal of Neuroscience* **23**, 2284–2293.

YOKOSAKI, Y., MATSUURA, N., HIGASHIYAMA, S., MURAKAMI, I., OBARA, M., YAMAKIDO, M., SHIGETO, N., CHEN, J. & SHEPPARD, D. (1998) Identification of the ligand binding site for the integrin alpha9 beta1 in the third fibronectin type III repeat of tenascin-C. *The Journal of biological chemistry* **273**, 11423–11428. American Society for Biochemistry and Molecular Biology.

YOKOSAKI, Y., PALMER, E.L., PRIETO, A.L., CROSSIN, K.L., BOURDON, M.A., PYTELA, R. & SHEPPARD, D. (1994) The integrin alpha 9 beta 1 mediates cell attachment to a non-RGD site in the third fibronectin type III repeat of tenascin. *The Journal of biological chemistry* **269**, 26691–26696.

YOSHII, A. & CONSTANTINE-PATON, M. (2007) BDNF induces transport of PSD-95 to dendrites through PI3K-AKT signaling after NMDA receptor activation. *Nature neuroscience* **10**, 702–711. Nature Publishing Group.

YOSHIMURA, T., KAWANO, Y., ARIMURA, N., KAWABATA, S., KIKUCHI, A. & KAIBUCHI, K. (2005) GSK-3 beta regulates phosphorylation of CRMP-2 and neuronal polarity. *Cell* **120**, 137–149.

YU, Y.M., CRISTOFANILLI, M., VALIVETI, A., MA, L., YOO, M., MORELLINI, F. & SCHACHNER, M. (2011) The Extracellular Matrix Glycoprotein Tenascin-C Promotes Locomotor Recovery After Spinal Cord Injury in Adult Zebrafish. *Neuroscience* **183**, 238–250.

ZAIDEL-BAR, R., ITZKOVITZ, S., MA'AYAN, A., IYENGAR, R. & GEIGER, B. (2007) Functional atlas of the integrin adhesome. *Nature cell biology* **9**, 858–867. Nature Publishing Group.

ZHANG, J., GAO, Z., YIN, J., QUON, M.J. & YE, J. (2008) S6K Directly Phosphorylates IRS-1 on Ser-270 to Promote Insulin Resistance in Response to TNF-alpha Signaling through IKK2. *The Journal of biological chemistry* **283**, 35375–35382. American Society for Biochemistry and Molecular Biology.

ZHANG, Y., ANDERSON, P.N., CAMPBELL, G., MOHAJERI, H., SCHACHNER, M. & LIEBERMAN, A.R. (1995a) Tenascin-C expression by neurons and glial cells in the rat spinal cord: Changes during postnatal development and after dorsal root or sciatic nerve injury. *Journal of neurocytology* **24**, 585–601. Kluwer Academic Publishers.

ZHANG, Y., ANDERSON, P.N., CAMPBELL, G., MOHAJERI, H., SCHACHNER, M. & LIEBERMAN, A.R. (1995b) Tenascin-C expression by neurons and glial cells in the rat spinal cord: changes during postnatal development and after dorsal root or sciatic nerve injury. *Journal of neurocytology* **24**, 585–601.

ZHANG, Y., WINTERBOTTOM, J.K., SCHACHNER, M., LIEBERMAN, A.R. & ANDERSON, P.N. (1997) Tenascin-C expression and axonal sprouting following injury to the spinal dorsal columns in the adult rat. *Journal of neuroscience research* **49**, 433–450. John Wiley & Sons, Inc.

ZHANG, Z., VUORI, K., WANG, H.-G., REED, J.C. & RUOSLAHTI, E. (1996) Integrin Activation by R-ras. *Cell* **85**, 61–69.

ZHANG, Z., YU, B., GU, Y., ZHOU, S., QIAN, T., WANG, Y., DING, G., DING, F. & GU, X. (2015) Fibroblast-derived tenascin-C promotes Schwann cell migration through β1-integrin dependent pathway during peripheral nerve regeneration. *Glia*, n/a–n/a.

ZHAO, L. & VOGT, P.K. (2008) Helical domain and kinase domain mutations in p110alpha of phosphatidylinositol 3-kinase induce gain of function by different mechanisms. *Proceedings of the National Academy of Sciences of the United States of America* **105**, 2652–2657. National Acad Sciences.

ZHENG, B., HO, C., LI, S., KEIRSTEAD, H., STEWARD, O. & TESSIER-LAVIGNE, M. (2003) Lack of Enhanced Spinal Regeneration in Nogo-Deficient Mice. *Neuron* **38**, 213–224.

ZHOU, D., LAMBERT, S., MALEN, P.L., CARPENTER, S., BOLAND, L.M. & BENNETT, V. (1998) AnkyrinG is required for clustering of voltage-gated Na channels at axon initial segments and for normal action potential firing. *The Journal of Cell Biology* **143**, 1295–1304.

ZHU, Y., SODERBLOM, C., TROJANOWSKY, M., LEE, D.-H. & LEE, J.K. (2015) Fibronectin Matrix Assembly after Spinal Cord Injury. *Journal of neurotrauma* **32**, 1158–1167. Mary Ann Liebert, Inc. 140 Huguenot Street, 3rd Floor New Rochelle, NY 10801 USA.

ZUKOR, K., BELIN, S., WANG, C., KEELAN, N., WANG, X. & HE, Z. (2013) Short hairpin RNA against PTEN enhances regenerative growth of corticospinal tract axons after spinal cord injury. *The Journal of Neuroscience* **33**, 15350–15361. Society for Neuroscience.